THEORY OF ELECTRON CAPTURE IN ION-ATOM COLLISIONS

by

Charles William Newby, B.Sc.

A thesis submitted to the University of Durham in candidature for the Degree of Doctor of Philosophy.

Department of Physics,
University of Durham,
England.

October, 1983.

ABSTRACT

Cross sections for electron capture by $^4He^{2+}$ ions from ground state atomic hydrogen are presented for a $^4He^{2+}$ laboratory energy range from 1 to 800 keV (0.25 to 200 keV amu^{-1}). The cross sections were calculated using a coupled channel approximation in which the electronic wavefunction was expanded in terms of a finite number of atomic orbital basis states centred upon the target and the projectile. Electron translation factors which incorporated a switching function were included in the basis states. The semi-classical impact parameter approximation was employed.

The cross sections presented are for electron capture into the 2s state of $^4He^+$, and into the n = 2 level of $^4He^+$ using two states and four states respectively in the basis expansion. Four functional forms of switching function were used in the translation factors.

The cross sections are compared with ones calculated using two-state and four-state atomic basis expansions which used plane-wave translation factors, and also with other theoretical and experimental cross sections. For energies $\leqslant$ 2.5 keV amu^{-1} fairly reasonable agreement is obtained with other data. For energies $\geqslant$2.5 keV amu^{-1} the present cross sections are in poor to extremely poor agreement with other data, steady divergence of the present results from existing data being observed with increasing energy.

The present results are discussed, and conclusions and suggestions for future work are made.

ACKNOWLEDGEMENTS

I wish to express my gratitude to my Supervisor, Professor B.H. Bransden for his supervision of this work, and also my gratitude to my additional Supervisor, Dr. D.R. Flower for his supervision during the periods of Professor Bransden's sabbatical leave.

In addition I wish to thank Dr. C.J. Noble, Dr. R. Shingal and Dr. A.M. Ermolaev for many useful discussions, and also I wish to thank my fellow graduate research students for contributing to the stimulating and convivial atmosphere in the office which we shared, with special thanks to Messrs. Robin Hewitt and Grahame Danby for numerous enlivening conversations.

I wish to thank Professor Bransden and Professor A. W. Wolfendale for providing the facilities of the Physics Department of the University of Durham, and also I wish to thank the University Computing Service for use of NUMAC (Newcastle University Multiple Access Computer), their IBM 370/168 machine, and also the Daresbury Laboratory for use of their AS 7000 machine. I wish to especially thank the Science and Engineering Research Council (SERC) for their provision of a research studentship.

Finally, a special debt of gratitude is owed to Mrs. Margaret Chipchase for her typing of the final manuscript.

CONTENTS

CHAPTER 1

INTRODUCTION

1.1 Electron capture in ion-atom collisions

The work presented in this thesis is concerned with the atomic collision process known as electron capture. This process is the transfer of one or more electrons during the collision of two atomic species which may be neutral atoms or electrically charged ions. Electron capture is also known by other titles, which are "charge exchange" and "charge transfer". In this thesis we shall be considering single-electron capture processes where only one electron is captured during the collision. Let us denote the projectile ion or atom by A and the target ion or atom by $(B + e^-)$. That is A and B represent singly or multiply charged ionic cores. The collision of A and $(B + e^-)$ may lead to one of a number of possible outcomes. These are listed as follows:-

$$A + (B + e^-) \longrightarrow A + (B + e^-), \text{ elastic;} \qquad (1.1.1a)$$

$$\Longrightarrow A + (B + e^-)^*, \text{ excitation;} \qquad (1.1.1b)$$

$$\longrightarrow (A + e^-) + B, \text{ capture to ground state} \qquad (1.1.1c)$$

$$\Longrightarrow (A + e^-)^* + B, \text{ capture to excited state;} \qquad (1.1.1d)$$

$$\Longrightarrow A + B + e^-, \text{ ionisation.} \qquad (1.1.1e)$$

The process (1.1.1a) involves no conversion of kinetic energy into internal energy and is termed elastic. This is not the case with process (1.1.1b) where the target system is excited (denoted by *). This inelastic process

is known as direct excitation, direct meaning there is no rearrangement of the particles during the collision.

Processes (1.1.1c) and (1.1.1d) are electron capture processes. They belong to the class of collisions known as rearrangement collisions. In process (1.1.1c) the electron is captured into the ground state of the $(A + e^-)$ system; in (1.1.1d) capture to an excited state occurs. The final process (1.1.1e) is ionisation. Here the electron is in a continuum state rather than a discrete bound state. At high energies electron capture occurs predominantly via the radiative process

$$A + (B + e^-) \longrightarrow (A + e^-)^* + B + \gamma \qquad (1.1.2)$$

where γ is a photon.

If A and B are the same, an electron capture process is termed "symmetric", if they are different the process is "asymmetric". If there is a zero (or nearly zero) energy defect between the initial and final systems, the process is termed "resonant"; if the energy defect is not zero, the term "non-resonant" is used. The process

$$H^+ + H(1s) \longrightarrow H(1s) + H^+ \qquad (1.1.3)$$

is an example of symmetrical resonance electron capture. However, the process

$$He^{2+} + H(1s) \longrightarrow He^+(2s) + H^+ \qquad (1.1.4)$$

is an example of asymmetrical (or accidental) resonance electron capture.

1.2 Controlled thermonuclear fusion

Electron capture processes have attracted much attention over the past few years owing to their relevance to the

field of controlled thermonuclear fusion. Specifically the magnitudes of cross sections (see next section) are of interest to workers trying to achieve the aim of harnessing the energy of thermonuclear fusion for peaceful purposes. Most of their effort has been directed toward a fusion reactor in which a magnetically confined plasma is heated to a temperature at which fusion occurs. The energy released is then used in a conventional manner to produce steam which is used to generate electricity in steam turbo-generators. The problems associated with the realisation of a viable fusion reactor are difficult. To bring about fusion in the plasma requires very high temperatures. This is because the Coulomb repulsion of the nuclei to be fused has to be overcome. As this is dependent upon the nuclear charges, nuclei with small nuclear charges must be used. This is no major problem, though, as the best isotopes, from this point of view, are those of hydrogen (deuterium, D and tritium, T). Deuterium occurs naturally in the form of "heavy water" (D_2O), and so may be obtained relatively cheaply from naturally occurring water. In fact the Coulomb repulsion is not such a great problem as quantum mechanical tunnelling through the Coulomb barrier can occur. A major problem in the fusion research work has been concerned with confining the plasma. One way of doing this is to have the plasma in a torus, confinement being achieved by a combination of poloidal and toroidal magnetic fields. Unfortunately a high-temperature plasma is highly unstable and successful confinement remains to be achieved alongside actual fusion occurring.

An attractive candidate for the fusion reaction is the so-called D-T reaction. This is

$$D + T \Rightarrow (^4He + 3.52\ MeV) + (n + 14.06\ MeV). \quad (1.2.1)$$

This process attains reaction rates sufficient for ignition at temperatures greater than ones corresponding to only 4-5 keV. The 3.52 MeV alpha particles remain in the fully ionised plasma where they give up their energy through collisions with the constituents. The neutrons must have their kinetic energy converted into heat by some means. One way envisaged of doing this is to surround the reactor vessel with a lithium blanket inside which the neutrons would be trapped, their kinetic energy being taken up in the form of heat by heat exchangers, which in turn would create steam by some means. This idea has the advantage that more tritium could be produced via the reaction

$$^6Li + n \Rightarrow ^4He + T + 4.80\ MeV. \quad (1.2.2)$$

The ^6Li lithium isotope occurs in natural lithium ($\sim 7.5\%$) and so may be obtained fairly easily. The driving of a 100 MW power station would require of the order of 10^{21} D-T reactions per second. This corresponds to temperatures being required of the order of 10^8K. At such temperatures the plasma must be kept from coming into contact with the reactor vessel and hence the need for confinement of the plasma.

The question arises as to how the plasma is heated. If magnetic confinement is the method used to confine the plasma, energy is supplied by means of ohmic heating

from the toroidal current induced in the plasma by the magnetic field. Beyond 2-3 keV this method of heating is ineffective, and at such energies, further heating cannot be produced by the alpha particles from the D-T fusion reaction (1.2.1). Supplementary heating is therefore, required by some means. A promising method is known as neutral-beam injection. This is where an intense beam of neutral deuterium atoms is injected into the plasma where the atoms are ionised either by electron capture or by direct ionisation. The resulting D^+ ions give up their energy in collisions with the plasma constituents. Neutral atoms must be used in the beam so that the magnetic field can be penetrated. The practical use of such a beam requires some kind of device to produce the beam. The design of such a device requires the knowledge of cross sections for atomic collision processes which include that of electron capture. The production of a neutral beam of deuterium atoms begins by accelerating a pulsed beam of D^+ ions produced by an ion source. Once at an energy of the order of 100 keV, This D^+ beam is passed through a gas (molecular deuterium D_2) or metallic vapour target. Partial conversion to fast neutral atoms or molecules takes place by electron capture, for example

$$D^+ + D_2 \longrightarrow D + D_2^+. \qquad (1.2.3)$$

Unfortunately this process has a small cross section at 100 keV and so the neutralisation process is somewhat inefficient An alternative is to use the "detachment" reaction

$$D^- + D_2 \longrightarrow D + e^- + D_2. \qquad (1.2.4)$$

This has a large cross section but the formation of a D^- beam is difficult. Assuming, though, that the beam of neutral deuterium atoms has been produced it is injected into the plasma and heating occurs by ionisation of the neutral deuterium atoms, as was stated earlier. The actual processes occurring in the plasma whereby the neutral D atoms are ionised are

$$D + D^+ \longrightarrow D^+ + D \qquad (1.2.5a)$$

$$D + T^+ \longrightarrow D^+ + T \qquad (1.2.5b)$$

$$D + D^+ \longrightarrow D^+ + D^+ + e^- \qquad (1.2.6a)$$

$$D + T^+ \longrightarrow D^+ + T^+ + e^- \qquad (1.2.6b)$$

$$e^- + D \longrightarrow D^+ + 2e^-. \qquad (1.2.7)$$

The cross sections for these processes have been measured for H and H^+ and the cross sections for D or T are the same at the same relative velocity. The electron capture processes (1.2.5a) and (1.2.5b) have associated cross sections of the order of $10^{-15}cm^2$ at beam energies of about 10 keV. The capture process is the most important process at this energy. At an energy of 100 keV, though, the capture processes have cross sections of the order of $10^{-17}cm^2$ but the ionisation processes (1.2.6a) and (1.2.6b) have cross sections larger by a factor of about 10. The electron ionisation process (1.2.7) is of little importance at the energies being considered.

The efficiency of neutral-beam heating is lowered by the presence of fully ionised impurity ions such as

C^{6+} and C^{8+}. Electron capture occurs resulting in highly-excited, short-lived states of the impurity ions, namely

$$X^{q+} + H \longrightarrow X^{(q-1)+} + H^{+} \qquad (1.2.8)$$

where X^{q+} is the impurity ion with charge q. These states then radiatively decay resulting in a loss of power. Also the ionisation process

$$X^{q+} + H \longrightarrow X^{q+} + H^{+} + e^{-} \qquad (1.2.9)$$

may occur. This can lead to cold electrons that can be detrimental to the density and temperature distribution of the plasma. Another possible process that can occur within the plasma is

$$H^{+} + X^{q+} \longrightarrow H + X^{(q+1)+} \qquad (1.2.10)$$

where X may be helium or an impurity. The resulting fast hydrogen atoms cannot be confined magnetically and thus escape. The increased charge of X results in further power loss by radiation.

As well as data concerning processes arising from neutral-beam heating being required, data are required on the electron capture processes

$$He^{2+} + H \rightleftharpoons He^{+} + H^{+} \qquad (1.2.11)$$

$$He^{+} + H \rightleftharpoons He + H^{+} \qquad (1.2.12)$$

in order that there be a better understanding of the energy and particle loss mechanisms which are associated with the alpha particle heating. Also the impurity ions may seriously affect the alpha particle heating. Data on the associated collisions are therefore of interest.

Another area where atomic physics can provide information of use in fusion research is that of plasma diagnostics. It is important to be able to measure the parameters of a plasma such as its density and temperature, and also the concentration of impurity ions and the depth of penetration of the neutral beam used to heat the plasma. Beams of hydrogen atoms with energies between 4 to 14 keV have been used as probes to investigate the plasma. By studying the attenuation of the beam and having a knowledge of the electron capture and ionisation cross sections for protons colliding with hydrogen, and also the cross section for ionisation of hydrogen atoms by electrons, in this case the plasma electrons, the path-averaged proton density in the plasma can be measured. Also it is possible to study the Doppler-shifted radiation emitted by decaying hydrogen atoms, formed by electron capture by plasma protons from injected hydrogen atoms, in order to measure the temperature of the plasma. The electron capture cross sections into the excited states of the subsequently decaying hydrogen atoms can be used to measure the proton density. In principle the impurities in the plasma can be investigated by this method.

Spectroscopic techniques can be applied to assessing the depth of penetration of the neutral beam used for heating. Electron capture by O^{8+} ions produces O^{7+} in levels corresponding to n = 5, 6 or 7. By determining the depth in the plasma from which radiation characteristic of these levels is emitted, an estimate of the penetration depth of the neutral beam can be obtained. However, fairly accurate spectroscopic

information is required for multiply charged ions such as O^{7+}. This information may be obtained by using beam-foil spectroscopy wherein a high energy beam of singly ionised particles is passed through a thin foil (often carbon) to produce an emergent beam of atomic species in many different excitation and ionisation states. The line radiation from these species can then be measured. Much more detailed discussions of various aspects of controlled nuclear fusion are given in the publication edited by McDowell and Ferendeci (1980).

1.3 Cross sections and reference frames

The quantities which characterise collision processes between "particles" such as atoms, molecules, etc. are called cross sections. Cross sections can usually be measured experimentally or alternatively a theoretical model can be constructed, based either wholly or in part upon quantum mechanics, the purpose of which is to predict the cross sections. A collision experiment is, in principle, very simple, consisting of a collimated, and very nearly monoenergetic beam of particles, A which is directed at a target containing scatterers, B. The products of the collision process occurring are detected in some way (see figure 1.1).

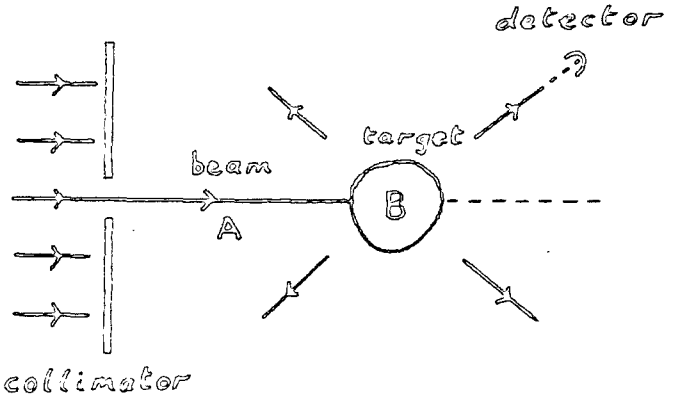

Figure 1.1
A simple collision experiment.

We define the cross section of a certain type of event in a given collision as the ratio of the number of events of this type per unit time and per unit scatterer to the relative flux of the incident particles with respect to the target. We shall illustrate this somewhat verbose definition by considering the total cross section.

Let us suppose that N_A particles A reach the target per unit time. We assume that these particles are parallel in direction (that is not straying from the beam) and are monoenergetic. We denote by $\mathcal{N}_A$ the mean number of particles A per unit volume in the incident beam, and by v their mean velocity with respect to the target. The flux of incident particles relative to the target, that is the number of particles A crossing per unit time a unit area perpendicular to the beam direction and at rest with respect to the target) we denote by Φ_A ; this is given by

$$\Phi = \mathcal{N}_A v = N_A / S \qquad (1.3.1)$$

where S is the area in cross section of the beam. We assume that the target is thin and denote by n_B the number of particles B within the "effective" target volume interacting with the target. If the target is a thin layer of thickness l then,

$$n_B = S l \mathcal{N}_B = S \hat{\mathcal{N}}_B \qquad (1.3.2)$$

where $\mathcal{N}_B$ is the number of particles B per unit volume of the target and $\hat{\mathcal{N}}_B$ is the surface density of the target particles. If N_{tot} is the total number of particles A which have interacted per unit time with the target scatterers,

then under the experimental conditions assumed, N_{tot} is proportional to the relative incident flux Φ_A and the number of target scatterers n_B . Thus

$$N_{tot} = \sigma_{tot} \Phi_A n_B \tag{1.3.3}$$

where the constant of proportionality (at a given collision energy) is called the total cross section for scattering of particle A by particle B. It should be stressed that the definition of equation (1.3.3) is only valid for a thin target. The total cross section σ_{tot} depends only upon the collision energy for a given quantum system being considered. It is a measure of the tendency of the particles A and B to interact at the energy being considered. The dimension of σ_{tot} is that of area; we may, indeed, consider σ_{tot} as an "effective area" which collects a certain amount of the incident beam, (see equation (1.3.3)).

The quantity σ_{tot} is the total cross section for all possible collision processes occurring when A and B collide. That is, it includes elastic scattering

$$A + B \longrightarrow A + B, \tag{1.3.4}$$

inelastic scattering,

$$A + B \longrightarrow A^* + B^*, \tag{1.3.5}$$

where * denotes that a possible charge in internal quantum state has occurred, and reactive scattering

$$A + B \longrightarrow C + D \tag{1.3.6}$$

$$A + B \longrightarrow C_1 + C_2 + \ldots\ldots + C_n \tag{1.3.7}$$

where two or more particles are produced which are different from A and B. The reactive processes (1.3.6) and (1.3.7) are called rearrangement collisions if they occur via the exchange of one or more elementary constituent particles. If a rearrangement collision produces only two particles, as in process (1.3.6), it is called a binary rearrangement collision. Electron capture processes are an example of binary rearrangement collisions, the elementary constituent particle or particles exchanged during the collision being one or more electrons. It is possible to consider total cross sections for particular processes occurring such as, say, elastic scattering. This has associated with it the <u>total elastic cross section</u> σ_{tot}^{el} which is defined in an analogous manner to σ_{tot} (see equation (1.3.3))

$$N_{tot}^{el} = \sigma_{tot}^{el} \Phi_A n_B \qquad (1.3.8)$$

where N_{tot}^{el} is the total number of particles A scattered elastically per unit time. If only elastic scattering occurs then $\sigma_{tot} = \sigma_{tot}^{el}$. However, if non-elastic processes occur too then we define the <u>total reaction cross section</u> σ_{tot}^{r} for all such processes by

$$\sigma_{tot}^{r} = \sigma_{tot} - \sigma_{tot}^{el}. \qquad (1.3.9)$$

It is important to note that the term "total" as applied to cross sections may have two different meanings. The formally correct use of the term is to distinguish between <u>total</u> cross sections and <u>differential</u> cross sections, the latter to be discussed shortly. We have used the formally correct terminology in this discussion. However, it is

very common in atomic collision physics for "total cross section" to mean the total cross section for scattering into all possible states being considered, whilst "cross section" means the total cross section for scattering into one or a small number of states. For instance the total cross section for capture into a particular nlm state of a hydrogenic ion would be called "cross section", the total cross section for capture into all nlm states would be called "total cross section".

The total cross sections discussed so far do not give any information about the angular distribution of the scattered particles. In order to deal with angular distributions, it is necessary to choose a co-ordinate frame. The two most common frames used are the laboratory (L) frame and the centres of mass (CM) frame, sometimes called the bary-centric frame. The laboratory frame is that where the target B is at rest; the centre of mass frame is that where the centre of mass of (A + B) is at rest. Working in the laboratory frame and considering elastic collisions, we denote by dN_{el} the number of particles A scattered per unit time into solid angle $d\Omega_L$ centred about the direction (θ_L, ϕ_L) shown in figure 1.2. Provided the target is thin

$$dN_{el} = \sigma_{el}(\theta_L, \phi_L)\, \bar{\Phi}_A\, n_B\, d\Omega_L. \qquad (1.3.10)$$

The quantity $\sigma_{el}(\theta_L, \phi_L)$ is the laboratory

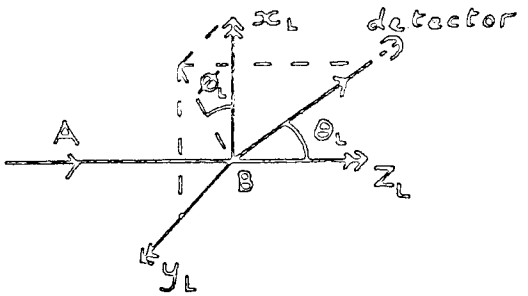

Figure 1.2
Scattering angles in the laboratory frame.

differential cross section for elastic scattering. It is also written

$$\sigma_{el}(\theta_L, \phi_L) = \frac{d\sigma_{el}(\theta_L, \phi_L)}{d\Omega_L}. \tag{1.3.11}$$

Similarly in the centre of mass frame

$$dN_{el} = \sigma_{el}(\theta_{CM}, \phi_{CM})\, \Phi_A\, n_B\, d\Omega_{CM} \tag{1.3.12}$$

where

$$\sigma_{el}(\theta_{CM}, \phi_{CM}) = \frac{d\sigma_{el}(\theta_{CM}, \phi_{CM})}{d\Omega_{CM}}. \tag{1.3.13}$$

Equations (1.3.10) and (1.3.12) show that

$$\frac{d\sigma_{el}(\theta_L, \phi_L)}{d\Omega_L} d\Omega_L = \frac{d\sigma_{el}(\theta_{CM}, \phi_{CM})}{d\Omega_{CM}} d\Omega_{CM} \tag{1.3.14}$$

and also the total elastic cross section is

$$\sigma_{el} = \int_{\Omega} \frac{d\sigma_{el}}{d\Omega_L}(\theta_L, \phi_L)\, d\Omega_L = \int_{\Omega} \frac{d\sigma_{el}}{d\Omega_{CM}}(\theta_{CM}, \phi_{CM})\, d\Omega_{CM} \tag{1.3.15}$$

which is independent of the co-ordinate frame. In a similar fashion, differential cross sections can be defined for non-elastic scattering.

1.4 Units

In the work of this thesis atomic units are used,

unless otherwise stated. This system of units is obtained by setting $e = m_e = \hbar = 1$, where $-e$ and m_e are the charge and rest-mass of the electron respectively. In this system the unit of length is the Bohr radius, a_0 (= 5.29×10^{-9}cm) which is the radius of the first Bohr orbit of the hydrogen atom. The Bohr radius is given by $a_0 = \hbar^2/m_e e^2$. Similarly the unit of velocity is the velocity of the electron in the first Bohr orbit of hydrogen $v_0 = e^2/\hbar$. The unit of energy is obtained by setting e, m_e and $\hbar$ to one in the expression for the ground state energy of the hydrogen atom which is $-m_e e^4/2\hbar^2$. In atomic units this is $-\frac{1}{2}$. Thus the atomic unit of energy is $m_e e^4/\hbar^2$, (27.2 eV in real units) which is twice the ionisation energy of the hydrogen atom, 13.6 e V. In atomic physics cross sections may be expressed in terms of a_0^2 (= 2.80×10^{-17} cm^2), though sometimes the units used are πa_0^2 (= 8.8×10^{-17} cm^2). However, the units often adopted are simply 10^{-16}cm^2 which are the units used in this thesis for cross sections.

Atomic units are not really suitable for measuring collision energies, though the collision velocity is usually in terms of atomic units. Ion-atom collision energies are usually measured in keV, either in the laboratory or centre of mass frames. If we denote the centre of mass energy by E_{CM} , and the laboratory energies for B being at rest and A being at rest by E_L^A and E_L^B respectively, that is E_L^A and E_L^B are the kinetic energies of A and B in the laboratory, then it is straightforward to show that

$$E_{CM} = \frac{M_B}{M_A+M_B} E_L^A = \frac{M_A}{M_A+M_B} E_L^B \qquad (1.4.1)$$

where M_A and M_B are the masses of A and B respectively. For an ion-atom collision, equations (1.4.1) apply if the mass of the electron is ignored. It should be noted that the laboratory energy is dependent upon whether A or B is at rest. In this work the convention is that B is at rest whilst A is moving. However, it is important to specify which of the colliding entities is the projectile or target when talking about laboratory energies, unless the meaning is clear. Hence the use of the phrases "the $^4He^{2+}$ laboratory energy" or "the $^4He^{2+}$ projectile energy" indicating that $^4He^{2+}$ is the projectile. It is also possible to divide the laboratory energy by the mass of the projectile and use this as the energy unit. For example, the $^4He^{2+}$ laboratory energy can be divided by 4(the mass of $^4He^{2+}$ in atomic mass units, amu) to give a laboratory energy in keV amu^{-1}. From equations (1.4.1) we see that $E_L^A/M_A = E_L^B/M_B$ which is proportional to the square of the relative velocity of A and B, and so there is no need to specify that A is the projectile. If the laboratory energy is, say, 125 keV amu^{-1} for A colliding with B, it is the same for B colliding with A. We note, finally, that one atomic unit of velocity corresponds to a laboratory energy of 24.97 keV amu^{-1}.

CHAPTER 2

EXISTING THEORY AND APPLICATIONS

2.1 Introduction

There are many excellent review articles and texts that deal either wholly or in part on the subject of electron capture in ion-atom collisions. For example, McDowell and Coleman (1970), Bransden (1972), Basu et al. (1978), Greenland (1982), McCarroll (1982) and Bransden (1983). This chapter is in no way intended to be an extensive review of the subject, but rather it is a discussion of some of the main aspects of the theory of electron capture relevant to the work presented in this thesis, with mention of some of the main applications of the theory.

We shall begin by discussing the full quantum mechanical treatment of the electron capture problem and then discuss the semi-classical impact parameter approximation which is extensively used in theoretical work on ion-atom collisions. We shall then examine the atomic expansion method and related expansions, for example, the pseudostate expansion, and also improvements to the basic atomic expansion method. Then we shall consider the molecular expansion method. Finally a brief discussion of electron capture at high energies will be given. It is possible to use techniques based upon classical mechanics to calculate electron capture cross sections. A discussion of the use of classical techniques is not given here, but the interested reader is referred to Section 6 of the review by Greenland (1982) for a discussion and references on this topic.

2.2 Quantum mechanical formulation

We begin by defining the single electron capture process

$$A + (B + e^-) \rightarrow (A + e^-) + B \qquad (2.2.1)$$

A and B may represent singly or multiply charged ionic cores. As through all this thesis, we adopt the convention that A is the projectile ion and B is the target ion. We require a co-ordinate system to describe the process and this is shown in figure 2.1.

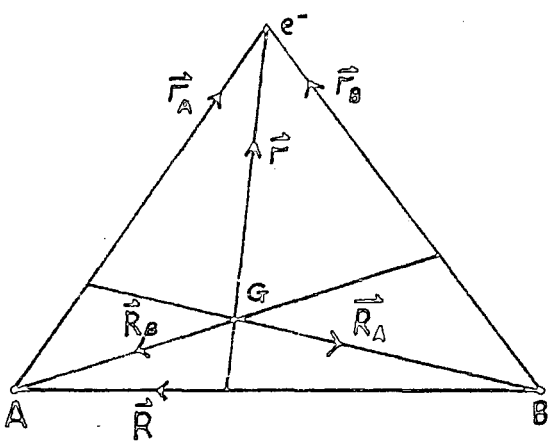

Figure 2.1
Electron capture centre of mass co-ordinates.

In Figure 2.1 $\vec{R}$ is the position vector of A with respect to B, $\vec{R}_A$ is the position vector of B with respect to the centre of mass of $(A + e^-)$, $\vec{R}_B$ is the position vector of A with respect to the centre of mass of $(B + e^-)$. Vectors $\vec{r}_A$ and $\vec{r}_B$ are the position vectors of the electron with respect to A and B respectively, and $\vec{r}$ is the position vector of the electron with respect to the centre of mass of A and B. We note, finally, that G is the centre of mass of the whole system $(A + B + e^-)$.

We denote by M_A and M_B the masses of A and B respectively, and by m_e the mass of the electron (here we denote electron mass by m_e even though $m_e = 1$ in atomic units). The total mass of the system, M is given by

$$M = M_A + M_B + m_e \,. \tag{2.2.2}$$

The kinetic energy, T_{CM} of the centre of mass of the system is given by

$$T_{CM} = \frac{P_{CM}^2}{2M} \tag{2.2.3}$$

where P_{CM} is the magnitude of the linear momentum of the centre of mass in the reference frame. When dealing with the theoretical analysis of a scattering problem, it is useful to separate the centre of mass motion from the problem (Farina, 1975) and work in the frame where the centre of mass is at rest. Hence P_{CM} and T_{CM} (from equation (2.2.3)) will both be zero. For the $(A+B+e^-)$ system we choose to work in the centre of mass frame, that is, point G in Figure 2.1 will be at rest.

In order to describe the dynamics of the system in the centre of mass frame one of three sets of independent centre of mass co-ordinates may be used, namely $(\vec{r}, \vec{R})$, $(\vec{r}_A, \vec{R}_A)$ or $(\vec{r}_B, \vec{R}_B)$. The centre of mass kinetic energy operator T may be written

$$T = \frac{P^2}{2\mu} + \frac{P^2}{2m} = \frac{P_A^2}{2\mu_A} + \frac{P_A^2}{2m_A} = \frac{P_B^2}{2\mu_B} + \frac{P_B^2}{2m_B} \tag{2.2.4}$$

where $\vec{P}$, $\vec{P}_A$ and $\vec{P}_B$ are momentum operators conjugate to

$\vec{R}$, $\vec{R}_A$ and $\vec{R}_B$ respectively, and $\vec{P}$, $\vec{P}_A$ and $\vec{P}_B$ are momentum operators conjugate to $\vec{r}$, $\vec{r}_A$ and $\vec{r}_B$ respectively. The various reduced masses in the expressions for T of equation (2.2.4) are given by

$$\mu = \frac{M_A M_B}{M_A + M_B} , \qquad \mu_A = \frac{M_B (M_A + m_e)}{M_A + M_B + m_e} ,$$

$$\mu_B = \frac{M_A (M_B + m_e)}{M_A + M_B + m_e} ; \qquad (2.2.5)$$

$$m = \frac{m_e (M_A + M_B)}{M_A + M_B + m_e} , \qquad m_A = \frac{m_e M_A}{M_A + m_e} ,$$

$$m_B = \frac{m_e M_B}{M_B + m_e} . \qquad (2.2.6)$$

When dealing with the general theory of collisions it is convenient to introduce the concept of arrangement channels (see, for example, Bransden (1983),Chapter 4). Working in the centre of mass frame, the total Hamiltonian of the system,H, is written

$$H = H_\alpha + V_\alpha , \qquad (2.2.7)$$

where the subscript α varies, and corresponds to a particular grouping of the particles into aggregates and single particles. H_α is the Hamiltonian of the system when the particles and aggregates are far apart and V_α is the interaction potential. Normally V_α tends to zero as time goes to plus or minus infinity. The various decompositions of H, labelled by subscript α , correspond to the arrangement

channels of the system. With each arrangement channel there is associated a set of channels. A channel corresponds to a particular state of the system before or after the collision.

When considering the $(A+B+e^-)$ system, the arrangement channels to be considered are the direct arrangement channel which corresponds to the centre A interacting with the $(B+e^-)$ system, and the rearrangement arrangement channel which corresponds to the centre B interacting with the $(A+e^-)$ system. For brevity it is usual to omit the word "arrangement" and talk of the direct and rearrangement channels. The process of excitation occurs in the direct channel whilst the electron capture occurs in the re-arrangement channel. We use the co-ordinates $(\vec{r}_B, \vec{R}_B)$ for describing scattering in the direct channel and the co-ordinates $(\vec{r}_A, \vec{R}_A)$ for describing scattering in the re-arrangement channel. The so-called adiabatic co-ordinates $(\vec{r}, \vec{R})$ are useful for dealing with the calculation of the molecular states of the system $(A+B+e^-)$.

The total Hamiltonian of the $(A+B+e^-)$ system is denoted by H. It is given by

$$H = T + V \qquad (2.2.8)$$

where the kinetic energy operator T was defined earlier in equation (2.2.4). The potential energy operator V is given by

$$V = V_{eA} + V_{eB} + V_{AB} \qquad (2.2.9)$$

where V_{eA} and V_{eB} are the potentials between the electron and A and B respectively and V_{AB} is the potential between A and B. For the case of electron capture where A and B are nuclei, these potentials are simple Coulomb ones. We now make the decomposition into direct and rearrangement channels and write the total Hamiltonian H as

$$H = H_d + V_d \qquad (2.2.10a)$$

or

$$H = H_r + V_r \qquad (2.2.10b)$$

where d and r refer to the direct and rearrangement channels respectively. We have that

$$H_d = T + V_{eB} \qquad (2.2.11a)$$

and

$$V_d = V_{eA} + V_{AB} \; ; \qquad (2.2.11b)$$

$$H_r = T + V_{eA} \qquad (2.2.12a)$$

and

$$V_r = V_{eB} + V_{AB} \; . \qquad (2.2.12b)$$

We denote by $\Phi_m^B(\vec{r}_B, \vec{R}_B)$ the asymptotic "free" state for the system being in the mth state in the direct channel. Thus

$$H_d \Phi_m^B = E_m \Phi_m^B \qquad (2.2.13)$$

where E_m are energy eigenvalues. Similarly we denote by $X_n^A(\vec{r}_A, \vec{R}_A)$ the asymptotic "free" state for the system being in the nth state in the rearrangement channel. Thus

$$H_r X_n^A = E_n X_n^A \; . \qquad (2.2.14)$$

The asymptotic state for the system being in the initial state i in the direct channel is $\Phi_i^B(\vec{r}_B, \vec{R}_B)$ and this is given by

$$\Phi_i^B(\vec{r}_B, \vec{R}_B) = \exp(i\vec{k}_i . \vec{R}_B)\, \phi_i^B(\vec{r}_B) \qquad (2.2.15)$$

where $\vec{k}_i$ is the initial wave vector of A relative to the centre of mass of $(B + e^-)$. The $\phi_i^B(\vec{r}_B)$ is the initial state eigenfunction of the $(B + e^-)$ system and we have

$$\left(-\frac{1}{2m_B}\nabla^2_{\vec{r}_B} + V_{eB}\right)\phi_i^B(\vec{r}_B) = \varepsilon_i\, \phi_i^B(\vec{r}_B) \qquad (2.2.16)$$

where ε_i is the energy eigenvalue of the initial state of $(B + e^-)$. We may relate the total energy E_i and ε_i by

$$E_i = \frac{k_i^2}{2\mu_B} + \varepsilon_i . \qquad (2.2.17)$$

The m_B and μ_B in equations (2.2.16) and (2.2.17) respectively are the reduced masses of B and e^-, and A and $(B + e^-)$ respectively. They are given by the expressions of equations (2.2.5) and (2.2.6).

We consider first scattering in the direct channel, that is excitation processes. We denote the final asymptotic "free" state in the direct channel by $\Phi_f^B(\vec{r}_B, \vec{R}_B)$. This is given by

$$\Phi_f^B(\vec{r}_B, \vec{R}_B) = \exp(i\vec{k}_f . \vec{R}_B)\, \phi_f^B(\vec{r}_B) \qquad (2.2.18)$$

where $\vec{k}_f$ is the final wave vector of A relative to the centre of mass of $(B + e^-)$. The function $\phi_f^B(\vec{r}_B)$ satisfies the equation

$$\left(-\frac{1}{2m_B}\nabla^2_{\vec{r}_B} + V_{eB}\right)\phi_f^B(\vec{r}_B) = \varepsilon_f\, \phi_f^B(\vec{r}_B). \qquad (2.2.19)$$

It is also true that

$$E_f = \frac{k_f^2}{2\mu_B} + \mathcal{E}_f . \qquad (2.2.20)$$

It turns out that for direct scattering the probability of scattering from an initial state $|\Phi_i^B\rangle$ to a final state $|\Phi_f^B\rangle$ is zero unless we work "on the energy shell" namely, we have

$$E_i = E_f = E . \qquad (2.2.21)$$

The scattering amplitude for the direct process $i \rightarrow f$ is given by (McDowell and Coleman, 1970)

$$f_{fi}^d(\hat{k}_i, \hat{k}_f) = -\frac{\mu_B}{2\pi} T_{fi}^d \qquad (2.2.22)$$

where T_{fi}^d is the transition (T-) matrix element for scattering in the direct channel between states labelled by i and f. The T-matrix element T_{fi}^d is given by

$$T_{fi}^d = \langle \Phi_f^B | V_d | \Psi_i^{(+)} \rangle . \qquad (2.2.23)$$

The $\Psi_i^{(+)}$ is the scattering wavefunction corresponding to the initial state i. It satisfies the Schrödinger equation

$$H\Psi_i^{(+)} = E\Psi_i^{(+)} . \qquad (2.2.24)$$

The (+) denotes that the wavefunction is the solution of the Schrödinger equation corresponding to outgoing scattered spherical waves. The differential scattering cross section in the direct channel is given by

$$\frac{d\sigma_{fi}^d}{d\Omega} = \frac{k_f}{k_i} \left| f_{fi}^d(\hat{k}_i, \hat{k}_f) \right|^2 , \qquad (2.2.25)$$

$$= \frac{\mu_B^2}{4\pi^2} \cdot \frac{k_f}{k_i} \left| T_{fi}^{d} \right|^2 . \qquad (2.2.26)$$

For rearrangement scattering, which corresponds to electron capture, we denote the final asymptotic state by $\chi_f^A(\vec{r}_A, \vec{R}_A)$. This is given by

$$\chi_f^A(\vec{r}_A, \vec{R}_A) = \exp(-i\vec{k}_f . \vec{R}_A)\, \chi_f^A(\vec{r}_A) \qquad (2.2.27)$$

where $\vec{k}_f$ is now the final wave vector of the centre of mass of $(A + e^-)$ relative to B. The function $\chi_f^A(\vec{r}_A)$ is the final state eigenfunction of the $(A + e^-)$ system and satisfies

$$\left(-\frac{1}{2m_A} \nabla_{\vec{r}_A}^2 + V_{eA} \right) \chi_f^A(\vec{r}_A) = \eta_f \chi_f^A(\vec{r}_A), \qquad (2.2.28)$$

where η_f is the final state energy eigenvalue of the $(A + e^-)$ system. The total energy corresponding to the final state f is E_f and we have

$$E_f = \frac{k_f^2}{2\mu_A} + \eta_f . \qquad (2.2.29)$$

The m_A and μ_A in equations (2.2.28) and (2.2.29) respectively are the reduced masses of A and e^-, and B and $(A+e^-)$ respectively (equations (2.2.5) and (2.2.6)). As for direct scattering, we must work on the energy shell in rearrangement scattering. Setting the total energy to be E, we have

$$E_i = E_f = E . \qquad (2.2.30)$$

The scattering amplitude for the rearrangement process $i \Rightarrow f$ is given by (McDowell and Coleman, 1970)

$$f^{r}_{fi}(\hat{k}_i, \hat{k}_f) = -\frac{\mu_A}{2\pi} T^{r}_{fi} \qquad (2.2.31)$$

where T^{r}_{fi} is the T-matrix element for the rearrangement process $i \rightarrow f$ given by

$$T^{r}_{fi} = \langle X^{A}_{f} | V_r | \Psi^{(+)}_{i} \rangle . \qquad (2.2.32)$$

The differential scattering cross section is given by

$$\frac{d\sigma^{r}_{fi}}{d\Omega} = \frac{\mu_B}{\mu_A} \cdot \frac{k_f}{k_i} \left| f^{r}_{fi}(\hat{k}_i, \hat{k}_f) \right|^2 \qquad (2.2.33)$$

$$= \frac{\mu_A \mu_B}{4\pi^2} \cdot \frac{k_f}{k_i} \left| T^{r}_{fi} \right|^2 . \qquad (2.2.34)$$

The total scattering cross sections for direct and rearrangement scattering are given respectively by

$$\sigma^{d}_{fi} = \int_{\Omega} \frac{d\sigma^{d}_{fi}}{d\Omega} . d\Omega \qquad (2.2.35)$$

$$\sigma^{r}_{fi} = \int_{\Omega} \frac{d\sigma^{r}_{fi}}{d\Omega} . d\Omega . \qquad (2.2.36)$$

The asymptotic boundary conditions upon the scattering wavefunction $\Psi^{(+)}_{i}$ corresponding to outgoing spherical scattered waves are given by

$$\Psi^{(+)}_{i} \underset{R_B \to \infty}{\sim} \sum_{m} \left[\delta_{mi} \exp(i\vec{k}_i . \vec{R}_B) + f^{d}_{mi} \exp \frac{ik_m R_B}{R_B} \right] \varphi^{B}_{m}(\vec{r}_B) \qquad (2.2.37)$$

$$\underset{R_A \to \infty}{\sim} \sum_{n} f^{r}_{ni} \exp \frac{ik_n R_A}{R_A} \chi^{A}_{n}(\vec{r}_A) . \qquad (2.2.38)$$

Equation (2.2.37) corresponds to the direct (excitation) channel. The first term in the square brackets represents the incident plane-wave of momentum $\vec{k}_i$ ($\hbar = 1$). The second term represents the outgoing spherical waves describing the scattered particle A leaving the $(B + e^-)$ system in the mth level represented by the eigenfunction

$\phi_m^B(\vec{r}_B)$. Equation (2.2.38) corresponds to the rearrangement (electron capture) channel. There is no incident plane-wave and so the full expression represents particle B leaving the $(A + e^-)$ system in the nth level represented by the eigenfunction $\chi_n^A(\vec{r}_A)$.

At very low energies the scattering wavefunction may be expanded on a basis of atomic or molecular orbital wavefunctions and a partial wave decomposition can be made. The problem becomes one of solving a set of coupled second-order differential equations. Alternatively, at high energies provided the $\Psi_i^{(+)}$ is only weakly perturbed by the collision, the wavefunction $\Psi_i^{(+)}$ may be represented approximately using the Born or distorted wave approximations. These methods are discussed in the review by Basu et al. (1978). When the collision energy is neither in the low energy nor high energy regions, approaches based on the full quantal treatment become impractical. However, the typical ion-atom collision system has a feature that enables a semi-classical approximation to be used in the system's description. This feature is that the masses of the centres A and B are very much greater than the mass of the electron being either excited or captured in the collision, and hence the motion of the centres may be treated classically owing to the associated de Broglie wavelength being very small as compared with atomic dimensions. The result of this is the semi-classical impact parameter approximation which will be discussed in more detail in the next section.

2.3 The impact parameter approximation

2.3.1 The impact parameter Schrödinger equation

In the previous section the quantum mechanical treatment of ion-atom collisions was discussed. We noted, though, that in practice it was not practical to employ the quantal treatment, but due to the much larger masses of the centres A and B as compared with the electron, it was possible to describe the motion of A and B classically as the de Broglie wavelength for the motion of A and B will be very much smaller than typical atomic dimensions. Quantitatively this means that the collision energy E will be such that

$$E \gtrsim eV\ amu^{-1}. \qquad (2.3.1)$$

In addition, if the collision energy E is much greater than the typical change in electronic energy during a collision ($\sim$ 10 eV for a slow collision), then the nuclear motion may be assumed as being independent of the electronic motion. Typically independence of nuclear and electronic motion is present if

$$E \gtrsim 100\ eV\ amu^{-1}. \qquad (2.3.2)$$

If the collision energy, E satisfies equation (2.3.2) then the impact parameter approximation is usually valid.

When the impact parameter approximation is applied to a collision problem, a trajectory equation is written down to describe the classical motion of the massive centres A and B. Figure 2.2 shows the co-ordinate system employed

when the impact parameter approximation is used and the motion of A and B is such that they move along straight-line paths. (From now on we shall describe the motion of A and B as "nuclear motion").

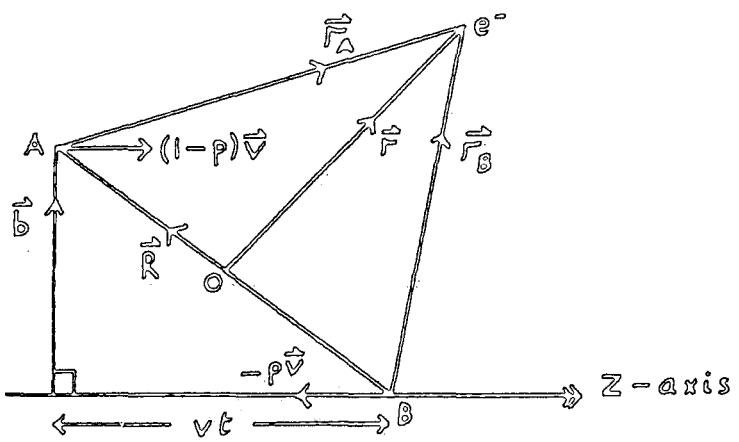

Figure 2.2
Impact parameter co-ordinate system (straight-line nuclear trajectories).

In figure 2.2 the parameter ρ determines where the position of the origin O is on the internuclear line AB. ρ is such that

$$0 \leq \rho \leq 1 \quad . \tag{2.3.3}$$

We note that

$$\left.\begin{aligned} \vec{BO} &= \rho\vec{R} \\ \vec{OA} &= (1-\rho)\vec{R} \end{aligned}\right\} . \tag{2.3.4}$$

The quantity $\vec{b}$ is the two-dimensional impact parameter vector. We use $\vec{r}$ to denote the electronic co-ordinate but unlike in the previous section $\vec{r}$ may have its origin at any point on AB. In general the nuclear motion is determined by some effective internuclear potential $U(\vec{R})$, and the internuclear co-ordinate $\vec{R}$ will be a function of time t for a given impact parameter $\vec{b}$. Thus

the trajectory equation takes the general form

$$\vec{R} = \vec{R}(\vec{b}, t). \qquad (2.3.5)$$

The electronic motion is described quantum mechanically and the associated time dependent (impact parameter) Schrödinger equation will now be derived.

The total Hamiltonian of the $(A+B+e^-)$ system is given by

$$H = T + V \qquad (2.3.6)$$

$$= -\frac{1}{2\mu}\nabla_{\vec{R}}^2 - \frac{1}{2m}\nabla_{\vec{r}}^2 + V_{eA} + V_{eB} + V_{AB}. \qquad (2.3.7)$$

from equations (2.2.4), (2.2.8) and (2.2.9). The reduced mass of A and B is μ, and the reduced mass of the electron and the (A + B) system is m (equations (2.2.5) and (2.2.6)). As the mass of the electron is very small compared to the masses of A and B, we may put $m \approx m_e = 1$ in atomic units. The Schrödinger equation for the system is thus given by

$$\left(-\frac{1}{2\mu}\nabla_{\vec{R}}^2 + U(\vec{R}) + H_{el} - E\right)\Phi(\vec{R}, \vec{r}) = 0 \qquad (2.3.8)$$

where the electronic Hamiltonian, H_{el} is given by

$$H_{el} = -\frac{1}{2}\nabla_{\vec{r}}^2 + V_{eA} + V_{eB} + (V_{AB} - U), \qquad (2.3.9)$$

and $\Phi(\vec{R},\vec{r})$ is the wavefunction of the system. The nuclear motion is described by a wavefunction $F(\vec{R})$ which satisfies the potential scattering equation

$$\left(-\frac{1}{2\mu}\nabla_{\vec{R}}^2 + U(\vec{R}) - E\right)F(\vec{R}). \qquad (2.3.10)$$

It is usually a good approximation to ignore the binding energy in the initial state $\mathcal{E}_i$ and so the energy E is given by

$$E = \frac{k_i^2}{2\mu} + \mathcal{E}_i$$
$$\approx \frac{k_i^2}{2\mu} = \frac{1}{2}\mu v^2 \qquad (2.3.11)$$

where v is the relative velocity of the centres A and B; (k_i is the wavenumber associated with the motion of A and B).

We write the wavefunction of the system $\Phi(\vec{R},\vec{r})$ as the product of the nuclear wavefunction $F(\vec{R})$ and a wavefunction for the electronic motion $\Psi(\vec{R},\vec{r})$

$$\Phi(\vec{R},\vec{r}) = F(\vec{R})\Psi(\vec{R},\vec{r}). \qquad (2.3.12)$$

Substituting for $\Phi(\vec{R},\vec{r})$ in equation (2.3.8) we obtain

$$-\frac{1}{2\mu}F(\vec{R})\nabla_{\vec{R}}^2\Psi(\vec{R},\vec{r}) - \frac{1}{\mu}\vec{\nabla}_{\vec{R}}F(\vec{R}).\vec{\nabla}_{\vec{R}}\Psi(\vec{R},\vec{r})$$
$$+ F(\vec{R})H_{el}\Psi(\vec{R},\vec{r}) = 0. \qquad (2.3.13)$$

We now write the nuclear wavefunction as

$$F(\vec{R}) = \exp iS(\vec{R}) \qquad (2.3.14)$$

where

$$S(\vec{R}) \approx \int ds\left[2\mu\{E - U(\vec{R})\}\right]^{1/2} \qquad (2.3.15)$$

which is consistent with nuclear motion being described

classically by the trajectory equation (2.3.5), and where the integration in equation (2.3.15) is along this trajectory. The approximation defined by equations (2.3.14) and (2.3.15) for the wavefunction $F(\vec{R})$ is the basic starting point of the semi-classical eikonal approximation (Bransden, 1983) and $F(\vec{R})$ as given by (2.3.14) is termed the eikonal wavefunction. At high energies the scattering is mainly into a forward cone of small angular width and the motion of the centres A and B can be approximated by a straight-line trajectory equation, namely

$$\vec{R} = \vec{b} + \vec{v}t \; ; \quad \vec{b}.\vec{v} = 0 . \tag{2.3.16}$$

The velocity vector is parallel to the z-axis (Figure 2.2). The straight-line trajectory case is consistent with the effective internuclear potential, $U(\vec{R})$ being ignored. This results in the wavefunction $F(\vec{R})$ being a plane-wave, that is

$$F(\vec{R}) \approx \exp i k_i Z_R$$

$$= \exp i\mu v Z_R \tag{2.3.17}$$

where Z_R is the z-component of $\vec{R}$. If equation (2.3.17) is used to substitute for $F(\vec{R})$ in equation (2.3.13), then the first term is found to be very much smaller than the second due to μ being a large parameter. The first term is neglected and equation (2.3.13) becomes

$$H_{el}\Psi(\vec{R},\vec{r}) = iv\frac{\partial}{\partial Z_R}\Psi(\vec{R},\vec{r}). \tag{2.3.18}$$

For the straight-line trajectory case $Z_R = vt$ and so we obtain a time dependent Schrödinger equation, also called the impact parameter Schrödinger equation

$$H_{el}\Psi(\vec{r},t) = i\left.\frac{\partial}{\partial t}\right]_{\vec{r}}\Psi(\vec{r},t) \qquad (2.3.19)$$

where the notation $\partial/\partial t]_{\vec{r}}$ means differentiate with respect to time keeping $\vec{r}$ fixed. It should be noted that if non-linear trajectories are considered, equation (2.3.19) is obtained in the same way by dropping the first term of equation (2.3.13). Now, though, the trajectory is given by equation (2.3.5) as determined by the particular $U(\vec{R})$ being used.

2.3.2 Boundary conditions

Before proceeding to consider how the impact parameter Schrödinger equation (2.3.19) can be solved, we must consider the boundary conditions of the problem. The unperturbed solutions of equation (2.3.19) are expressed in terms of the orthonomal sets of eigenfunctions $\phi_j^B(\vec{r}_B)$ and $\chi_k^A(\vec{r}_A)$ of the $(B + e^-)$ and $(A + e^-)$ systems respectively. These are solutions of the equations

$$\left(-\tfrac{1}{2}\nabla_{\vec{r}_B}^2 + V_{eB}\right)\phi_j^B(\vec{r}_B) = \varepsilon_j\,\phi_j^B(\vec{r}_B) \qquad (2.3.20)$$

and

$$\left(-\tfrac{1}{2}\nabla_{\vec{r}_A}^2 + V_{eA}\right)\chi_k^A(\vec{r}_A) = \eta_k\,\chi_k^A(\vec{r}_A) \qquad (2.3.21)$$

where ε_j and η_k are the energy eigenvalues of the systems. $\phi_j^B(\vec{r}_B)$ and $\chi_k^A(\vec{r}_A)$ are quantised with respect to the space-fixed z-axis. The unperturbed solutions of equation

(2.3.19) are denoted by $\Phi_j^0(\vec{r},t)$ and $X_k^A(\vec{r},t)$. The functions $\Phi_j^B(\vec{r},t)$ are given by

$$\Phi_j^B(\vec{r},t) = \phi_j^B(\vec{r}_B)\exp -i\left[\varepsilon_j t + \tfrac{1}{2}\rho^2 v^2 t + \rho\vec{v}.\vec{r}\right] \qquad (2.3.22)$$

and satisfy equation (2.3.19) in the asymptotic limit $t \Longrightarrow \pm\infty$ and $r_B \ll r_A$. We remember that the parameter ρ determines the position of the origin (equations (2.3.3) and (2.3.4)). Similarly the functions $X_k^A(\vec{r},t)$ are given by

$$X_k^A(\vec{r},t) = X_k^A(\vec{r}_A)\exp -i\left[\eta_k t + \tfrac{1}{2}(1-\rho)^2 v^2 t - (1-\rho)\vec{v}.\vec{r}\right] \qquad (2.3.23)$$

and these satisfy equation (2.3.19) in the asymptotic limit $t \rightarrow \pm\infty$ and $r_A \ll r_B$. We note the presence of the factors $\exp -i\left(\frac{1}{2}\rho^2 v^2 t + \rho\vec{v}.\vec{r}\right)$ and $\exp -i\left[\frac{1}{2}(1-\rho)^2 v^2 t - (1-\rho)\vec{v}.\vec{r}\right]$. These are necessary if the functions $\Phi_j^B(\vec{r},t)$ and $X_k^A(\vec{r},t)$ are to satisfy equation (2.3.19) in asymptopia. If the system is originally in the i th state of $(B + e^-)$, then the corresponding boundary condition is

$$\Psi(\vec{r},t) \underset{t\rightarrow-\infty}{\longrightarrow} \Phi_i^B(\vec{r},t). \qquad (2.3.24)$$

The probability amplitude for finding the system in the jth state of $(B + e^-)$ after the collision is given by

$$a_{ji}(\vec{b}) = \lim_{t\rightarrow+\infty}\int_V \Phi_j^{B*}(\vec{r},t)\,\Psi(\vec{r},t)\,d\vec{r} \qquad (2.3.25)$$

and the probability amplitude for finding the system in the k th state of $(A + e^-)$ after the collision is given by

$$c_{ki}(\vec{b}) = \lim_{t\rightarrow+\infty}\int_V X_k^{A*}(\vec{r},t)\,\Psi(\vec{r},t)\,d\vec{r}. \qquad (2.3.26)$$

The total cross sections for excitation σ_{ji}^d or electron

capture σ_{ki}^{r} are obtained by integrating $|a_{ji}(\vec{b})|^2$ or $|c_{ki}(\vec{b})|^2$ $(i \neq j)$ respectively over all two-dimensional impact parameter space, that is

$$\sigma_{ji}^{d} = \int |a_{ji}(\vec{b})|^2 \, d\vec{b} \tag{2.3.27}$$

$$= 2\pi \int_0^\infty |a_{ji}(b)|^2 \, b \, db \,, \quad i \neq j \tag{2.3.28}$$

and

$$\sigma_{ki}^{r} = \int |c_{ki}(\vec{b})|^2 \, d\vec{b} \tag{2.3.29}$$

$$= 2\pi \int_0^\infty |c_{ki}(b)| \, b \, db \tag{2.3.30}$$

where the integral over $d\vec{b}$ has been simplified due to azimuthal symmetry.

2.3.3. Solving the impact parameter Schrödinger equation

An approximate solution of equation (2.3.19) can be performed using a variational principle.

We define the functional $I(\Psi)$ where

$$I(\Psi) = \int_{-\infty}^{\infty} dt \int_V d\vec{r} \, \Psi^*(\vec{r},t) \left\{ H_{el} - i \frac{\partial}{\partial t} \right]_{\vec{r}} \Psi(\vec{r},t) \,. \tag{2.3.31}$$

We then vary Ψ and Ψ^* to first order by means of

$$\left.\begin{aligned} \Psi &\longrightarrow \Psi + \delta\Psi \\ \text{and} \quad \Psi^* &\longrightarrow \Psi^* + \delta\Psi^* \end{aligned}\right\} \tag{2.3.32}$$

but with the constraint that the boundary conditions are preserved. This requires $\delta\Psi(\vec{r},t) \to 0$ and $\delta\Psi^*(\vec{r},t) \to 0$ as $t \longrightarrow \pm\infty$. It can be shown that $\delta I = 0$ up to terms of the second order provided Ψ satisfies the Schrödinger equation (2.3.19).

We define a trial function $\Psi_T(\vec{r},t)$ in terms of two sets of linearly independent functions, $F_j(\vec{r},t)$ and

$G_k(\vec{r},t)$. These functions may be orthonormal for all t among themselves and indeed we choose them to be such, namely

$$\int_V F_{j'}^{*}(\vec{r},t)F_j(\vec{r},t)d\vec{r} = \delta_{j'j} \tag{2.3.33}$$

and

$$\int_V G_{k'}^{*}(\vec{r},t)G_k(\vec{r},t)d\vec{r} = \delta_{k'k} . \tag{2.3.34}$$

In order to satisfy the boundary conditions the F_j and G_k must tend to the unperturbed solutions of equation (2.3.19) as $t \to \pm\infty$, that is

$$F_j(\vec{r},t) \longrightarrow \Phi_j^{B}(\vec{r},t), \quad t \to \pm\infty \tag{2.3.35a}$$

$$G_k(\vec{r},t) \longrightarrow X_k^{A}(\vec{r},t), \quad t \to \pm\infty . \tag{2.3.35b}$$

The trial function $\Psi_\tau(\vec{r},t)$ we expand as

$$\Psi_\tau(\vec{r},t) = \sum_{j=1}^{M} a_j(t)F_j(\vec{r},t) + \sum_{k=1}^{N} c_k(t)G_k(\vec{r},t) . \tag{2.3.36}$$

In fact we could display explicitly a dependence upon the impact parameter $\vec{b}$ for the expansion coefficients a_j and c_k as well as for the functions F_j and G_k . For brevity, however, we omit this.

We obtain the coupled first-order differential equations a_j and c_k by requiring that

$$\int_V d\vec{r}\, F_j^{*}(\vec{r},t)\left\{H_{el} - i\left[\frac{\partial}{\partial t}\right]_{\vec{r}}\right\}\Psi_\tau(\vec{r},t) = 0, \quad j = 1,2,\ldots M \tag{2.3.37}$$

$$\int_V d\vec{r}\, G_k^{*}(\vec{r},t)\left\{H_{el} - i\left[\frac{\partial}{\partial t}\right]_{\vec{r}}\right\}\Psi_\tau(\vec{r},t) = 0, \quad k = 1,2,\ldots N \tag{2.3.38}$$

which are consistent with the variational principle discussed earlier. The differential equations are (in matrix form)

$$i\left[\dot{\underline{a}}(t) + \underline{N}\,\dot{\underline{c}}(t)\right] = \underline{H}\,\underline{a}(t) + \underline{K}\,\underline{c}(t) \tag{2.3.39a}$$

$$i\left[\underline{N}^{\dagger}\dot{\underline{a}}(t) + \dot{\underline{c}}(t)\right] = \overline{\underline{K}}\,\underline{a}(t) + \overline{\underline{H}}\,\underline{c}(t) \tag{2.3.39b}$$

where $\dagger$ denotes Hermition adjoint. We see that these can be written in a more compact form, namely

$$i \underset{\sim}{S} \dot{\underset{\sim}{A}}(t) = \underset{\sim}{M} \underset{\sim}{A}(t) \tag{2.3.40}$$

where

$$\underset{\sim}{S} = \begin{pmatrix} \underset{\sim}{I} & \underset{\sim}{N} \\ \underset{\sim}{N}^{\dagger} & \underset{\sim}{I} \end{pmatrix} , \quad \underset{\sim}{M} = \begin{pmatrix} \underset{\sim}{H} & \underset{\sim}{K} \\ -\underset{\sim}{K}^{*} & -\underset{\sim}{H}^{*} \end{pmatrix} \tag{2.3.41}$$

and

$$\underset{\sim}{A}(t) = \begin{pmatrix} \underset{\sim}{a}(t) \\ \underset{\sim}{c}(t) \end{pmatrix} . \tag{2.3.42}$$

The boundary conditions subject to which equations (2.3.39a) and (2.3.39b) must be solved are

$$a_j(-\infty) = \delta_{ji} , \quad c_k(-\infty) = 0 \tag{2.3.43}$$

where index i corresponds to the initial state of the $(B + e^{-})$ system. As $t \rightarrow +\infty$ the coefficients tend to the probability amplitudes for excitation and capture defined by equations (2.3.25) and (2.3.26)

$$a_{ji}(\vec{b}) = \lim_{t \rightarrow +\infty} a_j(t) \tag{2.3.44a}$$

$$c_{ki}(\vec{b}) = \lim_{t \rightarrow +\infty} c_k(t) . \tag{2.3.44b}$$

The elements of the matrices in equations (2.3.39a) and (2.3.39b) are given by

$$N_{jk}(t) = \int_v F_j^{*}(\vec{r}, t) G_k(\vec{r}, t) \, d\vec{r} \tag{2.3.45}$$

$$H_{jk}(t) = \int_v F_j^{*}(\vec{r}, t) \left\{ H_{el} - i \frac{\partial}{\partial t} \right]_{\vec{r}} \Bigg\} F_k(\vec{r}, t) \, d\vec{r} \tag{2.3.46}$$

$$\bar{H}_{jk}(t) = \int_v G_j^{*}(\vec{r}, t) \left\{ H_{el} - i \frac{\partial}{\partial t} \right]_{\vec{r}} \Bigg\} G_k(\vec{r}, t) \, d\vec{r} \tag{2.3.47}$$

$$K_{jk}(t) = \int_v F_j^{*}(\vec{r}, t) \left\{ H_{el} - i \frac{\partial}{\partial t} \right]_{\vec{r}} \Bigg\} G_k(\vec{r}, t) \, d\vec{r} \tag{2.3.48}$$

$$\bar{K}_{jk}(t) = \int_v G_j^{*}(\vec{r}, t) \left\{ H_{el} - i \frac{\partial}{\partial t} \right]_{\vec{r}} \Bigg\} F_k(\vec{r}, t) \, d\vec{r} . \tag{2.3.49}$$

The $\underset{\sim}{N}$ matrix is known as the overlap matrix. The $\underset{\sim}{H}$ and $\underset{\sim}{\bar{H}}$ matrices are known as the direct matrices. The $\underset{\sim}{K}$ and $\underset{\sim}{\bar{K}}$ matrices are known as the exchange matrices.

Green (1965) has shown that the Hamiltonian H_{el} being Hermitian implies that the Ψ_T trial solutions ensure that there is conservation of probability (unitarity), that is

$$\frac{d}{dt}\langle \Psi_T | \Psi_T \rangle = 0 . \tag{2.3.50}$$

From this it can be shown that

$$i\dot{\underset{\sim}{S}} = \underset{\sim}{M}^{\dagger} - \underset{\sim}{M} . \tag{2.3.51}$$

Equation (2.3.51) yields a related expression

$$i\dot{\underset{\sim}{N}} = \underset{\sim}{\bar{K}}^{\dagger} - \underset{\sim}{K} \tag{2.3.52a}$$

and also $$\underset{\sim}{H} = \underset{\sim}{H}^{\dagger}, \quad \underset{\sim}{\bar{H}} = \underset{\sim}{\bar{H}}^{\dagger} . \tag{2.3.52b}$$

A further result of probability conservation is Green's unitarity relation (Green, 1965).

$$\underset{\sim}{A}^{\dagger}\underset{\sim}{S}\underset{\sim}{A} = 1 . \tag{2.3.53}$$

Probability conservation is also expressed by the expression

$$\sum_{j=1}^{M} |a_j(+\infty)|^2 + \sum_{k=1}^{N} |c_k(+\infty)|^2 = 1 . \tag{2.3.54}$$

The expressions of equations (2.3.51) to (2.3.54) are useful in actual calculations as a check upon the numerical procedures being used. The excitation and electron capture cross sections σ_{ji}^{d} and σ_{ki}^{r} are given by

$$\sigma_{ji}^{d} = 2\pi \int_0^{\infty} |a_j(+\infty)|^2 \, b \, db, \quad i \neq j \tag{2.3.55}$$

and

$$\sigma_{ki}^{r} = 2\pi \int_{0}^{\infty} |C_k(+\infty)|^2 \, b \, db \, . \qquad (2.3.56)$$

2.3.4 Differential cross sections

It is possible to derive expressions for differential cross sections within the impact parameter approximation. For excitation it can be seen intuitively that the differential cross section is given by

$$\frac{d\sigma_{ji}^{d}}{d\Omega} = \frac{d\sigma^{c}(\theta)}{d\Omega} \, |a_j(b,+\infty)|^2 \qquad (2.3.57)$$

where $d\sigma^{c}(\theta)/d\Omega$ is the classical differential cross section for scattering by the potential U, θ is the scattering angle and the impact parameter b is a function of angle θ, that is, $b = b(\theta)$. The classical differential cross section is given by

$$\frac{d\sigma^{c}(\theta)}{d\Omega} = 2\pi \frac{b(\theta)}{\sin\theta} \cdot \frac{db}{d\theta} \, . \qquad (2.3.58)$$

Similarly for electron capture the differential cross section is given by

$$\frac{d\sigma_{ki}^{r}}{d\Omega} = \frac{d\sigma^{c}(\theta)}{d\Omega} \, |C_k(b,+\infty)|^2 \, . \qquad (2.3.59)$$

However, the expressions of equations (2.3.57) and 2.3.59) are only approximately true. It is possible to derive a more accurate expression for the differential cross section beginning with the quantal expression for the scattering amplitude. This expression applies even if the effective internuclear potential $U(\vec{R})$ is zero, and the nuclear trajectories are linear. We consider excitation scattering - the expression for electron capture scattering is derived in an analogous manner.

The scattering amplitude is given by

$$f^{d}_{ji}(\theta) = -\frac{\mu}{2\pi} T^{d}_{ji} \qquad (2.3.60)$$

where T^{d}_{ji} is the T-matrix element for excitation of the j th state of $(B + e^{-})$ from the initial state i, μ is the reduced mass of A and B. Strictly μ should be μ_B (equation (2.2.22)) but we know $\mu \approx \mu_B$ as the mass of the electron is much smaller than the masses of A and B. The T-matrix element is given by (after equation (2.2.23))

$$T^{d}_{ji} = \langle \Phi^{B}_{j}(\vec{r}_B, \vec{R}_B) | V_d | \Psi^{(+)}_{i} \rangle \qquad (2.3.61)$$

where the $\Phi^{B}_{j}(\vec{r}_B, \vec{R}_B)$ is the final asymptotic state (the arguments have been included to avoid confusion of notation) and the $\Psi^{(+)}_{i}$ is the scattering wavefunction corresponding to the initial state. The potential V_d is given by

$$V_d = V_{eA} + V_{AB} . \qquad (2.3.62)$$

In the full quantal treatment the $\Phi^{B}_{j}(\vec{r}_B, \vec{R}_B)$ would be given by equation (2.2.15). Similarly the $\Psi^{(+)}_{i}$ would be represented by some appropriate wave mechanical expression. However, we now bring in the semi-classical approximation used to derive the impact parameter equation and approximate the scattering wavefunction $\Psi^{(+)}_{i}$ and the asymptotic wavefunction $\Phi^{B}_{j}(\vec{r}_B, \vec{R}_B)$ by eikonal wavefunctions corresponding to linear trajectories; that is

$$\Phi^{B}_{j}(\vec{r}_B, \vec{R}_B) \approx \exp i\mu \vec{v}_f . \vec{R} \; . \; \Phi^{B}_{j}(\vec{R}, \vec{r}) \qquad (2.3.63)$$

where $\vec{v}_f$ is the final relative velocity after the collision, and $|\vec{v}_f| = |\vec{v}|$. The wavefunction $\Phi^{B}_{j}(\vec{R}, \vec{r})$ is

equivalent to $\Phi_j^B(\vec{r},t)$ given by equation (2.3.22) which is the solution of the impact parameter Schrödinger equation (2.3.19) in asymptopia. Similarly the scattering wavefunction $\Psi_i^{(+)}$ is given by

$$\Psi_i^{(+)} \approx \exp i\mu\vec{v}.\vec{R} \; . \; \Psi(\vec{R},\vec{r}) \qquad (2.3.64)$$

where $\Psi(\vec{R},\vec{r})$ is equivalent to the solution of the impact parameter Schrödinger equation $\Psi(\vec{r},t)$. Combining these results we have that the scattering amplitude is given by

$$f_{ji}^{d}(\theta) = -\frac{\mu}{2\pi i}\int d\vec{R}\int d\vec{r}\, e^{-i\mu\vec{v}_f.\vec{R}}\, \Phi_j^{B*}(\vec{R},\vec{r})(V_{eA}+V_{AB}) \times e^{i\mu\vec{v}.\vec{R}}\Psi(\vec{R},\vec{r}). \qquad (2.3.65)$$

We make the small angle approximation that $(\vec{v}-\vec{v}_f).\vec{R} \approx (\vec{v}-\vec{v}_f).\vec{b}$ and use the result that

$$(V_{eA}+V_{AB})\Phi_j^{B*} = \left\{H_{el}+i\left[\frac{\partial}{\partial t}\right]_{\vec{r}}\right\}\Phi_j^{B*} = \left\{H_{el}+iv\frac{\partial}{\partial Z_A}\right\}\Phi_j^{B*} \qquad (2.3.66)$$

to obtain (integrating by parts with respect to Z_A)

$$f_{ji}^{d}(\theta) = -\frac{i\mu v}{2\pi}\int d\vec{b}\int d\vec{r}\, e^{i\vec{q}.\vec{b}}\left|\Phi_j^{B*}\Psi\right|_{t=-\infty}^{\infty} \qquad (2.3.67)$$

where $\vec{q} = \mu(\vec{v}_f-\vec{v})$; $|\vec{q}| = 2\mu v \sin(\theta/2)$.

It is then possible to show using the expansion of equation (2.3.36) that

$$f_{ji}^{d}(\theta) = -\frac{i\mu v}{2\pi}\int d\vec{b}\, e^{i\vec{q}.\vec{b}}\left[a_j(b,+\infty)-\delta_{ij}\right] = -i\mu v\int_0^\infty b\, J_0(qb)\left[a_j(b,+\infty)-\delta_{ij}\right]db. \qquad (2.3.68)$$

The differential cross section is obtained from

$$\frac{d\sigma_{ji}^{d}}{d\Omega} = |f_{ji}^{d}(\theta)|^2 . \qquad (2.3.69)$$

Similarly for electron capture the scattering amplitude is given by

$$f_{ki}^{r}(\theta) = -i\mu v \int_0^{\infty} b\, J_0(qb)\, C_k(b, +\infty)\, db \qquad (2.3.70)$$

and

$$\frac{d\sigma_{ki}^{r}}{d\Omega} = |f_{ki}^{r}(\theta)|^2 . \qquad (2.3.71)$$

A full quantal derivation of equation (2.3.70) has been given by Mc Carroll and Salin (1968). The magnitude of the momentum transfer vector $\vec{q}$ is large, except when θ or v are very small. This means that the Bessel function $J_0(qb)$ may be replaced by the asymptotic form

$$J_0(qb) \sim \left(\frac{2}{\pi bq}\right)^{1/2} \sin\left(bq + \frac{\pi}{4}\right) . \qquad (2.3.72)$$

It is then possible to show that the expressions for the differential cross sections reduce to the form given in equation (2.3.57). Greenland (1982) shows that for the particular case of the nuclear motion being due to the Coulomb repulsion between the centres A and B, the expression for the classical differential cross section $d\sigma^c/d\Omega$ in equation (2.3.57) is simply the Rutherford differential cross section.

2.3.5. Choosing the basis functions

Going back to the expansion of the trial wavefunction $\Psi_T(\vec{r}, t)$ in terms of the basis functions $F_j(\vec{r}, t)$ and $G_k(\vec{r}, t)$, equation (2.3.36) these functions must be chosen carefully in order to be consistent with the particular physical aspects of the problem. As more terms

are included in the expansion for Ψ_T, the nearer Ψ_T comes to the exact wavefunction Ψ. However, the rate of convergence is very much dependent upon the basis functions being used. The main consideration is that of the speed of the collision. For very slow collisions ($v \ll 1$ a.u.) the adiabatic approximation is appropriate. Due to the slow relative speed of the centres A and B, the electron will adjust adiabatically to their motion and a virtual quasimolecule will be formed. The nuclear motion will then cause certain excitations of this molecule which correspond to electron capture occurring. (The adiabatic approximation (Born and Fock, 1928) corresponds to where the Hamiltonian of the system varies slowly with time and so the solutions of the Schrödinger equation can be approximated by stationary eigenfunctiuons of the instantaneous Hamiltonian and so an eigenfunction at one time goes over continuously to the corresponding eigenfunction at a later time - see, for example, Schiff (1955)). When the adiabatic approximation is applied the basis functions are given by combinations of the molecular eigenfunctions of the quasimolecular system comprising (for a simple one-electron system) the nuclei and the electron. These molecular eigenfunctions are denoted by $\Psi_n(\vec{r};\vec{R})$ which satisfy

$$H_{el}\,\Psi_n(\vec{r};\vec{R}) = \varepsilon_n(R)\,\Psi_n(\vec{r};\vec{R}). \qquad (2.3.73)$$

The $\Psi_n(\vec{r};\vec{R})$ are found for fixed values of $\vec{R}$ and so the dependence of $\Psi_n(\vec{r};\vec{R})$ upon $\vec{R}$ is parametric. The functions $\Psi_n(\vec{r};\vec{R})$ are known as Born-Oppenheimer electronic eigen-

functions.

For fast ($V \gg 1$ a.u.) collisions molecular eigenfunctions are not suitable for describing the collision as they cannot change adiabatically as the internuclear distance varies, in this case, rapidly. At such speeds the electron cannot adjust easily to the motion of the projectile and electron capture is improbable. For fast collisions the basis functions are best represented in terms of atomic eigenfunctions. In an actual calculation, the coupled differential equations (2.3.39a) and (2.3.39b) must be integrated. In order to minimise computing time, it is preferable to use an expansion which includes only a small number of states that are strongly coupled. This is termed the close-coupling approximation. Ideally one requires as small as possible number of states being strongly coupled. At low velocities this is the case for the molecular basis expansion whilst at high velocities it is true for the atomic basis expansion.

The atomic basis and molecular basis expansion methods are very much used in work on ion-atom collisions. In the next two sections of this chapter these expansion methods will be discussed in more detail.

2.4 Atomic and related expansion methods

2.4.1 Basic atomic expansion method

When the velocity of the incident ion is comparable with or greater than the orbital velocity of the electron in the target atom, an expansion in terms of atomic orbital wavefunctions, or related functions such as pseudostates, is appropriate. This is consistent with the fact that at such

velocities the electron spends most of its time bound either to one or the other ionic centre. In this subsection the basic atomic expansion method will be discussed.

Let us remind ourselves that we are seeking a solution of the impact parameter Schrödinger equation

$$\left\{H_{el} - i\left[\frac{\partial}{\partial t}\right]_{\vec{r}}\right\}\Psi(\vec{r},t) = 0 \qquad (2.4.1)$$

where the electronic Hamiltonian H_{el} is given by

$$H_{el} = -\tfrac{1}{2}\nabla_r^2 + V_{eA} + V_{eB} + V_{AB} \; . \qquad (2.4.2)$$

We describe the nuclear motion by the straight-line trajectory equation

$$\vec{R} = \vec{b} + \vec{v}t \; , \quad \vec{b}.\vec{v} = 0 \qquad (2.4.3)$$

(see figure 2.2).

The electronic wavefunction $\Psi(\vec{r},t)$ is expanded in terms of two sets of orthonormal basis functions $\{F_j(\vec{r},t)\}$ and $\{G_k(\vec{r},t)\}$

$$\Psi(\vec{r},t) = \sum_{j=1}^{M} a_j(t) F_j(\vec{r},t) + \sum_{k=1}^{N} c_k(t) G_k(\vec{r},t) \; . \qquad (2.4.4)$$

In the atomic expansion method the basis functions are written as follows:-

$$F_j(\vec{r},t) = \phi_j^B(\vec{r}_B)\exp -i\left[\varepsilon_j t + \tfrac{1}{2}p^2v^2t + p\vec{v}.\vec{r}\right] \qquad (2.4.5)$$

$$G_k(\vec{r},t) = \chi_k^A(\vec{r}_A)\exp -i\left[\eta_k t + \tfrac{1}{2}(1-p)^2v^2t - (1-p)\vec{v}.\vec{r}\right] \qquad (2.4.6)$$

where $\phi_j^B(\vec{r}_B)$ and $\chi_k^A(\vec{r}_A)$ are atomic eigenfunctions

for $(B+e^-)$ and $(A+e^-)$ with energy eigenvalues ε_j and η_k respectively. When we discussed the solution of the Schrödinger equation (2.4.1) in the previous section of this chapter, we noted the presence of the factors $\exp -i\left[\frac{1}{2}\rho^2 v^2 t + \rho\vec{v}.\vec{r}\right]$ and $\exp -i\left[\frac{1}{2}(1-\rho)^2 v^2 t - (1-\rho)\vec{v}.\vec{r}\right]$ in the unperturbed solutions of equation (2.4.1) (see equations (2.3.22) and (2.3.23)). Similarly we see that these factors are included in the basis states $F_j(\vec{r},t)$ and $G_k(\vec{r},t)$. The factors are known as electron translation factors and they need not be of the form given in equations (2.4.5) and (2.4.6). The particular form shown here are known as plane-wave translation factors. Electron translation factors are required to account for the fact that the electron, if captured, will acquire a momentum $\vec{v}$ by virtue of the relative motion of the ionic centres A and B. Translation factors are required in this formulation if the boundary conditions are to be satisfied and also if the theory is to be invariant under Gallilean transformation, that is the probability amplitudes must be independent of the choice of the origin of co-ordinates. The need for translation factors in theoretical descriptions of electron capture was first recognised by Bates and Mc Carroll (1958), though within the context of slow collisions using molecular basis functions. Shortly after, Bates (1958) proposed using plane-wave translation factors with an atomic basis expansion.

In order to derive the explicit forms of the matrix elements we consider the effect of the operator $\left\{H_{el} - i\,\partial/\partial t\right\}_r$ upon the basis functions $F_j(\vec{r},t)$ and $G_k(\vec{r},t)$ as given by

equations (2.4.5) and (2.4.6). We remember that the notation $\partial/\partial t\big]_{\vec{r}}$ means differentiate with respect to time keeping the electronic co-ordinate $\vec{r}$ fixed. It is straightforward to show that

$$H_{el} F_j(\vec{r},t) = \Big[\big(\varepsilon_j + V_{eA} + V_{AB} + \tfrac{1}{2}p^2v^2\big)\phi_j^B(\vec{r}_B) + ip\vec{v}.\vec{\nabla}_{\vec{r}}\phi_j^B(\vec{r}_B)\Big]\exp -i\big(\varepsilon_j t + \tfrac{1}{2}p^2v^2t + p\vec{v}.\vec{r}\big) \qquad (2.4.7)$$

where we have used the relation

$$\big(-\tfrac{1}{2}\nabla_{\vec{r}}^2 + V_{eB} - \varepsilon_j\big)\phi_j^B(\vec{r}_B) = 0. \qquad (2.4.8)$$

The operator $\partial/\partial t\big]_{\vec{r}}$ may be written as

$$\frac{\partial}{\partial t}\Big]_{\vec{r}} = \frac{\partial}{\partial t}\Big]_{\vec{r}_B} + p\vec{v}.\vec{\nabla}_{\vec{r}} \qquad (2.4.9)$$

or

$$\frac{\partial}{\partial t}\Big]_{\vec{r}} = \frac{\partial}{\partial t}\Big]_{\vec{r}_A} - (1-p)\vec{v}.\vec{\nabla}_{\vec{r}}\ . \qquad (2.4.10)$$

Using equation (2.4.9) yields

$$-i\frac{\partial}{\partial t}\Big]_{\vec{r}} F_j(\vec{r},t) = \Big[-\big(\varepsilon_j + \tfrac{1}{2}p^2v^2\big)\phi_j^B(\vec{r}_B) - ip\vec{v}.\vec{\nabla}_{\vec{r}}\phi_j^B(\vec{r}_B)\Big] \times \exp -i\big(\varepsilon_j t + \tfrac{1}{2}p^2v^2t + p\vec{v}.\vec{r}\big)\ . \qquad (2.4.11)$$

Combining equations (2.4.7) and (2.4.11) we obtain

$$\Big\{H_{el} - i\frac{\partial}{\partial t}\Big]_{\vec{r}}\Big\} F_j(\vec{r},t) = \big(V_{eA} + V_{AB}\big)F_j(\vec{r},t)\ . \qquad (2.4.12)$$

Similarly

$$\Big\{H_{el} - i\frac{\partial}{\partial t}\Big]_{\vec{r}}\Big\} G_k(\vec{r},t) = \big(V_{eB} + V_{AB}\big)G_k(\vec{r},t). \qquad (2.4.13)$$

The coupled differential equations are obtained from the relations

$$\int_v F_j^{*}(\vec{r},t)\Big\{H_{el} - i\frac{\partial}{\partial t}\Big]_{\vec{r}}\Big\}\Psi(\vec{r},t)\,d\vec{r} = 0 \qquad (2.4.14)$$

and

$$\int_V G_k^*(\vec{r},t)\left\{H_{el} - i\left[\frac{\partial}{\partial t}\right]_{\vec{r}}\right\}\Psi(\vec{r},t)\,d\vec{r} = 0 \qquad (2.4.15)$$

which give using equations (2.4.12) and (2.4.13) the standard coupled differential equations

$$i\left[\underset{\sim}{\dot{a}}(t) + \underset{\sim}{N}\,\underset{\sim}{\dot{c}}(t)\right] = \underset{\sim}{H}\,\underset{\sim}{a}(t) + \underset{\sim}{K}\,\underset{\sim}{c}(t) \qquad (2.4.16a)$$

$$i\left[\underset{\sim}{N}^{\dagger}\,\underset{\sim}{\dot{a}}(t) + \underset{\sim}{\dot{c}}(t)\right] = \underset{\sim}{\bar{K}}\,\underset{\sim}{a}(t) + \underset{\sim}{\bar{H}}\,\underset{\sim}{c}(t) \qquad (2.4.16b)$$

where the matrix elements are given by

$$N_{jk} = \langle \phi_j^B(\vec{r}_B) \mid e^{i\vec{v}.\vec{r}} \mid \chi_k^A(\vec{r}_A)\rangle\, e^{i(\varepsilon_j - \eta_k)t} \qquad (2.4.17)$$

$$H_{jk} = \langle \phi_j^B(\vec{r}_B) \mid V_{eA} \mid \phi_k^B(\vec{r}_B)\rangle\, e^{i(\varepsilon_j - \varepsilon_k)t} + V_{AB}\,\delta_{jk} \qquad (2.4.18)$$

$$\bar{H}_{jk} = \langle \chi_j^A(\vec{r}_A) \mid V_{eB} \mid \chi_k^A(\vec{r}_A)\rangle\, e^{i(\eta_j - \eta_k)t} + V_{AB}\,\delta_{jk} \qquad (2.4.19)$$

$$K_{jk} = \langle \phi_j^B(\vec{r}_B) \mid V_{eB}\, e^{i\vec{v}.\vec{r}} \mid \chi_k^A(\vec{r}_A)\rangle\, e^{i(\varepsilon_j - \eta_k)t} + V_{AB}N_{jk} \qquad (2.4.20)$$

$$\bar{K}_{jk} = \langle \chi_j^A(\vec{r}_A) \mid V_{eA}\, e^{-i\vec{v}.\vec{r}} \mid \phi_j^B(\vec{r}_B)\rangle\, e^{i(\eta_j - \varepsilon_k)t} + V_{AB}N_{kj}^{*}\,. \qquad (2.4.21)$$

The coupled equations are solved subject to the boundary conditions given in equation (2.3.43).

For the case where the ionic centres A and B are nuclei, the potential V_{AB} is given by

$$V_{AB} = \frac{Z_A Z_B}{R}\,. \qquad (2.4.22)$$

This internuclear potential V_{AB} only affects the phase of the amplitudes $a_j(t)$ and $c_k(t)$. Hence total cross sections for excitation and capture are not dependent upon V_{AB} as they are calculated from $|a_j(\infty)|^2$ and $|c_k(\infty)|^2$ which are phase

independent. However, as may be seen from equations (2.3.68) and (2.3.70), differential cross sections are dependent upon the phase of the amplitudes and so depend upon V_{AB} . Also the total elastic cross section depends upon V_{AB} as it is calculated from $|a_i(\infty)-1|^2$ which is phase dependent. It is possible to simplify the matrix elements by a simple phase transformation involving V_{AB} . We put

$$a_j(t) = \exp\left[-i\,\phi(t)\right] a_j'(t) \tag{2.4.23}$$

$$c_k(t) = \exp\left[-i\,\phi(t)\right] c_k'(t) \tag{2.4.24}$$

where

$$\phi(t) = \int_{-\infty}^{t} V_{AB}(t')\,dt'. \tag{2.4.25}$$

The coupled differential equations become

$$i\left[\dot{\underset{\sim}{a}}'(t) + \underset{\sim}{N}\,\dot{\underset{\sim}{c}}'(t)\right] = \underset{\sim}{H}'\,\underset{\sim}{a}'(t) + \underset{\sim}{K}'\,\underset{\sim}{c}'(t) \tag{2.4.26a}$$

$$i\left[\underset{\sim}{N}^{\dagger}\,\dot{\underset{\sim}{a}}'(t) + \dot{\underset{\sim}{c}}'(t)\right] = \underset{\sim}{\bar{K}}'\,\underset{\sim}{a}'(t) + \underset{\sim}{\bar{H}}'\,\underset{\sim}{c}'(t) \tag{2.4.26b}$$

where

$$H'_{jk} = \langle \phi_j^B(\vec{r}_B)|\, V_{cA}\,|\phi_k^B(\vec{r}_B)\rangle\, e^{i(\varepsilon_j-\varepsilon_k)t} \tag{2.4.27}$$

$$\bar{H}'_{jk} = \langle \chi_j^A(\vec{r}_A)|\, V_{cB}\,|\chi_k^A(\vec{r}_A)\rangle\, e^{i(\eta_j-\eta_k)t} \tag{2.4.28}$$

$$K'_{jk} = \langle \phi_j^B(\vec{r}_B)|\, V_{cB}\, e^{i\vec{v}.\vec{r}}\,|\chi_k^A(\vec{r}_A)\rangle\, e^{i(\varepsilon_j-\eta_k)t} \tag{2.4.29}$$

$$\bar{K}'_{jk} = \langle \chi_j^A(\vec{r}_A)|\, V_{cA}\, e^{-i\vec{v}.\vec{r}}\,|\phi_k^B(\vec{r}_B)\rangle\, e^{i(\eta_j-\varepsilon_k)t}\,. \tag{2.4.30}$$

If we examine the form of the matrix elements, we observe the factors $\exp(\pm i\vec{v}.\vec{r})$ in the overlap and exchange elements. These correspond physically to the increase in the captured electron's momentum. At low energies ($\lesssim$ 1 keV) it is possible

to approximate the factors by unity. At higher energies the effect of the factors is to cause the $\underset{\sim}{K}$ and $\underset{\sim}{\bar{K}}$ matrix elements to rapidly decrease owing to the factors oscillating rapidly and this is the reason why electron capture cross sections fall off very rapidly at high energy as compared with excitation cross sections which are dependent upon the direct matrices $\underset{\sim}{H}$ and $\underset{\sim}{\bar{H}}$ which do not contain such factors.

For the simple one-electron system the direct elements can be found analytically. However, the overlap and exchange elements can only be calculated numerically owing to the presence of the awkward momentum factors $\exp(\pm i\vec{v}.\vec{r})$. There are various techniques available for dealing with the overlap and exchange matrix elements involving the factors. Three such methods are described in Appendix 4.3 of Mc Dowell and Coleman (1970). The first method uses prolate spheroidal co-ordinates. The method is described more fully in Chapter 4 of this thesis as it was the main method used to evaluate the matrix elements specific to the calculations presented in Chapter 5. The second method is known as the Fourier transform method. It was developed by Sin Fai Lam in connection with work on electron capture by protons from helium atoms (Bransden and Sin Fai Lam, 1966: Sin Fai Lam 1967). The required matrix elements can be expressed in terms of families of one-dimensional integrals after a reduction process has taken place. Noble (1980) has developed a computer package based on this Fourier transform method. Finally, Cheshire (1967) and Chatterjee et al. (1967) have developed a method which is based upon expressing the required matrix elements in terms of a solution

of a first-order differential equation.

In a coupled channel calculation as the size of the basis set increases, the computational time required for calculating the matrix elements increases substantially. One way round this is to use a two-state approximation in which only the initial target state and the final projectile state are retained in the expansion of the electronic wavefunction (Bates, 1958). Although this method is not as accurate as elaborate calculations involving more states being coupled, the two-state approximation can provide reasonably accurate cross sections in the energy range where the total cross section is a maximum. This has been used by Lin and collaborators in their work dealing with capture from inner shells of heavy ions (Lin, 1978a, 1978b; Lin et al. 1978; Lin and Tunnell, 1979). Mc Carroll (1961) applied the two-state approximation to symmetrical resonant electron capture in proton-hydrogen collisions, namely

$$H^+ + H(1s) \longrightarrow H(1s) + H^+. \qquad (2.4.31)$$

For symmetrical resonance the two-state coupled differential equations are

$$i(\dot{a} + n\dot{c}) = ha + kc \qquad (2.4.32a)$$

$$i(n^*\dot{a} + \dot{c}) = ka + hc \qquad (2.4.32b)$$

where

$$n = N_{11} \qquad (2.4.33)$$

$$h = H_{11} = \bar{H}_{11} \qquad (2.4.34)$$

$$k = K_{11} = \bar{K}_{11}\,, \qquad (2.4.35)$$

the matrix elements with subscripts 11 being given by equations (2.4.17) to (2.4.21). We now introduce the new amplitudes

$$A_{\pm}(t) = a(t) \pm c(t) \tag{2.4.36}$$

and also set

$$M = \frac{h - nk}{1 - |n|^2} , \tag{2.4.37}$$

$$L = \frac{k - nh}{1 - |n|^2} . \tag{2.4.38}$$

This yields the uncoupled equations

$$i \dot{A}_{\pm}(t) = (M \pm L) A_{\pm}(t) , \tag{2.4.39}$$

which are to be solved subject to the boundary condition

$$A_{\pm}(-\infty) = 1 . \tag{2.4.40}$$

The solutions are

$$A_{\pm}(t) = \exp\left\{-i \int_{-\infty}^{t} (M \pm L)\, dt'\right\} \tag{2.4.41}$$

from which we have

$$a(t) = \cos\left\{\int_{-\infty}^{t} L\, dt'\right\} \exp\left\{-i \int_{-\infty}^{t} M\, dt'\right\} \tag{2.4.42}$$

$$c(t) = \sin\left\{\int_{-\infty}^{t} L\, dt'\right\} \exp\left\{-i \int_{-\infty}^{t} M\, dt'\right\} . (-i) . \tag{2.4.43}$$

The transition probability for electron capture is given by

$$|c(+\infty)|^2 = \sin^2\left\{\int_{-\infty}^{\infty} L\, dt'\right\}$$

$$= \sin^2\left\{\int_{-\infty}^{\infty} \frac{k - nh}{1 - |n|^2}\, dt'\right\} . \tag{2.4.44}$$

Mc Carroll's calculations were for incident energies from 0.1 keV to 1 MeV. The total cross sections are in rough agreement with the experimental results of Wittkower et al. (1966) between 40 and 250 keV. At high energies the cross section tends to the first-order Brinkman-Kramers approximation (Brinkman and Kramers, 1930). In this approximation $C(+\infty)$ is approximated by

$$C(+\infty) = \int_{-\infty}^{\infty} L_{BK}\, dt' \qquad (2.4.45)$$

where

$$L_{BK} = \int_V \phi^*(\vec{r}_A)\, e^{i\vec{v}\cdot\vec{r}}\, \frac{1}{r_A}\, \phi(\vec{r}_B)\, d\vec{r}\,. \qquad (2.4.46)$$

The corresponding Brinkman-Kramers cross section σ_{BK} varies at high energies like v^{-12}. The two-state cross section approaches σ_{BK} very slowly and very high energies must be reached before there is reasonable agreement between the two cross sections.

If the capture process is not one of symmetrical resonance, the two-state equations do not decouple and must be solved numerically. At very high energies the coupling between the initial and final states becomes weak and the coupled equations become

$$i\dot{a} = M a \qquad (2.4.47a)$$

$$i\dot{c} = \bar{M} c + \bar{L} a \qquad (2.4.47b)$$

where

$$M = \frac{H_{00} - N_{00}\bar{K}_{00}}{1 - |N_{00}|^2} \qquad (2.4.48)$$

$$\bar{M} = \frac{\bar{H}_{00} - N_{00}^{*}K_{00}}{1 - |N_{00}|^2} \qquad (2.4.49)$$

$$\bar{L} = \frac{\bar{K}_{00} - N_{00}^{*}H_{00}}{1 - |N_{00}|^2} \qquad (2.4.50)$$

with the solution

$$c(+\infty) = -i\int_{-\infty}^{\infty}\left[\bar{L}(t)\exp\left\{\int_{-\infty}^{t}\{M(t') - \bar{M}(t')\}dt'\right\}\right]dt. \qquad (2.4.51)$$

This approximation is a form of the distorted-wave Born approximation applied to this problem (Bates, 1958). Ryufuku and Watanabe (1978, 1979a, 1979b) have developed a method based upon this distorted-wave solution which they term the Unitarised Distorted-Wave Born Approximation (UDWA). They make the approximation of neglecting the $|N_{00}|^2$ term in the denominators of the expressions of equations (2.4.48) to (2.4.50). The total propability for capture is $P(b)$ where b is the impact parameter and this is unitarised by writing

$$P(b) = \sin^2\left[p(b)\right]^{1/2} \qquad (2.4.52)$$

where

$$p(b) = \sum_{nlm} \left| c_{nlm}^{DW}(+\infty) \right|^2 \qquad (2.4.53)$$

and where

$$c_{nlm}^{DW}(+\infty) \equiv c(+\infty) \qquad (2.4.54)$$

$C(+\infty)$ being given by equation (2.4.51). The $n\ell m$ are the quantum numbers of the captured states. Ryufuku and Watanabe applied the method quite successfully to electron capture from atomic hydrogen by fully stripped ions, (H^+, He^{2+}, Li^{3+}, etc.). Ryufuku (1982) has extended the UDWA method method to the calculation of ionisation and excitation cross sections as well as capture cross sections for fully stripped ions (H^+, Li^{3+}, B^{5+}, C^{6+} and Si^{14+}) on atomic hydrogen.

Bransden et al. (1980) have also studied electron capture by fully stripped ions from atomic hydrogen. They considered the ions He^{2+}, Li^{3+}, Be^{4+} and B^{5+} having impact energies between 5 and 200 keV amu^{-1}. The two-state approximation was used with no neglect of coupling between the initial and final states. The total cross sections were calculated by summing the individual nlm quantum state cross sections. Reasonable agreement was obtained with experiment and other theories, though below about 25 keV amu^{-1} this method seemed to overestimate the cross section somewhat. A copy of the paper describing the work of Bransden et al. is to be found at the rear of this thesis, p293.

The two-state approximation is limited in its effectiveness for describing a capture process and it is a much better approximation to include more states in the expansion that are strongly coupled. The proton-hydrogen system has been the subject of much study using the two-centre atomic basis expansion method. A useful compilation of atomic and related basis close-coupling calculations using the impact parameter approximation is given in Table 1 of the review article by Delos (1981). Part of this table is reproduced

as Table 2.1.

Reference	Radial functions	Rotating (R) or nonrotating (NR) angular functions
McCarroll (1961)	$1s$ atomic	
Cheshire (1968); McCarroll, Piacentini and Salin (1970)	$\bar{1}s$ atomic, varying orbital exponent	
Lovell and McElroy (1965)	$1s_A 2s_A 2s_B$ and other combinations	
Fulton and Mittleman (1965)	$1s$ atomic, including antitraveling orbitals	
Flannery (1969)	$1s_A 2s_A 2p_{xA}\ 2p_{zA}$ (no exchange)	
Wilets and Gallaher (1966)	$1s2s2p_x2p_z$ atomic	R
Gallaher and Wilets (1968)	$1s2s2p_x2p_z$ Sturmian	R
Rapp, Dinwiddie, Storm, and Sharp (1972)	$1s2s2p_x2p_z$ atomic	R
Rapp and Dinwiddie (1972)	$1s2s2p_x2p_z$ atomic $1s2s2p_x2p_z3s3p_x3p_z$ atomic	R R
Cheshire, Gallaher, and Taylor (1970)	$1s2s2p_x2p_z$ atomic $1s2s2p_x2p_z\bar{3}s\bar{3}p_x\bar{3}p_z$ atomic and pseudostate	R R
Sullivan, Coleman, and Bransden (1972)	$1s_A 2s_A 2p_{x_A} 2p_{z_A}$ +closure (no exchange)	NR
Shakeshaft (1976)	$1s$-$\tilde{6}s$, $2p$-$\tilde{4}p$ Sturmian	NR

Table 2.1 Close-coupled calculations of proton-hydrogen collisions based on atomic representations (after Delos (1981)).

Referring to Table 2.1, the non-rotating functions (NR) are quantised in the space-fixed frame. Rotating functions (R) are quantised along the internuclear line. If such functions are used, the form of the direct and exchange matrix elements is modified by a term involving the y-component of the angular momentum operator in the rotating (body-fixed) frame. A discussion of this is given in Section 2.3.5 of the review of Bransden (1972).

More detailed discussions of these proton-hydrogen calculations are given in the review of Delos (1981), and also atomic basis calculations on the proton-hydrogen system are discussed by Basu et al. (1978) in their review. Of these calculations, three of note are the ones performed by Wilets and Gallaher (1966), Cheshire et al. (1970) and Rapp and Dinwiddie (1972). In these calculations the 1s, 2s and 2p states were coupled. It was found that the cross section was not affected greatly by the inclusion of the 2s and 2p states at energies below 20 keV ., Above this energy, the 2s and 2p states influence the final result by about 10%. Rapp and Dinwiddie also included the 3s and 3p states but found that the coupling with them had little effect upon the final result.

Collisions between alpha particles and atomic hydrogen have been investigated theoretically by a number of workers. Table 2.2 shows some important calculations on the He^{2+}-H system using atomic expansions. We shall refer to some of the calculations shown in the table later in Chapter 5 as the He^{2+}-H system was the subject of the work of this thesis.

Two recent calculations using atomic basis states with the He^{2+}-H system being the subject of study , are those of Bransden and Noble (1981) and Bransden et al. (1983). The former of these is included in table 2.2. In the work of Bransden and Noble an 8-state model was used in which the 1s, 2s and 2p states were retained on the H and He centres. Close agreement was found with experiment up to an energy of 75 keV amu^{-1}. Bransden and Noble also used the same

Authors	Basis	States		Energy range	Comments
[Ref.]		H	He	keV/amu	
Basu et al. (1967)	Atomic	1s	1s 2s 2p	0.4 → 8	No translation factors
Malaviya (1969)	Atomic	1s	1s 2s 2p	1.58 → 200	
Rapp (1973)	Atomic	1s 2s 2p	1s 2s 2p	0.25 → 150	Known to contain errors
Rapp (1974)	Atomic	1s 2s 2p 1s 2s 2p	1s 2s 2p 1s 2s 2p 3s 3p	0.25 → 150	
Belkic and Janev (1973)	Atomic	1s	1s 2s 2p 3s 3p	6.25 → 750	Continuum Distorted Wave Calculation
Msezane and Gallagher (1973)	Atomic	1s 2s 2p	1s 2s 2p pseudostates	1.6 → 1000	Pseudostates used to reproduce united atom wavefunction
Bransden and Noble (1981)	Atomic	1s 2s 2p	1s 2s 2p	2.5 → 250	

Table 2.2 Calculations on He^{2+}-H using atomic basis states (after Table 4 of Greenland (1982) with slight amendments).

model to investigate electron capture by protons from $He^{+}(1s)$. Only up to about 19 keV amu^{-1} was there agreement with experiment. The cause of this was attributed to the coupling with continuum intermediate states not being accounted for in the calculation. Bransden et al. (1983) extended the 8-state work by including the n = 3 states on the centres, that is a 20-state calculation, and also they used the pseudo-states due to Callaway and Wooten (1974) to investigate proton-He^{+} capture. They obtained results that were in harmony with experiment and other theory. Work similar to that of Bransden and co-workers has been done by Fujiwara (1981) on the He^{2+}-H system. Fujiwara used all states up to n=2 on the H centre and all states up to n=3 on the He centre. Fairly good agreement was obtained with experimental

data. Bransden and Noble (1982) have also investigated Li^{3+}-H collisions using a 20-atomic state model.

The atomic basis state expansion begins to become unsatisfactory at high energies owing to the need for inclusion of continuum states. We shall now discuss three attempts to include these states that have been found to be reasonably successful.

2.4.2 Sturmian functions

Gallaher and Wilets (1968) first introduced Sturmian functions to take into account the continuum in their work on proton-hydrogen collisions. The atomic eigenfunctions used in the two-centre expansion are replaced by functions of the form

$$\hat{\phi}_k(\vec{r}) = \frac{1}{r} S_{n\ell}(r) Y_{\ell m}(\theta,\phi), \quad k \equiv \{n,\ell,m\} \qquad (2.4.55)$$

where $S_{n\ell}(r)$ is a radial function which satisfies

$$\left(-\frac{1}{2}\frac{d^2}{dr^2} + \frac{\ell(\ell+1)}{2r^2} - \frac{\alpha_{n\ell}}{r}\right) S_{n\ell}(r) = E_\ell S_{n\ell}(r) . \qquad (2.4.56)$$

This is the Sturmian equation and is similar to the Schrödinger equation except that the energy E_ℓ is treated as a fixed parameter and the effective charge $\alpha_{n\ell}$ acts as the eigenvalue. In Gallaher and Wilets' work E_ℓ was taken as

$$E_\ell = -\frac{1}{2(\ell+1)^2} . \qquad (2.4.57)$$

The boundary conditions on $S_{n\ell}(r)$ are that it is zero at the origin and that it decays exponentially at infinity. The Sturmian functions $\hat{\phi}_{n\ell}(\vec{r})$ are members of an infinite, discrete and complete set of states. There is no continuum

unlike hydrogenic functions.

The Sturmian functions are related to scaled radial hydrogenic functions via the relation

$$S_{n\ell}(r) = \alpha_{n\ell}^{1/2} R_{n\ell}(\alpha_{n\ell} r) \quad . \tag{2.4.58}$$

Normalisation is expressed by

$$\langle \hat{\phi}_k | \hat{\phi}_k \rangle = 1 \tag{2.4.59}$$

but the Sturmian functions are not orthogonal unless a weighting factor of $1/r$ is included. Taking E_ℓ as given by equation (2.4.57), $\alpha_{n\ell}$ is given by

$$\alpha_{n\ell} = \frac{n}{\ell + 1} \tag{2.4.60}$$

which gives a mean energy of

$$\bar{E}_k = \langle \hat{\phi}_k | H_0 | \hat{\phi}_k \rangle$$

$$= -\frac{1}{n(\ell+1)} + \frac{1}{2(\ell+1)^3} \quad . \tag{2.4.61}$$

With this definition of the Sturmian basis set, the 1s, 2p and 3d Sturmian states coincide with the hydrogenic $\phi_{n\ell}$. Problems arise, however, in defining the transition amplitudes using Sturmian functions. The resulting transition probabilities have oscillating components which do not vanish as $t \rightarrow \infty$. However, if a large Sturmian basis set is used, this problem can be solved as was shown by Shakeshaft (1976) in his work on proton-hydrogen collisions. He included the 1s to 6s and 2p to 4p Sturmian states on both centres. Electron capture in proton-He^+ and He^{2+}-H collisions has been studied using Sturmian functions

by Winter (1982). Between 19 and 24 Sturmian functions were used as a basis.

2.4.3 Pseudostate expansion

Cheshire et al. (1970) introduced pseudostate functions in their work on proton-hydrogen collisions. The Sturmian expansion discussed previously does not represent the 2s state of hydrogen well, and this is a major defect as the degenerate 2s and 2p states are strongly coupled at large internuclear separations, and so the 2s state must be adequately described in coupled channel calculations. In the work of Cheshire et al. the 1s, 2s and 2p hydrogenic states were used in the expansion together with $\overline{3s}$ and $\overline{3p}$ pseudostates. The pseudostate wavefunctions are given by

$$\overline{\phi}_k(\vec{r}) = \exp(-\lambda_i r)\left[\sum_{q=1}^{j+3-i} \alpha_{ijq}\, r^{q+i-2}\right] Y_{lm}(\theta,\phi)\,,$$

$$i = l+1\,,\quad j \geq 1\,,\quad k = 3j+l+m+2\,. \qquad (2.4.62)$$

The parameters are such that the functions are orthogonal with the 1s, 2s and 2p hydrogenic states. The total capture cross sections calculated by Cheshire et al. agree well with the experimental results of Bayfield (1969). The cross sections for capture into the 2s state of hydrogen are in good agreement with the experimental results of Bayfield (1969) and Ryding et al. (1966). There is discrepancy between Cheshire et al.'s results for capture to the 2p state of hydrogen and the experimental results of Stebbings et al. (1965) (corrected by Young et al. (1968)). Figures 8.2 and 8.3 of Basu et al. (1978) display the 2s and 2p

capture results.

Dose and Semini (1974) have used Gaussian functions to study the proton-hydrogen system, Gaussian functions being another type of pseudostate function. The advantage of Gaussian functions is that the overlap and exchange matrix elements containing the $\exp(\pm i\vec{v}.\vec{r})$ factors can be calculated analytically. Only capture into the 1s state of hydrogen was investigated but good agreement was achieved with the results of Cheshire et al. (1970). In the review of Basu et al. (1978), Table 8.3 compares the results of Dose and Semini with the 4 atomic state and 7 atomic/pseudostate ground state capture results of Cheshire et al. and with the results of Shakeshaft's Sturmian expansion work.

2.4.4. Scaled hydrogenic basis set

The Sturmian and pseudostate expansions take into account coupling with continuum states and so may be used for calculations of ionisation cross sections. Shakeshaft (1978b) has used a scaled hydrogenic basis set to do such calculations. This set of basis functions is very similar to the Sturmian functions, but the scaling factors are such that the atomic Hamiltonian is diagonalised. The states almost coincide with the 1s, 2s, 2p, 3s, 3p and 3d states and overlap the low energy part of the continuum. The scaled hydrogenic functions $\tilde{\phi}_{nlm}(\vec{r})$ satisfy

$$\left(-\tfrac{1}{2}\nabla_r^2 - \frac{\lambda_{nl}}{r} + \tfrac{1}{2}\frac{\lambda_{nl}^2}{n^2}\right)\tilde{\phi}_{nlm}(\vec{r}) = 0 \,. \qquad (2.4.63)$$

Shakeshaft used 35 of these functions centred about each

proton with $0 \leq l \leq 2$, $0 \leq m \leq l$, $l \leq n \leq N_l$ where $N_0=9$, $N_1=8$, $N_2=6$. The scale factors λ_{nl} were chosen as follows: $\lambda_{n0} = 0.75n$, $\lambda_{n1} = 0.7n$, $\lambda_{n2} = 0.6n$. Shakeshaft's total ionisation cross section was in fairly good agreement with the experimental results of Park et al. (1977). The work of Shakeshaft is interesting in that it shows that below about 60 keV the cross section for "charge transfer to the continuum" (CTTC) is larger than the cross section for direct ionisation. Shakeshaft describes this as being "remarkable" and shows that any ionisation approximation which neglects CTTC for proton-hydrogen collisions will be inadequate below about 100 keV.

2.4.5 Other improvements based on the atomic expansion method

Apart from the three methods discussed previously, there are other methods which are based upon the atomic expansion.

One method is due to Cheshire (1968) who used atomic wavefunctions with variable charges $Z(t)$ which were determined using the Euler-Lagrange variational principle. The main problem with this method is the large amount of computer time needed. Mc Carroll et al. (1970) used the method to study proton-hydrogen collisions in the two-state approximation. They calculated the differential cross section and the capture probability as a function of the incident proton energy for different scattering angles. Recently Campos et al. (1983) have calculated total cross sections for the resonance capture process

$$H^+ + H(1s) \longrightarrow H(1s) + H^+ \qquad (2.4.64)$$

using a variable effective charge $Z(R)$. However, Campos et al. used the virial theorem to find $Z(R)$ rather than the Euler-Lagrange method in order to economise on computer time. Another method is to expand the wavefunction about three centres instead of two, namely the nuclei A and B and their centre of charge (Anderson et al., 1974). Anderson et al. considered proton-hydrogen collisions and used 1s and 2s hydrogenic states on the centres A and B with a 1s He^+ state on centre C, the centre of charge. The inclusion of the 1s He^+ state partially represented the hydrogenic continuum and united atom states. An elaborate expansion method using a modified system of elliptical co-ordinates and orthogonal polynomials has been used by Morrison and Öpik (1978) on the proton-hydrogen and He^{2+}-H systems. If the charge Z_A of the projectile nucleus is much less than the charge Z_B of the target nucleus, then the interaction between the incident particle A and the electron can be treated as a perturbation and the scattering wavefunction can be expanded in terms of atomic states and pseudo-states centred on the target. Reading and co-workers (Reading et al. 1976; Ford et al. 1977) have used this method for calculating K-shell ionisation cross sections for light, fully stripped ions incident upon heavy, neutral target atoms (Z_B = 13 - 30). Fitchard et al. (1977) applied the method to n = 2 and n = 3 excitation and ionisation in proton-hydrogen collisions. Between projectile energies of 50 and 200 keV excellent agreement was obtained with experi-

ment. The method was extended (Reading et al. 1979; Reading and Ford, 1979) to electron capture processes by fully stripped ions from heavy target atoms. Specifically inner shell ionisation and electron capture in proton-argon collisions in an overall energy range 1 to 12 MeV were studied by Ford et al. (1979a, 1979b) using this method. The work was extended by Becker et al. (1980) to He^{2+} and C^{6+} incident upon argon in the energy range 1-9 MeV , and then by Ford et al. (1981) to H^{+}, He^{2r} and Li^{3+} incident upon neon (0.4 - 4.0 MeV amu^{-1}) and carbon (0.2 to 2.0 MeV amu^{-1}).

An interesting development of the above single-centred expansion (SCE) work of Reading and co-workers has been a method which is termed the one and a half centred expansion (OHCE), (Reading et al. 1981). The method utilises a wave-function expansion of the form

$$\Psi(\vec{r},t)=\sum_{j} a_j(b,t)\,\bar{\Phi}_j(\vec{r},t)+\sum_{k} c_k(b,\infty)f(t)\chi_k(\vec{r},t)\,. \qquad (2.4.65)$$

The first sum is centred on the target and includes real and pseudostates. The second sum is centred on the projectile and contains atomic states of importance needed to describe the capture channels adequately. The wavefunction $\Psi(\vec{r},t)$ satisfies the boundary conditions provided the predetermined function $f(t)$ satisfies

$$\left.\begin{aligned} f(t) &\longrightarrow 0\,, \quad t \longrightarrow -\infty \\ f(t) &\longrightarrow 1\,, \quad t \longrightarrow +\infty \end{aligned}\right\}\,. \qquad (2.4.66)$$

A variational procedure is applied and yields a set of coupled first-order differential equations for the amplitudes $a_j(t)$ coupled with algebraic equations for the coefficients $c_k(b,\infty)$. Reading et al. (1981) applied the OHCE method successfully to proton-hydrogen collisions. The SCE method failed for excitation and ionisation (Fitchard et al., 1977) below 50 keV due to electron capture being the dominant process in this energy region. However, the OHCE method gave accurate results down to 15 keV, the lowest energy considered. The OHCE method was also applied by Reading et al. (1982) to ionization and electron capture in H^+ - He^+ and He^{2+} - H collisions. Some disagreement was found between other theory and experiment for the H^+ - He^+ collisions but good agreement was achieved when He^{2+} - H was considered. The energy range was 25 - 482.5 keV amu^{-1} for both H^+ - He^+ and He^{2+} - H. Ford et al. (1982) have considered collisions involving lithium ions using the OHCE method. They considered H^+ - Li^+ for an energy range 70 - 400 keV amu^{-1} and also H^+ - Li^{2+} for an energy range 50 - 200 keV amu^{-1}. Both ionisation and electron capture cross sections were calculated; for H^+ - Li^+ the ionisation result was in good agreement with experiment but the capture result was lower than experiment. Time reversal was used to extract capture cross sections for the processes Li^{2+} - H and Li^{3+} - H. These were higher than experiment. This work was the first test of the OHCE method when more than one electron was present. Fritsch and Lin (1982a) have proposed a modified two-centre atomic orbital expansion which includes united

atom orbitals as well as separated atom orbitals. Wilets and Gallaher (1966) noted that for the H^+ - H system the atomic orbital expansion fails at low velocities due to the poor representation of the united atom orbitals even by the full bound spectrum of the separated atoms. Investigations by Fritsch and Lin (1982a, b) on the H^+ - H and He^+ - H systems showed that model sensitive partial cross sections and impact parameter-dependent transition probabilities, calculated using their modified atomic orbital (AO+) expansion, agreed well with (low velocity) molecular orbital expansion calculations. Fritsch and Lin (1982c) have applied the method to Li^{3+} - H collisions for $^7Li^{3+}$ impact energies of 1.4 to 140 keV and obtained excellent agreement with experiment. They have also investigated H^+ - Li and He^{2+} - Li collisions (Fritsch and Lin, 1983). The calculated total and partial capture cross sections are the first published origin-independent results in the energy range 0.5 to 20 keV for H^+ - Li and in the range 0.1 to 2.0 ke V amu^{-1} for He^{2+} - Li. For H^+ - Li the total capture cross sections agreed well with experiment but for He^{2+} - Li the low energy capture cross sections were much larger than comparable molecular orbital results.

Lüdde and Dreizler (1981) have introduced a method which is based upon a numerical solution of the impact parameter Schrödinger equation using a two- centre basis set of the Hylleraas type. Lüdde and Dreizler have applied this method to proton-hydrogen collisions (Lüdde and Dreizler, 1981: 1982a) and also to collisions of He^{2+}, Li^{3+}, Be^{4+}

and B^{5+} with atomic hydrogen (Lüdde and Dreizler, 1982b). Recently Lüdde and Driezler (1983) have obtained differential cross sections and capture probabilities for proton-hydrogen collisions at 1 and 2 keV.

The final improvement we consider is the one most relevant to the work presented in this thesis. The improvement is that of including a "switching function" in the electron translation factor when using a two-centre atomic basis expansion. Equations (2.4.5) and (2.4.6) show the expressions for the basis states when plane-wave translation factors are used. The modified basis states $F_j^s(\vec{r},t)$ and $G_k^s(\vec{r},t)$, where the superscript s signifies switching function, are given by

$$F_j^s(\vec{r},t) = \phi_j^B(\vec{r}_B)\exp -i\left[\varepsilon_j t + \frac{1}{8}v^2 t - \frac{1}{2}f(\vec{r},\vec{R})\vec{v}.\vec{r}\right] \qquad (2.4.67)$$

$$G_k^s(\vec{r},t) = \chi_k^A(\vec{r}_A)\exp -i\left[\eta_k t + \frac{1}{8}v^2 t - \frac{1}{2}f(\vec{r},\vec{R})\vec{v}.\vec{r}\right] . \qquad (2.4.68)$$

The function $f(\vec{r},\vec{R})$ is the switching function. In equations (2.4.67) and (2.4.68) the parameter p (see equations (2.4.5) and (2.4.6)) which determines the position of the origin, has been set to 1/2. The idea of switching functions (also known as switching factors) was introduced by Schneiderman and Russek (1969) in their work on electron capture in proton-hydrogen collisions. More will be said about switching functions in the next section of this chapter which deals with molecular expansion methods as switching functions have been used a great deal in conjunction with such methods.

However, there have been no previous calculations to date employing switching functions with a two-centre atomic basis expansion. The main properties of the switching function are that it "switches" in value between -1 and +1 as the electron is transferred from the target centre to the projectile centre, and also it tends to zero as the internuclear separation tends to zero (united atom limit). It thus gives the atomic expansion more flexibility by giving it a more molecular character than the plane-wave translational factors can in the interaction region where internuclear separation is small and probability of electron capture is high.

2.5 Molecular expansion methods

2.5.1 Introduction

The molecular state expansion method is the appropriate way of theoretically describing excitation or electron capture in ion-atom collisions when the relative collision velocity is small as compared with the classical velocity of an electron in a Bohr orbit of the target atom. Physically the effect of the slow projectile is to cause the electron to move into an orbit around the two nuclear centres so that a quasimolecule is formed adiabatically. Similarly the orbit will "unform" adiabatically leaving the electron in its initial state. Excitation or electron capture occurs because the quasimolecule is excited due to the kinetic energy associated with the relative motion of the charged centres, and the final state of the system is where the target is excited or capture has occurred.

Molecular expansion methods are based upon expanding the electronic wavefunction in terms of electronic molecular states. At low energies only a few such states are usually required to give a reasonable description of the process whereas many atomic states would normally be required. We shall see that the relative motion gives rise to electron-nuclear coupling matrix elements which are associated with transitions between the molecular states. However, the transitions between these states can only take place where there is near degeneracy of the electronic energy levels associated with the quasimolecule.

The method of using stationary molecular states to describe slow inelastic collisions of ions and atoms is called the perturbed stationary states (PSS) method. The PSS method was introduced by Massey and Smith (1933). though the idea of expanding the wavefunction in terms of molecular states was proposed by Mott (1931) using the semi-classical impact parameter approximation. The PSS method is discussed by Mott and Massey in their well-known text (Mott and Massey, 1965). We shall now discuss the basic quantum PSS method. In subsection 2.5.5 of this chapter an illustration of its use will be given.

For simplicity we consider a single-electron diatomic molecule (Figure 2.3).

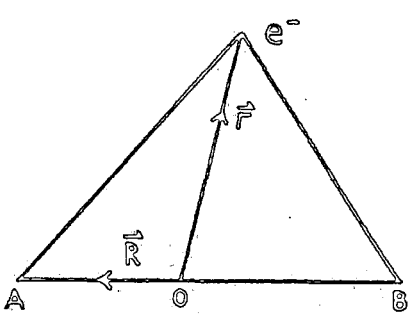

Figure 2.3

Molecular (adiabatic) co-ordinates for the ABe^- system. O is the centre of mass of (A+B).

The total Hamiltonian H of the system is given by

$$H = T_{nuc} + H_{el} \tag{2.5.1}$$

where T_{nuc} is the kinetic energy operator associated with the nuclear motion. We have

$$T_{nuc} = -\frac{1}{2\mu}\nabla_R^2 \tag{2.5.2}$$

where μ is the reduced mass of the nuclei, namely

$$\mu = \frac{M_A M_B}{M_A + M_B} \tag{2.5.3}$$

and the electronic Hamiltonian H_{el} is given by

$$H_{el} = -\frac{1}{2}\nabla_r^2 + V(\vec{r},\vec{R}) \tag{2.5.4}$$

where

$$V(\vec{r},\vec{R}) = V_{eA} + V_{eB} + V_{AB} \quad . \tag{2.5.5}$$

We apply the Born-Oppenheimer approximation (Born and Oppenheimer, 1927) to the problem and write the stationary molecular state wavefunctions $\Psi_j(\vec{r},\vec{R})$ as

$$\Psi_j(\vec{r},\vec{R}) = F_{jn}(\vec{R})\,\psi_j(\vec{r};\vec{R}) \tag{2.5.6}$$

where $F_{jn}(\vec{R})$ are vibrational wavefunctions for the nuclei and $\psi_j(\vec{r};\vec{R})$ are the adiabatic (Born-Oppenheimer) electronic wavefunctions which depend parametrically upon $\vec{R}$. The electronic and nuclear wavefunctions satisfy respectively

$$H_{el}\,\psi_j(\vec{r};\vec{R}) = \varepsilon_j(R)\,\psi(\vec{r};\vec{R}) \tag{2.5.7}$$

and

$$\left[T_{nuc} + \varepsilon_j(R)\right] F_{jn}(\vec{R}) = E_{jn} F_{jn}(\vec{R}) \tag{2.5.8}$$

where $\varepsilon_j(R)$ are the electronic energy eigenvalues and E_{jn}

are the vibrational (nuclear) energy eigenvalues. If we have an arbitrary state having total energy E then the total wavefunction $\Psi(\vec{r},\vec{R})$ satisfies the Schrödinger equation.

$$H\Psi(\vec{r},\vec{R}) = E\Psi(\vec{r},\vec{R}). \tag{2.5.9}$$

Expanding $\Psi(\vec{r},\vec{R})$ on the basis $\Psi_j(\vec{r},\vec{R})$ we have

$$\Psi(\vec{r},\vec{R}) = \sum_j \Psi_j(\vec{r},\vec{R})$$

$$= \sum_j F_j(\vec{R})\Psi_j(\vec{r};\vec{R}) \tag{2.5.10}$$

where we have dropped the index n from $F_j(\vec{R})$. It is straightforward to show that this gives

$$\sum_j \left\{\psi_j\left[T_{nuc} + \varepsilon_j(R) - E\right]F_j + F_j T_{nuc}\psi_j - \frac{1}{\mu}\vec{\nabla}_{\vec{R}}\psi_j \cdot \vec{\nabla}_{\vec{R}}F_j\right\} = 0. \tag{2.5.11}$$

Projecting upon ψ_k gives the coupled equations

$$\left\{\nabla^2_{\vec{R}} + 2\mu\left[E - \varepsilon_j(R)\right]\right\}F_j(\vec{R})$$

$$= \sum_k (2\vec{A}_{jk}\cdot\vec{\nabla}_{\vec{R}} + B_{jk})F_k(\vec{R}) \tag{2.5.12}$$

where the coupling matrices $\vec{A}_{jk}$ and B_{jk} are given by

$$\vec{A}_{jk}(R) = \int_v \psi_j^* \vec{\nabla}_{\vec{R}}\psi_k \, d\vec{r} \tag{2.5.13}$$

and

$$B_{jk}(R) = \int_v \psi_j^* \nabla^2_{\vec{R}}\psi_k \, d\vec{r}. \tag{2.5.14}$$

It should be noted that the operators $\vec{\nabla}_{\vec{R}}$ and $\nabla^2_{\vec{R}}$ operate with $\vec{r}$ fixed. Equations (2.5.13) and (2.5.14) are the electron-nuclear coupling terms. If they are neglected then equation (2.5.12) becomes

$$\left\{\nabla^2_{\vec{R}} + 2\mu\left[E - \varepsilon_j(R)\right]\right\}F_j(\vec{R}) = 0 \tag{2.5.15}$$

which is, in fact, the same as the Born-Oppenheimer nuclear equation, equation (2.5.8) with $E = E_{j\Lambda}$. The electron-nuclear couplings arise due to the nuclear kinetic energy T_{nuc} and are non-diagonal in the basis of adiabatic (Born-Oppenheimer) states $\psi_j(\vec{r};\vec{R})$. It is these terms that lead to transitions between the electronic states. Massey and Smith (1933) recognised that adiabatic states could be used for describing the electronic states in slow ion-atom collisions. Neglecting the electron-nuclear couplings corresponds to no electronic transitions occurring and only elastic scattering may be described. Retaining these couplings, transitions can occur and inelastic scattering may be described.

Before proceeding to discuss in more detail molecular state expansion methods, some notation must be introduced to describe the molecular states and also correlation diagrams introduced. If we denote by L_z the operator associated with the component of angular momentum along the inter-nuclear line, then it is the case that $\psi_j(\vec{r};\vec{R})$ are eigenfunctions of L_z , that is

$$L_z \psi_j(\vec{r};\vec{R}) = \lambda_j \psi_j(\vec{r};\vec{R}) \qquad (2.5.16)$$

where λ_j are the quantum numbers associated with L_z . The modulus of λ_j is one quantum number used to describe molecular states. One way of choosing the others required is to consider the united atom limit $(R \to 0)$. The wavefunction becomes hydrogenic for single-electron molecules and three quantum numbers n, ℓ, m describe the state. In this limit λ_j and m are the same. The molecular states may be denoted

by using the united atom quantum numbers n, l plus a lower-case Greek letter $\sigma, \pi, \delta \ldots$ to denote $|\lambda_j| = 0, 1, 2 \ldots$. Hence we have the notation $1s\sigma$, $2p\sigma$, $2p\pi$, ... etc. For more than one electron upper case Greek letters are used, that is $\Sigma, \Pi, \Delta, \ldots$. As an alternative we may consider the separated atom limit $(R \to \infty)$. As $R \to \infty$ the molecular wavefunction must tend to an atomic wavefunction representing the case when the electron is attached to one or other of the centres, or to a linear combination of such functions. We may denote molecular states using the notation $|\lambda_j| n' l'$ where n' and l' are separated atom quantum numbers. If the two nuclei are the same then the system is invariant under the transformation $\vec{r} \Longrightarrow -\vec{r}$ and the molecular states must be labelled gerade (g) or ungerade (u) which are even or odd parity solutions.

Associated with the adiabatic molecular states are the adiabatic potential energy curves $\mathcal{E}_j(R)$ which vary with R. An important visual aid in work on molecular expansion methods is that of the potential energy correlation diagram which relates energy levels in the united atom limit with those in the separated atom limit and displays the potential energy curves $\mathcal{E}_j(R)$. Figure 2.4 shows the correlation diagram for the $(HeH)^{2+}$ system. It shows the molecular states and separated atomic systems with which they correlate. An important theorem associated with adiabatic potential energy curves is that if levels j and k belong to the same symmetry class then the curves $\mathcal{E}_j(R)$ and $\mathcal{E}_k(R)$ cannot cross as R goes from 0 to ∞ . For heteronuclear systems this

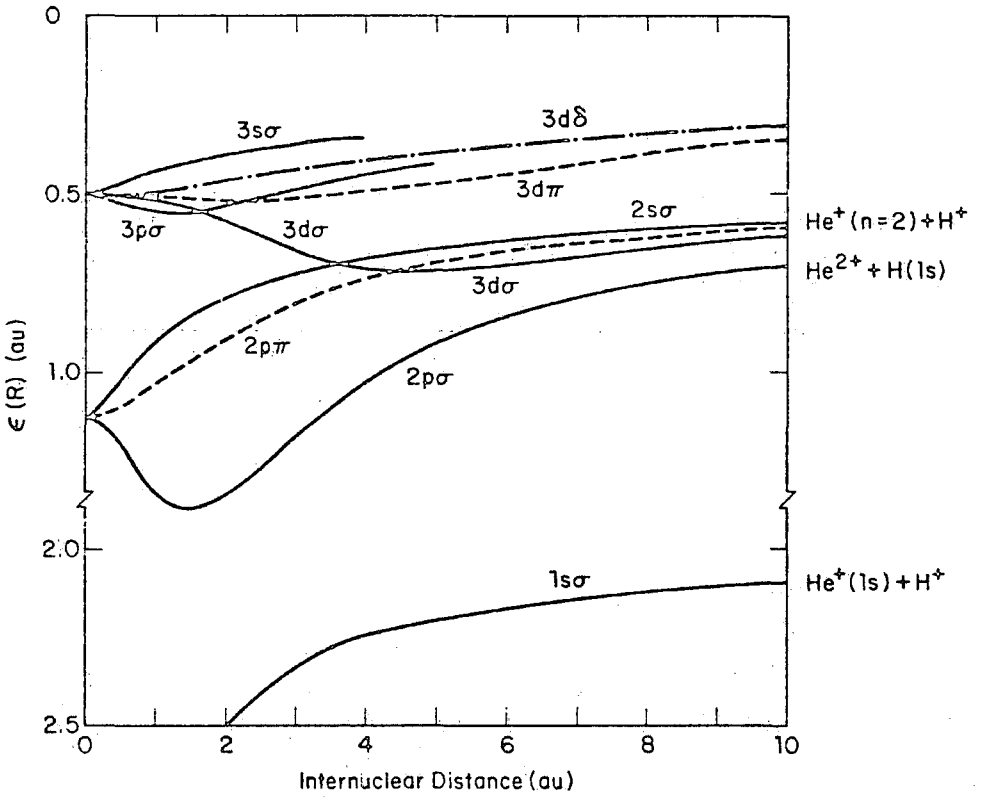

Figure 2.4 The adiabatic potential energies of $(HeH)^{2+}$ (after fig. 9-5 Bransden, 1983).

theorem requires that two curves with the same $|\lambda_j|$ may not cross (Neumann and Wigner, 1929). For homonuclear molecules, states with the same S and $|\lambda_j|$ cannot cross, where S is a separation constant arising due to the extra symmetry of the problem. The no-crossing theorem was proved by Teller (1937).

2.5.2 The impact parameter PSS method

Although the molecular state expansion is appropriate for describing collisions in the low energy region, it is

still necessary (above energies of the order of 100 eV amu^{-1}) to use the impact parameter approximation. Therefore the nuclear motion is treated classically whilst the electronic motion is treated quantum mechanically and thus we must solve the Schrödinger equation

$$\left\{H_{el} - i\left[\frac{\partial}{\partial t}\right]_{\vec{r}}\right\} \Psi(\vec{r}, t) \qquad (2.5.17)$$

where $\Psi(\vec{r}, t)$ is the electronic wavefunction and the Hamiltonian H_{el} is given by

$$H_{el} = -\frac{1}{2}\nabla_r^2 + V_{eA} + V_{eB} + V_{AB} . \qquad (2.5.18)$$

We intend to expand $\Psi(\vec{r}, t)$ on a basis of adiabatic molecular wavefunctions $\psi_j(\vec{r}; \vec{R})$ which satisfy

$$H_{el}\, \psi_j(\vec{r}; \vec{R}) = \varepsilon_j(R)\, \psi_j(\vec{r}; \vec{R}) . \qquad (2.5.19)$$

For the heteronuclear case $\psi_j(\vec{r}; \vec{R})$ will tend in the separated atom limit to an atomic wavefunction centred upon A or B, that is

$$\psi_j(\vec{r}; \vec{R}) \underset{R\to\infty}{\sim} \phi_j^B(\vec{r}_B) \qquad (2.5.20)$$

$$\psi_k(\vec{r}; \vec{R}) \underset{R\to\infty}{\sim} \chi_k^A(\vec{r}_A) . \qquad (2.5.21)$$

Sometimes the superscripts A or B are added to the ψ-functions to indicate to which centre the electron will be attached to as $R \to \infty$.

For the homonuclear case $\psi_j(\vec{r}; \vec{R})$ will tend to linear combinations of atomic orbital wavefunctions, namely

$$\psi_j^g(\vec{r}; \vec{R}) \underset{R\to\infty}{\sim} \frac{1}{\sqrt{2}}\left[\phi_j^B(\vec{r}_B) + \chi_j^A(\vec{r}_A)\right] \qquad (2.5.22)$$

$$\psi_k^u(\vec{r}; \vec{R}) \underset{R\to\infty}{\sim} \frac{1}{\sqrt{2}}\left[\phi_k^B(\vec{r}_B) - \chi_k^A(\vec{r}_A)\right] . \qquad (2.5.23)$$

The g and u refer to gerade or ungerade symmetry.

Earlier in this chapter we discussed the general solution of the impact parameter Schrödinger equation (Subsection 2.3.3). We saw how the trial wavefunction was expanded in terms of two orthonormal sets of functions $F_j(\vec{r},t)$ and $G_k(\vec{r},t)$ (equation (2.3.36)), the F_j - functions being associated with centre B, and the G_k - functions being associated with centre A via the limits given in equations (2.3.35a) and (2.3.35b). In the atomic expansion method the F_j - and G_k-functions were expressed in terms of atomic wavefunctions $\phi_j^B(\vec{r}_B)$ and $\chi_k^A(\vec{r}_A)$ respectively. In the molecular expansion method F_j and G_k are expressed in terms of $\psi_j^B(\vec{r};\vec{R})$ and $\psi_k^A(\vec{r};\vec{R})$ molecular wavefunctions for heteronuclear systems, that is

$$\left.\begin{aligned} F_j(\vec{r},t) &\sim \psi_j^B(\vec{r};\vec{R}) \\ G_k(\vec{r},t) &\sim \psi_k^A(\vec{r};\vec{R}) \end{aligned}\right\} \qquad (2.5.24)$$

or in terms of linear combinations of gerade and ungerade molecular wavefunctions for the homonuclear case, that is

$$\left.\begin{aligned} F_j(\vec{r},t) &\sim \frac{1}{\sqrt{2}}\left[\psi_j^g(\vec{r};\vec{R}) + \psi_j^u(\vec{r};\vec{R})\right] \\ G_k(\vec{r},t) &\sim \frac{1}{\sqrt{2}}\left[\psi_k^g(\vec{r};\vec{R}) - \psi_k^u(\vec{r};\vec{R})\right] \end{aligned}\right\} . \qquad (2.5.25)$$

There is no reason why the wavefunction $\Psi(\vec{r},t)$ has to be expanded in terms of two series in the basic PSS method, though. In the impact parameter version of the PSS method the electronic wavefunction $\Psi(\vec{r},t)$ is expanded as follows:-

$$\begin{aligned} \Psi(\vec{r},t) &= \sum_j a_j(t)\,\bar{\Phi}_j(\vec{r},t) \\ &= \sum_j a_j(t)\,\psi_j(\vec{r};\vec{R})\exp\left[-i\int_{-\infty}^{t}\varepsilon_j(R)\,dt'\right] . \end{aligned} \qquad (2.5.26)$$

From this expression a set of coupled first-order differential

equations can be obtained

$$i\dot{a}_j = \sum_{j'=j} a_{j'} V_{jj'} \exp\left[i \int_{-\infty}^{t} (\varepsilon_j - \varepsilon_{j'}) \, dt' \right] \qquad (2.5.27)$$

where $$V_{jj'} = \langle \gamma_j | \frac{\partial}{\partial t}\Big]_{\mathcal{F}} | \gamma_{j'} \rangle \, . \qquad (2.5.28)$$

The coupled equations (2.5.27) are the PSS equations using the impact parameter approximation.

The matrix elements $V_{jj'}$ are calculated assuming that the time derivative is with respect to the fixed space axes Molecular wavefunctions are quantised with respect to the rotating internuclear line and so this rotation must be accounted for somehow. It is simple to show that

$$\frac{\partial}{\partial t}\Big]_{\mathcal{F}} = \dot{R} \frac{\partial}{\partial R} + i \frac{bv}{R^2} L_{y'} \qquad (2.5.29)$$

(Greenland, 1982) where $L_{y'}$ is the y'-component of the angular momentum operator, prime denoting the rotating frame. The $\partial/\partial R$ term gives rise to matrix elements known as radial couplings whilst the $L_{y'}$ term gives rise to matrix elements known as rotational couplings.

If we examine the PSS equations (2.5.27), we see the presence of the exponential phase factor

$$\exp\left[i \int_{-\infty}^{t} (\varepsilon_j - \varepsilon_{j'}) \, dt' \right] . \qquad (2.5.30)$$

If the potential energy difference $(\varepsilon_j - \varepsilon_{j'})$ is large for all internuclear separation R, the states j and j' are weakly coupled. If $(\varepsilon_j - \varepsilon_{j'})$ vanishes, then the coupling is strong.

We know that from the no-crossing theorem two potential energy curves corresponding to states of the same symmetry may not cross in the adiabatic representation. However, they may

approach one another closely. Such a place where this occurs is known as a pseudocrossing (or avoided crossing). In the region of a pseudocrossing the radial coupling is large and the two states concerned are strongly coupled. Figure 2.5 shows two pseudocrossings for the N^{7+}-H (1s) system.

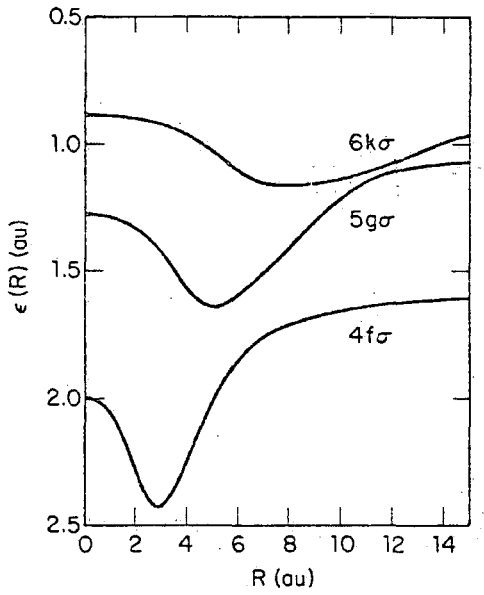

Figure 2.5 Some σ levels of the system (N^{7+}+H) illustrating pseudocrossings at 11.6 and 6.4 a.u. (after figure 9-4 of Bransden, 1983).

The pseudocrossings occur between the $6k\sigma$ and $5g\sigma$ levels at 11.6 a.u. and the $5g\sigma$ and $4f\sigma$ levels at 6.4 a.u. It is possible to solve the coupled equations connecting the two levels at a crossing or pseudocrossing within an analytic approximation due to Landau (1932), Zener (1932) and Stückelberg (1932). A discussion of the Landau-Zener-Stückelberg approximation is given in the text by Bransden (1983).

For the fully-stipped ion-atom system (A^{z+} + H(1s)) where A^{z+} is the fully-stripped ion and $z \neq 1$, the number of pseudo-

crossings is few and so the number of states strongly coupled to the initial channel is small. This means that at low velocities ($v \lesssim 1$ a.u.) capture takes place to very specific final states and other cross sections (for excitation and ionisation) are small. Let us consider the z = 2 case and refer to figure 2.4. The initial channel is represented by the $2p\sigma$ orbital which goes over to He^{2+} + H(1s) as $R \to \infty$. The $2p\sigma$ and $3d\sigma$ states have a pseudocrossing at R = 4.5 a.u. and the associated radial coupling is strong. The other coupling of importance is rotational between the $2p\pi$ and $2p\sigma$ levels which is effective for small R values as the $2p\pi$ and $2p\sigma$ levels are degenerate in the united atom limit. Hence a qualitative idea of the behaviour of the cross section may be obtained using a molecular basis comprising the $2p\sigma$, $2p\pi$ and $3d\sigma$ states. The $2p\pi$ and $3d\sigma$ levels correlate to the n = 2 level of He^+ as $R \to \infty$. Hence at low energies the dominant reaction is

$$He^{2+} + H(1s) \longrightarrow He^{+}(n = 2) + H^{+}. \qquad (2.5.31)$$

In the region of a pseudocrossing, the radial coupling matrix element varies rapidly and is difficult to calculate numerically. It is for this reason that an orthogonal transformation is sometimes made on the adiabatic basis to produce a new basis in which the radial coupling vanishes. The new basis is termed a diabatic basis (Smith, 1969; Baer, 1975; Heil and Dalgarno, 1979). In the diabatic basis the Hamiltonian H_{el} is no longer diagonal. Also levels i and j which have a pseudocrossing at R_c in the

adiabatic basis have a real crossing $(H_{el})_{ii}(R_c) = (H_{el})_{jj}(R_c)$ in the diabatic basis.

The PSS coupling matrix elements $V_{jj'}$ exhibit behaviour which is somewhat peculiar as will be demonstrated. The operator $\partial/\partial t]_{\vec{r}}$ may be written

$$\left.\frac{\partial}{\partial t}\right]_{\vec{r}} = \left.\frac{\partial}{\partial t}\right]_{\vec{r}_B} + \rho\vec{v}.\vec{\nabla}_{\vec{r}_B} \qquad (2.5.32)$$

or

$$\left.\frac{\partial}{\partial t}\right]_{\vec{r}} = \left.\frac{\partial}{\partial t}\right]_{\vec{r}_A} - (1-\rho)\vec{v}.\vec{\nabla}_{\vec{r}_A} . \qquad (2.5.33)$$

Taking equation (2.5.33) and coupling states j and k

$$V_{jk} = \langle\psi_j|\left.\frac{\partial}{\partial t}\right]_{\vec{r}_A}|\psi_k\rangle - (1-\rho)\langle\psi_j|\vec{v}.\vec{\nabla}_{\vec{r}_A}|\psi_k\rangle \qquad (2.5.34)$$

we see that V_{jk} depends upon the choice of origin as determined by ρ. If the states ψ_j and ψ_k both go over to atomic orbitals centred upon centre A, that is

$$\left.\begin{aligned}\psi_j(\vec{r};\vec{R}) &\underset{R\to\infty}{\sim} \chi_j^A(\vec{r}_A)\\ \psi_k(\vec{r};\vec{R}) &\underset{R\to\infty}{\sim} \chi_k^A(\vec{r}_A)\end{aligned}\right\} , \qquad (2.5.35)$$

then from equation (2.5.34)

$$V_{jk} = \langle\psi_j|\left.\frac{\partial}{\partial t}\right]_{\vec{r}}|\psi_k\rangle$$

$$\underset{t\to\infty}{\sim} -(1-\rho)\langle\chi_j^A(\vec{r}_A)|\vec{v}.\vec{\nabla}_{\vec{r}_A}|\chi_k^A(\vec{r}_A)\rangle \qquad (2.5.36)$$

as

$$\langle\chi_j^A(\vec{r}_A)|\left.\frac{\partial}{\partial t}\right]_{\vec{r}_A}|\chi_k^A(\vec{r}_A)\rangle = 0 . \qquad (2.5.37)$$

If states χ_j^A and χ_k^A are connected by a dipole transition then equation (2.5.36) implies that V_{jk} is not zero at very large internuclear separation which is not correct physically. Bates et al. (1953) investigated slow inelastic collisions using the PSS method. Later Bates and McCarroll (1958) improved the PSS method by including translation factors in the formulation and thereby eliminated these problems

of origin dependent couplings and non-zero asymptotic couplings.

Despite its shortcomings, the impact parameter PSS method has been used by a number of workers to calculate cross sections. The first PSS study of the He^{2+}-H system was carried out by Piacentini and Salin (1974, 1976, 1977) who calculated total cross sections. Prior to this most theoretical studies had been on the proton-hydrogen system (Chidichimo-Frank and Piacentini, 1974). (It should be noted that in the work of Piacentini and Salin, the paper of 1974 contains incorrect results. The corrected results are in their paper of 1977).

The impact parameter PSS method has been applied to collisions between fully stripped ions and atomic hydrogen. Harel and Salin (1977) took Be^{4+}, B^{5+} and O^{8+} as the fully-stripped ions. Salop and Olson (1977, 1979) have used the PSS method to study C^{6+} and O^{8+} fully-stripped ions colliding with atomic hydrogen.

2.5.3 Plane-wave translation factors

Bates and McCarroll (1958) realised that the standard PSS expansion of $\Psi(\vec{r},t)$, equation (2.5.26), did not satisfy the Schrödinger equation for large R due to the relative motion of the two centres A and B. They introduced plane-wave translation factors into the molecular basis. Considering the heteronuclear case, we separate the direct and re-arrangement channels and expand $\Psi(\vec{r},t)$ as

$$\Psi(\vec{r},t) = \sum_j \left[a_j(t)\ \Phi_j^B(\vec{r},t) + c_j(t)\ \Phi_j^A(\vec{r},t) \right] \qquad (2.5.38)$$

where the basis functions are given by

$$\Phi_j^B(\vec{r},t) = \psi_j^B(\vec{r};\vec{R}) \exp\left[-ip\vec{v}.\vec{r} - i\int_{-\infty}^{t}(\varepsilon_j^B + \tfrac{1}{2}p^2v^2)dt'\right] \quad (2.5.39)$$

$$\Phi_j^A(\vec{r},t) = \psi_j^A(\vec{r};\vec{R}) \exp\left[i(1-p)\vec{v}.\vec{r} - i\int_{-\infty}^{t}\{\varepsilon_j^A + \tfrac{1}{2}(1-p)^2v^2\}dt'\right]. \quad (2.5.40)$$

It can be shown that

$$\left\{H_{el} - i\frac{\partial}{\partial t}\right]_{\vec{r}}\right\}\Phi_j^B(\vec{r},t) = -i\left\{\left[\frac{\partial}{\partial t}\right]_{\vec{r}_B}\psi_j^B\right\}\exp\left[-ip\vec{v}.\vec{r} - i\int_{-\infty}^{t}(\varepsilon_j^B + \tfrac{1}{2}p^2v^2)dt'\right] \quad (2.5.41)$$

$$\left\{H_{el} - i\frac{\partial}{\partial t}\right]_{\vec{r}}\right\}\Phi_j^A(\vec{r},t) = -i\left\{\left[\frac{\partial}{\partial t}\right]_{\vec{r}_A}\psi_j^A\right\}\exp\left[i(1-p)\vec{v}.\vec{r} - i\int_{-\infty}^{t}\{\varepsilon_j^A + \tfrac{1}{2}(1-p)^2v^2\}dt'\right]. \quad (2.5.42)$$

Using equations (2.5.41) and (2.5.42) and the Schrödinger equation, equation (2.5.17) yields the coupled equations

$$i\left[\dot{a}_j + \sum_k N_{jk}\dot{c}_k\right] = \sum_k H_{jk}a_k + \sum_k K_{jk}c_k \quad (2.5.43a)$$

$$i\left[\sum_k N_{kj}^{*}\dot{a}_k + \dot{c}_j\right] = \sum_k K_{jk}a_k + \sum_k \bar{H}_{jk}c_k \quad (2.5.43b)$$

where

$$N_{jk} = \langle\Phi_j^B \mid \Phi_k^A\rangle$$

$$= \langle\psi_j^B|e^{i\vec{v}.\vec{r}}|\psi_k^A\rangle \exp\left[i\int_{-\infty}^{t}(\varepsilon_j^B - \varepsilon_k^A)dt'\right], \quad (2.5.44)$$

$$H_{jk} = \langle\Phi_j^B \mid H_{el} - i\frac{\partial}{\partial t}\right]_{\vec{r}} \mid \Phi_k^B\rangle$$

$$= -i\langle\psi_j^B|\left[\frac{\partial}{\partial t}\right]_{\vec{r}_B}|\psi_k^B\rangle \exp\left[i\int_{-\infty}^{t}(\varepsilon_j^B - \varepsilon_k^B)dt'\right], \quad (2.5.45)$$

$$\bar{H}_{jk} = \langle\Phi_j^A \mid H_{el} - i\frac{\partial}{\partial t}\right]_{\vec{r}} \mid \Phi_k^A\rangle$$

$$= -i\langle\psi_j^A|\left[\frac{\partial}{\partial t}\right]_{\vec{r}_A}|\psi_k^A\rangle \exp\left[i\int_{-\infty}^{t}(\varepsilon_j^A - \varepsilon_k^A)dt'\right], \quad (2.5.46)$$

$$K_{jk} = \langle \Phi_j^B | H_{el} - i\frac{\partial}{\partial t}\Big]_{\vec{r}} | \Phi_k^A \rangle$$
$$= -i\langle \psi_j^B | e^{i\vec{v}.\vec{r}} \frac{\partial}{\partial t}\Big]_{\vec{r}_A} | \psi_k^A \rangle \exp\left[i\int_{-\infty}^{t} (\varepsilon_j^B - \varepsilon_k^A)\, dt' \right] \quad (2.5.47)$$

$$\bar{K}_{jk} = \langle \Phi_j^A | H_{el} - i\frac{\partial}{\partial t}\Big]_{\vec{r}} | \Phi_k^B \rangle$$
$$= -i\langle \psi_j^A | e^{-i\vec{v}.\vec{r}} \frac{\partial}{\partial t}\Big]_{\vec{r}_B} | \psi_k^B \rangle \exp\left[i\int_{-\infty}^{t} (\varepsilon_j^A - \varepsilon_k^B)\, dt' \right]. \quad (2.5.48)$$

Comparing this with the general solution of the Schrödinger equation, we see that the basis states used here, $\Phi_j^B(\vec{r},t)$ and $\Phi_j^A(\vec{r},t)$ correspond to the general basis states $F_j(\vec{r},t)$ and $G_k(\vec{r},t)$ respectively. We note that unitarity is expressed by the relations

$$i\dot{\underset{\sim}{N}} = \underset{\sim}{\bar{K}}^{\dagger} - \underset{\sim}{K} \quad (2.5.49)$$

and
$$\underset{\sim}{H} = \underset{\sim}{H}^{\dagger} \; , \quad \underset{\sim}{\bar{H}} = \underset{\sim}{\bar{H}}^{\dagger} \; . \quad (2.5.50)$$

The introduction of plane-wave translation factors removes the problems of the PSS method. The matrix elements are not dependent upon the origin and they all vanish at large R. The disadvantage is that the exchange elements K_{jk} and $\bar{K}_{jk}$ are not easy to evaluate owing to the presence of the momentum transfer factors $\exp(\pm i\vec{v}.\vec{r})$ which also mean that the elements must be evaluated at each collision velocity required. This has resulted in there being few applications of this method.

Winter and Lane (1978) used the PSS method to investigate He^{2+}-H collisions using up to 22 basis states. Prior to this Piacentini and Salin (1974, 1976, 1977) had studied the system using the PSS method but using only three basis states ($2p\sigma$, $2p\pi$ and $3d\sigma$). In the work of Hatton

et al. (1979) and Winter and Hatton (1980) the molecular expansion method with plane-wave translation factors was used to calculate total cross sections for $^4He^{2+}$-H collisions in the $^4He^{2+}$ energy range 1-70 keV. Excellent agreement was obtained with experimental data for capture into all states down to 8 keV. However, the agreement was poor at lower energies. Winter et al. (1980) investigated the inverse process of protons on $^4He^+$ ions for centre of mass collision energies from 1.6 to 14 keV using plane-wave translation factors in the molecular basis. Their total cross section results were in very good agreement with the experimental results of Peart et al. (1977).

The difficulties associated with the matrix elements arising from using plane-wave factors has led to various approximations being tried. One is to expand $\exp(i\vec{v}.\vec{r})$ in powers of $\vec{v}$ and only retain the leading terms when low velocity collisions are being considered. Within this approximation the coupled equations become

$$i\dot{a}_j = \sum_k H_{jk}\, a_k + \sum_k K_{jk}\, c_k \qquad (2.5.51a)$$

$$i\dot{c}_j = \sum_k \overline{K}_{jk}\, a_k + \sum_k \overline{H}_{jk}\, c_k \qquad (2.5.51b)$$

where

$$K_{jk} = -i\langle \psi_j^B \left| \frac{\partial}{\partial t} \right]_{\vec{r}_A} \left| \psi_k^A \right\rangle \exp\left[i \int_{-\infty}^{t} (\varepsilon_j^B - \varepsilon_k^A)\, dt' \right] \qquad (2.5.52)$$

$$\overline{K}_{jk} = -i\langle \psi_j^A \left| \frac{\partial}{\partial t} \right]_{\vec{r}_B} \left| \psi_k^B \right\rangle \exp\left[i \int_{-\infty}^{t} (\varepsilon_j^A - \varepsilon_k^B)\, dt' \right]. \qquad (2.5.53)$$

The disadvantage of this is that unitarity is not satisfied. Briggs and Taulbjerg (1975) used exchange elements calculated at a common origin which was chosen to be the centre of mass of the system in order to force unitarity. Bates and Williams (1964) used the mean value of K_{jk} and $\overline{K}_{jk}$ to force unitarity.

One final point about the plane-wave translation factors of Bates and McCarroll (1958) is that it can be shown that they arise naturally by solving the PSS equations in the asymptotic region assuming that straight-line trajectories are used to describe the nuclear motion. This is demonstrated by Greenland (1982). He also shows how the use of a Coulomb trajectories causes the factors to be modified.

The idea of using translation factors of a type other than the plane-wave type is a further improvement of the basic method. This will be discussed in the next subsection.

2.5.4 Other translation factors

Although the introduction of plane-wave translation factors results in the theory being independent of the choice of origin and free from non-zero asymptotic couplings, the major defect of the plane-wave factor approach is that the plane-wave factors associate the electron with one or other of the two centres even in the interaction region. However, in the region of interaction the electron belongs to neither of the two centres. Thus plane-wave factors do not allow adiabatic relaxation of the system to occur.

Schneiderman and Russek (1969) proposed that the plane-wave translation factors should be modified by the introduction

of what is now termed a switching function $f(\vec{r},\vec{R})$ (Thorson and Delos, 1978a, 1978b). $\vec{r}$ is the electronic co-ordinate and $\vec{R}$ is the internuclear co-ordinate. We remember that in the PSS method the electronic wavefunction is expanded as

$$\Psi(\vec{r},t) = \sum_j a_j(t)\,\Phi_j(\vec{r},t) \qquad (2.5.54)$$

where

$$\Phi_j(\vec{r},t) = \psi_j(\vec{r};\vec{R})\exp\left[-i\int_{-\infty}^{t}\varepsilon_j(R)\,dt'\right] , \qquad (2.5.55)$$

the $\psi_j(\vec{r};\vec{R})$ being adiabatic electronic wavefunctions.

In the Bates and McCarroll (1958) treatment the $\Phi_j(\vec{r},t)$ become

$$\Phi_j(\vec{r},t) = \psi_j^{B,A}(\vec{r};\vec{R})\exp\left[\mp\tfrac{1}{2}i\vec{v}.\vec{r} - i\int_{-\infty}^{t}(\varepsilon_j^{B,A}+\tfrac{1}{8}v^2)\,dt'\right] \qquad (2.5.56)$$

where the origin position parameter p is taken as being 1/2, that is, the origin is at the centre of the internuclear line. Schneiderman and Russek (1969) working on the proton-hydrogen capture process proposed that $\Phi_j(\vec{r},t)$ should be given by

$$\Phi_j(\vec{r},t) = \psi_j(\vec{r};\vec{R})\exp\left[\tfrac{1}{2}if(\vec{r},\vec{R})\vec{v}.\vec{r} - i\int_{-\infty}^{t}\left(\varepsilon_j+\tfrac{1}{8}\int_v|\psi_j|^2\left\{\vec{\nabla}_{\vec{r}}(\vec{v}.\vec{r}f)\right\}^2 d\vec{r}\right)dt'\right] \qquad (2.5.57)$$

where $f(\vec{r},\vec{R})$ is such that

$$\left.\begin{array}{ll} f(\vec{r},\vec{R}) \to -1 & \text{for} \quad r_B \ll r_A \\ f(\vec{r},\vec{R}) \to +1 & \text{for} \quad r_A \ll r_B \end{array}\right\} \quad \text{as} \quad R \to \infty \qquad (2.5.58)$$

and

$$f(\vec{r},\vec{R}) \to 0 \quad \text{as} \quad R \to 0. \qquad (2.5.59)$$

Schneiderman and Russek give a table of conditions which they state the function $f(\vec{r},\vec{R})$ should satisfy, equations (2.5.58) and (2.5.59) being the main ones. They also propose a switching function which is of the form

$$f(\vec{r},\vec{R}) = -\cos\theta / [1 + (a/R)^3] \qquad (2.5.60)$$

where θ is the angle between $\vec{R}$ and $-\vec{r}$, and a is a relatively small distance below which the electron essentially "sees" a united atom and ceases to "belong" to either nucleus individually. We shall now obtain the coupled equations which arise when a switching function is used. The electronic wavefunction $\Psi(\vec{r},t)$ is expanded as

$$\Psi(\vec{r},t) = \sum_j a_j(t)\,\psi_j(\vec{r};\vec{R})\,\exp\left[\tfrac{1}{2} i f \vec{v}.\vec{r} - i\int_{-\infty}^{t}\left\{\varepsilon_j(R) + \tfrac{1}{8}v^2\right\}dt'\right]. \qquad (2.5.61)$$

The coupled equations are

$$i\dot{a}_j = \sum_{k\neq j} a_k V_{jk} \exp\left[i\int_{-\infty}^{t}(\varepsilon_j - \varepsilon_k)\,dt'\right] \qquad (2.5.62)$$

where

$$V_{jk} = -i\langle\psi_j|\left.\frac{\partial}{\partial t}\right]_{\vec{r}}|\psi_k\rangle - \frac{i}{2}\langle\psi_j|\vec{\nabla}_{\vec{r}}(f\vec{v}.\vec{r}).\vec{\nabla}_{\vec{r}}|\psi_k\rangle$$

$$-\frac{i}{8}\langle\psi_j|\nabla_{\vec{r}}^2(f\vec{v}.\vec{r})|\psi_k\rangle + \frac{1}{8}\langle\psi_j|[\vec{\nabla}_{\vec{r}}(f\vec{v}.\vec{r})]^2|\psi_k\rangle + \frac{1}{2}\langle\psi_j|\left.\frac{\partial}{\partial t}\right]_{\vec{r}}(f\vec{v}.\vec{r})|\psi_k\rangle. \qquad (2.5.63)$$

There have been various forms of switching function proposed. Levy and Thorson (Thorson and Levy, 1969; Levy and Thorson, 1969a, 1969b) working on impact ionisation in the proton-hydrogen system proposed the switching function

$$f(\vec{r},\vec{R}) = -\frac{(r_A^2 - r_B^2)}{r_A^2 + r_B^2} \quad . \tag{2.5.64}$$

Thorson and his collaborators (Lebeda et al. 1971; Sethu Raman et al., 1973; Rankin and Thorson, 1978) proposed switching functions which were dependent upon the particular discrete states with which they were associated. Rankin and Thorson's proposal for the switching function was

$$f_j = -\tanh R\left\{\tfrac{1}{2}\beta_j\left[(Z_A + Z_B)(r_A - r_B)/R + (Z_A - Z_B)\right] + \alpha_j \log_e(Z_B/Z_A)\right\} \tag{2.5.65}$$

where Z_A and Z_B are nuclear charges and α_j and β_j are parameters variationally chosen so that the coupling between the discrete state j and the continuum is a minimum. Rankin and Thorson were dealing with the ionisation problem but they proposed that the f_j of equation (2.5.65) should be useful for discrete-discrete close-coupling excitation and capture processes. An equivalent form of f_j is

$$f_j = -\tanh\left[\bar{\beta}_j R(\eta - \eta_j^\circ)\right] \tag{2.5.66}$$

where η is equal to $(r_A - r_B)/R$ -one of the prolate spheroidal co-ordinates (ξ, η, ϕ), and $\bar{\beta}_j$ and η_j° are parameters to be determined. An extension of the work of Rankin and Thorson (1978) was the work of Thorson et al. (1981) who

derived a set of switching functions for the H_2^+ system by an analytical two-centre decomposition of the exact molecular wavefunctions. The switching functions obtained were closely approximated by the form $f = -\tfrac{1}{2}\tanh(b\eta)$ and the parameters involved were in excellent agreement with those obtained by the earlier heuristic optimisation scheme of Rankin and Thorson.

Kimura and Thorson (1981a) used these analytically derived switching functions to calculate excitation and capture cross sections for $H^+ + H(1s) \Rightarrow H^+ + H(nl)$ collisions at projectile energies from 1 to 7 keV. Their results agreed with experiment better than in a comparable theoretical study by Crothers and Hughes (1978, 1979). In this work Crothers and Hughes took f to be a function of R only, namely $f = f(R)$ which was determined using Euler-Lagrange optimisation. However, in this work the function $f(R)$ was not a true switching function. Kimura and Thorson (1981b) have also obtained excitation and capture cross sections for He^{2+} - H(1s) collisions at He^{2+} projectile energies of 1-20 keV, and for H^+ - He^+ (1s) collisions at centre of mass energies 1.6 to 8 keV. For He^{2+} - H their results were in good agreement with the plane-wave translation factor work of Hatton et al. (1979) and Winter and Hatton (1980). However, for H^+ - He^+ there were significant differences between the results and those of Winter et al. (1980). Good agreement was obtained with experiment, though, for both He^{2+} - H and H^+ - He^+ systems. One point of note

about this work of Kimura and Thorson on the HeH^{2+} system was that they used switching functions whose parameters were determined by the optimisation scheme of Rankin and Thorson (1978). This was because the analytically derived switching functions (Thorson et al., 1981) had parameters which were in not as good agreement with the optimised ones for the HeH^{2+} system as were the parameters of the analytically derived switching functions with the optimised ones for the H_2^+ system. Recently Kimura and Thorson (1983) have used their switching functions, equation (2.5.66), to obtain total cross sections for electron capture in Li^{3+}, Be^{4+} and B^{5+} collisions with atomic hydrogen in the ground state. The projectile energy range was 1-15 keV amu^{-1}. A combination of the analytical and optimisation schemes were used to determine the parameters $\bar{\beta}_j$ and η_j^0. Good agreement was obtained with other theory and experiment.

As a follow-on to the work of Taulbjerg et al. (1975), Vaaben and Briggs (1977) and Fritsch and Wille (1977), Vaaben and Taulbjerg (1979, 1981) obtained the switching function

$$f(\vec{r},\vec{R}) = -\frac{(Z_B r_A^3 - Z_A r_B^3)}{(Z_B r_A^3 + Z_A r_B^3)} - \frac{(Z_A - Z_B)}{Z_A + Z_B} \qquad (2.5.67)$$

where $\vec{r}$ is from the centre of charge of the system. Vaaben and Taulbjerg determined their switching function using the criterion that the associated translation factors must relax adiabatically at intermediate and small internuclear distances. Vaaben and Taulbjerg (1979) have applied their

switching function to the He^{2+} - H electron capture process.

Riley and Green (1971) have applied the Euler-Lagrange variational method to the problem of determining a general plane-wave translation factor (which may include a switching function) of the electron co-ordinates and time. They considered three types of translation factor all of which resulted in complicated optimisation equations. Ponce (1979) used the Euler-Lagrange method to obtain optimised translation factors for H^+ - H collisions, the wavefunction being expanded in terms of the $1s\sigma_g$, $2p\sigma_u$ and $2p\pi_u$ molecular states. Each of these three adiabatic states was given a translation factor of the form

$$T_j = \exp\left[i f_j(\vec{r}, t)\right]. \qquad (2.5.68)$$

Crothers and Todd (1981a) have also adopted the Euler-Lagrange variational method to the determination of translation factors with specific consideration being given to adiabatic states of HeH^{2+}. This work is an improvement of the earlier work of Crothers and Hughes (1978, 1979) mentioned earlier which also used the Euler-Lagrange method. In the work of Crothers and Todd the translation factors are state dependent and are given by

$$T_j = \exp\left[i f_j(\vec{R})\vec{v}.\vec{r}/2\right] \qquad (2.5.69)$$

where $f_j(\vec{R})$ are the switching functions. Crothers and Todd (1981b) have applied their variationally determined translation factors to electron capture in He^{2+} - H collisions

for $^4He^{2+}$ collision energies of 2-25 keV. Five adiabatic molecular states ($2p\sigma$, $2p\pi$, $3d\sigma$, $3d\pi$, $2s\sigma$) were employed in the expansion of the wave-function. Good agreement was obtained with experiment for the total capture process.

An interesting approach to the switching function probem has recently been proposed by Dickinson and McCarroll (1983). They suggest a switching function $f(t)$ having the form

$$f(t) = 1 - \exp(-\gamma|t - t_0|), \quad |t| > t_0 > 0 \qquad (2.5.70a)$$

$$= 0 \qquad |t| < t_0 \qquad (2.5.70b)$$

such that in the interaction region $f(t)$ is zero (equation (2.5.70b)) and hence the scattering equations take on the usual PSS form here. However, outside this region the function $f(t)$ gives the correct asymptotic behaviour to the basis states (equation (2.5.70a)). In equation (2.5.70a) γ is a frequency which is low compared with the natural frequency of the problem. The time t_0 is chosen such that the molecular wavefunctions have assumed their atomic character. Dickinson and McCarroll term $f(t)$ an "adiabatic switching factor" (function). Allan et al. (1983) have used the adiabatic switching function to calculate electron capture cross sections in H^+ - Li collisions for centre of mass collision energies below 20 keV. Reasonable agreement was obtained in the energy range 0.5 to 8 keV but the results were very sensitive to the choice of the origin of co-ordinates, the method being essentially the PSS method with slight

modification.

The theory of electronic translational momentum and applications of the theory have produced many other scientific papers over the past few years, for example Thorson and Delos (1978a, 1978b), Green (1981a, 1981b), Green et al. (1981, 1982), Shipsey et al. (1983). A useful review of the work up to 1981 is given in the review by Delos (1981).

2.5.5. The quantum mechanical PSS method

At very low collision energies ($\lesssim 100$ eV amu^{-1}) the change in electronic energy during a collision will become comparable with the collision energy. If this is so, the impact parameter approximation may not generally be applied and a full quantum mechanical treatment is required.

In the introduction of this chapter, the basic quantum PSS method was presented. The total wavefunction was expanded in terms of molecular states, namely

$$\Psi(\vec{r},\vec{R}) = \sum_j F_j(\vec{R})\,\psi_j(\vec{r};\vec{R}). \qquad (2.5.71)$$

Projecting upon the basis set $\{\psi_k\}$ gave the coupled equations

$$\left\{\nabla_{\vec{R}}^2 + 2\mu[E-\varepsilon_j(R)]\right\} F_j(\vec{R}) = \sum_k (2\vec{A}_{jk}.\vec{\nabla}_{\vec{R}} + B_{jk})\,F_k(\vec{R}) \qquad (2.5.72)$$

where μ is the reduced mass of the nuclei and the coupling matrices $\vec{A}_{jk}$ and B_{jk} are given by

$$\vec{A}_{jk} = \int_v \psi_j^* \vec{\nabla}_{\vec{R}}\,\psi_k\,d\vec{r} \qquad (2.5.73)$$

and

$$B_{jk} = \int_v \psi^* \nabla_{\vec{R}}^2 \psi_k\,d\vec{r}. \qquad (2.5.74)$$

As an example, let us consider the simple case of symmetric resonant electron capture, namely

$$A^+ + A(1s) \longrightarrow A(1s) + A^+. \qquad (2.5.75)$$

The total wavefunction is taken as

$$\Psi(\vec{r},R) = F_g(\vec{R})\Psi_g(\vec{r};\vec{R}) + F_u(\vec{R})\Psi_u(\vec{r};\vec{R}), \qquad (2.5.76)$$

that is, a simple two-state expansion. Coupled equations analogous to those of equation (2.5.72) are obtained.

After making suitable approximations, the uncoupled equations for F_g and F_u are obtained, namely

$$-\frac{1}{2\mu}\nabla_R^2 F_g + (E-\varepsilon_g)F_g = 0 \qquad (2.5.77)$$

$$-\frac{1}{2\mu}\nabla_R^2 F_u + (E-\varepsilon_u)F_u = 0. \qquad (2.5.78)$$

We define the scattering amplitudes $f_g(\theta)$ and $f_u(\theta)$ by

$$F_{g,u}(\vec{R}) \underset{R\to\infty}{\sim} \left[\exp(i\vec{k}.\vec{R}) + \frac{1}{R}\exp(ikR) f_{g,u}(\theta)\right] \qquad (2.5.79)$$

where θ is the scattering angle. As $R\to\infty$ the initial and final atomic states are obtained from linear combinations of Ψ_g and Ψ_u

$$\left.\begin{aligned} \frac{1}{\sqrt{2}}(\Psi_g + \Psi_u) &\underset{R\to\infty}{\sim} \phi_0(\vec{r}_B) \\ \frac{1}{\sqrt{2}}(\Psi_g - \Psi_u) &\underset{R\to\infty}{\sim} \phi_0(\vec{r}_A) \end{aligned}\right\} \qquad (2.5.80)$$

where $\phi_0(\vec{r})$ is the wavefunction of the ground state of A.

The ground state eigenenergy $\mathcal{E}_0$ is given by

$$\mathcal{E}_0 = \lim_{R\to\infty} \mathcal{E}_g(R) = \lim_{R\to\infty} \mathcal{E}_u(R) . \qquad (2.5.81)$$

It can be shown that the differential cross section for electron capture is given by

$$I_{cap} = \frac{1}{4} |f_g(\theta) - f_u(\theta)|^2 . \qquad (2.5.82)$$

The total cross section is

$$\sigma = \frac{\pi}{2} \int_0^{\pi} |f_g(\theta) - f_u(\theta)|^2 \sin\theta \, d\theta . \qquad (2.5.83)$$

The scattering amplitudes $f_{g,u}(\theta)$ are calculated by using the partial wave decomposition

$$f_{g,u}(\theta) = \frac{1}{2ik} \sum_{L=0}^{\infty} (2L+1) \left[\exp(2i\eta^L_{g,u}) - 1 \right] P_L(\cos\theta) . \qquad (2.5.84)$$

The phase shifts $\eta_L^{g,u}$ are obtained from the solutions of

$$\left[\frac{d^2}{dR^2} - \frac{L(L+1)}{R^2} + k^2 - 2\mu \mathcal{E}_{g,u} \right] G^L_{g,u}(R) = 0 \qquad (2.5.85)$$

which have the asymptotic form

$$G^L_{g,u} \sim \frac{1}{k} \sin(kR - \tfrac{1}{2} L\pi + \eta^L_{g,u}) . \qquad (2.5.86)$$

The total cross section may be expressed in terms of $\eta^L_{g,u}$ by means of

$$\sigma = \frac{\pi}{k^2} \sum_{L=0}^{\infty} (2L+1) \sin^2(\eta^L_g - \eta^L_u) . \qquad (2.5.87)$$

The formula of equation (2.5.87) was used by Dalgarno

and Yadav (1953) to calculate cross sections when A was hydrogen and the incident energy range was 1eV to 10 keV. Bates and McCarroll (1958) suggested improving the expansion of equation (2.5.76) by including plane-wave translation factors. They had

$$\Psi(\vec{r},\vec{R}) = F_g(\vec{R})\chi_g(\vec{r},\vec{R}) + F_u(\vec{R})\chi_u(\vec{r},\vec{R}) \qquad (2.5.88)$$

where

$$\chi_{g,u}(\vec{r},\vec{R}) = \tfrac{1}{2}\left[\{\gamma_g + \gamma_u\}\exp\left(-\tfrac{1}{2}i\vec{v}.\vec{r}\right) \pm \{\gamma_g - \gamma_u\}\exp\left(\tfrac{1}{2}i\vec{v}.\vec{r}\right)\right] \qquad (2.5.89)$$

the plus (minus) in the middle of the expression corresponding to gerade (ungerade) symmetry.

The expression for the cross section σ for symmetrical resonance, equation (2.5.87) is not convenient at energies above about 100 eV. The wave number k becomes large and the functions $G^{L}_{g,u}$ oscillate rapidly with R. Integration of equation (2.5.85) becomes time consuming and also more partial waves are required as k increases. It is then necessary to use the impact parameter approximation. Bates et al. (1953) showed that for symmetrical resonance, using the impact parameter approximation, the cross section was given by

$$\sigma = 2\pi\int_0^\infty b\sin^2 P(b)\,db \qquad (2.5.90)$$

where

$$P(b) = \frac{1}{v}\int_b^\infty (\varepsilon_g - \varepsilon_u)\left[1 - \frac{b^2}{R^2}\right]^{-1/2} dR . \qquad (2.5.91)$$

2.6 Electron capture at high energies

Discussion of electron capture at high energies begins with the Born series. Using the impact parameter approximation the amplitude for electron capture to the k th state of $(A+e^-)$ is given by

$$c_k(b,\infty) = \lim_{t\to\infty}\int_v \chi_k^{A*}(\vec{r},t)\,\Psi(\vec{r},t)\,d\vec{r} \qquad (2.6.1)$$

where $\Psi(\vec{r},t)$ satisfies

$$\left\{H_{el} - i\frac{\partial}{\partial t}\right]_{\vec{r}}\Psi(\vec{r},t) \qquad (2.6.2)$$

and $\chi_k^A(\vec{r},t)$ is the unperturbed solution of equation (2.6.2) for $r_A \ll r_B$. It is simple to show that (Bransden 1983)

$$c_k(b,\infty) = -i\langle \chi_k^A | V^B | \Psi \rangle \qquad (2.6.3)$$

where

$$V^B = V_{eB} + V_{AB} . \qquad (2.6.4)$$

Using the iterative solution for Ψ the Born series for $c_k(b,\infty)$ can be obtained

$$c_k(b,\infty) = -i\langle \chi_k^A | V^B + V^B G^0 V^A + \ldots | \Phi_i^B \rangle \qquad (2.6.5)$$

where $\Phi_i^B(\vec{r},t)$ is the unperturbed solution of equation (2.6.2) for $r_0 \ll r_A$ corresponding to the initial state i. V^A is given by

$$V^A = V_{eA} + V_{AB} \tag{2.6.6}$$

and G° is the free particle Green's operator. Oppenheimer (1928) and Brinkman and Kramers (1930) pointed out that the internuclear potential V_{AB} should not significantly affect the electron capture probability. At high energies the paths of the nuclei will be straight and in this case the capture cross section should be independent of the internuclear potential. If V_{AB} is omitted from equation (2.6.5) the so-called Brinkman-Kramers series for $c_k(b,\infty)$ is obtained. Taking the first terms of the Born series and the Brinkman-Kramers series gives the first Born approximation and the first-order Brinkman-Kramers approximation respectively

$$c_k^{B1}(b,\infty) = -i\langle \chi_k^A | V_{eB} + V_{AB} | \Phi_i^B \rangle \tag{2.6.7}$$

$$c_k^{BK1}(b,\infty) = -i\langle \chi_k^A | V_{eB} | \Phi_i^B \rangle \tag{2.6.8}$$

($B \equiv$ Born ; $BK \equiv$ Brinkman-Kramers).

Unfortunately neither the first Born approximation nor the first Brinkman-Kramers approximation give reliable results because higher order terms are large at all energies. In the energy region up to a few MeV amu^{-1} the Brinkman-Kramers series has been shown to be slowly convergent and

not to be of practical use in calculations. Simony and McGuire (1981) have done calculations on the symmetrical resonance process

$$H^+ + H(1s) \longrightarrow H(1s) + H^+ \qquad (2.6.9)$$

and their results show that the second-order Brinkman-Kramers cross section is larger than the first-order cross section which already exceeds experimental data for energies below 3 MeV. The first-order Brinkman-Kramers cross section is of interest, though, as there is some evidence that it provides a useful estimate of the ratios of cross sections for capture into the nl excited state, especially for large n. Considering bare nuclei A and B with charges Z_A and Z_B, Sil (1954) has shown that Brinkman-Kramers cross sections can be found analytically for capture into level nl from any level of the target. For capture from the ground state into level n

$$\sigma_n^{BK1}(Z_A, Z_B) = n^2 \sigma_1^{BK1}(Z_B, Z_A/n) \qquad (2.6.10)$$

where

$$\sigma_1^{BK1}(Z_A, Z_B) = \frac{2^8 \pi (Z_A Z_B)^5}{5v^2 (Z_B^2 + \alpha^2)^5} \qquad (2.6.11)$$

and where

$$\alpha = (v^2 + Z_A^2 - Z_B^2)/2v \ . \qquad (2.6.12)$$

For large n σ_n^{BK1} decreases as $1/n^3$, which is known as the Oppenheimer rule.

At asymptotically high velocities the electron capture cross section is given by the second Born approximation. Drisko (1955) has shown that for the process of equation (2.6.9) the second Born asymptotic cross section is given by

$$\sigma_1^{B2} \sim \left(0.295 + \frac{5\pi v}{2^{12}}\right)\tilde{\sigma}_1^{BK1} \qquad (2.6.13)$$

where $\tilde{\sigma}_1^{BK1}$ is the asymptotic first-order Brinkman-Kramers cross section given by

$$\tilde{\sigma}_1^{BK1} = \frac{2^{18}\pi}{5v^{12}} . \qquad (2.6.14)$$

The result of equation (2.6.13) shows that the v^{-12} behaviour arising from the first-order term is overtaken by a v^{-11} behaviour arising from the second-order term. Drisko gave arguments to show that the third Born term modifies the coefficient 0.295 in equation (2.6.13) to 0.315, but does not alter the v^{-11} behaviour at large v. This was confirmed by Shakeshaft (1978a).

An interesting fact is that Thomas (1927) predicted the v^{-11} behaviour of the cross section using a classical model. In this binary encounter model of Thomas, the electron acquires the speed of the projectile, v and is deflected toward the target nucleus. Then the electron is deflected into a direction parallel with the projectile with loss

of speed. A discrete atomic orbital expansion cannot represent these intermediate states and this is why the continuum must be accounted for, especially at high energies. A most satisfactory model of high-energy electron capture is the continuum distorted wave (CDW) model of Cheshire (1964) which has been applied to electron capture from hydrogen by protons and alpha particles (He^{2+}) for energies above 25 keV amu^{-1} and up to 10 MeV amu^{-1} (Belkic and Gayet, 1977). Good agreement with experiment was obtained for total capture and capture into s states. Belkic and McCarroll (1977) have used the CDW model to study capture by highly charged ions ($1 < Z_A < 30$) from atomic hydrogen. The results agree well with experiment. Belkic et al. (1979) have produced an excellent review on electron capture in high-energy ion-atom collisions.

This brings Chapter 2 to a close. In the next chapter the presentation of the work of this thesis will be started.

CHAPTER 3

TWO - CENTRE ATOMIC BASIS METHOD USING SWITCHING FUNCTIONS : BASIC THEORY

3.1 Introduction

In this chapter the basic theory of this work will be presented. We shall be considering the single-electron capture process

$$A + (B + e^-) \longrightarrow (A + e^-) + B \qquad (3.1.1)$$

where A is the fully-stripped projectile ion and $(B+e^-)$ is the single-electron atom or ion target.

The co-ordinate system used is shown in figure 3.1. The origin O of the system is at the mid-point of the inter-nuclear line AB. The (x,y,z) co-ordinate frame is fixed in space with the x- and z- axes as shown. The y- axis is out of the paper.

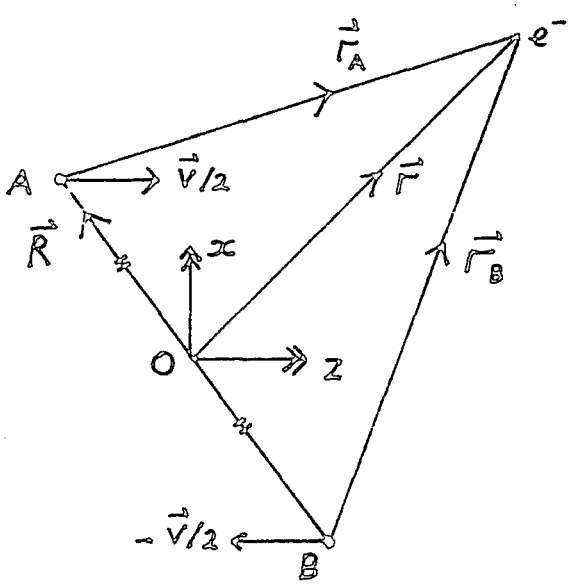

Fig. 3.1
The co-ordinate system. (Space-fixed x,y,z co-ordinates).

3.2 Nuclear motion

In this section the theory of the nuclear motion will be discussed. The motion is treated classically as the impact parameter approximation will be employed. Thus we may consider the two ion-centres, A and B, as travelling along classical trajectories, their motion being described mathematically by a general trajectory equation

$$\vec{R} = \vec{R}(\vec{b}, t) \qquad (3.2.1)$$

where $\vec{R}$ is the internuclear vector (figure 3.1) and $\vec{b}$ is the two-dimensional impact parameter vector and t is the time variable. In general the impact parameter vector is defined as the vector perpendicular to the linear trajectories produced by having no internuclear potential, (figure 3.2), (dashed lines).

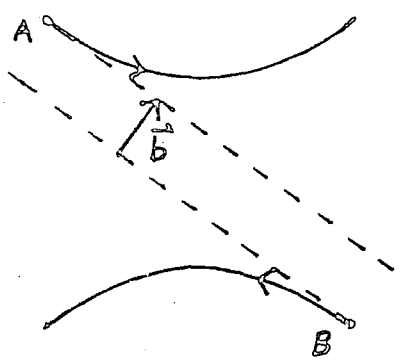

Fig. 3.2

Diagram defining impact parameter vector $\vec{b}$ for non-linear trajectories.

At high impact velocities the trajectories are very near being linear, the actual scattering being mainly in the forward direction. However, at low velocities the internuclear potential $V_{AB} = Z_A Z_B / R$ has a greater effect and it is more appropriate to use Coulomb trajectories. We shall see, however, that the straight-line trajectory case (much used in work on electron capture) is simply a special case of the Coulomb trajectory with the potential "turned

off".

The problem of the dynamics of two particles repelling one another by a Coulomb-type potential $\mathcal{J}/R$ is well-known and is treated in most standard texts on classical mechanics, for example Landau and Lifshitz (1960). The potential is $\mathcal{J}/R$ with $\mathcal{J} > 0$ in our case. It is both central (dependent only on $|\vec{R}|$) and repulsive. The motion can be written in terms of the following parametric equations

$$R = (\gamma^2 + b^2)^{1/2} \cosh w + \gamma, \qquad (3.2.2)$$

$$t = \frac{1}{v_i}\left[(\gamma^2 + b^2)^{1/2} \sinh w + \gamma w\right], \qquad (3.2.3)$$

where $$\gamma = \mathcal{J}/\mu v_i^2. \qquad (3.2.4)$$

μ is the reduced mass of the two nuclei A and B, v_i is the initial relative velocity of A and B, b is the modulus of $\vec{b}$ and w is the parameter coupling eqs. (3.2.2) and (3.2.3).

It is normal to introduce another parameter τ given by

$$\tau = (\gamma^2 + b^2)^{1/2} \sinh w. \qquad (3.2.5)$$

We see from equations (3.2.2) and (3.2.3) that when w (or τ) is equal to zero, that R is a minimum and t is equal to zero.

If we set $\mathcal{J} = 0$, that is "turn off" the internuclear potential, we see from equation (3.2.4) that $\gamma = 0$ and equations (3.2.2) and (3.2.3) reduce to

$$R = b \cosh w , \tag{3.2.6}$$

$$t = \frac{b}{v_i} \sinh w . \tag{3.2.7}$$

This is consistent with the straight-line trajectory relation

$$R^2 = b^2 + v_i^2 t^2 \tag{3.2.8}$$

which is obtained from the well-known straight-line trajectory equation

$$\vec{R} = \vec{b} + \vec{v} t \tag{3.2.9}$$

with $$\vec{b} \cdot \vec{v} = 0 , \tag{3.2.10}$$

and where $\vec{v} = \vec{v}_i$ = constant vector.

If the straight-line trajectory approach is used the diagram shown in figure 3.1 must be amended. Figure 3.3 shows the well-known diagram for the co-ordinates used when straight-line trajectories are employed. We note that $Z = vt$.

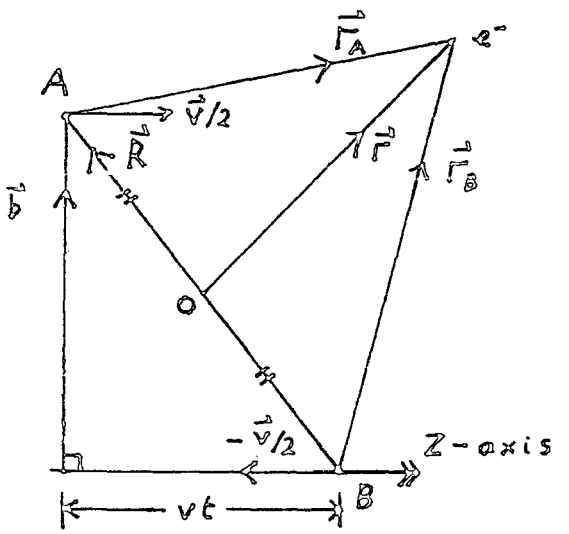

Fig. 3.3

The co-ordinate system (straight line trajectory case).

The quantity γ defined by equation (3.2.4) measures the strength of the Coulomb repulsion. Clearly as v_i decreases the trajectories (which are hyperbolae) will become more curved and similarly as ζ increases they become more curved. For electron capture $\zeta = Z_A Z_B$ and so increasing nuclear charge will lead to more curved trajectories.

The formulation given in the next section will assume the use of a general trajectory, and the velocity $\vec{v}$ is a function of t. For the straight-line case we take $\vec{v}$ as being constant.

3.3 Formulation of the problem

This section will present the basic theoretical formulation of the two-centre atomic basis method using a switching function. As in most theoretical work on electron capture, much of the work centres around the quantum mechanical matrix elements, namely their derivation and evaluation. Chapter 4 will be devoted to discussing the evaluation of the matrix elements, but in this chapter we shall deal with their derivation and also simplifications that can be made to their form.

We describe the electronic motion using the time-dependent Schrödinger equation in the impact parameter approximation

$$\left\{ H_{el} - i \frac{\partial}{\partial t} \right]_{\vec{r}} \right\} \Psi(\vec{r}, t) = 0 \qquad (3.3.1)$$

where $\Psi(\vec{r}, t)$ is the electronic wavefunction, and H_{el} is the electronic Hamiltonian given by

$$H_{el} = -\frac{1}{2} \nabla_{\vec{r}}^2 + V_{eA} + V_{eB} + V_{AB} . \qquad (3.3.2)$$

The potentials in H_{el} are

$$V_{eA} = -\frac{Z_A}{r_A}, \quad V_{eB} = -\frac{Z_B}{r_B} \quad \& \quad V_{AB} = \frac{Z_A Z_B}{R} . \qquad (3.3.3)$$

The close-coupling approximation (Chapter 2, p 36) is used, the trial wavefunction $\Psi_T(\vec{r}, t)$ being expanded in terms of two sets of orthonormal basis functions $F_j^s(\vec{r}, t)$ and $G_k^s(\vec{r}, t)$ as follows

$$\Psi_T(\vec{r}, t) = \sum_{j=1}^{M} a_j(t) F_j^s(\vec{r}, t) + \sum_{k=1}^{N} c_k(t) G_k^s(\vec{r}, t) . \qquad (3.3.4)$$

We obtain the usual coupled first-order differential equations for the coefficients $a_j(t)$ and $c_k(t)$ (written in matrix form)

$$i\left[\dot{\underset{\sim}{a}}(t) + \underset{\sim}{N}\,\dot{\underset{\sim}{c}}(t)\right] = \underset{\sim}{H}\,\underset{\sim}{a}(t) + \underset{\sim}{K}\,\underset{\sim}{c}(t) \qquad (3.3.5a)$$

$$i\left[\underset{\sim}{N}^{\dagger}\dot{\underset{\sim}{a}}(t) + \dot{\underset{\sim}{c}}(t)\right] = \bar{\underset{\sim}{K}}\,\underset{\sim}{a}(t) + \bar{\underset{\sim}{H}}\,\underset{\sim}{c}(t) \qquad (3.3.5b)$$

which are to be solved subject to the boundary conditions

$$a_j(-\infty) = \delta_{ji} \quad , \quad c_k(-\infty) = 0 \qquad (3.3.6)$$

where index i corresponds to the initial state of $(B + e^-)$.

The capture amplitudes $c_{ki}(\vec{b})$ for capture from the i th state of $(B+e^-)$ to the k th state of $(A + e^-)$ are given by

$$c_{ki}(\vec{b}) = \lim_{t \to \infty} c_k(t) . \qquad (3.3.7)$$

The total electron capture cross sections ($i \to k$) are given by

$$\sigma_{ki} = \int |C_{ki}(\vec{b})|^2 d^2\vec{b} \qquad (3.3.8)$$

which, owing to azimuthal symmetry, may be written

$$\sigma_{ki} = 2\pi \int_0^\infty |C_k(+\infty)|^2 b\, db \ . \qquad (3.3.9)$$

The units of σ_{ki} are a_o^2 where a_o is the Bohr radius (5.29×10^{-9}cm).

The matrix elements of the matrices in equations (3.3.5a) and (3.3.5b) are in Dirac notation, given by

$$N_{jk} = \langle F_j^s | G_k^s \rangle \qquad (3.3.10)$$

$$H_{jk} = \langle F_j^s | H_{el} - i\, \partial/\partial t]_{\vec{r}} | F_k^s \rangle \qquad (3.3.11)$$

$$\bar{H}_{jk} = \langle G_j^s | H_{el} - i\, \partial/\partial t]_{\vec{r}} | G_k^s \rangle \qquad (3.3.12)$$

$$K_{jk} = \langle F_j^s | H_{el} - i\, \partial/\partial t]_{\vec{r}} | G_k^s \rangle \qquad (3.3.13)$$

$$\bar{K}_{jk} = \langle G_j^s | H_{el} - i\, \partial/\partial t]_{\vec{r}} | F_k^s \rangle \ . \qquad (3.3.14)$$

The theory presented so far applies for any two orthonormal sets of basis functions $F_j^s(\vec{r},t)$ and $G_k^s(\vec{r},t)$ which satisfy

$$F_j^s(\vec{r},t) \xrightarrow[r_B \ll r_A]{t \to \pm\infty} \phi_j^B(\vec{r}_B) \exp -i\left(\varepsilon_j t + \tfrac{1}{8}v^2 t + \tfrac{1}{2}\vec{v}.\vec{r}\right) \qquad (3.3.15)$$

$$G_k^s(\vec{r},t) \xrightarrow[r_A \ll r_B]{t \to \pm\infty} \chi_k^A(\vec{r}_A) \exp -i\left(\eta_k t + \tfrac{1}{8}v^2 t - \tfrac{1}{2}\vec{v}.\vec{r}\right), \qquad (3.3.16)$$

the asymptotic boundary conditions on $F_j^s(\vec{r},t)$ and $G_k^s(\vec{r},t)$. As usual, $\phi_j^B(\vec{r}_B)$ are atomic eigenfunctions for the $(B+e^-)$ system with energy eigenvalues ε_j, and $\chi_k^A(\vec{r}_A)$ are atomic eigenfunctions for the $(A+e^-)$ system with energy eigenvalues η_k.

We now specify the form of the basis functions $F_j^s(\vec{r},t)$ and $G_k^s(\vec{r},t)$.

$$F_j^s(\vec{r},t) = \phi_j^B(\vec{r}_B)\exp -i\left[\varepsilon_j t + \frac{1}{8}v^2 t - \frac{1}{2}f_j(\vec{r},\vec{R})\vec{v}\cdot\vec{r}\right] \quad (3.3.17)$$

$$G_k^s(\vec{r},t) = \chi_k^A(\vec{r}_A)\exp -i\left[\eta_k t + \frac{1}{8}v^2 t - \frac{1}{2}g_k(\vec{r},\vec{R})\vec{v}\cdot\vec{r}\right]. \quad (3.3.18)$$

The functions $f_j(\vec{r},\vec{R})$ and $g_k(\vec{r},\vec{R})$ are the switching functions. Their main properties are

$$\begin{aligned} f_j(\vec{r},\vec{R}) &\to -1 \quad \text{for} \quad r_B \ll r_A \quad \text{as} \quad R\to\infty \\ g_k(\vec{r},\vec{R}) &\to -1 \quad \text{for} \quad r_B \ll r_A \quad \text{as} \quad R\to\infty, \end{aligned} \quad (3.3.19)$$

and

$$\begin{aligned} f_j(\vec{r},\vec{R}) &\to +1 \quad \text{for} \quad r_A \ll r_B \quad \text{as} \quad R\to\infty \\ g_k(\vec{r},\vec{R}) &\to +1 \quad \text{for} \quad r_A \ll r_B \quad \text{as} \quad R\to\infty. \end{aligned} \quad (3.3.20)$$

Also their united atom limit is

$$\left.\begin{aligned} f_j(\vec{r},\vec{R}) &\to 0 \\ g_k(\vec{r},\vec{R}) &\to 0 \end{aligned}\right\} \quad \text{as} \quad R\to 0. \quad (3.3.21)$$

We note that in general the switching functions may be channel dependent.

The basis functions defined by equations (3.3.17) and (3.3.18) are orthonormal with respect to one another by virtue of the fact that the atomic eigenfunctions are orthonormal with one another, that is

$$\langle F_j^s | F_m^s \rangle = \delta_{jm} \quad , \quad \langle G_k^s | G_n^s \rangle = \delta_{kn} \, , \tag{3.3.22}$$

as

$$\langle \phi_j^B | \phi_m^B \rangle = \delta_{jm} \, , \quad \langle \chi_k^A | \chi_n^A \rangle = \delta_{kn} \, . \tag{3.3.23}$$

We now make the simplification of replacing the channel dependent switching functions $f_j(\vec{r},\vec{R})$ and $g_k(\vec{r},\vec{R})$ by a single channel independent switching function $f(\vec{r},\vec{R})$ and henceforth the theory and results presented will be for this specific case. The conditions (3.3.19), (3.3.20) and (3.3.21) now reduce to

$$f(\vec{r},\vec{R}) \rightarrow -1 \qquad \text{for } r_B \ll r_A \text{ as } R \rightarrow \infty \, , \tag{3.3.24}$$

$$f(\vec{r},\vec{R}) \rightarrow +1 \qquad \text{for } r_A \ll r_B \text{ as } R \rightarrow \infty \, , \tag{3.3.25}$$

and

$$f(\vec{r},\vec{R}) \rightarrow 0 \qquad \text{as} \quad R \rightarrow 0 \, . \tag{3.3.26}$$

For completeness we note the new form of the basis functions using $f(\vec{r},\vec{R})$ instead of $f_j(\vec{r},\vec{R})$ and $g_k(\vec{r},\vec{R})$.

$$F_j^s(\vec{r},t) = \phi_j^B(\vec{r}_B) \exp -i\left[\varepsilon_j t + \tfrac{1}{8} v^2 t - \tfrac{1}{2} f(\vec{r},\vec{R})\, \vec{v}.\vec{r}\right], \tag{3.3.27}$$

$$G_k^s(\vec{r},t) = \chi_k^A(\vec{r}_A) \exp -i\left[\eta_k t + \tfrac{1}{8} v^2 t - \tfrac{1}{2} f(\vec{r},\vec{R})\, \vec{v}.\vec{r}\right]. \tag{3.3.28}$$

We now require the explicit expressions for the matrix elements (3.3.10) to (3.3.14) obtained when we use the basis functions $F_j^s(\vec{r},t)$ and $G_k^s(\vec{r},t)$ as given by equations (3.3.27) and (3.3.28). The expression for the overlap matrix N_{jk} is trivial. It is

$$N_{jk} = \langle \phi_j^B(\vec{r}_B) | \chi_k^A(\vec{r}_A) \rangle \exp i(\varepsilon_j - \eta_k)t \,. \qquad (3.3.29)$$

The expressions for the direct matrix elements H_{jk} and $\bar{H}_{jk}$, and the exchange matrix elements K_{jk} and $\bar{K}_{jk}$ are obtained by considering the effect of the operators H_{el} and $-i\,\partial/\partial t]_{\vec{r}}$ upon the basis functions $F_j^s(\vec{r},t)$ and $G_k^s(\vec{r},t)$. Algebraic manipulation then yields the expressions for the elements. The expressions resulting from H_{el} and $-i\,\partial/\partial t]_{\vec{r}}$ operating upon the basis functions are quite lengthy. Their derivation and they themselves are given in Apprndix A1.

The direct and exchange matrix elements are given on the following four pages.

Direct 1 matrix $\underline{\underline{H}}$

$$
\begin{aligned}
H_{jk} = {} & \langle \phi_j^B(\vec{r}_B) \mid V_{eA} \mid \phi_k^B(\vec{r}_B) \rangle e^{i(\varepsilon_j - \varepsilon_k)t} \\
& - \frac{i}{2} \langle \phi_j^B(\vec{r}_B) \mid f\, \vec{v}.\vec{\nabla}_{\vec{r}} \mid \phi_k^B(\vec{r}_B) \rangle e^{i(\varepsilon_j - \varepsilon_k)t} \\
& - \frac{i}{2} \langle \phi_j^B(\vec{r}_B) \mid (\vec{v}.\vec{r})(\vec{\nabla}_{\vec{r}} f).\vec{\nabla}_{\vec{r}} \mid \phi_k^B(\vec{r}_B) \rangle e^{i(\varepsilon_j - \varepsilon_k)t} \\
& - \frac{i}{2} \langle \phi_j^B(\vec{r}_B) \mid \vec{v}.\vec{\nabla}_{\vec{r}} f \mid \phi_k^B(\vec{r}_B) \rangle e^{i(\varepsilon_j - \varepsilon_k)t} \\
& - \frac{i}{4} \langle \phi_j^B(\vec{r}_B) \mid (\vec{v}.\vec{r}) \nabla_{\vec{r}}^2 f \mid \phi_k^B(\vec{r}_B) \rangle e^{i(\varepsilon_j - \varepsilon_k)t} \\
& + \frac{v^2}{8} \langle \phi_j^B(\vec{r}_B) \mid f^2 \mid \phi_k^B(\vec{r}_B) \rangle e^{i(\varepsilon_j - \varepsilon_k)t} \\
& + \frac{i}{4} \langle \phi_j^B(\vec{r}_B) \mid f(\vec{v}.\vec{r})\, \vec{v}.\vec{\nabla}_{\vec{r}} f \mid \phi_k^B(\vec{r}_B) \rangle e^{i(\varepsilon_j - \varepsilon_k)t} \\
& + \frac{1}{8} \langle \phi_j^B(\vec{r}_B) \mid (\vec{v}.\vec{r})^2 (\vec{\nabla}_{\vec{r}} f)^2 \mid \phi_k^B(\vec{r}_B) \rangle e^{i(\varepsilon_j - \varepsilon_k)t} \\
& + \frac{1}{2} \langle \phi_j^B(\vec{r}_B) \mid (\vec{v}.\vec{r}) \left\{ \frac{\partial}{\partial t} \right]_{\vec{r}} f \Big\} \mid \phi_k^B(\vec{r}_B) \rangle e^{i(\varepsilon_j - \varepsilon_k)t} \\
& + \frac{i}{2} \langle \phi_j^B(\vec{r}_B) \mid f\vec{r}.\frac{d\vec{v}}{dt} \mid \phi_k^B(\vec{r}_B) \rangle e^{i(\varepsilon_j - \varepsilon_k)t} \\
& - \frac{i}{2} \langle \phi_j^B(\vec{r}_B) \mid \vec{v}.\vec{\nabla}_{\vec{r}} \mid \phi_k^B(\vec{r}_B) \rangle e^{i(\varepsilon_j - \varepsilon_k)t} \\
& + \left\{ V_{AB} - \frac{1}{8}\left[v^2 + t\,\frac{d(v^2)}{dt} \right] \right\} \delta_{jk} .
\end{aligned}
\tag{3.3.30}
$$

Direct 2 matrix $\overline{\overline{H}}$

$$\overline{H}_{jk} = \langle \chi_j^A(\vec{r}_A) | V_{eB} | \chi_k^A(\vec{r}_A) \rangle e^{i(\eta_j - \eta_k)t}$$

$$- \frac{i}{2} \langle \chi_j^A(\vec{r}_A) | f \vec{v}.\vec{\nabla}_r | \chi_k^A(\vec{r}_A) \rangle e^{i(\eta_j - \eta_k)t}$$

$$- \frac{i}{2} \langle \chi_j^A(\vec{r}_A) | (\vec{v}.\vec{r})(\vec{\nabla}_r f).\vec{\nabla}_r | \chi_k^A(\vec{r}_A) \rangle e^{i(\eta_j - \eta_k)t}$$

$$- \frac{i}{2} \langle \chi_j^A(\vec{r}_A) | \vec{v}.\vec{\nabla}_r f | \chi_k^A(\vec{r}_A) \rangle e^{i(\eta_j - \eta_k)t}$$

$$- \frac{i}{4} \langle \chi_j^A(\vec{r}_A) | (\vec{v}.\vec{r}) \nabla_r^2 f | \chi_k^A(\vec{r}_A) \rangle e^{i(\eta_j - \eta_k)t}$$

$$+ \frac{v^2}{8} \langle \chi_j^A(\vec{r}_A) | f^2 | \chi_k^A(\vec{r}_A) \rangle e^{i(\eta_j - \eta_k)t}$$

$$+ \frac{1}{4} \langle \chi_j^A(\vec{r}_A) | f (\vec{v}.\vec{r}) \vec{v}.\vec{\nabla}_r f | \chi_k^A(\vec{r}_A) \rangle e^{i(\eta_j - \eta_k)t}$$

$$+ \frac{1}{8} \langle \chi_j^A(\vec{r}_A) | (\vec{v}.\vec{r})^2 (\vec{\nabla}_r f)^2 | \chi_k^A(\vec{r}_A) \rangle e^{i(\eta_j - \eta_k)t}$$

$$+ \frac{1}{2} \langle \chi_j^A(\vec{r}_A) | (\vec{v}.\vec{r}) \left\{ \left[\frac{\partial}{\partial t} \right]_{\vec{r}} f \right\} | \chi_k^A(\vec{r}_A) \rangle e^{i(\eta_j - \eta_k)t}$$

$$+ \frac{1}{2} \langle \chi_j^A(\vec{r}_A) | f \vec{r}.\frac{d\vec{v}}{dt} | \chi_k^A(\vec{r}_A) \rangle e^{i(\eta_j - \eta_k)t}$$

$$+ \frac{i}{2} \langle \chi_j^A(\vec{r}_A) | \vec{v}.\vec{\nabla}_r | \chi_k^A(\vec{r}_A) \rangle e^{i(\eta_j - \eta_k)t}$$

$$+ \left\{ V_{AB} - \frac{1}{8} \left[v^2 + t \frac{d(v^2)}{dt} \right] \right\} \delta_{jk} . \qquad (3.3.31)$$

Exchange 1 matrix K

$$
\begin{aligned}
K_{jk} = {} & \langle \phi_j^B(\vec{r}_B) | V_{eB} | \chi_k^A(\vec{r}_A) \rangle e^{i(\varepsilon_j - \eta_k)t} \\
& - \frac{i}{2} \langle \phi_j^B(\vec{r}_B) | f \vec{v} . \vec{\nabla}_r | \chi_k^A(\vec{r}_A) \rangle e^{i(\varepsilon_j - \eta_k)t} \\
& - \frac{i}{2} \langle \phi_j^B(\vec{r}_B) | (\vec{v} . \vec{r})(\vec{\nabla}_r f) . \vec{\nabla}_r | \chi_k^A(\vec{r}_A) \rangle e^{i(\varepsilon_j - \eta_k)t} \\
& - \frac{i}{2} \langle \phi_j^B(\vec{r}_B) | \vec{v} . \vec{\nabla}_r f | \chi_k^A(\vec{r}_A) \rangle e^{i(\varepsilon_j - \eta_k)t} \\
& - \frac{i}{4} \langle \phi_j^B(\vec{r}_B) | (\vec{v} . \vec{r}) \nabla_r^2 f | \chi_k^A(\vec{r}_A) \rangle e^{i(\varepsilon_j - \eta_k)t} \\
& + \frac{v^2}{8} \langle \phi_j^B(\vec{r}_B) | f^2 | \chi_k^A(\vec{r}_A) \rangle e^{i(\varepsilon_j - \eta_k)t} \\
& + \frac{1}{4} \langle \phi_j^B(\vec{r}_B) | f (\vec{v} . \vec{r}) \vec{v} . \vec{\nabla}_r f | \chi_k^A(\vec{r}_A) \rangle e^{i(\varepsilon_j - \eta_k)t} \\
& + \frac{1}{8} \langle \phi_j^B(\vec{r}_B) | (\vec{v} . \vec{r})^2 (\vec{\nabla}_r f)^2 | \chi_k^A(\vec{r}_A) \rangle e^{i(\varepsilon_j - \eta_k)t} \\
& + \frac{1}{2} \langle \phi_j^B(\vec{r}_B) | (\vec{v} . \vec{r}) \left\{ \left[\frac{\partial}{\partial t} \right]_{\vec{r}} f \right\} | \chi_k^A(\vec{r}_A) \rangle e^{i(\varepsilon_j - \eta_k)t} \\
& + \frac{1}{2} \langle \phi_j^B(\vec{r}_B) | f \vec{r} . \frac{d\vec{v}}{dt} | \chi_k^A(\vec{r}_A) \rangle e^{i(\varepsilon_j - \eta_k)t} \\
& + \frac{i}{2} \langle \phi_j^B(\vec{r}_B) | \vec{v} . \vec{\nabla}_r | \chi_k^A(\vec{r}_A) \rangle e^{i(\varepsilon_j - \eta_k)t} \\
& + \left\{ V_{AB} - \frac{1}{8} \left[v^2 + t \frac{d(v^2)}{dt} \right] \right\} N_{jk} \, .
\end{aligned}
$$

(3.3.32)

Exchange 2 matrix $\overline{K}$

$$\overline{K}_{jk} = \langle \chi_j^A(\vec{r}_A) | V_{eA} | \phi_k^B(\vec{r}_B) \rangle e^{i(\eta_j - \varepsilon_k)t}$$

$$- \frac{i}{2} \langle \chi_j^A(\vec{r}_A) | f \vec{v}.\vec{\nabla}_r | \phi_k^B(\vec{r}_B) \rangle e^{i(\eta_j - \varepsilon_k)t}$$

$$- \frac{i}{2} \langle \chi_j^A(\vec{r}_A) | (\vec{v}.\vec{r})(\vec{\nabla}_r f).\vec{\nabla}_r | \phi_k^B(\vec{r}_B) \rangle e^{i(\eta_j - \varepsilon_k)t}$$

$$- \frac{i}{2} \langle \chi_j^A(\vec{r}_A) | \vec{v}.\vec{\nabla}_r f | \phi_k^B(\vec{r}_B) \rangle e^{i(\eta_j - \varepsilon_k)t}$$

$$- \frac{i}{4} \langle \chi_j^A(\vec{r}_A) | (\vec{v}.\vec{r}) \nabla_r^2 f | \phi_k^B(\vec{r}_B) \rangle e^{i(\eta_j - \varepsilon_k)t}$$

$$+ \frac{v^2}{8} \langle \chi_j^A(\vec{r}_A) | f^2 | \phi_k^B(\vec{r}_B) \rangle e^{i(\eta_j - \varepsilon_k)t}$$

$$+ \frac{1}{4} \langle \chi_j^A(\vec{r}_A) | f (\vec{v}.\vec{r}) \vec{v}.\vec{\nabla}_r f | \phi_k^B(\vec{r}_B) \rangle e^{i(\eta_i - \varepsilon_k)t}$$

$$+ \frac{1}{8} \langle \chi_j^A(\vec{r}_A) | (\vec{v}.\vec{r})^2 (\vec{\nabla}_r f)^2 | \phi_k^B(\vec{r}_B) \rangle e^{i(\eta_j - \varepsilon_k)t}$$

$$+ \frac{1}{2} \langle \chi_j^A(\vec{r}_A) | (\vec{v}.\vec{r}) \left\{ \left[\frac{\partial}{\partial t} \right]_{\vec{r}} f \right\} | \phi_k^B(\vec{r}_B) \rangle e^{i(\eta_j - \varepsilon_k)t}$$

$$+ \frac{1}{2} \langle \chi_j^A(\vec{r}_A) | f \vec{r}.\frac{d\vec{v}}{dt} | \phi_k^B(\vec{r}_B) \rangle e^{i(\eta_j - \varepsilon_k)t}$$

$$- \frac{i}{2} \langle \chi_j^A(\vec{r}_A) | \vec{v}.\vec{\nabla}_r | \phi_k^B(\vec{r}_B) \rangle e^{i(\eta_j - \varepsilon_k)t}$$

$$+ \left\{ V_{AB} - \frac{1}{8} \left[v^2 + t \frac{d(v^2)}{dt} \right] \right\} N_{kj}^{*} . \qquad (3.3.33)$$

For ease of reference we denote the individual matrix elements as follows:-

Overlap

$$N_{jk}^{BA} \equiv \langle \phi_j^B(\vec{r}_B) | \chi_k^A(\vec{r}_A) \rangle . \qquad (3.3.34)$$

Direct 1

$$A_{jk}^{BB} \equiv \langle \phi_j^B(\vec{r}_B) | V_{cA} | \phi_k^B(\vec{r}_B) \rangle . \qquad (3.3.35)$$

$$B_{jk}^{BB} \equiv \langle \phi_j^B(\vec{r}_B) | f \vec{v}.\vec{\nabla}_r | \phi_k^B(\vec{r}_B) \rangle . \qquad (3.3.36)$$

$$C_{jk}^{BB} \equiv \langle \phi_j^B(\vec{r}_B) | (\vec{v}.\vec{r})(\vec{\nabla}_r f).\vec{\nabla}_r | \phi_k^B(\vec{r}_B) \rangle . \qquad (3.3.37)$$

$$D_{jk}^{BB} \equiv \langle \phi_j^B(\vec{r}_B) | \vec{v}.\vec{\nabla}_r f | \phi_k^B(\vec{r}_B) \rangle . \qquad (3.3.38)$$

$$F_{jk}^{BB} \equiv \langle \phi_j^B(\vec{r}_B) | (\vec{v}.\vec{r}) \nabla_r^2 f | \phi_k^B(\vec{r}_B) \rangle . \qquad (3.3.39)$$

$$G_{jk}^{BB} \equiv \langle \phi_j^B(\vec{r}_B) | f^2 | \phi_k^B(\vec{r}_B) \rangle . \qquad (3.3.40)$$

$$H_{jk}^{BB} \equiv \langle \phi_j^B(\vec{r}_B) | f (\vec{v}.\vec{r}) \vec{v}.\vec{\nabla}_r f | \phi_k^B(\vec{r}_B) \rangle . \qquad (3.3.41)$$

$$J_{jk}^{BB} \equiv \langle \phi_j^B(\vec{r}_B) | (\vec{v}.\vec{r})^2 (\vec{\nabla}_r f)^2 | \phi_k^B(\vec{r}_B) \rangle . \qquad (3.3.42)$$

$$K_{jk}^{BB} \equiv \langle \phi_j^B(\vec{r}_B) | (\vec{v}.\vec{r}) \left\{ \left[\frac{\partial}{\partial t} \right]_{\vec{r}} f \right\} | \phi_k^B(\vec{r}_B) \rangle . \qquad (3.3.43)$$

$$\Lambda_{jk}^{BB} \equiv \langle \phi_j^B(\vec{r}_B) | f \vec{r}.\frac{d\vec{v}}{dt} | \phi_k^B(\vec{r}_B) \rangle . \qquad (3.3.44)$$

$$L_{jk}^{BB} \equiv \langle \phi_j^B(\vec{r}_B) | \vec{v}.\vec{\nabla}_r | \phi_k^B(\vec{r}_B) \rangle . \qquad (3.3.45)$$

Direct 2

$$A_{jk}^{AA} \equiv \langle \chi_j^A(\vec{r}_A) | V_{ee} | \chi_k^A(\vec{r}_A) \rangle . \tag{3.3.46}$$

$$B_{jk}^{AA} \equiv \langle \chi_j^A(\vec{r}_A) | f \vec{v} . \vec{\nabla}_r | \chi_k^A(\vec{r}_A) \rangle . \tag{3.3.47}$$

$$C_{jk}^{AA} \equiv \langle \chi_j^A(\vec{r}_A) | (\vec{v} . \vec{r})(\vec{\nabla}_r f) . \vec{\nabla}_r | \chi_k^A(\vec{r}_A) \rangle . \tag{3.3.48}$$

$$D_{jk}^{AA} \equiv \langle \chi_j^A(\vec{r}_A) | \vec{v} . \vec{\nabla}_r f | \chi_k^A(\vec{r}_A) \rangle . \tag{3.3.49}$$

$$F_{jk}^{AA} \equiv \langle \chi_j^A(\vec{r}_A) | (\vec{v} . \vec{r}) \nabla_r^2 f | \chi_k^A(\vec{r}_A) \rangle . \tag{3.3.50}$$

$$G_{jk}^{AA} \equiv \langle \chi_j^A(\vec{r}_A) | f^2 | \chi_k^A(\vec{r}_A) \rangle . \tag{3.3.51}$$

$$H_{jk}^{AA} \equiv \langle \chi_j^A(\vec{r}_A) | f (\vec{v} . \vec{r}) \vec{v} . \vec{\nabla}_r f | \chi_k^A(\vec{r}_A) \rangle . \tag{3.3.52}$$

$$J_{jk}^{AA} \equiv \langle \chi_j^A(\vec{r}_A) | (\vec{v} . \vec{r})^2 (\vec{\nabla}_r f)^2 | \chi_k^A(\vec{r}_A) \rangle . \tag{3.3.53}$$

$$K_{jk}^{AA} \equiv \langle \chi_j^A(\vec{r}_A) | (\vec{v} . \vec{r}) \left\{ \left[\frac{\partial}{\partial t} \right]_{\vec{r}} f \right\} | \chi_k^A(\vec{r}_A) \rangle . \tag{3.3.54}$$

$$\Lambda_{jk}^{AA} \equiv \langle \chi_j^A(\vec{r}_A) | f \vec{r} . \frac{d\vec{v}}{dt} | \chi_k^A(\vec{r}_A) \rangle . \tag{3.3.55}$$

$$L_{jk}^{AA} \equiv \langle \chi_j^A(\vec{r}_A) | \vec{v} . \vec{\nabla}_r | \chi_k^A(\vec{r}_A) \rangle . \tag{3.3.56}$$

Exchange 1

$$A^{BA}_{jk} \equiv \langle \phi^B_j(\vec{r}_B) | V_{eB} | \chi^A_k(\vec{r}_A) \rangle . \qquad (3.3.57)$$

$$B^{BA}_{jk} \equiv \langle \phi^B_j(\vec{r}_B) | f \vec{v} . \vec{\nabla}_r | \chi^A_k(\vec{r}_A) \rangle . \qquad (3.3.58)$$

$$C^{BA}_{jk} \equiv \langle \phi^B_j(\vec{r}_B) | (\vec{v} . \vec{r})(\vec{\nabla}_r f) . \vec{\nabla}_r | \chi^A_k(\vec{r}_A) \rangle . \qquad (3.3.59)$$

$$D^{BA}_{jk} \equiv \langle \phi^B_j(\vec{r}_B) | \vec{v} . \vec{\nabla}_r f | \chi^A_k(\vec{r}_A) \rangle . \qquad (3.3.60)$$

$$F^{BA}_{jk} \equiv \langle \phi^B_j(\vec{r}_B) | (\vec{v} . \vec{r}) \nabla_r^2 f | \chi^A_k(\vec{r}_A) \rangle . \qquad (3.3.61)$$

$$G^{BA}_{jk} \equiv \langle \phi^B_j(\vec{r}_B) | f^2 | \chi^A_k(\vec{r}_A) \rangle . \qquad (3.3.62)$$

$$H^{BA}_{jk} \equiv \langle \phi^B_j(\vec{r}_B) | f (\vec{v} . \vec{r}) \vec{v} . \vec{\nabla}_r f | \chi^A_k(\vec{r}_A) \rangle . \qquad (3.3.63)$$

$$J^{BA}_{jk} \equiv \langle \phi^B_j(\vec{r}_B) | (\vec{v} . \vec{r}) (\vec{\nabla}_r f)^2 | \chi^A_k(\vec{r}_A) \rangle . \qquad (3.3.64)$$

$$K^{BA}_{jk} \equiv \langle \phi^B_j(\vec{r}_B) | (\vec{v} . \vec{r}) \left\{ \left[\frac{\partial}{\partial t} \right]_{\vec{r}} f \right\} | \chi^A_k(\vec{r}_A) \rangle . \qquad (3.3.65)$$

$$\Lambda^{BA}_{jk} \equiv \langle \phi^B_j(\vec{r}_B) | f \vec{r} . \frac{d\vec{v}}{dt} | \chi^A_k(\vec{r}_A) \rangle . \qquad (3.3.66)$$

$$L^{BA}_{jk} \equiv \langle \phi^B_j(\vec{r}_B) | \vec{v} . \vec{\nabla}_r | \chi^A_k(\vec{r}_A) \rangle . \qquad (3.3.67)$$

Exchange 2

$$A_{jk}^{AB} \equiv \langle \chi_j^A(\vec{r}_A) | V_{eA} | \phi_k^B(\vec{r}_B) \rangle . \qquad (3.3.68)$$

$$B_{jk}^{AB} \equiv \langle \chi_j^A(\vec{r}_A) | f \vec{v} . \vec{\nabla}_r | \phi_k^B(\vec{r}_B) \rangle . \qquad (3.3.69)$$

$$C_{jk}^{AB} \equiv \langle \chi_j^A(\vec{r}_A) | (\vec{v} . \vec{r})(\vec{\nabla}_r f) . \vec{\nabla}_r | \phi_k^B(\vec{r}_B) \rangle . \qquad (3.3.70)$$

$$D_{jk}^{AB} \equiv \langle \chi_j^A(\vec{r}_A) | \vec{v} . \vec{\nabla}_r f | \phi_k^B(\vec{r}_B) \rangle . \qquad (3.3.71)$$

$$F_{jk}^{AB} \equiv \langle \chi_j^A(\vec{r}_A) | (\vec{v} . \vec{r}) \nabla_r^2 f | \phi_k^B(\vec{r}_B) \rangle . \qquad (3.3.72)$$

$$G_{jk}^{AB} \equiv \langle \chi_j^A(\vec{r}_A) | f^2 | \phi_k^B(\vec{r}_B) \rangle . \qquad (3.3.73)$$

$$H_{jk}^{AB} \equiv \langle \chi_j^A(\vec{r}_A) | f (\vec{v} . \vec{r}) \vec{v} . \vec{\nabla}_r f | \phi_k^B(\vec{r}_B) \rangle . \qquad (3.3.74)$$

$$J_{jk}^{AB} \equiv \langle \chi_j^A(\vec{r}_A) | (\vec{v} . \vec{r})^2 (\vec{\nabla}_r f)^2 | \phi_k^B(\vec{r}_B) \rangle . \qquad (3.3.75)$$

$$K_{jk}^{AB} \equiv \langle \chi_j^A(\vec{r}_A) | (\vec{v} . \vec{r}) \left\{ \left[\frac{\partial}{\partial t} \right]_{\vec{r}} f \right\} | \phi_k^B(\vec{r}_B) \rangle . \qquad (3.3.76)$$

$$\Lambda_{jk}^{AB} \equiv \langle \chi_j^A(\vec{r}_A) | f \vec{r} . \frac{d\vec{v}}{dt} | \phi_k^B(\vec{r}_B) \rangle . \qquad (3.3.77)$$

$$L_{jk}^{AB} \equiv \langle \chi_j^A(\vec{r}_A) | \vec{v} . \vec{\nabla}_r | \phi_k^B(\vec{r}_B) \rangle . \qquad (3.3.78)$$

We see that the matrix elements obtained in this formulation are much more complicated than the corresponding plane-wave matrix elements, equations (2.4.17) to (2.4.21). We note that the relative velocity vector of the nuclear motion, $\vec{v}$, is given by

$$\vec{v}(t) = \frac{\partial \vec{R}}{\partial t} \tag{3.3.79}$$

where $\vec{R}$ is the internuclear vector. For straight-line trajectories $\vec{v}$ is constant. If we look at the expressions for the direct and exchange matrix elements, equations (3.3.30) to (3.3.33), we see that in the straight-line trajectory case the Λ-type elements, which contain $d\vec{v}/dt$ will be equal to zero. Also the final terms of the expressions containing $d(v^2)/dt$ will vanish.

We now write down expressions for the matrix elements N_{jk}, H_{jk}, $\bar{H}_{jk}$, K_{jk} and $\bar{K}_{jk}$ in terms of simpler matrix elements N^{BA}_{jk}, v_{jk}, w_{jk}, k_{jk} and h_{jk}, the aim being to remove the internuclear potential terms, and the exponential eigen-energy phase factors. We have

$$N_{jk} = N^{BA}_{jk} \exp i(\varepsilon_j - \eta_k)t \,. \tag{3.3.80}$$

$$H_{jk} = (V_{AB}\delta_{jk} + v_{jk}) \exp i(\varepsilon_j - \varepsilon_k)t \,. \tag{3.3.81}$$

$$\bar{H}_{jk} = (V_{AB}\delta_{jk} + w_{jk}) \exp i(\eta_j - \eta_k)t \,. \tag{3.3.82}$$

$$K_{jk} = (V_{AB}N^{BA}_{jk} + k_{jk}) \exp i(\varepsilon_j - \eta_k)t \,. \tag{3.3.83}$$

$$\bar{K}_{jk} = (V_{AB}N^{BA*}_{kj} + h^{*}_{kj}) \exp i(\eta_j - \varepsilon_k)t \,. \tag{3.3.84}$$

The matrices $\underset{\sim}{v}$, $\underset{\sim}{w}$, $\underset{\sim}{k}$ and $\underset{\sim}{h}^{\dagger}$, where † denotes Hermitian adjoint, are given by the following expressions (in matrix form).

$$\underset{\sim}{v} = \underset{\sim}{A}^{BB} + \frac{v^2}{8}\underset{\sim}{G}^{BB} + \frac{1}{4}\underset{\sim}{H}^{BB} + \frac{1}{8}\underset{\sim}{J}^{BB} + \frac{1}{2}\underset{\sim}{K}^{BB} + \frac{1}{2}\underset{\sim}{\Lambda}^{BB} - \frac{1}{8}\left[v^2 + t\frac{d(v^2)}{dt}\right]\underset{\sim}{I} - i\left(\frac{1}{2}\underset{\sim}{B}^{BB} + \frac{1}{2}\underset{\sim}{C}^{BB} + \frac{1}{2}\underset{\sim}{D}^{BB} + \frac{1}{4}\underset{\sim}{E}^{BB} + \frac{1}{2}\underset{\sim}{L}^{BB}\right). \qquad (3.3.85)$$

$$\underset{\sim}{w} = \underset{\sim}{A}^{AA} + \frac{v^2}{8}\underset{\sim}{G}^{AA} + \frac{1}{4}\underset{\sim}{H}^{AA} + \frac{1}{8}\underset{\sim}{J}^{AA} + \frac{1}{2}\underset{\sim}{K}^{AA} + \frac{1}{2}\underset{\sim}{\Lambda}^{AA} - \frac{1}{8}\left[v^2 + t\frac{d(v^2)}{dt}\right]\underset{\sim}{I} - i\left(\frac{1}{2}\underset{\sim}{B}^{AA} + \frac{1}{2}\underset{\sim}{C}^{AA} + \frac{1}{2}\underset{\sim}{D}^{AA} + \frac{1}{4}\underset{\sim}{E}^{AA} - \frac{1}{2}\underset{\sim}{L}^{AA}\right). \qquad (3.3.86)$$

where $\underset{\sim}{I}$ is the unit matrix.

$$\underset{\sim}{k} = \underset{\sim}{A}^{BA} + \frac{v^2}{8}\underset{\sim}{G}^{BA} + \frac{1}{4}\underset{\sim}{H}^{BA} + \frac{1}{8}\underset{\sim}{J}^{BA} + \frac{1}{2}\underset{\sim}{K}^{BA} + \frac{1}{2}\underset{\sim}{\Lambda}^{BA} - \frac{1}{8}\left[v^2 + t\frac{d(v^2)}{dt}\right]\underset{\sim}{N}^{BA} - i\left(\frac{1}{2}\underset{\sim}{B}^{BA} + \frac{1}{2}\underset{\sim}{C}^{BA} + \frac{1}{2}\underset{\sim}{D}^{BA} + \frac{1}{4}\underset{\sim}{E}^{BA} - \frac{1}{2}\underset{\sim}{L}^{BA}\right). \qquad (3.3.87)$$

$$\underset{\sim}{h}^{\dagger} = \underset{\sim}{A}^{AB} + \frac{v^2}{8}\underset{\sim}{G}^{AB} + \frac{1}{4}\underset{\sim}{H}^{AB} + \frac{1}{8}\underset{\sim}{J}^{AB} + \frac{1}{2}\underset{\sim}{K}^{AB} + \frac{1}{2}\underset{\sim}{\Lambda}^{AB} - \frac{1}{8}\left[v^2 + t\frac{d(v^2)}{dt}\right](\underset{\sim}{N}^{BA})^{\dagger} - i\left(\frac{1}{2}\underset{\sim}{B}^{AB} + \frac{1}{2}\underset{\sim}{C}^{AB} + \frac{1}{2}\underset{\sim}{D}^{AB} + \frac{1}{4}\underset{\sim}{E}^{AB} + \frac{1}{2}\underset{\sim}{L}^{AB}\right). \qquad (3.3.88)$$

3.4 Simplification of the matrix expressions

In the previous section rather complicated expressions for the matrices $\underset{\sim}{v}$, $\underset{\sim}{w}$, $\underset{\sim}{k}$ and $\underset{\sim}{h}^{\dagger}$ were obtained in terms of the various individual matrices $\underset{\sim}{A}^{BB}$, $\underset{\sim}{B}^{BB}$, $\underset{\sim}{C}^{BB}$, $\underset{\sim}{D}^{BB}$, ... etc. In this section it will be shown how the expressions for $\underset{\sim}{v}$, $\underset{\sim}{w}$, $\underset{\sim}{k}$ and $\underset{\sim}{h}^{\dagger}$ (equations (3.3.85) to (3.3.88)) may be reduced down to simpler expressions.

We begin by first combining some of the matrices in the expressions together and replacing the combination by one matrix which we shall denote by $\underset{\sim}{Y}$. The following expressions show this.

$$\underset{\sim}{Y}^{BB} = \frac{v^2}{8}\underset{\sim}{G}^{BB} + \frac{1}{4}\underset{\sim}{H}^{BB} + \frac{1}{8}\underset{\sim}{J}^{BB} + \frac{1}{2}\underset{\sim}{K}^{BB} + \frac{1}{2}\underset{\sim}{\Delta}^{BB} - \frac{1}{8}\left[v^2 + t\frac{d(v^2)}{dt}\right]\underset{\sim}{I}. \qquad (3.4.1)$$

$$\underset{\sim}{Y}^{AA} = \frac{v^2}{8}\underset{\sim}{G}^{AA} + \frac{1}{4}\underset{\sim}{H}^{AA} + \frac{1}{8}\underset{\sim}{J}^{AA} + \frac{1}{2}\underset{\sim}{K}^{AA} + \frac{1}{2}\underset{\sim}{\Delta}^{AA} - \frac{1}{8}\left[v^2 + t\frac{d(v^2)}{dt}\right]\underset{\sim}{I}. \qquad (3.4.2)$$

$$\underset{\sim}{Y}^{BA} = \frac{v^2}{8}\underset{\sim}{G}^{BA} + \frac{1}{4}\underset{\sim}{H}^{BA} + \frac{1}{8}\underset{\sim}{J}^{BA} + \frac{1}{2}\underset{\sim}{K}^{BA} + \frac{1}{2}\underset{\sim}{\Delta}^{BA} - \frac{1}{8}\left[v^2 + t\frac{d(v^2)}{dt}\right]\underset{\sim}{N}^{BA}. \qquad (3.4.3)$$

$$\underset{\sim}{Y}^{AB} = \frac{v^2}{8}\underset{\sim}{G}^{AB} + \frac{1}{4}\underset{\sim}{H}^{AB} + \frac{1}{8}\underset{\sim}{J}^{AB} + \frac{1}{2}\underset{\sim}{K}^{AB} + \frac{1}{2}\underset{\sim}{\Delta}^{AB} - \frac{1}{8}\left[v^2 + t\frac{d(v^2)}{dt}\right](\underset{\sim}{N}^{BA})^{\dagger}. \qquad (3.4.4)$$

It will now be shown how the $\underset{\sim}{B}$, $\underset{\sim}{C}$, $\underset{\sim}{D}$ and $\underset{\sim}{E}$ matrices may be combined. We begin by considering the small direct 1 matrix expression, equation (3.3.85).

From equations (3.3.37) and (3.3.39) we have that the elements C_{jk}^{BB} and F_{jk}^{BB} are, in integral form

$$C_{jk}^{BB} = \int_V \phi_j^{B*}(\vec{r}_B)(\vec{v}.\vec{r})(\vec{\nabla}_r f).\vec{\nabla}_r \phi_k^B(\vec{r}_B)\,d\vec{r} \qquad (3.4.5)$$

and

$$F_{jk}^{BB} = \int_V \phi_j^{B*}(\vec{r}_B)(\vec{v}.\vec{r})(\nabla_r^2 f)\phi_k^B(\vec{r}_B)\,d\vec{r}. \qquad (3.4.6)$$

setting

$$\overline{\phi}_j(\vec{r}) = (\vec{v}.\vec{r})\phi_j^B(\vec{r}_B) \qquad (3.4.7)$$

we have

$$C_{jk}^{BB} = \int_V \overline{\phi}_j^*(\vec{r})(\vec{\nabla}_r f).\vec{\nabla}_r \phi_k^B(\vec{r}_B)\,d\vec{r} \qquad (3.4.8)$$

$$F_{jk}^{BB} = \int_V \overline{\phi}_j^*(\vec{r})(\nabla_r^2 f)\phi_k^B(\vec{r}_B)\,d\vec{r}\,. \qquad (3.4.9)$$

If we have complex functions $\Phi(\vec{r})$ and $\Psi(\vec{r})$ which tend asymptotically to zero as $|\vec{r}|\to\infty$, and a real function $f(\vec{r})$, then it can be shown (Appendix A2) that

$$2\int_V \Phi^*(\vec{r})\vec{\nabla}_r f(\vec{r}).\vec{\nabla}_r \Psi(\vec{r})\,d\vec{r} + \int_V \Phi^*(\vec{r})\left\{\nabla_r^2 f(\vec{r})\right\}\Psi(\vec{r})\,d\vec{r}$$

$$= \int_V \left\{\nabla_r^2 \Phi^*(\vec{r})\right\} f(\vec{r})\Psi(\vec{r})\,d\vec{r} - \int_V \Phi^*(\vec{r}) f(\vec{r})\nabla_r^2 \Psi(\vec{r})\,d\vec{r}. \qquad (3.4.10)$$

Using equation (3.4.10) we can show that

$$2C_{jk}^{BB} + F_{jk}^{BB} = \int_v \nabla_r^2 \left[(\vec{v}.\vec{r}) \phi_j^{B*}(\vec{r}_B) \right] f \phi_k^B(\vec{r}_B)\, d\vec{r}$$

$$- \int_v (\vec{v}.\vec{r}) \phi_j^{B*}(\vec{r}_B) f \nabla_r^2 \phi_k^B(\vec{r}_B)\, d\vec{r}. \qquad (3.4.11)$$

Now

$$\nabla_r^2 \left[(\vec{v}.\vec{r}) \phi_j^{B*}(\vec{r}_B) \right] = (\vec{v}.\vec{r}) \nabla_r^2 \phi_j^{B*}(\vec{r}_B)$$

$$+ 2\vec{v}.\vec{\nabla}_r \phi_j^{B*}(\vec{r}_B) \qquad (3.4.12)$$

and also

$$\nabla_r^2 \phi_k^B(\vec{r}_B) = 2(V_{eB} - \varepsilon_k) \phi_k^B(\vec{r}_B) \qquad (3.4.13)$$

$$\nabla_r^2 \phi_j^{B*}(\vec{r}_B) = 2(V_{eB} - \varepsilon_j) \phi_j^{B*}(\vec{r}_B). \qquad (3.4.14)$$

Using equations (3.4.12) to (3.4.14), equation (3.4.11) can be re-written, after some algebra

$$2C_{jk}^{BB} + F_{jk}^{BB} = -2B_{jk}^{BB} - 2D_{jk}^{BB} - 2(\varepsilon_j - \varepsilon_k) U_{jk}^{BB} \qquad (3.4.15)$$

where the B_{jk}^{BB} and D_{jk}^{BB} are given by equations (3.3.36) and (3.3.38) respectively, and U_{jk}^{BB} is given by

$$U_{jk}^{BB} = \langle \phi_j^B(\vec{r}_B) | f(\vec{v}.\vec{r}) | \phi_k^B(\vec{r}_B) \rangle. \qquad (3.4.16)$$

Rearrangement of equation (3.4.15) gives

$$2B_{jk}^{BB} + 2C_{jk}^{BB} + 2D_{jk}^{BB} + F_{jk}^{BB} = -2(\varepsilon_j - \varepsilon_k) U_{jk}^{BB}. \qquad (3.4.17)$$

Similarly one can show for the direct 2 elements that

$$2B_{jk}^{AA} + 2C_{jk}^{AA} + 2D_{jk}^{AA} + F_{jk}^{AA} = -2(\eta_j - \eta_k) U_{jk}^{AA} \qquad (3.4.18)$$

where

$$U_{jk}^{AA} = \langle \chi_j^A(\vec{r}_A) | f(\vec{v}.\vec{r}) | \chi_k^A(\vec{r}_A) \rangle . \qquad (3.4.19)$$

To simplify the exchange 1 expression equation (3.3.87) we begin with the C_{jk}^{BA} and F_{jk}^{BA} which are

$$C_{jk}^{BA} = \int_v \phi_j^{B*}(\vec{r}_B)(\vec{v}.\vec{r})(\vec{\nabla}_r f).\vec{\nabla}_r \chi_k^A(\vec{r}_A)\, d\vec{r} \qquad (3.4.20)$$

and

$$F_{jk}^{BA} = \int_v \phi_j^{B*}(\vec{r}_B)(\vec{v}.\vec{r})(\nabla_r^2 f)\chi_k^A(\vec{r}_A)\, d\vec{r} . \qquad (3.4.21)$$

Using the relation (3.4.10) plus the fact that

$$\nabla_r^2 \phi_j^{B*}(\vec{r}_B) = 2(V_{eB} - \varepsilon_j)\phi_j^{B*}(\vec{r}_B) \qquad (3.4.22)$$

and

$$\nabla_r^2 \chi_k^A(\vec{r}_A) = 2(V_{eA} - \eta_k)\chi_k^A(\vec{r}_A), \qquad (3.4.23)$$

we obtain, in a similar manner to the direct expressions, the following, that

$$2B_{jk}^{BA} + 2C_{jk}^{BA} + 2D_{jk}^{BA} + F_{jk}^{BA} = 2X_{jk}^{BA} \qquad (3.4.24)$$

where

$$X_{jk}^{BA} = V_{jk}^{BA} - W_{jk}^{BA} - (\varepsilon_j - \eta_k) U_{jk}^{BA}, \tag{3.4.25}$$

and where

$$V_{jk}^{BA} = \langle \phi_j^B(\vec{r}_B) | f(\vec{v}.\vec{r}) V_{eB} | \chi_k^A(\vec{r}_A) \rangle, \tag{3.4.26}$$

$$W_{jk}^{BA} = \langle \phi_j^B(\vec{r}_B) | f(\vec{v}.\vec{r}) V_{eA} | \chi_k^A(\vec{r}_A) \rangle, \tag{3.4.27}$$

and

$$U_{jk}^{BA} = \langle \phi_j^B(\vec{r}_B) | f(\vec{v}.\vec{r}) | \chi_k^A(\vec{r}_A) \rangle. \tag{3.4.28}$$

Similarly

$$2B_{jk}^{AB} + 2C_{jk}^{AB} + 2D_{jk}^{AB} + F_{jk}^{AB} = -2X_{jk}^{AB} \tag{3.4.29}$$

where

$$X_{jk}^{AB} = V_{jk}^{AB} - W_{jk}^{AB} + (\eta_j - \varepsilon_k) U_{jk}^{AB} \tag{3.4.30}$$

and where

$$V_{jk}^{AB} = \langle \chi_j^A(\vec{r}_A) | f(\vec{v}.\vec{r}) V_{eB} | \phi_k^B(\vec{r}_B) \rangle \tag{3.4.31}$$

$$W_{jk}^{AB} = \langle \chi_j^A(\vec{r}_A) | f(\vec{v}.\vec{r}) V_{eA} | \phi_k^B(\vec{r}_B) \rangle \tag{3.4.32}$$

$$U_{jk}^{AB} = \langle \chi_j^A(\vec{r}_A) | f(\vec{v}.\vec{r}) | \phi_k^B(\vec{r}_B) \rangle. \tag{3.4.33}$$

We now bring together these results. For the direct elements using equations (3.4.1) and (3.4.2) plus equations (3.4.17)

and (3.4.18), we find that

$$\underset{\sim}{v} = \underset{\sim}{A}^{BB} + \underset{\sim}{Y}^{BB} + \frac{i}{2}(\underset{\sim}{\bar{U}}^{BB} - \underset{\sim}{L}^{BB}) \qquad (3.4.34)$$

$$\underset{\sim}{w} = \underset{\sim}{A}^{AA} + \underset{\sim}{Y}^{AA} + \frac{i}{2}(\underset{\sim}{\bar{U}}^{AA} + \underset{\sim}{L}^{AA}) \qquad (3.4.35)$$

where

$$\bar{U}_{jk}^{BB} = (\varepsilon_j - \varepsilon_k)\langle \phi_j^B(\vec{r}_B)|f(\vec{v}.\vec{r})|\phi_k^B(\vec{r}_B)\rangle \qquad (3.4.36)$$

and

$$\bar{U}_{jk}^{AA} = (\eta_j - \eta_k)\langle \chi_j^A(\vec{r}_A)|f(\vec{v}.\vec{r})|\chi_k^A(\vec{r}_A)\rangle . \qquad (3.4.37)$$

For the exchange elements using equations (3.4.3) and (3.4.4) plus equations (3.4.24) and (3.4.29), we find that

$$\underset{\sim}{k} = \underset{\sim}{A}^{BA} + \underset{\sim}{Y}^{BA} - \frac{i}{2}(\underset{\sim}{X}^{BA} - \underset{\sim}{L}^{BA}) \qquad (3.4.38)$$

$$\underset{\sim}{h}^{\dagger} = \underset{\sim}{A}^{AB} + \underset{\sim}{Y}^{AB} + \frac{i}{2}(\underset{\sim}{X}^{AB} - \underset{\sim}{L}^{AB}). \qquad (3.4.39)$$

It is possible to obtain the matrix $\underset{\sim}{h}$ in terms of BA-type exchange elements as we shall now see. This is useful from a computational point of view as we only need to compute BA-type elements in order to obtain the $\underset{\sim}{h}^{\dagger}$ matrix. The $\underset{\sim}{h}$ matrix is given by

$$\underset{\sim}{h} = (\underset{\sim}{A}^{AB})^{\dagger} + (\underset{\sim}{Y}^{AB})^{\dagger} - \frac{i}{2}\left[(\underset{\sim}{X}^{AB})^{\dagger} - (\underset{\sim}{L}^{AB})^{\dagger}\right]. \qquad (3.4.40)$$

It is easy to show that

$$(\underset{\sim}{X}^{AB})^{\dagger} = \underset{\sim}{X}^{BA} \quad \& \quad (\underset{\sim}{Y}^{AB})^{\dagger} = \underset{\sim}{Y}^{BA}. \qquad (3.4.41)$$

Integrating by parts, it can be shown that

$$(\underset{\sim}{L}^{AB})^{\dagger} = -\underset{\sim}{L}^{BA}. \tag{3.4.42}$$

and finally

$$(\underset{\sim}{A}^{AB})^{\dagger} = \underset{\sim}{\bar{A}}^{BA} \tag{3.4.43}$$

where

$$\bar{A}^{BA}_{jk} = \langle \phi^{B}_{j}(\vec{r}_{B}) | V_{CA} | \chi^{A}_{k}(\vec{r}_{A}) \rangle . \tag{3.4.44}$$

And so we obtain

$$\underset{\sim}{h} = \underset{\sim}{\bar{A}}^{BA} + \underset{\sim}{Y}^{BA} - \frac{i}{2}\left(\underset{\sim}{X}^{BA} + \underset{\sim}{L}^{BA}\right). \tag{3.4.45}$$

This concludes this chapter. We shall proceed in the next chapter to look at methods of evaluating the matrix elements.

CHAPTER 4

EVALUATION OF THE MATRIX ELEMENTS

4.1 Introduction

In the previous chapter, the basis functions $F_j^s(\vec{r}, t)$ and $G_k^s(\vec{r}, t)$, given in equations (3.3.27) and (3.3.28), were used to derive expressions for the matrix elements which have to be evaluated as part of the calculation of electron capture cross sections. It was seen that the basis functions $F_j^s(\vec{r}, t)$ and $G_k^s(\vec{r}, t)$ contained a switching function $f(\vec{r}, \vec{R})$.

Although the expressions for the direct and exchange matrix elements, equations (3.3.30) to (3.3.33), were complicated, it was shown in Section 3.4 of the previous chapter how some of the individual matrix elements could be combined to yield simpler expressions for the matrix elements V_{jk}, W_{jk}, k_{jk} and h_{jk} . The final results of Section 3.4 were equations (3.4.33) and (3.4.34); and equations (3.4.37) and (3.4.44). The problem of evaluating the individual matrix elements remaining in the expressions for V_{jk} , W_{jk} , k_{jk} and h_{jk} was not dealt with though.

The calculations presented in the next chapter were done using a numerical technique for integrating the individual elements because this was a general method suited to the use of different functional forms of switching function. However, one form of switching function, the "simple" switching function f_s given by

$$f_s = - \frac{R^2}{R^2 + \rho^2} \eta \qquad (4.1.1)$$

where

$$\eta = \frac{r_A - r_B}{R} \quad , \tag{4.1.2}$$

and where p is a parameter, was such that an analytic method could be used to compute the elements. Although limited in that only one switching function could be employed, the analytic method was useful as a computational check against the numerical method. Also this analytic method was such that it could be used with a switching function of the form

$$f = -\frac{R^2}{R^2 + p^2} Q(\eta) \tag{4.1.3}$$

where $Q(\eta)$ is a polynomial of η

$$Q(\eta) = b_1 \eta + b_3 \eta^3 + b_5 \eta^5 + \ldots + b_{2n+1} \eta^{2n+1} \quad . \tag{4.1.4}$$

The coefficients b_1, b_3 , b_5 , etc. must be such that

$$Q(\pm 1) = \pm 1 \tag{4.1.5}$$

in order that the function f of equation (4.1.3) satisfies the switching conditions equations (3.3.24) and (3.3.25) of the previous chapter. The variable η , defined in equation (4.1.2) is one of the three Prolate Spheroidal Co-ordinates (ξ , η, ϕ) which were used in evaluating the elements. These co-ordinates and their use will be discussed later on in this chapter. The variable η is such that

$$-1 \leq \eta \leq 1 \tag{4.1.6}$$

and hence the polynomial $Q(\eta)$ is bounded between plus and minus one.

In this chapter we shall go on to see how the matrix elements may be evaluated - a central part of the work presented in this thesis. Both the general numerical method and the special analytic method will be discussed together with theoretical aspects common to both methods.

4.2 General form of the individual matrix elements and the atomic orbitals

On pages 117 to 120 (Chapter 3) lists of the individual matrix elements are given. We saw in Section 3.4 of Chapter 3 how simplifications meant that some of the elements, namely the B-, C-, D- and F- type elements did not have to be calculated. Instead matrix elements of simpler forms appeared in the formulation, namely $\bar{U}^{BB}_{jk}$ and $\bar{U}^{AA}_{jk}$ elements, equations (3.4.35) and (3.4.36), and also V^{BA}_{jk}, W^{BA}_{jk} and U^{BA}_{jk} elements equations (3.4.26) to (3.4.28). This is good from a calculational point of view as the B and C elements involve a gradient operator $\vec{\nabla}_{\vec{r}}$ acting upon an atomic orbital state $|\phi^{B}_{j}(\vec{r}_B)\rangle$ or $|\chi^{A}_{k}(\vec{r}_A)\rangle$, and this would lead to awkward expressions. In a similar vein, we shall see later in this chapter (Section 4.4) how the L- type expressions which contain $\vec{v}.\vec{\nabla}_{\vec{r}}$ may be recast to avoid the $\vec{\nabla}_{\vec{r}}$. Hence all the elements to be calculated are of the general form

$$M_{jk}(t) = \langle \gamma^{B,A}_{j} | m(\vec{r},t) | \gamma^{B,A}_{k} \rangle \qquad (4.2.1)$$

where

$$|\chi_j^B\rangle \equiv |\phi_j^B(\vec{r}_B)\rangle \qquad (4.2.2a)$$

and

$$|\chi_k^A\rangle \equiv |\chi_k^A(\vec{r}_A)\rangle , \qquad (4.2.2b)$$

and where $m(\vec{r},t)$ is a function of $\vec{r}$ and t and is not an operator acting upon the atomic orbital states. For example, for the J-type elements $m(\vec{r},t)$ is $(\vec{v}.\vec{r})^2(\vec{\nabla}_r f)^2$.

A choice has to be made as to the form of the atomic orbital wavefunctions used. In the calculations presented in this thesis hydrogenic wavefunctions of the general form

$$\chi_{n\ell m}(\vec{r}) = R_{n\ell}(r)\bar{Y}_{\ell m}(\theta,\phi) \qquad (4.2.3)$$

where used.

The $R_{n\ell}(r)$ are the hydrogenic radial wavefunctions which are given by

$$R_{n\ell}(r) = e^{-\lambda r}\sum_{i=1}^{n-\ell} c_i r^{\ell-1+i} \qquad (4.2.4)$$

(c_i are coefficients),

and where

$$\bar{Y}_{\ell m}(\theta,\phi) = N_m\left[Y_{\ell m}(\theta,\phi) + Y^*_{\ell m}(\theta,\phi)\right], \quad m \geq 0 \qquad (4.2.5)$$

with $N_m = 1/2$ if $m = 0$, (4.2.6a)

$N_m = 1/\sqrt{2}$ if $m > 0$. (4.2.6b)

The spherical harmonics $Y_{\ell m}(\theta,\phi)$ are given by

$$Y_{\ell m}(\theta,\phi) = (-1)^m\left[\frac{(2\ell+1)}{4\pi}\cdot\frac{(\ell-m)!}{(\ell+m)!}\right]^{1/2} P_\ell^m(\cos\theta)e^{im\phi}, \quad m \geq 0, \qquad (4.2.7)$$

where the $P_l^m(\cos\theta)$ are associated Legendre functions. We see from the presence of the $(-1)^m$ phase factor that the Condon-Shortley phase convention is adopted. The functions $\bar{Y}_{lm}(\theta,\phi)$ defined by equation (4.2.5) are known as real spherical harmonics. As their name implies, they are real functions. The use of real spherical harmonics means that the hydrogenic orbital wavefunctions $\chi_{nlm}(\vec{r})$ of equation (4.2.3) are real which simplifies the analysis somewhat. In particular, if we note that the expressions for the $\underset{\sim}{v}$, $\underset{\sim}{w}$, $\underset{\sim}{k}$ and $\underset{\sim}{h}$ matrices derived in Chapter 3, Section 3.4 are

$$\underset{\sim}{v} = \underset{\sim}{A}^{BB} + \underset{\sim}{Y}^{BB} + \frac{i}{2}\left(\underset{\sim}{\bar{U}}^{BB} - \underset{\sim}{L}^{BB}\right), \qquad (4.2.8)$$

$$\underset{\sim}{w} = \underset{\sim}{A}^{AA} + \underset{\sim}{Y}^{AA} + \frac{i}{2}\left(\underset{\sim}{\bar{U}}^{AA} + \underset{\sim}{L}^{AA}\right), \qquad (4.2.9)$$

$$\underset{\sim}{k} = \underset{\sim}{A}^{BA} + \underset{\sim}{Y}^{BA} - \frac{i}{2}\left(\underset{\sim}{X}^{BA} - \underset{\sim}{L}^{BA}\right), \qquad (4.2.10)$$

and $$\underset{\sim}{h} = \underset{\sim}{\bar{A}}^{BA} + \underset{\sim}{Y}^{BA} - \frac{i}{2}\left(\underset{\sim}{X}^{BA} + \underset{\sim}{L}^{BA}\right). \qquad (4.2.11)$$

We see that using real atomic orbital wavefunctions means that the expressions display explicitly their real and imaginary parts.

Using equation (4.2.7), equation (4.2.5) may be re-written

$$\bar{Y}_{lm}(\theta,\phi) = N_m C_{lm} P_l^m(\cos\theta)\cos m\phi \qquad (4.2.12)$$

where

$$C_{lm} = 2(-1)^m\left[\frac{2l+1}{4\pi}\cdot\frac{(l-m)!}{(l+m)!}\right]^{1/2}. \qquad (4.2.13)$$

The atomic orbital wavefunctions are given by

$$\phi_j^B(\vec{r}_B) = R_{(n_B)_j (l_B)_j}(r_B)\, \overline{Y}_{(l_B)_j (m_B)_j}(\theta_B, \phi_B) \qquad (4.2.14)$$

$$\chi_k^A(\vec{r}_A) = R_{(n_A)_k (l_A)_k}(r_A)\, \overline{Y}_{(l_A)_k (m_A)_k}(\theta_A, \phi_A)\,. \qquad (4.2.15)$$

We also note the explicit expressions for the radial wavefunctions and the real spherical harmonics

$$R_{(n_B)_j (l_B)_j}(r_B) = e^{-\nu_j r_B} \sum_{q=1}^{(n_B)_j - (l_B)_j} b_{jq}\, r_B^{[(l_B)_j - 1 + q]}\,, \qquad (4.2.16)$$

$$R_{(n_A)_k (l_A)_k}(r_A) = e^{-\mu_k r_A} \sum_{p=1}^{(n_A)_k - (l_A)_k} a_{kp}\, r_A^{[(l_A)_k - 1 + p]}\,; \qquad (4.2.17)$$

after equation (4.2.4).

$$\overline{Y}_{(l_B)_j (m_B)_j}(\theta_B, \phi_B) = N_{(m_B)_j}\, C_{(l_B)_j (m_B)_j}\, P^{(m_B)_j}_{(l_B)_j}(\cos\theta_B) \cos (m_B)_j \phi_B\,, \qquad (4.2.18)$$

$$\overline{Y}_{(l_A)_k (m_A)_k}(\theta_A, \phi_A) = N_{(m_A)_k}\, C_{(l_A)_k (m_A)_k}\, P^{(m_A)_k}_{(l_A)_k}(\cos\theta_A) \cos (m_A)_k \phi_A\,, \qquad (4.2.19)$$

after equation (4.2.12).

Having now specified the form of the atomic orbital wavefunctions, equations (4.2.14) and (4.2.15), we may now proceed to evaluate the general matrix elements $M_{jk}(t)$ of equation (4.2.1).

4.3 Space-fixed and body-fixed frames and prolate spheroidal co-ordinates

In the previous section of this chapter the forms of the atomic orbitals were chosen. We noted that their angular parts were real spherical harmonics which resulted in the orbitals being real. In this section it will be shown how

matrix elements of the form

$$M_{jk}(t) = \langle \psi_j^{B,A} | m(\vec{r}, t) | \psi_k^{B,A} \rangle \qquad (4.3.1)$$

where

$$| \psi_j^B \rangle \equiv | \phi_j^B(\vec{r}_B) \rangle \qquad (4.3.2)$$

and

$$| \psi_k^A \rangle \equiv | \chi_k^A(\vec{r}_A) \rangle \qquad (4.3.3)$$

may be evaluated as the matrix elements required for calculating electron capture cross sections for the method presented in this thesis, are of the form given in equation (4.3.1).

The formulation given in Chapter 3 assumed that the (x,y,z) co-ordinate frame was fixed in space. This space-fixed frame was such that its z-axis lay parallel to the velocity vectors $\pm \vec{v}/2$ at time $t = 0$, (Figure 4.1).

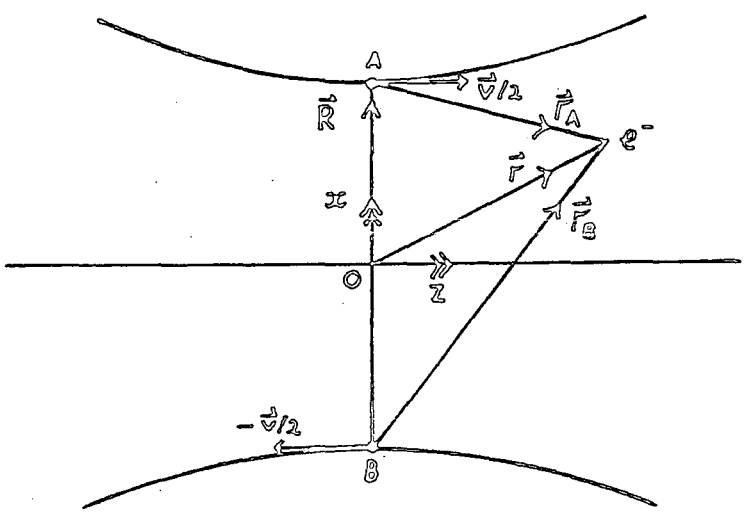

Fig. 4.1

The co-ordinates at $t = 0$ in the space-fixed frame (y-axis is out of the paper).

We note in Figure 4.1 the case of curved hyperbolic Coulomb nuclear trajectories is shown. The two trajectories would be replaced by lines parallel to the z-axis for the straight-line trajectory case.

The overlap and required exchange BA-type matrix elements presented in Chapter 3 are of the general form (excluding the L-type elements)

$$M_{jk}^{BA}(t) = \int_V \phi_j^{B*}(\vec{r}_B)\, m(\vec{r},t)\, \chi_k^A(\vec{r}_A)\, d\vec{r} \qquad (4.3.4)$$

where $m(\vec{r},t)$ is some function of $\vec{r}$ and t. The L-type matrix elements are not of the form in equation (4.3.4) but we shall later in Section 4.4 see that they may be written in terms of elements of the form given in equation (4.3.4). Integrals of the form shown in equation (4.3.4) are known as two-centre integrals and are generally not straightforward to evaluate. Although not explicitly shown in equation (4.3.4), the matrix elements $M_{jk}^{BA}(t)$ are in the space-fixed frame owing to the fact that the formulation was performed using this as the co-ordinate frame.

The rest of this section will be devoted to showing how the elements of the form shown in equation (4.3.4) may be evaluated by performing the necessary integration in the body-fixed frame using prolate spheroidal co-ordinates. A transformation is then done into the space-fixed frame. (The meaning of these terms will be explained anon). The direct matrix elements (BB-type and AA-type, equations (3.3.35) to (3.3.56), Chapter 3) were also evaluated using this method.

More will be said about the direct elements at the end of this section.

Figure 4.2 shows the co-ordinates at some time $t > 0$ and also shows the body-fixed (x',y',z') co-ordinates.

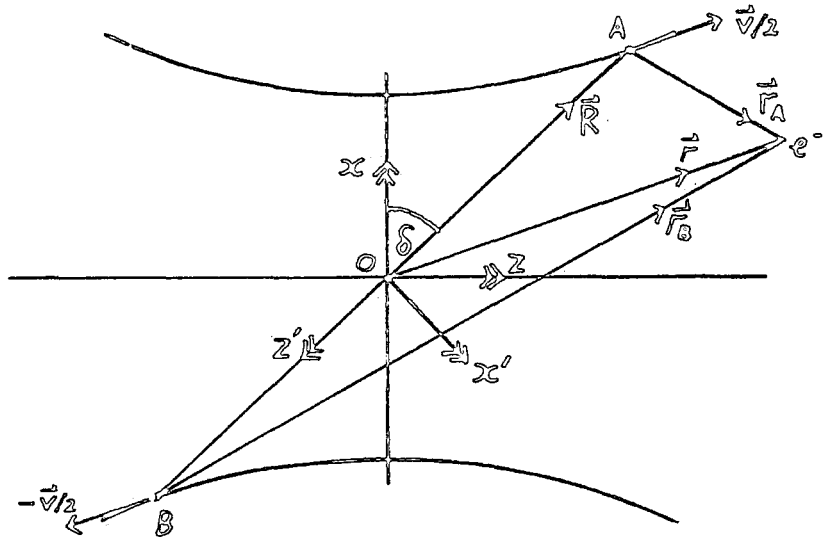

Figure 4.2

Space-fixed (x,y,z) and body-fixed (x',y',z') co-ordinate frames. (y and y' axes out of the paper).

Figure 4.2 also shows the angle δ which is the angle between $\vec{R}$ and the x-axis. We note that the z'-axis lies in the same line as the $\vec{R}$ vector, though opposite in direction. As the collision proceeds, the body-fixed frame will move with the vector $\vec{R}$ as seen from the space-fixed frame.

If we consider the general BA-type matrix element in the space-fixed frame, equation (4.3.4), we may re-write it

$$\left[M^{BA}_{jk}\right]^{SF} = \int_V R_{(n_B)_j (L_B)_j}(r_B)\, \overline{Y}^{SF}_{(L_B)_j (m_B)_j}(\theta_B, \phi_B)\, m(\vec{r}, t)$$

$$\times R_{(n_A)_k (L_A)_k}(r_A)\, \overline{Y}^{SF}_{(L_A)_k (m_A)_k}(\theta_A, \phi_A)\, d\vec{r} \,. \qquad (4.3.5)$$

Use has been made of the expressions for the atomic orbital wavefunctions $\phi_j^B(\vec{r}_B)$ and $\chi_k^A(\vec{r}_A)$ given in the previous section by equations (4.2.14) and (4.2.15). Also the real spherical harmonics have been labelled SF to show that they are in the space-fixed frame. The transformation between the space-fixed and body-fixed frames is purely rotational and so lengths are preserved. Hence the radial wavefunctions are unaffected by the transformation. The $m(\vec{r}, t)$ functions are invariant under rotation for all the elements required. Some of the m -functions contain the switching function $f(\vec{r}, \vec{R})$. This is equivalent to a function in terms of $\vec{r}_A$ and $\vec{r}_B$ which we call $g(\vec{r}_A, \vec{r}_B)$, that is

$$g(\vec{r}_A, \vec{r}_B) \equiv f(\vec{r}, \vec{R}) . \qquad (4.3.6)$$

In general the function $g(\vec{r}_A, \vec{r}_B)$ will not be invariant under rotation due to the angular dependence upon (θ_A, ϕ_A) and (θ_B, ϕ_B). However, in this work only switching functions involving r_A and r_B (moduli of $\vec{r}_A$ and $\vec{r}_B$) have been used, which are invariant under rotation. Thus when considering the transformation from the body-fixed frame to the space-fixed frame, it is the relationship between spherical harmonics in these frames that is important.

If we consider the rotation of one co-ordinate frame with respect to another defined by two Euler angles α and β (Figure 4.3),

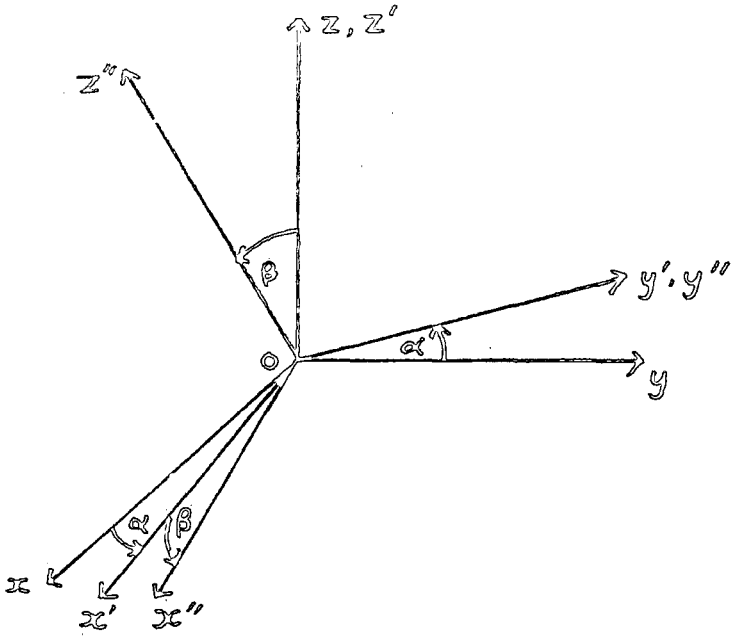

Figure 4.3

Euler angles ($\gamma = 0$).

we may relate spherical harmonics in one frame (primed) to those in another (unprimed) frame via the relation

$$Y_{\ell m}(\theta,\phi) = \sum_{m'=-\ell}^{m'=\ell} D^{\ell}_{m'm}(\alpha,\beta,0)\, Y_{\ell m'}(\theta',\phi') \qquad (4.3.7)$$

where the $D^{\ell}_{m'm}$ are elements of the rotation matrix $\mathcal{D}^{\ell}$, (Rose, 1957). The point (θ, ϕ) is the same point in space as (θ', ϕ') but measured relative to the new unprimed co-ordinate system.

If we consider Figure 4.2 we see that for our system the Euler angles are $\alpha = 0$ and $\beta = \delta + (\pi/2)$. The presence of the $\pi/2$ in the expression for β is in order to get the correct sense of rotation.

From equation (4.3.7) we may thus relate the space-fixed spherical harmonics to the body-fixed ones by use of the relation

$$Y^{SF}_{\ell m}(\theta,\phi) = \sum_{m'=-\ell}^{m'=\ell} D^{\ell}_{m'm}(0,\beta,0)\, Y^{BF}_{\ell m'}(\theta',\phi') . \qquad (4.3.8)$$

A corresponding relation exists relating the real spherical harmonics. It is

$$\bar{Y}^{SF}_{\ell m}(\theta,\phi) = \sum_{m'=0}^{m'=\ell} \mathcal{D}^{\ell}_{m'm}(\beta)\, \bar{Y}^{BF}_{\ell m'}(\theta',\phi') , \qquad (4.3.9)$$

where

$$\mathcal{D}^{\ell}_{m'm}(\beta) = \frac{N_m}{N_{m'}}\left[d^{\ell}_{m'm}(\beta) + (-1)^{m'} d^{\ell}_{-m'm}(\beta)\right]\cdot\frac{1}{\delta_{m'0}+1} . \qquad (4.3.10)$$

The N_m factors were defined in the previous section of this chapter, equations (4.2.6a) and (4.2.6b). The $\underset{\sim}{d}^{\ell}(\beta)$ are Wigner reduced rotation matrices (Rose, 1957). The derivation of equation (4.3.9) is given in Appendix A3.

We now substitute expressions for the space-fixed real spherical harmonics from equation (4.3.9), in the expression for the general BA-type matrix elements in the space-fixed frame, $\left[M^{BA}_{jk}\right]^{SF}$, equation (4.3.5).

$$\left[M^{BA}_{jk}\right]^{SF} = \int_V R_{(n\omega)_j(\ell_B)_j}(r_B) \sum_{m'=0}^{(\ell_B)_j} \mathcal{D}^{(\ell_B)_j}_{m'(m_B)_j}(\beta)\, \bar{Y}^{BF}_{(\ell_B)_j m'}(\theta_B',\phi_B')$$

$$\times\, \chi_m(\vec{r},t)\, R_{(n_A)_k(\ell_A)_k}(r_A) \sum_{n'=0}^{(\ell_A)_k} \mathcal{D}^{(\ell_A)_k}_{n'(m_A)_k}(\beta)\, \bar{Y}^{BF}_{(\ell_A)_k n'}(\theta_A',\phi_A')\, d\vec{r} . \qquad (4.3.11)$$

We may write the matrix elements $\left[M^{BA}_{jk}\right]^{SF}$ more explicitly

$$\left[M^{BA}_{jk}\right]^{SF} = \left\{ M^{BA}\left[(n_B)_j (l_B)_j (m_B)_j \; ; \; (n_A)_k (l_A)_k (m_A)_k\right] \right\}^{SF} \qquad (4.3.12)$$

where specific dependence upon the quantum numbers has been displayed. We use the notation of equation (4.3.12) to re-write equation (4.3.11) as

$$\left\{ M^{BA}\left[(n_B)_j (l_B)_j (m_B)_j \; ; \; (n_A)_k (l_A)_k (m_A)_k\right] \right\}^{SF}$$

$$= \sum_{m'=0}^{(l_B)_j} \sum_{\Lambda'=0}^{(l_A)_k} \mathcal{D}^{(l_B)_j}_{m'(m_B)_j}(\beta)\, \mathcal{D}^{(l_A)_k}_{\Lambda'(m_A)_k}(\beta) \left\{ M^{BA}\left[(n_B)_j (l_B)_j m' \; ; \; (n_A)_k (l_A)_k \Lambda'\right] \right\}^{BF} . \qquad (4.3.13)$$

Hence we have a relation linking the matrix elements in the space-fixed frame, $\left[M^{BA}_{jk}\right]^{SF}$ with those in the body-fixed frame, $\left[M^{BA}_{jk}\right]^{BF}$. We see from equation (4.3.13) that the relation involves summations over all the magnetic substates for given $(l_B)_j$ and $(l_A)_k$. In order to see this more clearly let us consider a simple example. Take the element

$$M^{SF}(B,1s|A,2p_0) = \int_V \left[\phi^{B*}_{1s}(\vec{r}_B)\right]^{SF} m(\vec{r},t) \left[\chi^{A}_{2p_0}(\vec{r}_A)\right]^{SF} d\vec{r}, \qquad (4.3.14)$$

where we have introduced fairly obvious notation. Use of equation (4.3.13) yields

$$M(B,1s|A,2p_0) = \mathcal{D}^{0}_{00}(\beta)\mathcal{D}^{1}_{00}(\beta)\, M^{BF}(B,1s|A,2p_0) + \mathcal{D}^{0}_{00}(\beta)\mathcal{D}^{1}_{10}(\beta)\, M^{BF}(B,1s|A,2p_1), \qquad (4.3.15)$$

where

$$M^{BF}(B,1s|A,2p_0) = \int_V \left[\phi^{B*}_{1s}(\vec{r}_B)\right]^{BF} m(\vec{r},t) \left[\chi^{A}_{2p_0}(\vec{r}_A)\right]^{BF} d\vec{r}. \qquad (4.3.16)$$

A similar expression exists for $M^{BF}(B,1s|A,2p^1)$. We see, therefore, that in order to obtain an element corresponding to one pair of magnetic substates in the space-fixed frame we must calculate the elements corresponding to all the magnetic substates in the body-fixed frame for given values of angular momentum quantum numbers $(l_B)_j$ and $(l_A)_k$.

Before proceeding to discuss the evaluation of the body-fixed elements, we must consider the angle δ between the space-fixed and body-fixed frames in a little more detail as it is a needed quantity in the process of relating space-fixed and corresponding body-fixed matrix elements. We saw in Chapter 3, Section 3.2 that the nuclear motion can be described by the parametric equations

$$R = (\gamma^2 + b^2)^{1/2} \cosh w + \gamma \,, \tag{4.3.17}$$

$$t = \frac{1}{v_i}\left[(\gamma^2 + b^2)^{1/2} \sinh w + \gamma w\right] \,, \tag{4.3.18}$$

where $\gamma = \zeta / \mu v_i^2$. (4.3.19).

This is for Coulomb nuclear trajectories. Using the new parameter τ defined by

$$\tau = (\gamma^2 + b^2)^{1/2} \sinh w \tag{4.3.20}$$

the equations (4.3.17) and (4.3.18) become

$$R(\tau) = (\tau^2 + \gamma^2 + b^2)^{1/2} + \gamma \tag{4.3.21}$$

$$t(\tau) = \frac{1}{v_i}\left[\tau + \gamma \sinh^{-1}\frac{\tau}{(\gamma^2 + b^2)^{1/2}}\right] . \tag{4.3.22}$$

There is a one-to-one relation between the parameter τ and the position of the nuclei on their trajectories for a given impact parameter b .

When the electron capture matrix elements are computed, they are calculated at given (b, τ) points. That is, a given b -value is selected and matrix elements for different τ -points are found. Thus an expression for the angle δ in terms of b and τ must be found.

In fact the expression is

$$\delta = 2\tan^{-1}\left\{\frac{(\gamma^2+b^2)^{1/2}-\gamma}{b}\cdot\frac{\left[(\tau^2+\gamma^2+b^2)^{1/2}-(\gamma^2+b^2)^{1/2}\right]}{\tau}\right\} \quad . \qquad (4.3.23)$$

It is derived in Appendix A4.

We remember that setting $\gamma=0$ (equation(4.3.19)) corresponded to the straight-line trajectory case. Putting $\gamma=0$ in equation (4.3.21) yields

$$R = (\tau^2+b^2)^{1/2} \qquad (4.3.24)$$

which if we compare with equation (3.2.8) of Chapter 3, shows that

$$\tau = v_i t = z \qquad (4.3.25)$$

in the straight-line case. Hence from equation (4.3.23), setting $\gamma=0$ gives (after some algebra)

$$\delta = \tan^{-1}\frac{z}{b} \qquad (4.3.26)$$

which is consistent with the straight-line trajectory situation (Figure 4.4).

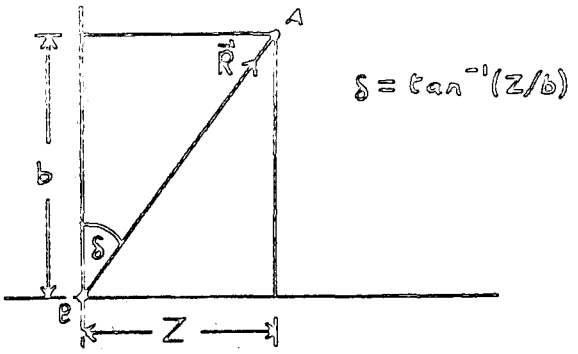

Fig. 4.4

Angle δ in the straight-line trajectory case.

We have shown, therefore, how to obtain the space-fixed BA-type matrix elements in terms of the body-fixed BA-type matrix elements, equation (4.3.13), and also we have an expression for angle δ in terms of b and τ, equation (4.3.23). From this angle β can be found simply and rotation matrix elements for the real spherical harmonics, $D^{l}_{m'm}(\beta)$ may be calculated. The next topic we must consider, is that of the actual integration of the BA-type body-fixed matrix elements.

The integration of the body-fixed elements is performed by using a set of co-ordinates which lend themselves readily to two-centre problems. These are the prolate spheroidal co-ordinates mentioned earlier in this section. They are a set of orthogonal curvilinear co-ordinates defined by

$$\xi = \frac{1}{R}(r_A + r_B), \quad 1 \leq \xi < \infty \qquad (4.3.27a)$$

$$\eta = \frac{1}{R}(r_A - r_B), \quad -1 \leq \eta \leq 1 \qquad (4.3.27b)$$

$$\phi \text{ (azimuthal angle)}, \quad 0 \leq \phi \leq 2\pi. \qquad (4.3.27c)$$

A discussion of these co-ordinates is given in Morse and Feshbach (1953) and also in Arfken (1970). Figure 4.5 shows the $\vec{r}_A$, $\vec{r}_B$ and $\vec{R}$ vectors in the body-fixed frame, and also the azimuthal angle ϕ .

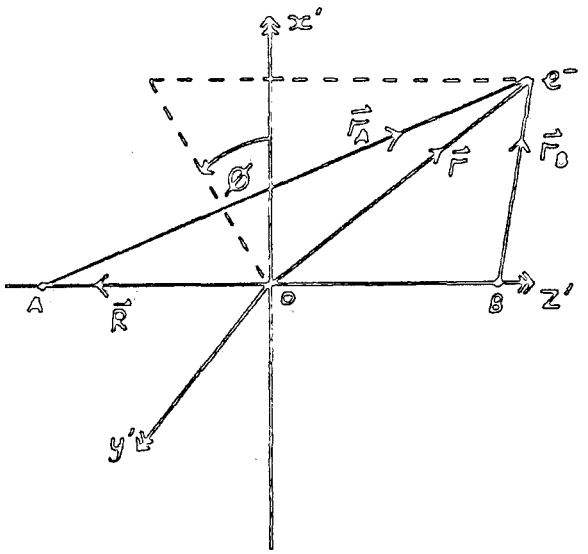

Fig. 4.5
The electron co-ordinates in the body-fixed co-ordinate frame. Angle ϕ has been found by projecting $\vec{r}$ onto the x'y'-plane.

An important point arising from Figure 4.5 is that the vectors $\vec{r}_A$, $\vec{r}_B$ and $\vec{R}$ have the same azimuthal co-ordinate ϕ in the body-fixed frame. That is

$$\phi_A = \phi_B = \phi \quad . \tag{4.3.28}$$

The integration of a typical BA-type element in the body-fixed frame is fairly straightforward. Transformation is made to the (ξ, η, ϕ) co-ordinates and the volume element $d\vec{r}$ is replaced by using

$$d\vec{r} \equiv \frac{R^3}{8}(\xi^2 - \eta^2)\, d\xi\, d\eta\, d\phi \quad . \tag{4.3.29}$$

The integration is then performed. Details of this will be discussed later in this chapter. In Appendix A5 expressions are derived for quantities needed in the integration in terms of (ξ, η, ϕ) co-ordinates.

To recap, we began by having a general BA-type matrix element in the space-fixed frame, $M^{BA}_{jk}(t)$ given in equation (4.3.4). We saw how we could relate this to BA-type matrix elements in the body-fixed frame via the relation of equation (4.3.13). Finally, we have seen that it is possible to integrate the body-fixed elements using prolate sphoidal co-ordinates (ξ, η, ϕ) . Hence we have a prescription for evaluating the BA-type matrix elements, and this was used in the actual calculations of cross sections presented in the next chapter.

The direct matrix elements, equations (3.3.35) to (3.3.56), Chapter 3, all involve the switching function $f(\vec{r}, \vec{R})$, except for the potential matrix elements A^{BB}_{jk} and A^{AA}_{jk} , and the direct L-type elements L^{BB}_{jk} and L^{AA}_{jk} . We saw earlier in this section that we may write the switching function as $g(\vec{r}_A, \vec{r}_B)$, (equation (4.3.6)), that is, it depends in general upon $\vec{r}_A$ and $\vec{r}_B$, though in this work it depends upon r_A and r_B . Hence the direct elements involving the switching function have a "two-centre" character.

The method which has been described in this section for evaluating the two-centre BA-type matrix elements, was used to evaluate all the direct BB- and AA- type matrix elements, including the direct potential matrix elements and the direct L-type elements, which it was possible to do.

In Sections 4.6 and 4.7 of this chapter the numerical and analytic methods of computing the overlap, direct and exchange body-fixed matrix elements will be discussed.

However, before dealing with these, the next two sections will deal with the L-type elements, and the $(\vec{v}.\vec{F})$ - factor in (ξ, η, ϕ) co-ordinates respectively.

4.4 The L-type elements

In section 4.2 mention was made that the L-type matrix elements (which contain $\vec{v}.\vec{\nabla}_{\vec{F}}$) can be recast so as to avoid the awkward $\vec{\nabla}_{\vec{F}}$ operator acting upon an atomic orbital state. In this section is will be shown how this may be done using some of the results of Section 3.4 of Chapter 3 which dealt with simplifying the matrix element expressions.

We begin with the direct matrix elements. Equation (3.4.17) we remember was

$$2B^{BB}_{jk} + 2C^{BB}_{jk} + 2D^{BB}_{jk} + F^{BB}_{jk} = -2(\varepsilon_j - \varepsilon_k) U^{BB}_{jk}. \quad (4.4.1)$$

We may write this more fully as

$$\langle \phi^B_j(\vec{r}_B) | 2f \vec{v}.\vec{\nabla}_{\vec{F}} + 2(\vec{v}.\vec{F})(\vec{\nabla}_{\vec{F}} f).\vec{\nabla}_{\vec{F}} + 2(\vec{v}.\vec{\nabla}_{\vec{F}} f)$$

$$+ (\vec{v}.\vec{F})(\nabla^2_{\vec{F}} f) | \phi^B_k(\vec{r}_B) \rangle = -2(\varepsilon_j - \varepsilon_k) \langle \phi^B_j(\vec{r}_B) | f(\vec{v}.\vec{F}) | \phi^B_k(\vec{r}_B) \rangle. \quad (4.4.2)$$

Setting $f = 1$ in equation (4.4.2) we obtain

$$\langle \phi^B_j(\vec{r}_B) | \vec{v}.\vec{\nabla}_{\vec{F}} | \phi^B_k(\vec{r}_B) \rangle = -(\varepsilon_j - \varepsilon_k) \langle \phi^B_j(\vec{r}_B) | \vec{v}.\vec{F} | \phi^B_k(\vec{r}_B) \rangle. \quad (4.4.3)$$

The left-hand side of equation (4.4.3) is L^{BB}_{jk} hence

$$L^{BB}_{jk} = -(\varepsilon_j - \varepsilon_k) \langle \phi^B_j(\vec{r}_B) | \vec{v}.\vec{F} | \phi^B_k(\vec{r}_B) \rangle. \quad (4.4.4)$$

In an analogous manner we find that

$$L_{jk}^{AA} = -(\eta_j - \eta_k)\langle \chi_j^A(\vec{r}_A)|\, \vec{v}.\vec{r}\, |\chi_k^A(\vec{r}_A)\rangle \,. \qquad (4.4.5)$$

For the exchange elements we use the expression given by equation (3.4.24), namely

$$2B_{jk}^{BA} + 2C_{jk}^{BA} + 2D_{jk}^{BA} + F_{jk}^{BA} = 2X_{jk}^{BA} \qquad (4.4.6)$$

where $$X_{jk}^{BA} = V_{jk}^{BA} - W_{jk}^{BA} - (\varepsilon_j - \eta_k)U_{jk}^{BA} \,, \qquad (4.4.7)$$

and the V_{jk}^{BA}, W_{jk}^{BA} and U_{jk}^{BA} matrix elements being given by equations (3.4.26) to (3.4.28). As for the direct matrix elements, we set $f=1$ and the C-, D- and F- type elements vanish giving

$$L_{jk}^{BA} = \langle \phi_j^B(\vec{r}_B)|\, \vec{v}.\vec{\nabla}_r |\chi_k^A(\vec{r}_A)\rangle$$

$$= \langle \phi_j^B(\vec{r}_B)|\left[V_{eB} - V_{eA} - (\varepsilon_j - \eta_k)\right](\vec{v}.\vec{r})|\chi_k^A(\vec{r}_A)\rangle \,. \qquad (4.4.8)$$

In a similar manner an expression for L_{jk}^{AB} can be obtained from equation (3.4.29)

$$L_{jk}^{AB} = \langle \chi_j^A(\vec{r}_A)|\left[V_{eA} - V_{eB} - (\eta_j - \varepsilon_k)\right](\vec{v}.\vec{r})|\phi_k^B(\vec{r}_B)\rangle \,. \qquad (4.4.9)$$

We see that equations (4.4.8) and (4.4.9) are consistent with the relation

$$(\underset{\sim}{L}^{AB})^{\dagger} = -\underset{\sim}{L}^{BA} \,. \qquad (4.4.10)$$

We have therefore obtained expressions for the L-type matrix elements, equations (4.4.4), (4.4.5), (4.4.8) and (4.4.9) which do not involve the $\vec{\nabla}_r$ operator. It was stated in Section 3.4 that in an actual calculation only the BA-type

exchange matrix elements are computed. Hence the expression for L^{AB}_{jk}, equation (4.4.9), is not required in practice.

4.5 The $(\vec{v}.\vec{r})$-factor in (ξ,η,ϕ) co-ordinates

A factor which occurs in almost all of the individual matrix elements of this work is $(\vec{v}.\vec{r})$. In this section an expression for this factor will be derived in terms of the prolate spheroidal co-ordinates, (ξ,η,ϕ).

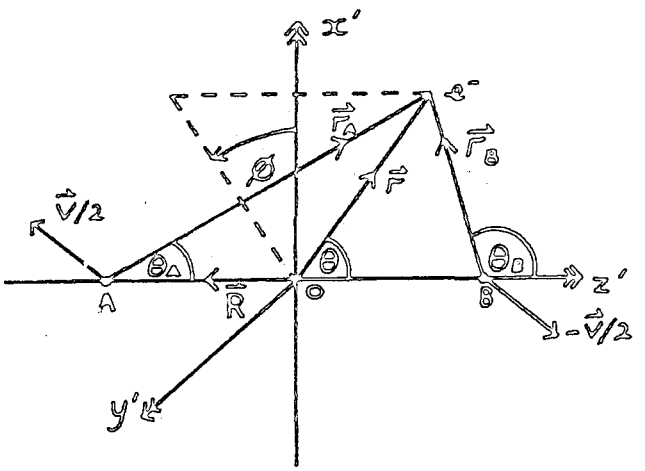

Figure 4.6
Electron co-ordinates in the body-fixed frame.

Figure 4.6 shows a diagram of the co-ordinates in the body-fixed frame. We note that the velocity vector $\vec{v}$ lies in the x'z'-plane and so has no y'-component. Thus in the body-fixed frame (indicated by prime notation)

$$\vec{v}.\vec{r} = v_{x'}x' + v_{z'}z' \quad . \tag{4.5.1}$$

This may be re-written in terms of spherical polar co-ordinates (r,θ,ϕ) as

$$\vec{v}.\vec{r} = v_{x'}r\sin\theta\cos\phi + v_{z'}r\cos\theta \quad . \tag{4.5.2}$$

From some of the results of Appendix A5, namely equations (A5.19a) to (A5.19c), equation (4.5.2) may be written

$$\vec{v}.\vec{r} = \frac{v_{x'}R}{2}\left[(\xi^2-1)(1-\eta^2)\right]^{1/2}\cos\phi + \frac{v_{z'}R}{2}\xi\eta \,. \qquad (4.5.3)$$

We need, finally, to obtain expressions for the velocity components $v_{x'}$ and $v_{z'}$.

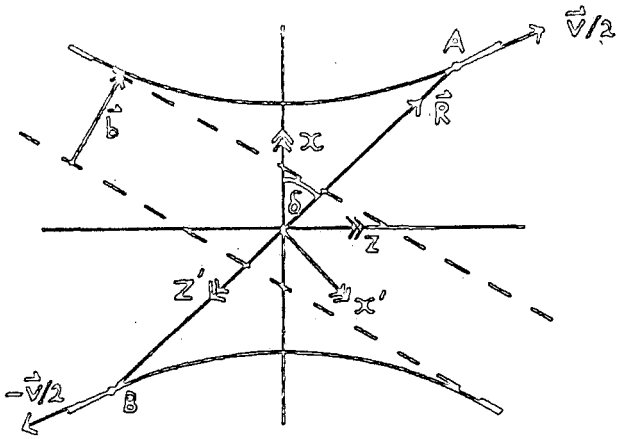

Figure 4.7
The space-fixed and body-fixed frames.

Figure 4.7 shows the space-fixed and body-fixed frames. We also note the angle δ which is important in determining the amount of rotation required to transform between the two frames. In the body-fixed frame the vector $\vec{v}$ may be written

$$\vec{v} = v_{x'}\hat{i}_b + v_{z'}\hat{k}_b \qquad (4.5.4)$$

where $v_{x'}$ and $v_{z'}$ are the components of $\vec{v}$ in the body-fixed frame, and $\hat{i}_b$ and $\hat{k}_b$ are body-fixed unit vectors, parallel to the x'- and z'-axes respectively. It follows from Figure 4.7 that

$$\vec{v} = R\frac{d\delta}{dt}\hat{i}_b - \frac{dR}{dt}\hat{k}_b \,. \qquad (4.5.5)$$

By conservation of angular momentum we have

$$v_i b = R^2\frac{d\delta}{dt} \qquad (4.5.6)$$

where v_i is the initial relative velocity of the nuclei A and B, and b is the modulus of the impact parameter vector $\vec{b}$. Hence using equation (4.5.6) we see that the velocity components are

$$v_{x'} = b v_i / R \tag{4.5.7}$$

and

$$v_{z'} = - dR/dt \ . \tag{4.5.8}$$

The final expression for $(\vec{v}.\vec{F})$ is thus

$$\vec{v}.\vec{F} = \tfrac{1}{2} b v_i \left[(\xi^2-1)(1-\eta^2)\right]^{1/2} \cos\phi - \tfrac{1}{2} R \frac{dR}{dt} \xi\eta \ . \tag{4.5.9}$$

The expression in equation (4.5.9) is completely general. For the special case of straight-line trajectory motion of the nuclei we begin with the well-known relation for the straight-line case (see equation (3.2.8)).

$$R^2 = b^2 + v_i^2 t^2 \ . \tag{4.5.10}$$

From this we obtain the straight-line trajectory $(\vec{v}.\vec{F})$-factor

$$\vec{v}.\vec{F} = \tfrac{1}{2} b v_i \left[(\xi^2-1)(1-\eta^2)\right]^{1/2} \cos\phi - \tfrac{1}{2} v_i^2 t \, \xi\eta \ . \tag{4.5.11}$$

We have thus obtained an expression for $(\vec{v}.\vec{F})$ in terms of (ξ,η,ϕ) given by equation (4.5.9).

4.6 Evaluating the body-fixed matrix elements - numerical method

In this section the numerical evaluation of the body-fixed matrix elements will be discussed. As was stated in the introduction to this chapter, this method was used for

obtaining the matrix elements used to calculate the final electron capture cross sections presented in Chapter 5 of this thesis. This was because it was best suited to investigating the effect of the use of different forms of switching functions.

The analytic method, which will be discussed in the next section of this chapter, could be used with the "simple" switching function f_s where

$$f_s = -\frac{R^2}{R^2+p^2}\,\eta \quad , \tag{4.6.1}$$

and the method could also be used with switching functions of the form

$$f = -\frac{R^2}{R^2+p^2}\,Q(\eta) \tag{4.6.2}$$

where the polynomial $Q(\eta)$ is given by equation (4.1.4).

The overlap and required BA-type matrix elements (excluding L-type elements) may be represented by general BA-type matrix elements of the form

$$M_{jk}^{BA} = \int_V \phi_j^{B*}(\vec{r}_B)\, m(\vec{r},t)\, \chi_k^A(\vec{r}_A)\, d\vec{r} \quad . \tag{4.6.3}$$

We know, however, that L-type elements may be written in terms of elements of the form given in equation (4.6.3) (Section 4.4). Although not explicitly shown, these elements are in the body-fixed co-ordinate frame. We may write equation (4.6.3) more explicitly using the expressions for the atomic orbital wavefunctions $\phi_j^B(\vec{r}_B)$ and $\chi_k^A(\vec{r}_A)$, equations (4.2.14) and (4.2.15) and the real spherical harmonics $\bar{Y}_{(l_B)_j(m_B)_j}(\theta_B,\phi_B)$, $\bar{Y}_{(l_A)_k(m_A)_k}(\theta_A,\phi_A)$

which occur in $\phi_j^B(\vec{r}_B)$ and $\chi_k^A(\vec{r}_A)$. The expressions for the real spherical harmonics are given in equations (4.2.18) and (4.2.19). The expression for M_{jk}^{BA} becomes

$$M_{jk}^{BA} = N_{(m_B)_j} C_{(l_B)_j (m_B)_j} N_{(m_A)_k} C_{(l_A)_k (m_A)_k}$$

$$\times \int_V R_{(n_B)_j (l_B)_j}(r_B) R_{(n_A)_k (l_A)_k}(r_A) P_{(l_B)_j}^{(m_B)_j}(\cos\theta_B) P_{(l_A)_k}^{(m_A)_k}(\cos\theta_A)$$

$$\times \cos(m_B)_j \phi_B \cos(m_A)_k \phi_A \, . \, m(\vec{r}, t) \, . \, d\vec{r} \quad . \qquad (4.6.4)$$

We define angular factors to make the expressions less complicated. They are

$$\alpha_k \equiv N_{(m_A)_k} C_{(l_A)_k (m_A)_k} \qquad (4.6.5a)$$

$$\beta_j \equiv N_{(m_B)_j} C_{(l_B)_j (m_B)_j} \quad . \qquad (4.6.5b)$$

We remember that the volume element in prolate spheroidal co-ordinates is given by

$$d\vec{r} = \frac{R^3}{8}(\xi^2 - \eta^2)\, d\xi\, d\eta\, d\phi \quad . \qquad (4.6.6)$$

From equation (A5.3c) of Appendix A5, this may be re-written as

$$d\vec{r} = \frac{R}{2} r_A r_B \, d\xi\, d\eta\, d\phi \, . \qquad (4.6.7)$$

Thus the M_{jk}^{BA} matrix elements become

$$M_{jk}^{BA} = \frac{R}{2}\beta_j \alpha_k \int_1^\infty d\xi \int_{-1}^{1} d\eta \int_0^{2\pi} d\phi \, . \, r_B R_{(n_B)_j (l_B)_j}(r_B) \, . \, r_A R_{(n_A)_k (l_A)_k}(r_A)$$

$$\times P_{(l_B)_j}^{(m_B)_j}(\cos\theta_B) P_{(l_A)_k}^{(m_A)_k}(\cos\theta_A) \, . \, m(\vec{r}, t) \, . \, \cos(m_B)_j \phi \cos(m_A)_k \phi \, . \qquad (4.6.8)$$

We note that the azimuthal angles ϕ_A and ϕ_B have been replaced by ϕ from equation (4.3.28). In a similar fashion the general direct matrix elements, M^{BB}_{jk} and M^{AA}_{jk} given by

$$M^{BB}_{jk} = \int_V \phi^{B*}_j(\vec{r}_B)\, m(\vec{r},t)\, \phi^B_k(\vec{r}_B)\, d\vec{r} \qquad (4.6.9)$$

and

$$M^{AA}_{jk} = \int_V \chi^{A*}_j(\vec{r}_A)\, m(\vec{r},t)\, \chi^A_k(\vec{r}_A)\, d\vec{r} \qquad (4.6.10)$$

are given by

$$M^{BB}_{jk} = \frac{R}{2}\beta_j\beta_k \int_1^\infty d\xi \int_{-1}^{1} d\eta \int_0^{2\pi} d\phi \cdot r_A r_B R_{(n_B)_j(l_B)_j}(r_B) R_{(n_B)_k(l_B)_k}(r_B)$$

$$\times P^{(m_B)_j}_{(l_B)_j}(\cos\theta_B)\, P^{(m_B)_k}_{(l_B)_k}(\cos\theta_B) \cdot m(\vec{r},t) \cdot \cos(m_B)_j\phi \cos(m_B)_k\phi \qquad (4.6.11)$$

and

$$M^{AA}_{jk} = \frac{R}{2}\alpha_j\alpha_k \int_1^\infty d\xi \int_{-1}^{1} d\eta \int_0^{2\pi} d\phi \cdot r_A r_B R_{(n_A)_j(l_A)_j}(r_A) R_{(n_A)_k(l_A)_k}(r_A)$$

$$\times P^{(m_A)_j}_{(l_A)_j}(\cos\theta_A)\, P^{(m_A)_k}_{(l_A)_k}(\cos\theta_A) \cdot m(\vec{r},t) \cdot \cos(m_A)_j\phi \cos(m_A)_k\phi \,. \qquad (4.6.12)$$

The functions $m(\vec{r},t)$ occurring in the expressions for M^{BA}_{jk} M^{BB}_{jk} and M^{AA}_{jk}, equations (4.6.8), (4.6.11) and (4.6.12), may depend upon $(\vec{v}.\vec{r})$ and the switching function $f(\vec{r},\vec{R})$, or quantities involving the gradient operator $\vec{\nabla}_{\vec{r}}$ acting upon $f(\vec{r},\vec{R})$. The m - functions must be determined in terms of (ξ,η,ϕ) co-ordinates prior to an actual calculation of matrix elements. We saw in Section 4.5, earlier in this chapter, how $(\vec{v}.\vec{r})$ was found in terms

of ξ, η and ϕ .

The azimuthal integration involved in integrating the matrix elements is fairly straightforward. The ϕ - integrals that may occur are of the three types as follows:-

$$ {}^{\phi}I_1(m_1, m_2) = \int_0^{2\pi} \cos m_1\phi \cos m_2\phi \, d\phi \, , \qquad (4.6.13) $$

$$ {}^{\phi}I_2(m_1, m_2) = \int_0^{2\pi} \cos m_1\phi \cos m_2\phi \cos\phi \, d\phi \, , \qquad (4.6.14) $$

and $$ {}^{\phi}I_3(m_1, m_2) = \int_0^{2\pi} \cos m_1\phi \cos m_2\phi \cos^2\phi \, d\phi \, , \qquad (4.6.15) $$

where m_1 and m_2 may be m_A or m_B with appropriate subscripts j or k . These angular integrals are evaluated in Appendix A6.

We are left, therefore, with a two-dimensional integration to perform over the variables ξ and η . This is performed numerically by using Gaussian integration - Gauss - Legendre integration for the η - integral and Gauss - Laguerre integration with transformed nodes and weights for the ξ - integral. More will be said about the numerical techniques used in Chapter 5.

We see that, in principle, the numerical method of evaluating the matrix elements is not too difficult, being based upon a two-dimensional numerical integration technique. In the next section of this chapter the analytic method will be discussed.

4.7 Evaluating the body-fixed matrix elements - analytic method

4.7.1 Introduction

In the previous section the numerical method of evaluating the body-fixed matrix elements was discussed. This method allowed the use of any functional form of switching function, and was used to obtain the electron capture cross sections presented in Chapter 5.

One of the switching functions used in this work was the "simple" switching function f_s mentioned earlier in this chapter. We remember that it was given by

$$f_s = -\frac{R^2}{R^2+\rho^2}\,\eta \qquad (4.7.1)$$

where ρ is a parameter and η is one of the prolate spheroidal co-ordinates which were discussed toward the end of Section 4.3 of this chapter. We remember that η was given by

$$\eta = \frac{1}{R}(r_A - r_B), \qquad -1 \leq \eta \leq 1 \quad . \qquad (4.7.2)$$

We note that the basic property of the switching function f_s is from equations (3.3.24) and (3.3.25) of Chapter 3.

$$f_s(\vec{r},\vec{R}) \longrightarrow -1 \qquad \text{for } r_B \ll r_A \quad \text{as } R \to \infty \ , \qquad (4.7.3)$$

$$f_s(\vec{r},\vec{R}) \longrightarrow +1 \qquad \text{for } r_A \ll r_B \quad \text{as } R \to \infty \ . \qquad (4.7.4)$$

We see that the switching behaviour of the function f_s is due to the fact that η varies between plus and minus one. The parameter ρ is present in the expression for f_s in order to give the correct united atom limit for f_s .

That is, as $R \to 0$, $f_s \to 0$ (equation (3.3.26) of Chapter 3). The absence of the parameter p would result in f_s being indeterminate at $R = 0$. We define a function $F(R)$ by

$$F(R) = \frac{R^2}{R^2 + p^2} \tag{4.7.5}$$

and so we may write f_s as

$$f_s = -F(R)\eta \,. \tag{4.7.6}$$

It turns out that if the switching function f_s is employed, it is possible to evaluate the matrix elements analytically.

The analytic method is such that it can be used when the function $f(\vec{r}, \vec{R})$ is of the form

$$f = -F(R)\mathcal{P}(\xi)Q(\eta) \tag{4.7.7}$$

where $\mathcal{P}(\xi)$ and $Q(\eta)$ are polynomials given by

$$\mathcal{P}(\xi) = a_0 + a_1\xi + a_2\xi^2 + a_3\xi^3 + \ldots + a_m\xi^m \tag{4.7.8}$$

and

$$Q(\eta) = b_0 + b_1\eta + b_2\eta^2 + b_3\eta^3 + \ldots + b_n\eta^n \,. \tag{4.7.9}$$

However, owing to the fact that ξ may range between one and infinity, namely

$$1 \leq \xi < \infty \,, \tag{4.7.10}$$

it would be impossible to have a switching function of the form given in equation (4.7.7) as it would not have the correct switching properties required. Hence a restriction must be made upon the form of the switching function suitable

for use with the analytic method of evaluating the matrix elements. The form was stated in the introduction to this chapter. It was

$$f = -\frac{R^2}{R^2+\rho^2}\, Q(\eta) \qquad (4.7.11)$$

where $Q(\eta)$ is now

$$Q(\eta) = b_1\eta + b_3\eta^3 + b_5\eta^5 + \ldots + b_{2n+1}\eta^{2n+1}\,, \qquad (4.7.12)$$

and where the coefficients $b_1, b_3, \ldots$etc. must be such that

$$Q(\pm 1) = \pm 1 \qquad (4.7.13)$$

in order to produce the correct switching behaviour of the switching function. The rest of this section will be devoted to discussing the analytic method of evaluating the elements using the switching function of the form given in equation (4.7.11).

4.7.2 Preliminary reduction of the matrix elements

We begin by considering the analytic evaluation of the overlap and exchange body-fixed matrix elements and we remember that these may be written as, or for the L-type elements, written in terms of, general BA-type matrix elements of the form

$$M_{jk}^{BA} = \int_V \phi_j^{B*}(\vec{r}_B)\, m(r,t)\, \chi_k^A(\vec{r}_A)\, dr\,. \qquad (4.7.14)$$

The fact that this is in the body-fixed frame is not explicitly shown. We consider the product of the atomic orbital wavefunctions $\phi_j^{B*}(\vec{r}_B)$ and $\chi_k^A(\vec{r}_A)$ in the integrand of the integral above and re-write it as

$$\phi_j^{B*}(\vec{r}_B)\chi_k^A(\vec{r}_A)=\beta_j\alpha_k\Omega_{jk}^{BA}(\vec{r}_B,\vec{r}_A)\,. \qquad (4.7.15)$$

The complex conjugation is, in fact, superfluous as we are using real orbitals. The function $\Omega_{jk}^{BA}(\vec{r}_B,\vec{r}_A)$ is given by

$$\Omega_{jk}^{BA}(\vec{r}_B,\vec{r}_A)=R_{(n_D)_j(l_D)_j}(r_B)R_{(n_A)_k(l_A)_k}(r_A)$$

$$\times P_{(l_D)_j}^{(m_D)_j}(\cos\theta_B)P_{(l_A)_k}^{(m_A)_k}(\cos\theta_A)\cos(m_D)_j\phi_B\cos(m_A)_k\phi_A\,. \qquad (4.7.16)$$

The angular factors α_k and β_j were defined in the previous section, equations (4.6.5a), (4.6.5b).

We may thus write equation (4.7.14) as

$$M_{jk}^{BA}=\beta_j\alpha_k\int_V\Omega_{jk}^{BA}(\vec{r}_B,\vec{r}_A)m(\vec{r},t)\,d\vec{r}\,. \qquad (4.7.17)$$

Prolate spheroidal co-ordinates (ξ,η,ϕ) are used to perform the integration. For each of the overlap and exchange BA-type matrix elements, the function $m(\vec{r},t)$ is written in terms of the variables ξ, η and ϕ, and where the switching function $f(\vec{r},\vec{R})$ is of the form given in equation (4.7.11). The volume element $d\vec{r}$ must be replaced by the expression of equation (4.6.6) of the previous section. The result of this is that the overlap and exchange BA-type elements are shown to be expressible in terms of triple integrals involving the variables ξ, η and ϕ. As a simple example, let us consider the potential matrix elements A_{jk}^{BA} which are

$$A_{jk}^{BA}=\int_V\phi_j^{B*}(\vec{r}_B)\frac{(-Z_B)}{r_B}\chi_k^A(\vec{r}_A)\,d\vec{r}\,. \qquad (4.7.18)$$

This becomes

$$A_{jk}^{BA} = -Z_i \beta_j \alpha_k \frac{R^2}{4} \left\{ \int_1^\infty d\xi \int_{-1}^{1} d\eta \int_0^{2\pi} d\phi \, \Omega_{jk}^{DA}(\vec{r}_B, \vec{r}_A)\, \xi \right.$$
$$\left. + \int_1^\infty d\xi \int_{-1}^{1} d\eta \int_0^{2\pi} d\phi \, \Omega_{jk}^{BA}(\vec{r}_B, \vec{r}_A)\, \eta \right\} , \qquad (4.7.19)$$

where the two triple integrals are enclosed in the curly brackets. The actual expressions for the other elements are rather tedious to derive, but once the expresions have been obtained it turns out that the triple integrals involved are of only three types which are as follows:-

$$\overset{A}{\Omega}I_{jk}^{BA}(m,n) = \int_1^\infty d\xi \int_{-1}^{1} d\eta \int_0^{2\pi} d\phi \, \Omega_{jk}^{BA} \xi^m \eta^n \qquad (4.7.20a)$$

$$\overset{B}{\Omega}I_{jk}^{BA}(m,n) = \int_1^\infty d\xi \int_{-1}^{1} d\eta \int_0^{2\pi} d\phi \, \Omega_{jk}^{BA} \xi^m \eta^n (\xi^2-1)^{1/2} (1-\eta^2)^{1/2} \cos\phi \qquad (4.7.20b)$$

$$\overset{C}{\Omega}I_{jk}^{BA}(m,n) = \int_1^\infty d\xi \int_{-1}^{1} d\eta \int_0^{2\pi} d\phi \, \Omega_{jk}^{BA} \xi^m \eta^n \cos^2\phi \qquad (4.7.20c)$$

where $m, n \geq 0$.

We call the above integrals Ω -triple integrals. The three Ω -triple integrals above can be performed analytically, and one of the reasons as to why this should be so is that they have ξ to the power m and η to the power n in their integrands, where m and n are non-negative integers. Now we can see why it was important to state that only a certain type of switching function could be used with the analytic method, namely one involving a simple polynomial function of η. Anything other than this would

result in Ω -triple integrals that contained perhaps awkward demoninators, trigonometric functions, etc., in their integrands. Such integrals could probably not be performed analytically, and certainly they could not be performed using the techniques yet to be described. Before moving on to see how the three Ω-triple integrals of equations (4.7.20a) to (4.7.20c) can be performed, we note that, in general, the switching function $f(\vec{r},\vec{R})$ could be of the form

$$f = -F(R)P(\xi)Q(\eta) \qquad (4.7.21)$$

as we stated earlier in this section. However, it was ruled invalid as it would not be a true "switching" function due to the presence of the polynomial $P(\xi)$.

4.7.3 The Ω-triple integrals ${}^{A}_{\Omega}I^{BA}_{jk}(m,n)$, ${}^{B}_{\Omega}I^{BA}_{jk}(m,n)$ and ${}^{C}_{\Omega}I^{BA}_{jk}(m,n)$

The integral ${}^{A}_{\Omega}I^{BA}_{jk}(m,n)$ is

$${}^{A}_{\Omega}I^{BA}_{jk}(m,n) = \int_{1}^{\infty} d\xi \int_{-1}^{1} d\eta \int_{0}^{2\pi} d\phi \, \Omega^{BA}_{jk} \xi^{m} \eta^{n} . \qquad (4.7.22)$$

We remember from equation (4.7.16) that the function Ω^{BA}_{jk} is given by

$$\Omega^{BA}_{jk} = R_{(n_B)_j(l_B)_j}(r_B) R_{(n_A)_k(l_A)_k}(r_A)$$

$$\times P^{(m_B)_j}_{(l_B)_j}(\cos\theta_B) P^{(m_A)_k}_{(l_A)_k}(\cos\theta_A) \cos(m_B)_j\phi \cos(m_A)_k\phi \qquad (4.7.23)$$

but where the azimuthal angles ϕ_A and ϕ_B have been replaced by angle ϕ from equation (4.3.28). Substituting for the radial wavefunctions using the explicit expressions given in section 4.2 of this chapter, equations (4.2.16) and

(4.2.17), equation (4.7.23) becomes (with a little re-arrangement),

$$\Omega_{jk}^{BA} = \sum_{p=1}^{(n_A)_k-(l_A)_k} \sum_{q=1}^{(n_B)_j-(l_B)_j} a_{kp} b_{jq} e^{-\mu_k r_A} e^{-\nu_j r_0} r_A^{[(l_A)_k-1+p]} r_B^{[(l_B)_j-1+q]}$$

$$\times P_{(l_A)_k}^{(m_A)_k}(\cos\theta_A) P_{(l_B)_j}^{(m_B)_j}(\cos\theta_B) \cos(m_A)_k\phi \cos(m_B)_j\phi \quad . \qquad (4.7.24)$$

Combining equations (4.7.22) and (4.7.24) gives

$${}_{\Omega}^{A}I_{jk}^{BA}(m,n) = {}^{\phi}I_1[(m_A)_k,(m_B)_j] \sum_{p=1}^{(n_A)_k-(l_A)_k} \sum_{q=1}^{(n_B)_j-(l_B)_j} a_{kp} b_{jq}\, {}^{BA}S_{jk}^{pq}(m,n) \qquad (4.7.25)$$

where the ${}^{\phi}I_1$ is one of the three azimuthal integrals that occurred when the numerical method was used, equations (4.6.13) to (4.6.15), and where ${}^{BA}S_{jk}^{pq}(m,n)$ is the integral

$${}^{BA}S_{jk}^{pq}(m,n) = \int_1^{\infty} d\xi \int_{-1}^{1} d\eta\, e^{-\mu_k r_A} e^{-\nu_j r_0} r_A^{[(l_A)_k-1+p]} r_B^{[(l_B)_j-1+q]}$$

$$\times \xi^m \eta^n P_{(l_A)_k}^{(m_A)_k}(\cos\theta_A) P_{(l_B)_j}^{(m_B)_j}(\cos\theta_B) \quad . \qquad (4.7.26)$$

Similarly for ${}_{\Omega}^{B}I_{jk}^{BA}(m,n)$

$${}_{\Omega}^{B}I_{jk}^{BA}(m,n) = {}^{\phi}I_2[(m_A)_k,(m_B)_j] \sum_{p=1}^{(n_A)_k-(l_A)_k} \sum_{q=1}^{(n_B)_j-(l_B)_j} a_{kp} b_{jq}\, {}^{BA}T_{jk}^{pq}(m,n) \qquad (4.7.27)$$

where ${}^{\phi}I_2$ is one of the three azimuthal integrals mentioned above and the integral ${}^{BA}T_{jk}^{pq}(m,n)$ is given by

$${}^{BA}T_{jk}^{pq}(m,n) = \int_1^{\infty} d\xi \int_{-1}^{1} d\eta\, e^{-\mu_k r_A} e^{-\nu_j r_0} r_A^{[(l_A)_k-1+p]} r_B^{[(l_B)_j-1+q]}$$

$$\times \xi^m (\xi^2-1)^{1/2} \eta^n (1-\eta^2)^{1/2} P_{(l_A)_k}^{(m_A)_k}(\cos\theta_A) P_{(l_B)_j}^{(m_B)_j}(\cos\theta_B) \quad . \qquad (4.7.28)$$

Finally the integral ${}^{C}_{\Omega}I^{BA}_{jk}(m,n)$ is given by

$$ {}^{C}_{\Omega}I^{BA}_{jk}(m,n) = {}^{\phi}I_{3}\left[(m_A)_k,(m_B)_j\right] \sum_{p=1}^{(n_A)_k-(m_A)_k} \sum_{q=1}^{(n_B)_j-(m_B)_j} a_{kp}\, b_{jq}\, {}^{BA}S^{pq}_{jk}(m,n) \qquad (4.7.29) $$

where the integral ${}^{BA}S^{pq}_{jk}(m,n)$ is given by equation (4.7.26).

We have reduced down the expressions for the three triple integrals ${}^{A}_{\Omega}I^{BA}_{jk}(m,n)$, ${}^{B}_{\Omega}I^{BA}_{jk}(m,n)$ and ${}^{C}_{\Omega}I^{BA}_{jk}(m,n)$ to expressions involving the two double integrals ${}^{BA}S^{pq}_{jk}(m,n)$ and ${}^{BA}T^{pq}_{jk}(m,n)$. The next stage is to obtain expressions for these double integrals.

4.7.4 The double integrals ${}^{BA}S^{pq}_{jk}(m,n)$ and ${}^{BA}T^{pq}_{jk}(m,n)$

The integrals ${}^{BA}S^{pq}_{jk}(m,n)$ and ${}^{BA}T^{pq}_{jk}(m,n)$ both contain associated Legendre functions $P^{(m_A)_k}_{(\ell_A)_k}(\cos\theta_A)$ and $P^{(m_B)_j}_{(\ell_B)_j}(\cos\theta_B)$ which must be expressed in terms of the integration variables ξ and η before the integration can be performed. In Appendix A7 lists of these associated Legendre functions are given in terms of ξ and η . If we inspect these expressions for the associated Legendre functions, we see that they all contain the factor $(\xi+\eta)$ or $(\xi-\eta)$, raised to the power $(\ell_A)_k$ or $(\ell_B)_j$ respectively, in the denominators. We know that

$$ r_A = \frac{R}{2}(\xi+\eta) \qquad \text{and} \qquad r_B = \frac{R}{2}(\xi-\eta) \qquad (4.7.30) $$

from equations (A5.2a) and (A5.2b) of Appendix A5, and so we may express the associated Legendre functions in terms of r_A and r_B . The result of this is that we obtain the following expressions for $P^{(m_A)_k}_{(\ell_A)_k}(\cos\theta_A)$ and $P^{(m_B)_j}_{(\ell_B)_j}(\cos\theta_B)$

$$P^{(m_A)_k}_{(\ell_A)_k}(\cos\theta_A) = \left(\frac{R}{2}\right)^{(\ell_A)_k} r_A^{-(\ell_A)_k}\, {}^{A}\bar{P}^{(m_A)_k}_{(\ell_A)_k}(\xi,\eta) \qquad (4.7.31)$$

$$P^{(m_B)_j}_{(\ell_B)_j}(\cos\theta_B) = \left(\frac{R}{2}\right)^{(\ell_B)_j} r_B^{-(\ell_B)_j}\, {}^{B}\bar{P}^{(m_B)_j}_{(\ell_B)_j}(\xi,\eta) \qquad (4.7.32)$$

where the functions ${}^{A}\bar{P}^{(m_A)_k}_{(\ell_A)_k}(\xi,\eta)$ and ${}^{B}\bar{P}^{(m_B)_j}_{(\ell_B)_j}(\xi,\eta)$ do not involve awkward $(\xi+\eta)$ or $(\xi-\eta)$ factors raised to the powers $(\ell_A)_k$ or $(\ell_B)_j$ respectively, in the denominators. As an example $P^2_2(\cos\theta_A)$ is given by

$$P^2_2(\cos\theta_A) = 3\sin^2\theta_A$$

$$= \frac{3(\xi^2-1)(1-\eta^2)}{(\xi+\eta)^2} \; . \qquad (4.7.33)$$

Using equations (4.7.30) and (4.7.31) gives us that

$$P^2_2(\cos\theta_A) = \left(\frac{R}{2}\right)^2 r_A^{-2}\, {}^{A}\bar{P}^2_2(\xi,\eta) \qquad (4.7.34)$$

where $${}^{A}\bar{P}^2_2(\xi,\eta) = 3(\xi^2-1)(1-\eta^2) \; . \qquad (4.7.35)$$

Substituting for the associated Legendre functions $P^{(m_A)_k}_{(\ell_A)_k}(\cos\theta_A)$ and $P^{(m_B)_j}_{(\ell_B)_j}(\cos\theta_B)$ in the expression for ${}^{BA}S^{pq}_{jk}(m,n)$, equation (4.7.26) we obtain

$${}^{BA}S^{pq}_{jk}(m,n) = \left(\frac{R}{2}\right)^{(\ell_B)_j+(\ell_A)_k} \int_1^\infty d\xi \int_{-1}^{1} d\eta\, e^{-\mu_k r_A} e^{-\nu_j r_B} r_A^{(p-n)} r_B^{(q-n)}$$

$$\times \xi^m \eta^n\, {}^{A}\bar{P}^{(m_A)_k}_{(\ell_A)_k}(\xi,\eta)\, {}^{B}\bar{P}^{(m_B)_j}_{(\ell_B)_j}(\xi,\eta) \; . \qquad (4.7.36)$$

We see immediately that the introduction of the functions ${}^{A}\bar{P}^{(m_A)_k}_{(\ell_A)_k}(\xi,\eta)$ and ${}^{B}\bar{P}^{(m_B)_j}_{(\ell_B)_j}(\xi,\eta)$ via equations (4.7.31) and (4.7.32) has resulted in the elimination of the factors $r_A^{(\ell_A)_k}$ and $r_B^{(\ell_B)_j}$ from the integrand of ${}^{BA}S^{pq}_{jk}(m,n)$.

By using the binomial expansion for $r_A^{(p-1)}$ and $r_B^{(q-1)}$ namely

$$r_A^{(p-1)} = \left(\frac{R}{2}\right)^{p-1}(\xi+\eta)^{p-1}$$

$$= \left(\frac{R}{2}\right)^{p-1}\sum_{r=0}^{p-1}\frac{(p-1)!}{r!(p-r-1)!}\,\xi^{p-r-1}\eta^{r} \qquad (4.7.37)$$

and

$$r_B^{(q-1)} = \left(\frac{R}{2}\right)^{q-1}(\xi-\eta)^{q-1}$$

$$= \left(\frac{R}{2}\right)^{q-1}\sum_{s=0}^{q-1}\frac{(q-1)!}{s!(q-s-1)!}(-1)^{s}\xi^{q-s-1}\eta^{s}, \qquad (4.7.38)$$

we obtain the following expression for ${}^{BA}S_{jk}^{pq}(m,n)$

$${}^{BA}S_{jk}^{pq}(m,n) = \left(\frac{R}{2}\right)^{(\ell_B)_j+(\ell_A)_k+p+q-2}(p-1)!\,(q-1)!$$

$$\times\sum_{r=0}^{p-1}\sum_{s=0}^{q-1}\frac{(-1)^{s}}{r!\,s!\,(p-r-1)!\,(q-s-1)!}\,{}^{BA}\bar{S}_{jk,rs}^{pq}(m,n) \qquad (4.7.39)$$

where ${}^{BA}\bar{S}_{jk,rs}^{pq}(m,n)$ is given by

$${}^{BA}\bar{S}_{jk,rs}^{pq}(m,n) = \int_1^{\infty}d\xi\int_{-1}^{1}d\eta\, e^{-\mu_k r_A}e^{-\nu_j r_B}\xi^{m+p+q-r-s-2}\eta^{n+r+s}$$

$$\times\,{}^{A}\bar{P}_{(\ell_A)_k}^{(m_A)_k}(\xi,\eta)\,{}^{B}\bar{P}_{(\ell_B)_j}^{(m_B)_j}(\xi,\eta). \qquad (4.7.40)$$

In a similar fashion the integral ${}^{BA}T_{jk}^{pq}(m,n)$ of equation (4.7.28) is given by

$${}^{BA}T_{jk}^{pq}(m,n) = \left(\frac{R}{2}\right)^{(\ell_B)_j+(\ell_A)_k+p+q-2}(p-1)!\,(q-1)!$$

$$\times\sum_{r=0}^{p-1}\sum_{s=0}^{q-1}\frac{(-1)^{s}}{r!\,s!\,(p-r-1)!\,(q-s-1)!}\,{}^{BA}\bar{T}_{jk,rs}^{pq}(m,n) \qquad (4.7.41)$$

where ${}^{BA}\bar{T}_{jk,rs}^{pq}(m,n)$ is given by

$$ {}^{BA}\bar{\bar{T}}^{pq}_{jk,rs}(m,n) = \int_1^\infty d\xi \int_{-1}^{1} d\eta\, e^{-\mu_k r_A} e^{-\nu_j r_B} \xi^{m+p+q-r-s-2} \eta^{n+r+s} $$

$$ \times (\xi^2-1)^{1/2} (1-\eta^2)^{1/2}\, {}^{A}\bar{P}^{(m_A)k}_{(\ell_A)k}(\xi,\eta)\, {}^{B}\bar{P}^{(m_B)j}_{(\ell_B)j}(\xi,\eta) . \qquad (4.7.42) $$

We have thus obtained the integrals ${}^{BA}\bar{S}^{pq}_{jk,rs}(m,n)$ and ${}^{BA}\bar{\bar{T}}^{pq}_{jk,rs}(m,n)$ which must be evaluated next.

4.7.5 The double integrals ${}^{BA}\bar{S}^{pq}_{jk,rs}(m,n)$ and ${}^{BA}\bar{\bar{T}}^{pq}_{jk,rs}(m,n)$

We begin by putting

$$ x \equiv m+p+q-r-s-2 \qquad (4.7.43) $$

and

$$ y \equiv n+r+s \qquad (4.7.44) $$

in the integrands of equations (4.7.40) and (4.7.42). x and y are non-zero integers. Hence ${}^{BA}\bar{S}^{pq}_{jk,rs}(m,n)$ and ${}^{BA}\bar{\bar{T}}^{pq}_{jk,rs}(m,n)$ become

$$ \bar{S}^{BA}_{jk}(x,y) = \int_1^\infty d\xi \int_{-1}^{1} d\eta\, e^{-\mu_k r_A} e^{-\nu_j r_B} \xi^{x} \eta^{y}\, {}^{A}\bar{P}^{(m_A)k}_{(\ell_A)k}\, {}^{B}\bar{P}^{(m_B)j}_{(\ell_B)j} \qquad (4.7.45) $$

and

$$ \bar{\bar{T}}^{BA}_{jk}(x,y) = \int_1^\infty d\xi \int_{-1}^{1} d\eta\, e^{-\mu_k r_A} e^{-\nu_j r_B} \xi^{x} \eta^{y} (\xi^2-1)^{1/2} (1-\eta^2)^{1/2} $$

$$ \times {}^{A}\bar{P}^{(m_A)k}_{(\ell_A)k}\, {}^{B}\bar{P}^{(m_B)j}_{(\ell_B)j} \qquad (4.7.46) $$

where the index notation has been changed.

The evaluation of the integrals is begun by inserting the appropriate expressions for the functions ${}^{A}\bar{P}^{(m_A)k}_{(\ell_A)k}(\xi,\eta)$ and ${}^{B}\bar{P}^{(m_B)j}_{(\ell_B)j}(\xi,\eta)$ into the integrands. The result of this is a set of expressions in terms of the integrals

$$ M^{BA}_{jk}(x,y) = \int_1^\infty d\xi \int_{-1}^{1} d\eta\, e^{-\mu_k r_A} e^{-\nu_j r_B} \xi^{x} \eta^{y} \qquad (4.7.47) $$

and

$$N^{BA}_{jk}(x,y)=\int_1^\infty d\xi\int_{-1}^{1}d\eta\, e^{-\mu_k r_A}e^{-\nu_j r_B}\xi^x(\xi^2-1)^{l_a}\eta^y(1-\eta^2)^{l_b}. \quad (4.7.48)$$

As an example, let us consider the 1s⇒2po capture transition. The integrals $\bar{S}^{BA}_{jk}(x,y)$ and $\bar{\bar{T}}^{BA}_{jk}(x,y)$ become

$$\bar{S}^{BA}_{1s,2p_o}(x,y)=\int_1^\infty d\xi\int_{-1}^{1}d\eta\, e^{-\mu_{2p_o}r_A}e^{-\nu_{1s}r_B}\xi^x\eta^y\,{}^A\bar{P}^o_1\,{}^B\bar{P}^o_0 \quad (4.7.49)$$

and

$$\bar{\bar{T}}^{BA}_{1s,2p_o}(x,y)=\int_1^\infty d\xi\int_{-1}^{1}d\eta\, e^{-\mu_{2p_o}r_A}e^{-\nu_{1s}r_B}\xi^x\eta^y(\xi^2-1)^{1/2}(1-\eta^2)^{1/2}\,{}^A\bar{P}^o_1\,{}^B\bar{P}^o_0. \quad (4.7.50)$$

The functions ${}^A\bar{P}^o_1(\xi,\eta)$ and ${}^B\bar{P}^o_0(\xi,\eta)$ are given by

$${}^A\bar{P}^o_1(\xi,\eta)=\xi\eta+1 \qquad \text{and} \qquad {}^B\bar{P}^o_0(\xi,\eta)=1 \quad (4.7.51)$$

Substituting for these functions in equations (4.7.49) and (4.7.50) we obtain

$$\bar{S}^{BA}_{1s,2p_o}(x,y)=\int_1^\infty d\xi\int_{-1}^{1}d\eta\, e^{-\mu_{2p_o}r_A}e^{-\nu_{1s}r_B}\xi^x\eta^y(\xi\eta+1) \quad (4.7.52)$$

$$\bar{\bar{T}}^{BA}_{1s,2p_o}(x,y)=\int_1^\infty d\xi\int_{-1}^{1}d\eta\, e^{-\mu_{2p_o}r_A}e^{-\nu_{1s}r_B}\xi^x\eta^y(\xi\eta+1)(\xi^2-1)^{1/2}(1-\eta^2)^{1/2}. \quad (4.7.53)$$

From equations (4.7.47) and (4.7.48) we see that these become

$$\bar{S}^{BA}_{1s,2p_o}(x,y)=M^{BA}_{1s,2p_o}(x+1,y+1)+M^{BA}_{1s,2p_o}(x,y) \quad (4.7.54)$$

and

$$\bar{\bar{T}}^{BA}_{1s,2p_o}(x,y)=N^{BA}_{1s,2p_o}(x+1,y+1)+N^{BA}_{1s,2p_o}(x,y). \quad (4.7.55)$$

In a similar manner the other $\bar{S}$ and $\bar{T}$ integrals can be expressed in terms of the M and N integrals. The final stage of this reduction process is to find expressions for the integrals $M_{jk}^{BA}(x,y)$ and $N_{jk}^{BA}(x,y)$ which will be dealt with next.

4.7.6 The double integrals $M_{jk}^{BA}(x,y)$ and $N_{jk}^{BA}(x,y)$

We begin the obtaining of expressions for $M_{jk}^{BA}(x,y)$ and $N_{jk}^{BA}(x,y)$ by dropping the channel indices j and k and the BA superscripts in order to simplify the notation a little. Thus we have

$$M(x,y)=\int_1^\infty d\xi \int_{-1}^{1} d\eta\, e^{-\mu r_A} e^{-\nu r_B} \xi^x \eta^y \qquad (4.7.56)$$

$$N(x,y)=\int_1^\infty d\xi \int_{-1}^{1} d\eta\, e^{-\mu r_A} e^{-\nu r_B} \xi^x (\xi^2-1)^{1/2} \eta^y (1-\eta^2)^{1/2}. \qquad (4.7.57)$$

It is at this stage that a distinction must be made between the case where the exponent factors μ and ν are unequal and the one where they are equal as this affects the outcome of the analysis. We deal first with the situation where $\mu \neq \nu$

1. $\mu \neq \nu$

We substitute the expressions for r_A and r_B in terms of ξ and η from equations (A5.2a) and (A5.2b) of Appendix A5 in the M and N integrals and obtain

$$M(x,y)=\int_1^\infty e^{-a\xi} \xi^x d\xi \cdot \int_{-1}^{1} e^{-b\eta} \eta^y d\eta \qquad (4.7.58)$$

and

$$N(x,y)=\int_1^\infty e^{-a\xi}\xi^x(\xi^2-1)^{1/2}d\xi\cdot\int_{-1}^1 e^{-b\eta}\eta^y(1-\eta^2)^{1/2}d\eta \qquad (4.7.59)$$

where $$a=\frac{R}{2}(\mu+\nu) \qquad (4.7.60a)$$

and $$b=\frac{R}{2}(\mu-\nu)\ . \qquad (4.7.60b)$$

The two integrals in equation (4.7.58) are given by expressions involving finite series. They are (from equations 5.1.8 and 5.1.9 Abramowitz and Stegun, 1965)

$$\begin{aligned}\alpha_x(a)&=\int_1^\infty e^{-a\xi}\xi^x d\xi\\ &=x!\,a^{-(x+1)}e^{-a}\sum_{j=0}^{x}\frac{a^j}{j!}\ ,\quad a>0\end{aligned} \qquad (4.7.61)$$

and

$$\begin{aligned}\beta_y(b)&=\int_{-1}^1 e^{-b\eta}\eta^y d\eta\\ &=y!\,b^{-(y+1)}\left[e^b\sum_{j=0}^{y}\frac{(-1)^j b^j}{j!}-e^{-b}\sum_{k=0}^{y}\frac{b^k}{k!}\right]\ .\end{aligned} \qquad (4.7.62)$$

Hence

$$M(x,y)=\alpha_x(a)\beta_y(b)\ . \qquad (4.7.63)$$

The N integral expression of equation (4.7.59) we re-write as

$$N(x,y)=A_x(a)\,B_y(b) \qquad (4.7.64)$$

where

$$A_x(a)=\int_1^\infty e^{-a\xi}\xi^x(\xi^2-1)^{1/2}d\xi \qquad (4.7.65)$$

and

$$B_y(b)=\int_{-1}^1 e^{-b\eta}\eta^y(1-\eta^2)^{1/2}d\eta\ . \qquad (4.7.66)$$

We may express $A_x(a)$ and $B_y(b)$ as

$$A_x(a) = (-1)^x (D_a)^x \int_1^\infty e^{-a\xi} (\xi^2-1)^{1/2} d\xi \qquad (4.7.67)$$

and

$$B_y(b) = (-1)^y (D_b)^y \int_{-1}^1 e^{-b\eta} (1-\eta^2)^{1/2} d\eta \qquad (4.7.68)$$

where $(D_a)^x \equiv \left(\frac{d}{da}\right)^x$ and $(D_b)^y \equiv \left(\frac{d}{db}\right)^y$. (4.7.69)

Hence $$A_x(a) = (-1)^x (D_a)^x A_0(a) \qquad (4.7.70)$$

and $$B_y(b) = (-1)^y (D_b)^y B_0(b) \, . \qquad (4.7.71)$$

The modified Bessel function $K_\nu(z)$ has the integral representation (equation 9.6.23 Abramowitz and Stegun, 1965)

$$K_\nu(z) = \frac{\pi^{1/2}(z/2)^\nu}{\Gamma(\nu+\frac{1}{2})} \int_1^\infty e^{-zt} (t^2-1)^{\nu-\frac{1}{2}} dt \, ,$$

$$\left(Re\{\nu\} > -\tfrac{1}{2} \, , \, |arg\, z| < \tfrac{1}{2}\pi\right) . \qquad (4.7.72)$$

Setting $t = \xi$, $z = a$ and $\nu = 1$ yields, after a little rearrangement,

$$A_0(a) = \int_1^\infty e^{-a\xi} (\xi^2-1)^{1/2} d\xi$$

$$= \frac{K_1(a)}{a} \, , \quad a > 0 \qquad (4.7.73)$$

where we have used the result

$$\Gamma\left(\tfrac{3}{2}\right) = \frac{\pi^{1/2}}{2} \, . \qquad (4.7.74)$$

Similarly the modified Bessel function $I_\nu(z)$ has the integral representation (equation 9.6.18 Abramowitz and Stegun, 1965)

$$I_\nu(Z)=\frac{(Z/2)^\nu}{\pi^{1/2}\Gamma(\nu+\frac{1}{2})}\int_{-1}^{1} e^{\pm Zt}(1-t^2)^{\nu-\frac{1}{2}}\,dt\,,$$

$$(\mathcal{R}e\{\nu\}>-\tfrac{1}{2})\,. \qquad (4.7.75)$$

Setting $t\equiv\eta$, $Z=a$ and $\nu=1$ (we take the minus option of the plus or minus choice in the exponent) we find

$$B_0(b)=\int_{-1}^{1} e^{-b\eta}(1-\eta^2)^{1/2}\,d\eta$$

$$=\frac{\pi I_1(b)}{b}\,. \qquad (4.7.76)$$

Thus, using these results for $A_0(a)$ and $B_0(b)$, we have from equations (4.7.70) and (4.7.71)

$$A_x(a)=(-1)^x(D_a)^x\left[K_1(a)/a\right] \qquad (4.7.77)$$

and $$B_y(b)=(-1)^y(D_b)^y\left[\pi I_1(b)/b\right]\,. \qquad (4.7.78)$$

Use of Leibnitz's Theorem gives

$$A_x(a)=\frac{x!}{a^{x+1}}\sum_{t=0}^{x}\frac{(-1)^t a^t}{t!}(D_a)^t\left[K_1(a)\right] \qquad (4.7.79)$$

and

$$B_y(b)=\frac{\pi y!}{b^{y+1}}\sum_{\nu=0}^{y}\frac{(-1)^\nu b^\nu}{\nu!}(D_b)^\nu\left[I_1(b)\right]\,. \qquad (4.7.80)$$

The derivatives of the modified Bessel functions can be obtained from the expression given by equation 9.6.29 of Abramowitz and Stegun (1965), which we re-write as

$$\mathcal{L}_\nu^{(k)}(Z)=\frac{1}{2^k}\sum_{s=0}^{k}\frac{k!}{s!\,(k-s)!}\,\mathcal{L}_{\nu-k+2s}(Z)\,,$$

$$(k=0,1,2,\ldots)\,, \qquad (4.7.81)$$

where $\mathcal{L}_\nu$ denotes I_ν or $e^{i\pi\nu}K_\nu$ or any linear combination of these functions. Using equation (4.7.81) gives

$$(D_a)^t K_\mu = \frac{1}{2^t}\sum_{u=0}^{t}\frac{(-1)^t\, t!}{u!\,(t-u)!}\,K_{\mu-t+2u} \qquad (4.7.82)$$

and

$$(D_b)^v I_\mu = \frac{1}{2^v}\sum_{w=0}^{v}\frac{v!}{w!\,(v-w)!}\,I_{\mu-v+2w}\ . \qquad (4.7.83)$$

Combining these expressions with the ones of equations (4.7.79) and (4.7.80), we obtain closed-form expressions for $A_x(a)$ and $B_y(b)$ which are

$$A_x(a) = \frac{x!}{a^{x+1}}\sum_{t=0}^{x}\left(\frac{a}{2}\right)^t\sum_{u=0}^{t}\frac{K_{\mu-t+2u}(a)}{u!\,(t-u)!} \qquad (4.7.84)$$

and

$$B_y(b) = \frac{\pi\, y!}{b^{y+1}}\sum_{v=0}^{y}\left(-\frac{b}{2}\right)^v\sum_{w=0}^{v}\frac{I_{\mu-v+2w}(b)}{w!\,(v-w)!}\ . \qquad (4.7.85)$$

The N integral is the product of $A_x(a)$ and $B_y(b)$ from equation (4.7.64) and so can be found from the expressions given in equations (4.7.84) and (4.7.85). The modified Bessel functions are fairly easy to generate computationally. More will be said about the computational aspects of the analytic method in Chapter 5.

We now deal with the case when $\mu = \nu$.

2. $\mu = \nu$

As for the $\mu \neq \nu$ case, the starting point of the analysis is the M and N integrals of equations (4.7.56) and (4.7.57) but where now $\mu = \nu$. Substituting for Γ_A

and Γ_B in terms of ξ and η from equations (A5.2a) and (A5.2b) of Appendix A5 gives

$$M(x,y)\Big|_{\mu\neq\nu} = \int_1^\infty e^{-\lambda\xi}\xi^x\,d\xi \cdot \int_{-1}^{1}\eta^y\,d\eta \qquad (4.7.86)$$

and

$$N(x,y)\Big|_{\mu=\nu} = \int_1^\infty e^{-\lambda\xi}\xi^x(\xi^2-1)^{1/2}\,d\xi \cdot \int_{-1}^{1}\eta^y(1-\eta^2)^{1/2}\,d\eta \qquad (4.7.87)$$

where $$\lambda = \mu R \ (=\nu R). \qquad (4.7.88)$$

The M integral we write as

$$M(x,y)\Big|_{\mu\neq\nu} = \alpha_x(\lambda)\int_{-1}^{1}\eta^y\,d\eta\,. \qquad (4.7.89)$$

The α integral is given in equation (4.7.61).

The η integral is simple. It is

$$\int_{-1}^{1}\eta^y\,d\eta = \frac{2}{y+1}, \quad y = 0,2,4,\ldots$$
$$= 0 \quad , \quad y = 1,3,5,\ldots \qquad (4.7.90)$$

Thus

$$M(x,y)\Big|_{\mu\neq\nu} = \frac{2\alpha_x(\lambda)}{y+1}, \quad y = 0,2,4,\ldots$$
$$= 0 \quad , \quad y = 1,3,5,\ldots \qquad (4.7.91)$$

The N integral we write as

$$N(x,y) = A_x(\lambda)\bar{B}_y \qquad (4.7.92)$$

where the A integral is defined in equation (4.7.65) and the expression for it (with argument α) is given by equation

(4.7.84). The integral $\bar{B}_y$ is given by

$$\bar{B}_y = \int_{-1}^{1} \eta^y (1-\eta^2)^{1/2}\, d\eta \quad . \tag{4.7.93}$$

For $y = 1, 3, 5, \ldots$ the integral $\bar{B}_y$ is zero as the integrand is an odd function of η. For $y = 0$, $\bar{B}_y = \pi/2$.

In order to deal with the $y = 2, 4, 6, \ldots$ case we set $y = 2m$, that is $m = 1, 2, 3, \ldots$

$$\bar{B}_y = \int_{-1}^{1} \eta^{2m} (1-\eta^2)^{1/2}\, d\eta, \quad m = 1, 2, 3, \ldots \tag{4.7.94}$$

This is equal to

$$\bar{B}_y = 2\int_{0}^{1} \eta^{2m} (1-\eta^2)^{1/2}\, d\eta, \quad m = 1, 2, 3, \ldots \tag{4.7.95}$$

because of the even integrand. We put $\eta = \sin\theta$ and $\bar{B}_y$ becomes

$$\bar{B}_y = 2\left\{ \int_{0}^{\pi/2} \sin^{2m}\theta\, d\theta - \int_{0}^{\pi/2} \sin^{2(m+1)}\theta\, d\theta \right\} \quad . \tag{4.7.96}$$

In general

$$\int_{0}^{\pi/2} \sin^{2n}\theta\, d\theta = \frac{1.3.5.\ldots.(2n-1)}{2.4.6.\ldots.2n} \cdot \frac{\pi}{2} \tag{4.7.97}$$

from equation 651 of the CRC Handbook of Chemistry and Physics (1975).

Thus $\bar{B}_y$ becomes

$$\bar{B}_y = 2\left\{ \prod_{k=1}^{m} \frac{2k-1}{2k} - \prod_{k=1}^{m+1} \frac{2k-1}{2k} \right\} \cdot \frac{\pi}{2} \tag{4.7.98}$$

or

$$\bar{B}_y = \frac{\pi}{2} \cdot \frac{1}{m+1} \prod_{k=1}^{m} \frac{2k-1}{2k} \quad , \tag{4.7.99}$$

where $m = 1, 2, 3, \ldots$

We remember that $y = 2m$ and that equation (4.7.99) is for the case when $y = 2, 4, 6, \ldots$ We have thus found expressions that can be used to compute the M and N integrals when $\mu = \nu$. Hence the M and N integrals have been found in terms of expressions that can be computed fairly easily which means that we have come to the end of this somewhat involved reduction process to evaluate the overlap and exchange body-fixed matrix elements. No mention has been made of the direct matrix elements. We shall see that these can be found analytically in a very similar fashion.

4.7.7. The direct matrix elements

As might be expected, the analytic evaluation of the direct matrix elements is very similar to the analytic evaluation of the overlap and exchange matrix elements. As with the overlap and exchange elements, the switching function f must be of the form given in equation (4.7.11).

We consider first the BB-type elements. The required direct BB-type elements are of the general form

$$M_{jk}^{BB} = \int_v \phi_j^{B*}(\vec{r}_B)\, m(\vec{r}, t)\, \phi_k^B(\vec{r}_B)\, d\vec{r} \,. \qquad (4.7.100)$$

The product of $\phi_j^{B*}(\vec{r}_B)$ and $\phi_k^B(\vec{r}_B)$ is given by

$$\phi_j^{B*}(\vec{r}_B)\,\phi_k^B(\vec{r}_B) = \beta_j \beta_k\, \Omega_{jk}^{BB}(\vec{r}_B) \qquad (4.7.101)$$

where

$$\Omega_{jk}^{BB}(\vec{r}_B) = R_{(n_B)_j (\omega_B)_j}(r_B)\, R_{(n_B)_k (\omega_B)_k}(r_B)$$

$$\times P^{(m_B)_j}_{(l_B)_j}(\cos\theta_B)\, P^{(m_B)_k}_{(l_B)_k}(\cos\theta_B)\, \cos(m_B)_j \phi_B \cos(m_B)_k \phi_B \,. \qquad (4.7.102)$$

The elements may be expressed in terms of the three integrals

$$ {}^{A}_{n}I^{BB}_{jk}(m,n) = \int_1^\infty d\xi \int_{-1}^{1} d\eta \int_0^{2\pi} d\phi \, \Omega^{BB}_{jk} \, \xi^m \eta^n \qquad (4.7.103a) $$

$$ {}^{B}_{n}I^{BB}_{jk}(m,n) = \int_1^\infty d\xi \int_{-1}^{1} d\eta \int_0^{2\pi} d\phi \, \Omega^{BB}_{jk} \, \xi^m \eta^n (\xi^2-1)^{1/2}(1-\eta^2)^{1/2} \cos\phi \qquad (4.7.103b) $$

$$ {}^{C}_{n}I^{BB}_{jk}(m,n) = \int_1^\infty d\xi \int_{-1}^{1} d\eta \int_0^{2\pi} d\phi \, \Omega^{BB}_{jk} \, \xi^m \eta^n \cos^2\phi \; . \qquad (4.7.103c) $$

These are given by

$$ {}^{A}_{n}I^{BB}_{jk}(m,n) = {}^{\sigma}I_1\left[(m_\sigma)_j,(m_\sigma)_k\right] \sum_{p=1}^{(n_\sigma)_j-(l_\sigma)_j} \sum_{q=1}^{(n_\sigma)_k-(l_\sigma)_k} b_{jp} b_{kq} \, {}^{BB}S^{pq}_{jk}(m,n) \qquad (4.7.104) $$

$$ {}^{B}_{n}I^{BB}_{jk}(m,n) = {}^{\sigma}I_2\left[(m_\sigma)_j,(m_\sigma)_k\right] \sum_{p=1}^{(n_\sigma)_j-(l_\sigma)_j} \sum_{q=1}^{(n_\sigma)_k-(l_\sigma)_k} b_{jp} b_{kq} \, {}^{BB}T^{pq}_{jk}(m,n) \qquad (4.7.105) $$

and

$$ {}^{C}_{n}I^{BB}_{jk}(m,n) = {}^{\sigma}I_3\left[(m_\sigma)_j,(m_\sigma)_k\right] \sum_{p=1}^{(n_\sigma)_j-(l_\sigma)_j} \sum_{q=1}^{(n_\sigma)_k-(l_\sigma)_k} b_{jp} b_{kq} \, {}^{BB}S^{pq}_{jk}(m,n) \, , \qquad (4.7.106) $$

where ${}^{BB}S^{pq}_{jk}(m,n)$ and ${}^{BB}T^{pq}_{jk}(m,n)$ are given by

$$ {}^{BB}S^{pq}_{jk}(m,n) = \int_1^\infty d\xi \int_{-1}^{1} d\eta \, e^{-\nu_j r_\sigma} e^{-\nu_k r_\sigma} \, r_\beta^{\left[(l_\beta)_j-1+p\right]} \, r_\beta^{\left[(l_\beta)_k-1+q\right]} $$

$$ \times \xi^m \eta^n P^{(m_\sigma)_j}_{(l_\sigma)_j}(\cos\theta_\sigma) P^{(m_\sigma)_k}_{(l_\sigma)_k}(\cos\theta_\sigma) \qquad (4.7.107) $$

and

$$ {}^{BB}T^{pq}_{jk}(m,n) = \int_1^\infty d\xi \int_{-1}^{1} d\eta \, e^{-\nu_j r_\sigma} e^{-\nu_k r_\sigma} \, r_\beta^{\left[(l_\beta)_j-1+p\right]} \, r_\beta^{\left[(l_\beta)_k-1+q\right]} $$

$$ \times \xi^m \eta^n (\xi^2-1)^{1/2}(1-\eta^2)^{1/2} P^{(m_\sigma)_j}_{(l_\sigma)_j}(\cos\theta_\sigma) P^{(m_\sigma)_k}_{(l_\sigma)_k}(\cos\theta_\sigma) \; . \qquad (4.7.108) $$

As with the BA-type elements, the S and T integrals are expressed in terms of $\bar{S}$ and $\bar{T}$ integrals, but where now only one summation is involved instead of two, that is

$$ {}^{BB}S^{pq}_{jk}(m,n) = \left(\frac{R}{2}\right)^{(\ell_B)_j+(\ell_B)_k+p+q-2}(p+q-2)! $$
$$ \times \sum_{r=0}^{p+q-2} \frac{(-1)^r}{r!(p+q-r-2)!}\,{}^{BB}\bar{S}^{pq}_{jk,r}(m,n) \qquad (4.7.109) $$

and

$$ {}^{BB}T^{pq}_{jk}(m,n) = \left(\frac{R}{2}\right)^{(\ell_B)_j+(\ell_B)_k+p+q-2}(p+q-2)! $$
$$ \times \sum_{r=0}^{p+q-2} \frac{(-1)^r}{r!(p+q-r-2)!}\,{}^{BB}\bar{T}^{pq}_{jk,r}(m,n) \qquad (4.7.110) $$

where

$$ {}^{BB}\bar{S}^{pq}_{jk,r}(m,n) = \int_1^\infty d\xi \int_{-1}^{1} d\eta\, e^{-\nu_j r_0} e^{-\nu_k r_0} \xi^{m+p+q-r-2} \eta^{n+r} $$
$$ \times {}^{B}\bar{P}^{(m_0)_j}_{(\ell_0)_j}\,{}^{B}\bar{P}^{(m_0)_k}_{(\ell_0)_k} \qquad (4.7.111) $$

and

$$ {}^{BB}\bar{T}^{pq}_{jk,r}(m,n) = \int_1^\infty d\xi \int_{-1}^{1} d\eta\, e^{-\nu_j r_0} e^{-\nu_k r_0} \xi^{m+p+q-r-2} \eta^{n+r} $$
$$ \times (\xi^2-1)^{1/2}(1-\eta^2)^{1/2}\,{}^{B}\bar{P}^{(m_0)_j}_{(\ell_0)_j}\,{}^{B}\bar{P}^{(m_0)_k}_{(\ell_0)_k} \,. \qquad (4.7.112) $$

Substitution of the appropriate ${}^{D}\bar{P}$ functions yields expressions in terms of the integrals

$$ M^{BB}_{jk}(x,y) = \int_1^\infty d\xi \int_{-1}^{1} d\eta\, e^{-\nu_j r_0} e^{-\nu_k r_0} \xi^{x} \eta^{y} \qquad (4.7.113) $$

and

$$N^{BB}_{jk}(x,y) = \int_1^\infty d\xi \int_{-1}^{1} d\eta\, e^{-\nu_j r_a} e^{-\nu_k r_b} \xi^x (\xi^2-1)^{1/2} \eta^y (1-\eta^2)^{1/2} \qquad (4.7.114)$$

where $$x \equiv m + p + q - r - 2 \qquad (4.7.115)$$

and $$y \equiv n + r \quad . \qquad (4.7.116)$$

We now substitute the ξ,η expression for r_s . We find that

$$M^{BB}_{jk}(x,y) = \int_1^\infty e^{-a\xi} \xi^x d\xi \cdot \int_{-1}^{1} e^{-b\eta} \eta^y d\eta$$

$$= \alpha_x(a)\beta_y(b) \qquad (4.7.117)$$

and

$$N^{BB}_{jk}(x,y) = \int_1^\infty e^{-a\xi} \xi^x (\xi^2-1)^{1/2} d\xi \cdot \int_{-1}^{1} e^{-b\eta} \eta^y (1-\eta^2)^{1/2} d\eta$$

$$= A_x(a) B_y(b) \qquad (4.7.118)$$

where $$a = \frac{R}{2}(\nu_j + \nu_k) \qquad (4.7.119a)$$

and $$b = -\frac{R}{2}(\nu_j + \nu_k) \quad . \qquad (4.7.119b)$$

We saw in Subsection 4.7.6 how the α, β, A and B integrals could be found. We see that the method of analytically evaluating the BB-type elements is similar to the method of evaluating the BA-type elements.

The direct AA-type elements can be found using the same analysis as for the BB-type elements. One slight difference is that in the expressions corresponding to those of equations (4.7.109) and (4.7.110), the factor $(-1)^r$ will not appear. This is because the expression in terms of ξ

and η for Γ_A contains the factor $(1+\eta)$, whereas the Γ_B expression contains $(1-\eta)$.

4.7.8 Concluding remarks on the analytic method

At first sight the analytic method of evaluating the matrix elements appears to be rather complicated as it involves a large amount of tedious algebra. However, the method is basically very simple in principle. The heart of the method is in the computation of the three triple integrals involving the Ω-functions (Ω-triple integrals). For the BA-type matrix elements, these triple integrals were given in equations (4.7.20a) to (4.7.20c). We saw how the integrals were progressively reduced down until they had been expressed in terms of simpler integrals which could be expressed in terms of series expansions of various types, all of which could be computed. More will be said in Chapter 5 about the computational aspects of this method, but it is centred around calling a subroutine OMEGA from the main program which returns the Ω-triple integrals. It is then a simple matter to compute the matrix elements. In Appendix A8 expressions are given for the BA-, BB-, and AA-type elements in terms of the Ω-triple integrals when the switching function is the simple one f_S given in equation (4.7.1). This brings Chapter 4 to a close. In the next chapter the results of this work will be presented and discussed.

CHAPTER 5

THE PRESENT RESULTS AND THEIR CALCULATION

5.1 Introduction

The previous two chapters form the theoretical background to this chapter wherein the results of this work will be presented. The aim of the work of this thesis has been to investigate the effect of including a switching function into the well-known two-centre atomic basis expansion for calculating electron capture cross sections.

It was decided to consider two specific capture processes, already much studied by other workers. The first was the asymmetrical (accidental) resonance process

$$^4He^{2+} + H(1s) \longrightarrow {}^4He^+(2s) + H^+ \qquad (5.1.1)$$

using a simple two-state approximation in which only the 1s target and 2s projectile states were retained in the expansion of the electronic wavefunction. The second process was electron capture into the n = 2 level of $^4He^+$, namely

$$^4He^{2+} + H(1s) \longrightarrow {}^4He^+(n = 2) + H^+ \qquad (5.1.2)$$

which is also an asymmetrical (accidental) resonance process. The process (5.1.2) was studied using a 4-state expansion, that is the 1s target state and the 2s, 2po and 2p $\pm$ 1 states being retained in the expansion. Quite a wide energy range was used in the calculations upon the processes (5.1.1) and (5.1.2). It was from a $^4He^{2+}$ laboratory energy of 1 keV to an energy of 800 keV. In terms of collision velocity this corresponded to a

range of 0.10 to 2.83 a.u.

Four functional forms of switching function were employed in the calculations. They were as follows:-

(a) the simple switching function, f_s

$$f_s = -F(R)\eta \qquad (5.1.3)$$

(b) the Schneiderman and Russek (1969) switching function, f_{SR}

$$f_{SR} = -F(R)\cos\theta \qquad (5.1.4)$$

where the angle θ is as shown in figure 5.1,

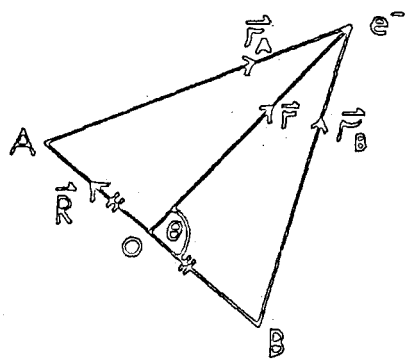

Figure 5.1

Angle θ occurring in f_{SR}.

that is

$$\cos\theta = -\frac{\vec{r}.\vec{R}}{rR} \qquad (5.1.5)$$

(c) the cubic switching function, f_c

$$f_c = -F(R)\eta^3 \qquad (5.1.6)$$

(d) the tanh switching function, f_T

$$f_T = -F(R)\tanh 3\eta . \qquad (5.1.7)$$

The variable η we know is one of the three prolate spheroidal co-ordinates (ξ, η, ϕ) equation (4.3.27b) and varies between minus one and plus one. It should be stated that the switching function f_T is an approximate switching function. The functions f_s , f_{SR} and f_c all beccme equal to plus or minus one for large R and $\Gamma_B \ll \Gamma_A$ or $\Gamma_A \ll \Gamma_B$ (i.e. $\eta = \mp 1$). However, the function $\tanh 3\eta$ takes on the values ∓ 0.995 when $\eta = \mp 1$ and so f_T will never be exactly plus or minus one, but this will have negligible (if any effect) upon the final cross sections.

The function $F(R)$ is given by

$$F(R) = \frac{R^2}{R^2 + \rho^2} \qquad (5.1.8)$$

where ρ is a parameter. A choice of the value of ρ had to be made. Taulbjerg et al. (1975) took ρ to be $1/Z_A$ a.u. and this prescription was chosen for the work presented here, namely ρ was taken as 1/2 Schneiderman and Russek (1969) took ρ to be of the order of 1/8 to 1/16. In both cases, these other workers were using molecular states as opposed to atomic states in the expansion basis. It should be stated that prior to full production of capture cross sections corresponding to the parameter ρ being 1/2 (0.5) cross sections were computed using the Schneiderman and Russek switching function f_{SR} using ρ set to 0.5 and also 0.3 for capture

into the 2s state of $^4He^+$ using two states in the expansion in the $^4He^{2+}$ laboratory energy range 8 keV to 400 keV. The change in the value of the cross sections was not significant, the accuracy of agreement being not less than two to three significant figures. Later, during production work, a run was done calculating the cross section for capture into the n = 2 level of $^4He^+$ (that is, four states were used in the expansion) using the parameter p set at 0.1 with the $^4He^{2+}$ laboratory energy being 400 keV. The cross section changed by about 0.3%. It was therefore considered that only one value of the parameter p be used, namely 0.5.

5.2 The method of calculating the cross sections

The calculation of the electron capture cross sections can be divided into two separate stages. In the first stage the matrix elements N_{jk}^{DA}, v_{jk}, w_{jk}, k_{jk} and h_{jk} are computed for different impact parameter values, the impact parameter represented by b, and also for different values of Z, where Z is as shown in figure 5.2

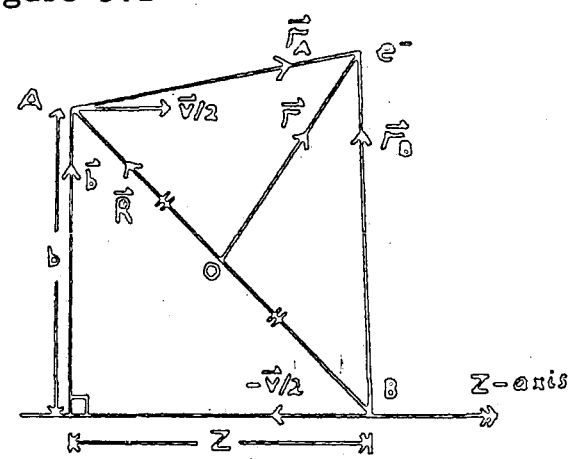

Figure 5.2

The impact parameter b and the Z co-ordinate.

The quantity Z is the Z-component of $\vec{R}$ and is such that $Z = vt$ where v is the collision velocity. It should be stressed that figure 5.2 is for the case of straight-line nuclear trajectories such that

$$\vec{R} = \vec{b} + \vec{v}t \qquad (5.2.1)$$

and

$$\vec{b}.\vec{v} = 0 \qquad (5.2.2)$$

that is

$$\begin{aligned} R^2 &= b^2 + v^2t^2 \\ &= b^2 + Z^2 \end{aligned} \qquad (5.2.3)$$

which is consistent with figure 5.2. In the calculations of this work, the trajectories were taken as being straight-line ones. We remember that the theory presented in Chapter 3 was for the case of Coulomb nuclear trajectories being used, and that setting a parameter γ, given by equation (3.2.4), to zero corresponded to straight-line trajectories being used so that the theory was still applicable to the straight-line trajectory situation.

It should be noted that if Coulomb trajectories were used, the matrix elements would be computed for different values of impact parameter b and τ instead of b and Z. The variable τ (which becomes equal to Z when $\gamma = 0$) is given by the expression of equation (3.2.5).

Prior to the calculation of the matrix elements, it is necessary to set up a mesh of (b, Z) points; the matrix elements are calculated at each (b, z) point. In practice this means that a given b value is selected

and then the matrix elements are calculated in turn at each point on a grid of Z points. Then, once this is done, a new b value is selected and the elements are calculated again at the points on the Z grid. Each value of b corresponds to a given nuclear trajectory and moving from each point on the grid of Z points corresponds to the nuclear motion along the trajectory. In practice either 12 or 30 b values were used. The number of Z points was 232. However, the elements only needed to be computed at 116 points because by having half of the Z grid negative and the other half positive it was possible to compute the elements in the negative part of the grid and use a simple relation to find the values of the corresponding elements in the positive part of the grid. Representing N_{jk}^{DA}, v_{jk}, w_{jk}, k_{jk} or h_{jk} by the element E_{jk}, the relation is

$$E_{jk}(-Z) = E_{jk}^{*}(Z)\, T_j\, T_k \qquad (5.2.4)$$

where

$$T_j = (-1)^{\ell_j + m_j} \qquad (5.2.5)$$

ℓ_j and m_j being angular momentum and magnetic quantum numbers associated with the state labelled by the index j. Clearly utilisation of equation (5.2.4) halves the computing time required. The matrix elements are stored in a file or files ready to be used in the second stage of the calculation.

The computation of the matrix elements requires the major part of the computer time required in any one

given calculation. This having been done, the second stage of the calculation may be performed. This consists essentially of integrating the coupled first-order differential equations for the expansion coefficients $a_j(t)$ and $c_k(t)$ (see equations (3.3.5a) and (3.3.5b)) subject to the boundary conditions given in equation (3.3.6). In practice the variable Z is used instead of t so the coefficients are $a_j(Z)$ and $c_k(Z)$. Assuming that $c_k(Z_f) \approx c_k(+\infty)$ where Z_f is the Z end point of the integration, the electron capture cross section for capture into the kth state of the $^4He^+$ ion from the ith state of H is found from

$$\sigma_{ki} = 2\pi \int_{b_i}^{b_f} |c_k(Z_f)|^2 \, b \, db \qquad (a_o^2) \qquad (5.2.6)$$

where b_i and b_f are the initial and final b values. The expression for σ_{ki} is an approximation of the one given in equation (3.3.9).

The work of this thesis is closely related to the work of Bransden and collaborators (Bransden et al., 1980; Bransden and Noble, 1981; Bransden et al. 1983) in that the method they used is very similar to the one described above. Indeed some of the computer programs used to calculate the cross section results presented in this chapter were based upon ones developed by Dr. C.J. Noble, who was one of the aforementioned collaborators. The work of Bransden and collaborators is similar to

the work presented here in that a two-centre atomic basis expansion was used, though with plane-wave translation factors incorporated. In the work of Bransden et al. of 1980 only two states were used in the expansion (two-state approximation) to calculate cross sections for collisions of He^{2+}, Li^{3+}, Be^{4+} and B^{5+} with H(1s) at laboratory energies from 5 to 200 keV amu^{-1}. An eight-state expansion model was used in the work of Bransden and Noble (1981) (1s, 2s, 2po, 2p $\pm$ 1 on each centre) to calculate cross sections for He^{2+} - H collisions and H^+ - He^+ collisions in the centre of mass energy range 2 to 200 keV. This work was extended by Bransden et al. (1983) by using twenty states in the expansion (that is, n = 3 states were used).

The main difference between the work of Bransden and collaborators and this present work is that in the present work the V_{jk} and W_{jk} matrix elements were calculated with the $N_{jk}^{\beta\alpha}$ and k_{jk}, h_{jk} elements at each (b, z) point, that is the V_{jk} and W_{jk} elements were computed in the first stage of the calculation. In the work of Bransden and collaborators, the V_{jk} and W_{jk} matrix elements were computed in the second stage of the calculation just prior to the integration of the differential equations. This was because plane-wave translation factors were being used and as a result these matrix elements were given by analytic expressions. It was possible, therefore, to code these into the program used to integrate the differential equations and calculate the cross sections.

As was seen in Chapter 3, the use of a switching function meant that the expressions for the matrix elements were complicated. In this work, therefore, V_{jk} and W_{jk} had to be integrated numerically together with the other elements.

5.3 The computer programs and numerical methods

5.3.1 Computing the matrix elements numerically

Five sets of matrix elements are required to obtain the cross sections in a given calculation. They are N_{jk}^{DA} V_{jk}, W_{jk}, K_{jk} and h_{jk}. A FORTRAN computer program was developed to calculate these elements when the simple switching function f_S was used. We shall refer to this program as SWITEL(S). Subsequently three other programs were developed from SWITEL(S) for computing the matrix elements when the Schneiderman and Russek switching function f_{SR}, the cubic switching function f_C and the tanh switching function f_T were used. These other programs we shall refer to as SWITEL(SR), SWITEL(C) and SWITEL(T) respectively. It should be noted, though, that all the SWITEL programs were very nearly the same. The only difference between the programs was that a small number of lines of code were different owing to the different functional forms of the switching functions, equations (5.1.3) and (5.1.4) and equations (5.1.6) and (5.1.7).

The SWITEL programs are fairly simple in principle. Basic data, namely the charges and masses of the target and projectile nuclei plus the laboratory energy, are read in from a data file. After reading control switches,

the nlm quantum numbers of the atomic basis states being used are read. A subroutine WFN is called in turn to calculate various quantities associated with the radial wavefunction expressions for first the target and then the projectile. Also calculated are the energy eigenvalues for the basis states ε_j and η_k , and the T-factors of equation (5.2.5). The next major step is to set up the b-z mesh discussed in the previous section. This is done in a fairly straightforward manner. The number of b values available is restricted to 12 or 30 with given values of b stored in BLOCK DATA. However, it is possible to choose the z grid without restriction, provided the arrays required are large enough. It is possible to divide the z grid up into a small number of regions, a different step-size being used in each region. In this way a large step-size can be used for large z where the centres of the target and projectile are far apart, and a small step-size can be used for small z where the centres are close together and the matrix elements may be varying fairly rapidly with respect to z . The number of points in the z grid may be chosen without restriction unlike the b grid. However it is possible to divide the b grid up so that a run can be done for say the first three b points, then the next run can be done for the second three points, etc. until the full 12 or 30 points have been done. The final data read are the numbers of Gauss-Legendre

and Gauss-Laguerre nodes in the numerical integration scheme. It is possible to have 4, 8, 16, 32 or 64 Gauss-Legendre nodes and 12 or 30 Gauss-Laguerre nodes.

The computation of the matrix elements begins by looping over the number of points in the b and z grids using two DO loops. A subroutine TRAJEC is called to calculate various factors associated with the classical nuclear motion such as the time derivatives of R, etc. Also returned by TRAJEC is the angle δ between the space-fixed and body-fixed frames (see figure 4.2) which is required later when the rotation between these frames is performed to obtain the space-fixed matrix elements, (we remember from Chapter 4 that the body-fixed elements are calculated and then the space-fixed elements are obtained from these). The number of target and projectile channels are looped over next and after calculating the α and β factors required (see equations (4.6.5a) and (4.6.5b)), calling a subroutine AZITH to calculate the $\mathcal{I}$-integrals (see equations (4.6.13) to (4.6.15)) which occur in some other factors, the actual integration of the B A-type elements begins. The theory of this integration was discussed in Section 4.6 of Chapter 4. It was noted there that a two-dimensional integration over the variables ξ' and η had to be performed. Gaussian integration (Hildebrand, 1974) is used to obtain the required integrals, Gauss-Laguerre integration being used for the ξ integral and Gauss-Legendre integration

being used for the η integral. It should be noted that the lower limit of the ξ integral is 1 not 0 and so the required nodes and weights must be transformed. The nodes and weights for both integrations are held in BLOCK DATA.

The end result of this is a set of arrays loaded with the N_{jk}^{BA}, k_{jk} and h_{jk} elements plus arrays loaded with the individual elements A_{jk}^{BA}, G_{jk}^{BA}, H_{jk}^{BA}, J_{jk}^{BA}, K_{jk}^{BA}, Λ_{jk}^{BA} (the Λ_{jk}^{BA} are all zero for straight-line trajectories), L_{jk}^{BA} and $\bar{A}_{jk}^{BA}$. All these elements are in the body fixed frame. A subroutine DIRECT is called twice, on the first call to calculate and return the matrix elements v_{jk} and on the second call to calculate and return the elements w_{jk}. Again these are in the body-fixed frame. In order to obtain the cross sections it is necessary to have the matrix elements in the space-fixed frame. The theory of this was discussed in Chapter 4. In the SWITEL programs the arrays containing the body-fixed elements are fed to a subroutine ROTATE together with angle δ mentioned earlier and n and l quantum numbers. The subroutine returns an array of elements in the space-fixed frame. The actual computation of the elements is now completed. It only remains to output them ready for the second stage of the calculation, namely the integration of the differential equations for the expansion coefficients and the calculation of the cross sections. The mode of outputting the matrix elements

may be performed in one of two ways. In the first way all the elements are read to a sequential line file. In the second way the $N_{jk}^{\mathbb{D}\mathbb{A}}$, k_{jk} and h_{jk} elements are read to one random access file and the V_{jk} and W_{jk} elements are read to another random access file. The second way is more versatile in that any number of basis states may be used, that is it can be used for both the two-state and the four-state expansion calculations. The first way is only used for two-state calculations, that is, it may only be applied to the process (5.1.1).

5.3.2 Computing the f_s matrix elements analytically

If the switching functions f_s and f_c are used, the matrix elements can be calculated using an analytic method which involves no numerical integration. The theory of this analytic method was presented in Section 4.7 of Chapter 4 and it was fairly involved. However, the method lends itself to computation fairly easily. Three analytic computer programs were developed for evaluating the matrix elements associated with the switching function f_s. The first we shall refer to an ANALYT(E). This program computes the $N_{jk}^{\mathbb{D}\mathbb{A}}$, k_{jk} and h_{jk} matrix elements using the analytic method. The other two programs will be called ANALYT(D1) and ANALYT(D2). These compute the V_{jk} and W_{jk} matrix elements respectively using the analytic method. All three ANALYT programs are very similar so for brevity only the ANALYT(E) program

will be discussed. One important point is that these programs were only developed to a point where they could output onto paper the matrix elements which could then be compared with similar output from the code SWITEL(S) which uses numerical integration as part of the element evaluation process. The ANALYT programs were only used as a check upon the SWITEL(S) program which was used for production work together with its related numerical programs SWITEL(SR), SWITEL(C) and SWITEL(T).

The program ANALYT(E) is more or less the same as the numerical program SWITEL(S) in the first part of its MAIN program where the charges and masses of the target and projectile nuclei and the laboratory energy are read in from the data file. The same subroutine WFN is called to calculate required radial wavefunction quantities, eigenenergies and T-factors. The b-z mesh is then set up. The points in the b and z grids are looped over in exactly the same fashion as in SWITEL(S), the subroutine TRAJEC is called to obtain various trajectory factors and then two DO loops are used to loop over the target and projectile channels. It is at this point that the similarities between the programs end. In Section 4.7 of Chapter 4 it was shown how the various individual matrix elements could be written in terms of three so-called Ω -triple integrals if the simple switching function f_S was used. These Ω-triple integrals are shown in equations (4.7.20a) to (4.7.20c), and also in Appendix

A8 expressions are given for the elements in terms of them. Having gone into the channel DO loops (in MAIN) a subroutine OMEGA is called. The input parameters are the channel indices, the internuclear distance divided by 2, $R/2$ and two positive integers used to define the size of some variably dimensioned arrays. OMEGA returns arrays containing the Ω -triple integrals which are used to calculate in a straightforward manner the individual matrix elements, certain combinations of which give the k_{jk} and h_{jk} matrix elements ($N_{jk}^{\beta\alpha}$ are individual matrix elements) which are in the body-fixed frame. A subroutine ROTATE calculates the required space-fixed matrix elements.

The first part of the subroutine OMEGA is more or less the same as the subroutine AZITH used in the program SWITEL(S) to calculate the φ -integrals. This having been done, two subroutines ALPBET and LINT are called. These load arrays ALP and BET, and AI and BI respectively (that is, ALPBET returns ALP and BET, LINT returns AI and BI) with the basic ξ and η integrals required for the calculation. These integrals were denoted by $\alpha_x(a)$ and (if the exponent factors μ and ν are not equal), $\beta_y(b)$ (ALP and BET) and by $A_x(a)$ and (if the exponent factors μ and ν are not equal) $B_y(b)$ (AI and BI), (see equations (4.7.61), (4.7.62), (4.7.65) and (4.7.66) in Chapter 4). If the exponent factors μ and ν are not equal then the integrals $\alpha_x(a)$, $\beta_y(b)$ and $A_x(a)$, $B_y(b)$ are given by the expressions of equations (4.7.61), (4.7.62) and (4.7.84), (4.7.85). The expressions

for $\alpha_{\varkappa}(a)$ and $\beta_{y}(b)$ are simple series expressions but the expressions for $A_{\varkappa}(a)$ and $B_{y}(b)$ involve modified Bessel functions of the second kind, $K_{n}(\varkappa)$, and of the first kind, $I_{n}(\varkappa)$ respectively. The subroutine LINT calls a subroutine BESLRK which returns an array of modified Bessel functions $K_{n}(\varkappa)$ where n is the order (n = 0, 1,2 .....) and $\varkappa$ is real. The subroutine BESLRK uses two NAG (Numerical Algorithms Group) subroutine functions: S18ACF which returns $K_{0}(\varkappa)$ and S18ADF which returns $K_{1}(\varkappa)$. BESLRK uses a simple recurrence relation to generate the higher order modified Bessel functions. LINT also calls a subroutine BESLRI which returns the modified Bessel functions $I_{n}(\varkappa)$. BESLRI was developed by Sookne (1973). It is also capable of returning Bessel functions $J_{n}(\varkappa)$. If the exponent factors μ and ν are equal ALPBET and LINT return the arrays ALP, BET and AI, BI loaded with the required values of the ξ and η integrals when $\mu \equiv \nu$.

The arrays ALP, BET and AI, BI now loaded, the subroutine OMEGA begins looping over various indices. During this process, which is to achieve a quadruple summation, a subroutine SELECT is called. A pointer is calculated within SELECT dependent upon the l and m quantum numbers of the target and projectile states and then the pointer determines as to where the calculation is to branch in SELECT as it is, in fact, here that the integrals $\bar{S}^{BA}_{jk}(x,y)$ and $\bar{\bar{T}}^{BA}_{jk}(x,y)$ are found (see equations (4.7.45) and (4.7.46)). These integrals are given in terms of the

ξ and η integrals computed by ALPBET and LINT, and the specific expressions depend upon which target and projectile states are being considered. SELECT therefore "selects" the correct expression in terms of the arrays ALP, BET and AI, BI. This is controlled by the l and m quantum numbers hence the reason for the l , m dependent pointer.

Finally the ϕ -integrals are multiplied into the results of the quadruple summation mentioned above and OMEGA returns the values of the Ω -triple integrals to MAIN. The final calculations are straightforward in MAIN to yield the required matrix elements.

5.3.3 Computing the cross sections

Subsection 5.3.1 described the SWITEL programs which computed the matrix elements N_{jk}^{BA}, v_{jk}, w_{jk}, k_{jk} and h_{jk} numerically. We noted that there were four versions of SWITEL corresponding to the four switching functions that were used. At the end of the subsection it was stated that the SWITEL programs could output the matrix elements in two ways. In the first way all the elements are read to one sequential line file. In the second way the N_{jk}^{BA}, k_{jk} and h_{jk} elements are read to one random access file and the v_{jk} and w_{jk} elements are read to another random access file. The second way would allow more than two states to be retained in the expansion. However, the first way was only used when there were two states.

Two programs for calculating the required capture cross sections were developed. Both were based upon programs written by Dr. C.J. Noble for the work of Bransden et al. (1980, 1983) and Bransden and Noble (1981) which were mentioned in Section 5.2. The main task in modifying the programs of Noble was to re-write parts of them so that the elements V_{jk} and W_{jk} could be read by the programs from the storage files. As we noted in Section 5.2, in the work of Bransden and collaborators the fact that plane-wave translation factors were being used resulted in the elements V_{jk} and W_{jk} being given by analytic expressions the coding for which was included in the cross section program.

The two cross section programs used in this work corresponded one to the SWITEL program reading the matrix elements to a sequential line file and this was used for two-state calculations of the cross sections for the process (5.1.1), and the other to the SWITEL program reading the matrix elements to two random access files. This was used for studying the process (5.1.2) using a four-state expansion, though it could be used for doing two-state calculations. The two-state cross section program will be referred to as CROSS2 whilst the more general multistate program which was used for the four-state calculations, will be referred to as CROSSM.

The program CROSSM is fairly straightforward. It begins by reading target and projectile data, namely charges and masses of the nuclei and quantities associated

with the radial wavefunctions. Also read are various control switches and the laboratory energy. The first major step in the calculation process is the calling of two very similar subroutines PHLNA and PHLNAD. These multiply the elements computed by SWITEL by their correct eigenenergy phase factors. In Chapter 3, equations (3.3.80) to (3.3.84), these are shown. The subroutine PHLNA multiplies N_{jk}^{DA}, k_{jk} and h_{jk} by $exp\,i(\varepsilon_j - \eta_k)t$ and PHLNAD multiplies v_{jk} and w_{jk} by $exp\,i(\varepsilon_j - \varepsilon_k)t$ and $exp\,i(\eta_j - \eta_k)t$ respectively. In both PHLNA and PHLNAD the elements are read from the random access storage files, the phase factors are added and then the new elements are read into temporary random access storage files. The integration of the coupled differential equations may now begin. It is necessary to go into a DO loop over the impact parameter grid. A subroutine START is called which computes the coefficients $a_j(Z)$ and $c_k(Z)$ at the initial integration Z point, Z_i. This having been done, the system of differential equations is integrated by calling the subroutine DE which is a standard Adams' program with automatic selection of order and step-size. (Shampine and Gordon, 1975). As part of the integration procedure, it is necessary to interpolate the matrix elements on the Z grid. This is done by the subroutines SLGINT and SLGIND. They use Lagrange four-point interpolation (Hildebrand, 1974). A useful check upon the numerical accuracy is done by using Green's unitarity relation equation (2.3.53) (see Chapter 2). As the inte-

gration proceeds from the initial Z point, Z_i to the final point, Z_f after each step Green's unitarity relation is computed. At the end of the integration for the particular impact parameter being dealt with, a routine ASCOR is called. In the original code written by Noble, this routine was required for asymptotically correcting the coefficients a_j and c_k, that is they had to be extrapolated out to $Z = +\infty$ in order to obtain the probabililty amplitudes $a_j(+\infty)$ and $c_k(+\infty)$ which could then be used to find cross sections associated with transitions to individual quantum states labelled by the indices j and k. Considering only the four-state (target 1s; projectile : 2s, 2po, 2p $\pm$ 1) case, in fact the coefficients a_{1s} and $c_{2p\pm1}$ do not need correcting, that is, the required probability amplitudes are equal to $a_{1s}(Z_f)$ and $c_{2p\pm1}(Z_f)$ provided Z_f is large enough. However, the coefficients c_{2s} and c_{2po} must be corrected as, in general, their values at $Z = Z_f$ are not approximately the same as those at $Z = +\infty$. The reason for this is the long-range dipole-type coupling between the 2s and 2po states of He^+. The method of correcting the coefficients by extrapolation along the trajectory is discussed by Wilets and Gallaher (1966) and Cheshire (1968). The subroutine ASCOR can correct coefficients calculated when plane-wave translation factors are used in the formulation. However, when a switching function is used, the correction procedure

will be much more complicated and so ASCOR should not be used. In fact the switching function coefficients are not asymptotically corrected by ASCOR, (the subroutine is called but it loads an array with the uncorrected coefficients which are then used). Thus only the cross section for capture into the n = 2 level of He^+ can be calculated. This is the sum of three cross sections for capture into the 2s, 2po and 2p $\pm$ 1 states of He^+ but of these individual cross sections, only the 2p $\pm$ 1 is correct. The final part of the MAIN program calls a subroutine XSECTN to calculate the cross sections using the integral expression of equation (5.2.6) (this expression assumes $C_k(Z_f) \approx C_k(+\infty)$. To be strictly correct the integrand should be $|C_k(+\infty)|^2 b$). One final and important point about CROSSM is that if the matrix elements are computed for plane-wave translation factors being used rather than switching function translation factors, CROSSM will output plane-wave factor cross sections. In fact a program PLANEL was written which computed N_{jk}^{BA}, v_{jk}, w_{jk}, k_{jk} and h_{jk} when plane-wave translation factors were used and this meant that CROSSM could be tested. More will be said about this in subsection 5.3.5. If CROSSM was used for finding plane-wave cross sections, the asymptotic correction routine ASCOR could be used fully.

In a similar fashion to CROSSM, the two-state cross section program CROSS2 begins by reading target and projectile

data together with switches, etc. The calculation begins with a DO loop over the b grid. Once in this loop, a subroutine ELEMS is called. This reads in the stored matrix elements and constructs arrays from which the elements required in the two-state calculation may be interpolated. It should be stated that the multistate program CROSSM solves the coupled equations when they are in the form

$$i\dot{\underset{\sim}{A}}(z) = \underset{\sim}{S}^{-1}\underset{\sim}{M}\underset{\sim}{A}(z) \qquad (5.3.1)$$

(see equations (2.3.40) to (2.3.42), Chapter 2). However, the two-state program solves equations which have been recast into a more convenient form by phase transforming the coefficients $a(z)$ and $c(z)$ to give new coefficients $A(z)$ and $C(z)$. The phase-functions are integrals of certain combinations of the matrix elements. The procedure for integrating the differential equations is the same as that in CROSSM. A subroutine START is called to compute $A(z_i)$ and $C(z_i)$ and then the subroutine DE is called to integrate the equations out to z_f. Unlike the program CROSSM, as the integration proceeds CROSS2 uses the matrix element unitarity relation given by equation (2.3.52a) as a numerical check upon the interpolation (Lagrange four-point) as the z-axis is stepped along. To check the accuracy of the integration procedure, the sums of the squares of the moduli of the coefficients A and C at $z = z_f$ are added together. This should be very near unity (equation 2.3.54). The subroutine XSECTN

is called to calculate the capture cross section. As for CROSSM, CROSS2 may be used to output cross sections for plane-wave translation factors being used. The program PLANEL supplies it with the required plane-wave matrix elements via a storage file.

These descriptions of the cross section programs are basic in that the programs have other secondary features not discussed. For example, the program CROSSM has the facilities to output the interpolated matrix elements and also output direct matrix elements H_{jk} and $\overline{H}_{jk}$ both at specific (b,z) points as an aid to checking the program. In subsection 5.3.5 more will be said about checking the programs but prior to this a little more will be said about the programs of Noble used in the work of Bransden and collaborators.

5.3.4 The plane-wave translation factor programs of Noble.

In the work of Bransden et al. (1980), Bransden and Noble (1981) and Bransden et al. (1983), the plane-wave matrix elements were computed using a program which will be referred to as FOURIER and uses the Fourier transform method of Sin Fai Lam (Sin Fai Lam, 1967). The FOURIER program was written by Noble (1980). It computes the N_{jk}^{BA}, k_{jk} and h_{jk} matrix elements when plane-wave translation factors are used. These are then read to either a sequential line file or a random access file according as to the whether

a two-state or multistate calculation is to be performed respectively.

The second stage of the calculation of plane-wave cross sections is carried out by one of two programs also written by Noble. The first we shall refer to as PLANX2 and the second as PLANXM. These are respectively two-state and multistate programs. The programs used in the present work, described in the previous subsection, CROSS2 and CROSSM, are based upon these programs. The programs PLANX2 and PLANXM compute the direct matrix elements, though, before the integration of the coupled differential equations and calculation of the cross sections are performed.

5.3.5 Testing the computer programs

It is vital that rigorous checks and tests are performed upon computer programs used in this kind of work. The programs which we are dealing with are the SWITEL programs that compute the matrix elements when a switching function is used in the formulation, and the CROSS2 and CROSSM programs that integrate the coupled differential equations and output the cross sections.

One very useful test of the simple switching function program SWITEL(S), which computes the matrix elements numerically, was to compare output from it with output from the analytic programs ANALYT(E), ANALYT(D1) and ANALYT(D2) which were discussed in Subsection 5.3.2. The SWITEL(S) and ANALYT programs were run at various energies and (b,z) points, mainly for the He^{2+} - H system

and coupling the 1s target and n = 2 projectile states. In all cases extremely good agreement was obtained between the numerical and analytic codes' output. As an example the codes were run for a $^4He^{2+}$ laboratory energy of 20keV at the point on the b-Z mesh $b = 4$, $Z = 5$ for the He^{2+} - H system with 1s target and n = 2 projectile states. Using a 16 /12 Gaussian quadrature scheme (16 Gauss-Legendre and 12 Gauss-Laguerre nodes) absolute agreement was achieved using an output format D16.8, that is, eight significant figure accuracy. The ANALYT program could only output matrix elements associated with the simple switching function f_s and so these programs could nct be used as diagnostic tools to check the other SWITEL programs SWITEL(SR), SWITEL(C) and SWITEL(T) which corresponded to the Schneiderman and Russek, the cubic and the tank switching functions respectively. However, the other three SWITEL programs were very similar to SWITEL(S). The only difference was that a few lines of code were different owing to the different forms of switching function. Thus this positive diagnostic result achieved by using the ANALYT programs to check SWITEL(S) could be considered valid for the other SWITEL programs provided very careful coding of the lines of code mentioned was performed.

Early in the development of the SWITEL programs it was decided to develop in parallel a program based upon SWITEL but which computed matrix elements when plane-wave translation factors were being used rather than

switching function translation factors. This program was named PLANEL and has been mentioned earlier in this section. The PLANEL program computed elements which were stored and then used by either CROSS2 or CROSSM for calculating plane-wave capture cross sections. These could then be compared directly with plane-wave capture cross section results from Noble's tried and tested programs PLANX2 and PLANXM which used elements computed by another Noble program FOURIER. Also comparisons were made between matrix elements computed by FOURIER and PLANEL. Good agreement was achieved between the cross sections produced by using PLANEL and CROSS2 and CROSSM and those produced by using Noble's programs FOURIER and PLANX2 or PLANXM. Table 5.1 shows the comparison between the plane-wave cross sections obtained using PLANEL and CROSS2, PLANEL and CROSSM, and FOURIER and PLANX2 for the process (5.1.1) capture into the 2s state of $^4He^+$ using two states in the expansion. The results in the table were obtained using 12 impact parameters whose values ranged from 3.472×10^{-2} to 11.13 a.u. The z grid began at -12 a.u. There is very good agreement between the PL2 results and the PLN results obtained using Noble's programs up to 40 keV. However, the accuracy of agreement goes down to that of two significant figures at 400 keV. The agreement is good between the PLM results and the PLN results with a similar decrease in accuracy of agreement at 400 keV.

Lab. energy (keV)	PL2	PLM	PLN
1	0.67695022-3	0.67694182-3	0.67695169-3
5	0.26763190+0	0.26763330+0	0.26763184+0
20	0.23231262+1	0.23231400+1	0.23231262+1
40	0.21119339+1	0.21119302+1	0.21119338+1
400	0.65477864-1	0.65478056-1	0.65119137-1

Table 5.1

Comparison of plane-wave translation factor cross section results for capture into 2s state of $^4He^+$.
PL2, results obtained using PLANEL & CROSS2;
PLM, results obtained using PLANEL & CROSSM;
PLN, results obtained using FOURIER & PLANX2.
The results are displayed in a format such that 1.23-4 = 1.23 x 10^{-4}.
(Cross section units : $10^{-16}cm^2$)

The results of table 5.1 used only two states in the expansion. Four-state tests were done comparing the total cross sections obtained using PLANEL and CROSSM with those obtained using Noble's programs FOURIER and PLANXM. The cross sections were for capture into the three n = 2 states of $^4He^+$. The results of this are displayed in table 5.2. There is good agreement between the results being compared in lines(a) and (b) (see table caption) though with a decrease in accuracy of agreement as the laboratory energy increases from 40 to

400 keV. The agreement is very good (5 to 6 significant figures) for 20 and 40 keV. As for the two-state comparison,

Lab. energy (keV)		nlm capture state		
		2so	2po	$2p^{\pm}1$
1	(a)	0.16442721-1	0.99307692-2	0.64168339-2
	(b)	0.16445727-1	0.99334556-2	0.64195141-2
5	(a)	0.69494132+0	0.13253467+1	0.84408687+0
	(b)	0.69497087+0	0.13255505+1	0.84422981+0
20	(a)	0.25112617+1	0.51997127+1	0.40949645+1
	(b)	0.25112930+1	0.51997108+1	0.40949595+1
40	(a)	0.18927889+1	0.51399597+1	0.39758756+1
	(b)	0.18927791+1	0.51399197+1	0.39758423+1
400	(a)	0.12844591+0	0.13145528+0	0.63796736-1
	(b)	0.12791546+0	0.13153327+0	0.63808077-1

Table 5.2

Comparison of plane-wave translation factor cross section results for capture into the n = 2 states of $^4He^+$.

Upper lines (a) : results obtained using PLANEL & CROSSM. Lower lines (b) : results obtained using FOURIER & PLANXM.

Results format as for table 5.1 . (Cross section units : $10^{-16}cm^2$).

12 impact parameters from 3.472×10^{-2} to 11.13 a.u. were used with a z grid beginning at -12 a.u.

The results of these comparisons between the cross section programs of this work, CROSS2 and CROSSM, and those written by Noble, PLANX2 and PLANXM, were indicative that the programs CROSS2 and CROSSM were reliable and could be used for production of switching function trans-

lation factor capture cross sections. However, the program PLANEL outputted matrix elements that could be compared with those from FOURIER, as was mentioned earlier. As would be expected from the cross section results, the matrix elements from these programs were in good agreement. This fact was a further recommendation of the reliability of the SWITEL programs upon which PLANEL was based. In fact, PLANEL was very similar to SWITEL; the same two-dimensional Gaussian integration method was used and the rotation routine ROTATE was the same. The main difference was in the integration of the azimuthal (that is, ϕ -) integral when calculating the N_{jk}^{DA}, k_{jk} and h_{jk} matrix elements which used the integral representation of the integer order Bessel functions (Arfken, 1970)

$$J_n(\alpha) = \frac{i^{-n}}{2\pi}\int_0^{2\pi} e^{i(\alpha\cos\phi + n\phi)}\,d\phi \qquad (5.3.2)$$

where

$$\alpha = \tfrac{1}{2} bv\left[(\xi^2-1)(1-\eta^2)\right]^{1/2}. \qquad (5.3.3)$$

This arose because of the $\exp(i\vec{v}.\vec{r})$ factor.

5.3.6 Preliminary runs - Gaussian quadrature convergence and choice of Z grid

The computer programs having been tested, it was necessary to do some preliminary runs of the programs as a prelude to production of final cross section results.

The SWITEL programs were going to be used for computing the matrix elements. The main question to be answered

about this first stage of the calculation was concerned with the number of nodes required in the Gaussian quadrature scheme. For each of the SWITEL programs (that is, SWITEL(S), SWITEL(SR), SWITEL(C) and SWITEL(T)) matrix elements were computed and outputted at four points on the $b-z$ mesh using four quadrature schemes 16 /12, 16/30, 32/12 and 32/30 (16 /12 means 16 Gauss-Legendre nodes, 12 Gauss-Laguerre nodes). The four points on the $b-z$ mesh (denoted by (b,z)) were (0.1,0.1), (0.1,10), (7,0.1) and (7,10). Comparing the elements computed using the four different quadratures showed that for the three switching functions f_S , f_C and f_T (simple, cubic and tanh) the use of a 16/12 quadrature was quite adequate. However, for the switching function f_{SR} (Schneiderman and Russek) it was found that, taken over all four (b,z) points, 16 /12 was not good enough. Comparing the 16 /12, 16 /30 and 32 /30 quadratures, the elements computed with 16 /12 usually only agreed to two significant figures with the 32/30 elements. However, the 16/30 elements agreed with the 32 /30 elements to three or four significant figures. Although better accuracy could have been achieved by using the 32/30 scheme, this would have required about twice as much computer time per run and hence the 16/30 quadrature scheme was chosen to be used when f_{SR} matrix elements were to be computed.

The matrix elements in the calculation are calculated on a grid of z points for each value of impact parameter b as was discussed in section 5.2. It was necessary to choose a suitable z grid. The one chosen began at

$z = -27.0$, had 22 steps of size 0.75 and then 93 steps of size 0.12. This corresponded to minimum and maximum possible initial and final points for integrating the differential equations of $z_i = -26.0$ and $z_f = +26.0$ respectively. It was necessary for z_i to at least lie between the second and third points on the z grid for the interpolation procedure to perform correctly. The outer region of the z grid, where the step-size was 0.75, was where the matrix elements were varying fairly slowly with respect to z. The inner region, where the step-size was 0.12, was where the elements were varying more rapidly. The choice of step-size in the inner region was the same as that in the work of Bransden et al. (1980). In that work the inner region had 92 steps of size 0.12. The step size in the outer region of 0.75, used in the present work, was larger than that used in the work of Bransden et al. In their outer region there were 6 steps of size 0.2. However, the first point of the grid in the present work had to be -27.0 whereas Bransden et al. had a first point of -12.0. Bearing in mind that the matrix elements had to be computed at each point of the grid, the larger step-size of 0.75 was used in the outer region in the present work in order to maintain economy of computer time.

The value of the first point of the grid used in the present work was -27.0. This was chosen by doing a series of full cross section calculations for capture into the n = 2 level of $^4He^+$ using the simple switching

function f_s at a $^4He^{2+}$ laboratory energy of 400 keV. The initial and final integration points on the z-axis for integrating the differential equations, that is z_i and z_f, were varied from $\pm$ 6.0 up to $\pm$ 49.0. The values of the cross section obtained are displayed in table 5.3. The usual impact parameter grid of 12 points from 3.472×10^{-2} to 11.13 was used. (The initial point z_i was the negative of the final point z_f and so only values of z_f are shown in table 5.3). The region of convergence was from z_f = 16.0 to z_f = 26.0. For values of z_f greater than 26.0 the cross section's increase in value is probably due to numerical inaccuracy. In all of the calculations of the present results the matrix elements were computed using the z grid beginning at -27.0. However, most of the cross sections were computed using more than one value of z_f (z_i) to ensure that convergence with respect to the value of z_f (z_i) had occurred. The values were in the region of convergence from 16.0 to 26.0. Some results, namely the ones computed using the Daresbury Laboratory AS 7000 machine, were only performed using a single value of z_f (z_i). In this case a value of 24.0 was used for z_f, with -24.0 for z_i.

Apart from the width of the z grid being large enough, it was necessary to test that the step-sizes being used, namely 0.75 in the outer region and 0.12 in the inner region, were small enough. This was done by simply halving the step-sizes so that there were 44 steps of 0.375

Z_f	$\sigma(n=2)$	Z_f	$\sigma(n=2)$
6.0	9.3862	29.0	9.7363
8.0	9.6574	31.0	9.7381
10.0	9.7232	33.0	9.7423
12.0	9.7339	35.0	9.7502
14.0	9.7347	37.0	9.7636
16.0	9.7347	39.0	9.7857
18.0	9.7346	41.0	9.8200
20.0	9.7345	43.0	9.8712
22.0	9.7348	45.0	9.9452
24.0	9.7348	47.0	10.050
26.0	9.7351	49.0	10.195
27.5	9.7355		

Table 5.3

Convergence of cross section results for capture in n = 2 level of $^4He^+$ at a $^4He^{2+}$ laboratory energy of 400 keV using the simple switching function f_s. $\sigma(n=2)$ denotes the cross section. (Units : Z_f in a.u.; $\sigma(n=2)$ in $10^{-16}cm^2$).

in the outer region and 186 steps of 0.06 in the inner region and then using this z grid in two full calculations of cross sections for capture into the three n = 2 states of $^4He^+$ using the simple switching function f_s . In the first calculation the $^4He^{2+}$ laboratory energy was 5 keV and in the second calculation it was 400 keV. The results of these calculations are displayed in table 5.4 together with corresponding results at 5 keV and 400 keV which were calculated using the original z grid of 22 steps of 0.75 and 93 steps of 0.12. In all the calculations Z_f was 24.0. At both energies used there

Lab. energy (keV)		nlm capture state		
		2so	2po	$2p^{\pm}1$
5	(a)	0.84523790+0	0.14265795+1	0.76193243+0
	(b)	0.84512118+0	0.14264635+1	0.76195279+0
400	(a)	0.30296729+1	0.48736342+1	0.18315204+1
	(b)	0.30295820+1	0.48734271+1	0.18315160+1

Table 5.4

Comparison of switching function cross section results for capture into the n = 2 states of $^4He^+$. Upper lines (a): results obtained using the z grid with 22 steps of 0.75 and 93 steps of 0.12. Lower lines (b) : results obtained using the z grid with 44 steps of 0.375 and 186 steps of 0.06. Results format as for table 5.1. (Cross section units : $10^{-16} cm^2$).

was very good agreement between the cross section results obtained using the two z grids. This was indicative that the grid with 22 steps of 0.75 and 93 steps of 0.12 was quite adequate for production work.

The number of points in the b grid could either be 12 or 30. The use of 12 points was cheaper computer time wise but results were also produced using 30 points. The final production results revealed that at low energies ($\lesssim$ 5-10 keV) 30 points were required. Above this, 12 points were enough. If 12 points were used their values ranged from 3.472×10^{-2} to 11.13 a.u; if 30 points were used their values ranged from 1.422×10^{-2} to 31.25 a.u.

5.3.7 A table displaying the programs

To end this section a table is given displaying the programs used and associated comments (table 5.5).

The table shows the matrix element programs and their corresponding cross section programs. Also shown are the number of states that can be dealt with and the type of translation factor used. It should be noted that

Matrix elements	Cross sections	Number of States	Type of Translation factor
FOURIER	PLANX2 PLANXM	2 $\geqslant 2$	plane-wave
PLANEL	CROSS2 CROSSM	2 $\geqslant 2$	plane-wave
SWITEL	CROSS2 CROSSM	2 $\geqslant 2$	switching function
ANALYT	-	2 $\geqslant 2$	simple switching function

TABLE 5.5

The computer programs referred to in the text.

SWITEL denotes either of the four SWITEL programs: SWITEL(S), SWITEL(SR), SWITEL(C) or SWITEL(T). ANALYT denotes ANALYT(E), ANALYT(D1) or ANALYT(D2). It was stated earlier that the ANALYT programs were not developed to the stage where they could be used together with the programs CROSS2 and CROSSM for calculation of cross sections.

5.4 The present results

5.4.1 Cross sections for capture into the 2s state of $^4He^+$

In this subsection capture cross section results are presented for the process (5.1.1), namely the capture

of the electron from atomic hydrogen by fully stripped helium ions (alpha particles) into the 2s state of the singly charged helium ion $^4He^+$. In all this presentation, the results are for helium nuclei having a mass of 4 amu. The energy range used for this study was from 1 keV to 800 keV ($^4He^{2+}$ laboratory energy). The results were calculated using the two-centre two-state atomic basis expansion with inclusion of a switching function. The four forms of switching function used were given in the introduction of this chapter, Section 5.1. The matrix elements were computed by the SWITEL programs which used Gaussian (numerical) integration. The cross sections were computed using CROSS2 and CROSSM. A useful comparison was between this work which used a switching function, and the work of Bransden et al. (1980) in which cross sections for capture into the 2s state of $^4He^+$ were among the results presented. Bransden et al. used a two-state approximation but with plane-wave translation factors instead of switching function translation factors. However, the energy range used by Bransden et al. was from 20 keV to 800 keV ($^4He^{2+}$ laboratory energy) and so some extra results were required at low energies. These were produced by using the programs PLANEL with CROSS2 and CROSSM. (Bransden et al. used the programs FOURIER and PLANX2). Table 5.6 displays all the two-state, plane-wave results for capture into the 2s state

of $^4He^+$. The table shows the programs used in the calculations and the number of impact parameters employed.

Lab. energy (keV)	Programs Used		Number of impact parameters	Cross section ($10^{-16}cm^2$)
	Matrix elements	Cross sections		
1	PLANEL	CROSSM	30	0.73-3
2.4	"	"	"	0.23-1
5	"	"	"	0.257
12	"	CROSS2	12	1.56
20	FOURIER	PLANX2	"	2.32
40	"	"	"	2.11
100	"	"	"	0.963
200	"	"	"	0.269
400	"	"	"	0.65-1
800	"	"	"	0.11-1

TABLE 5.6

Two-state plane-wave translation factor cross sections for capture into the 2s state of $^4He^+$. (0.73-3 = 0.73×10^{-3}).

All the cross sections in table 5.6 were computed on the IBM 370/168 machine (NUMAC) using double precision. The results for laboratory energies from 20 to 800 keV inclusive are those of Bransden et al. (1980).

Table 5.7 displays the present two-state switching function results for capture into the 2s state of $^4He^+$. The four forms of switching function are shown on the left of the table. The parameter p in $F(R)$ (see equation (5.1.8)) is 1/2. The 12 impact parameter results, labelled by a), were obtained using the IBM 370/168 machine (NUMAC). The 30 impact parameter results, labelled by b), were

Switching function	$^4He^{2+}$ Laboratory energy (keV)								
	1	2.4	5	10	20	40	100	400	800
$-F(R)\eta$	a) 0.25-3 b) 0.17-3	0.19-1 0.32-1	0.327 0.297	1.40 1.45	3.37 3.36	4.41 4.41	4.11 4.11	2.89 -	2.57 -
$-F(R)\cos\theta$	a) 0.25-3	0.19-1	0.319	1.37	3.25	4.13	3.55	1.95	1.39
$-F(R)\eta^3$	a) 0.25-3	0.21-1	0.353	1.53	3.82	5.24	5.69	6.40	8.60
$-F(R)\tanh 3\eta$	a) 0.24-3 b) 0.17-3	0.18-1 0.31-1	0.308 0.281	1.30 1.34	2.95 2.94	3.57 3.57	2.64 2.64	2.34 -	3.19 -

Table 5.7

Two-state switching function translation factor cross sections for capture into the 2s state of $^4He^+$. 12 impact parameter results are labelled by a); 30 impact parameter results by b). Cross sections are in units of $10^{-16}cm^2$.(0.25-3 = 0.25 x 10^{-3}).

obtained using the AS 7000 machine of the Daresbury Laboratory. All the results were computed using double precision.

The two-state results of the present work are also displayed graphically in figure 5.3 together with other theoretical data and experimental data. (The key to figure 5.3 is on the page after it).

The striking feature of the graph in figure 5.3 is the very large discrepancy at high energy between the present two-state atomic expansion cross sections using switching function translation factors and the cross section results of Bransden et al. (1980) who used a two-state atomic expansion with plane-wave translation factors. It can also be seen that at low energies the switching function and plane-wave translation factor results agree quite well. The divergence between the two-models would appear to begin in the region before the cross section's maximum, namely 2.5 to 4.0 keV amu^{-1}. This corresponds to a collision velocity of the order of 0.3 - 0.4 a.u. It is here also that the divergence between the results obtained using the four different forms of switching function becomes more pronounced. In contrast, for energies less than about 2.5 keV amu^{-1}, the results associated with the four switching functions are in good agreement, so much so that only the simple switching function results are plotted at energies below 2.5 keV amu^{-1}. One point which ought to be mentioned is that the plane-wave and switching function two-state results below 2.5 keV amu^{-1} were those obtained using 30 impact parameters. For

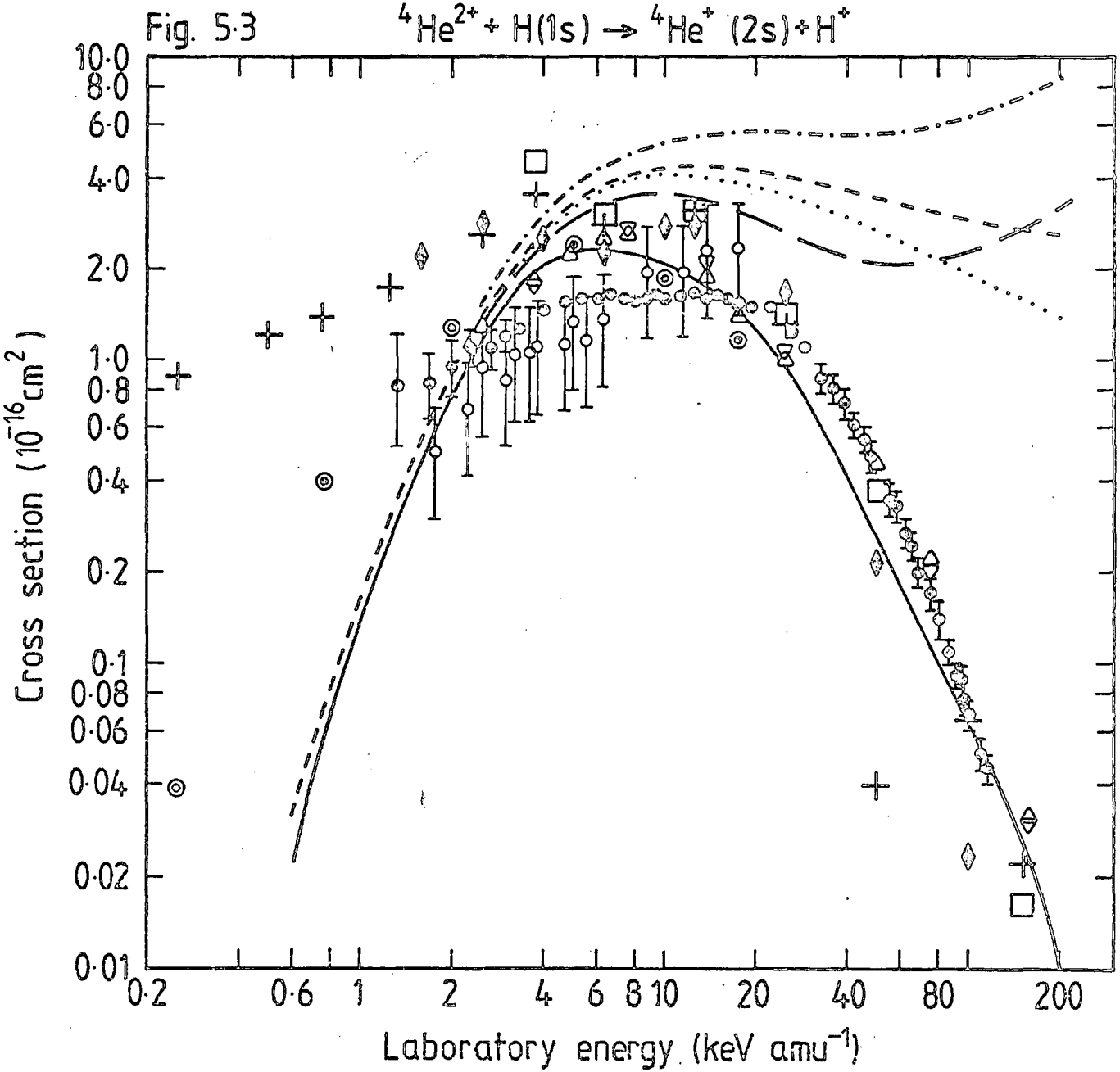
Fig. 5.3
$^4He^{2+} + H(1s) \rightarrow {}^4He^+ (2s) + H^+$
Cross section ($10^{-16} cm^2$)
10·0
8·0
6·0
4·0
2·0
1·0
0·8
0·6
0·4
0·2
0·1
0·08
0·06
0·04
0·02
0·01
0·2
0·6
1
2
4
6
8
10
20
40
80
200
Laboratory energy (keV amu^{-1})

Key to Figure 5.3

Cross sections for electron capture into the 2s state of $^4He^+$.

Theoretical cross sections :

———— , two-state atomic expansion with plane-wave translation factors, present work and Bransden et al. (1980);

– – – – – , two-state atomic expansion with simple switching function translation factors, present work;

····· , two-state atomic expansion with Schneiderman and Russek switching function translation factors, present work;

·–·–·–· , two-state atomic expansion with cubic switching function translation factors, present work;

—— —— , two-state atomic expansion with tanh switching function translation factors, present work;

△ , eight-state atomic expansion, Bransden and Noble (1981);

▽ , twenty-state atomic expansion, Bransden et al. (1983);

◇ , eight-state atomic expansion, Msezane and Gallaher (1973);

+ , eight-state and □ , eleven-state atomic expansion, Rapp (1974);

◎ , ten-state molecular expansion, Hatton et al. (1979).

Experimental cross sections:

I , Bayfield and Khayrallah (1975);

I , Shah and Gilbody (1978).

2.5 keV amu^{-1} and above, 12 impact parameters were used. Also the results for 0.25 keV amu^{-1} (that is, 1 keV) are not plotted owing to their smallness.

On the high energy side of the cross section's maximum the eight- and twenty- state plane-wave translation factor atomic expansion calculations of Bransden and Noble (1981) and Bransden et al. (1983) agree well with the experimental date of Shah and Gilbody (1978). This work was an extension of the two-state work of Bransden et al. (1980) which tends to underestimate the cross section in this energy region. The eight- and eleven- atomic state work of Rapp (1974) would appear to give good results in this region if the eight-state result at 50 keV amu^{-1} is disregarded and assumed to be spurious. It is, however, puzzling that there is notable disagreement between the eight-state results of Rapp and Msezane and Gallaher (1973) which should, in fact, agree. On the low energy side of the maximum the only other theoretical calculation worthy of note is that of Hatton et al. (1979). In this work a ten-state molecular expansion was used with plane-wave translation factors. Below about 1 keV amu^{-1} the two-state atomic expansion results (plane-wave and switching function) are in disagreement with Hatton et al.'s results by about one order of magnitude.

Data from three molecular expansion calculations, which were not plotted on the graph of figure 5.3, are compared with the data from the two-state atomic expansion calculations using plane-wave and switching function

translation factors and also with the results of Hatton et al.'s calculations for laboratory energies 0.25 - 5.0 keV amu^{-1} in table 5.8. Two of the molecular expansion calculations both employed optimised switching function translation factors. The one calculation due to Kimura and Thorson (1981b) used 10 basis functions; the other, due to Crothers and Todd (1981b), used 5 basis functions. There is good agreement between the two ten-state molecular calculations of Hatton et al. (1979) and Kimura and Thorson (1981b) with slightly less good agreement between these calculations and the five-state molecular one of Crothers and Todd (1981b). It is probably unfair to be critical of the lack of accord between these three molecular state calculations and the atomic state calculations A and B as the latter only used two states whilst the former calculations had five or ten states in the expansion. The three molecular calculations employing translation factors (H, KT and CT) are in better agreement with one another than with the three molecular state PSS calculations of Piacentini and Salin (1977) denoted by PS.

We end this subsection with a table of c.p.u. times for the computation of two-state matrix elements and cross sections for capture into the 2s state of $^4He^+$ at a laboratory energy of 400 keV (100 keV amu^{-1}) by the computer programs described in this chapter, table 5.9.

	Lab. energy (keV amu^{-1})			
	0.25	0.75	2.0	5.0
A	0.73-3	0.059*	0.78*	2.32
B	0.17-3	0.069*	0.90*	3.37
PS	-	0.28 *	0.98*	1.15*
H	0.39-1	0.397	1.27	2.37
KT	0.38-1	0.39 *	1.21	2.18
CT	-	0.395	1.46	2.90

* denotes graphical values.

Table 5.8

Comparison of cross sections for capture into the 2s state of $^4He^+$: A, two-state atomic expansion with plane-wave translation factors, present work and Bransden et al. (1980); B, two-state atomic expansion with simple switching function translation factors, present work; PS, three-state molecular expansion (PSS method in H ref. frame), Piacentini and Salin (1977); H, ten-state molecular expansion with plane-wave translation factors, Hatton et al. (1979); KT, ten-state molecular expansion with optimised switching function translation factors, Kimura and Thorson (1981b); CT, five-state molecular expansion with optimised switching function translation factors, Crothers and Todd (1981b). Cross sections are in units of $10^{-16}cm^2$. (0.73 - 3 = 0.73 x 10^{-3}).

	Program Name	C.p.u. time (s)	
		12i.p.	30i.p.
PW	M FOURIER C PLANX2	216 N 7	-
	M PLANEL C CROSS2	683 N 7	-
	M PLANEL C CROSSM	681 N 18	≈1700 N ≈ 40
SF	M SWITEL(S) C CROSS2	825 N 9	-
	M SWITEL(SR) C CROSS2	1700 N 9	-
	M SWITEL(C) C CROSS2	835 N 9	-
	M SWITEL(T) C CROSS2	876 N 9	-
	M SWITEL(S) C CROSSM	-	≈1800 D ≈ 36
	M SWITEL(T) C CROSSM	-	≈1575 D ≈ 36

Table 5.9

C.p.u. times for computation of matrix elements (M) and cross sections (C) for capture into the 2s state of $^4He^+$ at 400 keV for 12 and 30 impact parameters (i.p.). PW : plane-wave factors; SF : switching function factors. N : NUMAC (IBM 370/168); D : Daresbury (AS 7000).

5.4.2 Cross sections for capture into the n = 2 level of $^4He^+$

This subsection will follow similar lines to the previous one. In this subsection capture cross sections for the process (5.1.2) are presented where instead of the 2s state of $^4He^+$ being the final capture state, we shall be concerned with the cross section for capture into the n = 2 level of $^4He^+$ which is equal to the sum of the three individual cross sections for capture into the 2s, 2po and $2p^{\pm}1$ states. However, as we noted in subsection 5.3.3, it was not possible to asymptotically correct the 2s and 2po capture expansion coefficients when using switching function translation factors in the two-centre atomic basis and so only the cross sections for n = 2 level capture will be presented. The present calculations use four atomic states in the expansion : 1s target; 2s, 2po and $2p^{\pm}1$ projectile. This four-state work was very similar to the two-state work in that the energy range was from 1 keV to 800 keV ($^4He^{2+}$ laboratory energy) and the four SWITEL programs were used to compute the required matrix elements numerically using Gaussian integration. The program CROSSM was used to compute the cross sections. In addition to four-state atomic expansion switching function translation factor cross sections being calculated, cross sections were calculated using a four-state atomic expansion with plane-wave translation factors. Here it was possible to asymptotically correct the 2s and

2po coefficients and so individual capture cross sections are presented in addition to the summed n = 2 cross section. These results were computed using Noble's programs FOURIER (matrix elements) and PLANXM (differential equations and cross sections); they are given in table 5.10. FOURIER and PLANXM were used in preference to PLANEL and CROSSM owing to the FOURIER program being very much faster computationally than PLANEL (see table 5.12) especially as 30 impact parameter runs were done up to a laboratory energy of 100 keV (25 keV amu^{-1}). All the cross sections in table 5.10 were computed on the IBM 370/168 machine (NUMAC) using double precision.

Table 5.11 displays the present four-state switching function results for capture into the n = 2 level of $^4He^+$. The four forms of switching function are shown on the left of the table. The parameter p in $F(R)$ (see equation (5.1.8)) is 1/2. The 12 impact parameter results, labelled by a), were obtained using the IBM 370/168 machine (NUMAC). The 30 impact parameter results, labelled by b), were obtained using the AS 7000 machine of the Daresbury Laboratory. All the results were computed using double precision.

The four-state results of the present work are displayed graphically in figure 5.4 together with other theoretical data and some total capture experimental data. (The key to figure 5.4 is on the page after it).

Lab. energy (keV)	nlm capture state			n=2 capture
	2so	2po	$2p^{\pm}1$	
1	a) 0.16-1 b) 0.11-1	0.99-2 0.84-2	0.64-2 0.58-2	0.33-1 0.26-1
2.4	a) 0.231 b) 0.206	0.356 0.325	0.221 0.177	0.808 0.708
5.0	a) 0.695 b) 0.656	1.33 1.18	0.844 0.816	2.86 2.65
6.32	a) 0.962 b) 0.909	1.76 1.70	1.22 1.20	3.94 3.80
10	a) 1.67 b) 1.67	3.18 3.18	2.43 2.40	7.28 7.25
15.81	a) 2.43 b) 2.39	4.72 4.75	3.69 3.71	10.84 10.85
20	a) 2.51 b) 2.48	5.20 5.23	4.09 4.11	11.81 11.81
25	a) 2.36 b) 2.37	5.36 5.35	4.26 4.26	11.98 11.98
40	a) 1.89 b) "	5.14 "	3.98 "	11.01 "
50	a) 1.56 b) "	4.78 "	3.57 "	9.91 "
100	a) 1.12 b) "	2.67 "	1.80 "	5.59 "
200	a) 0.498	0.838	0.480	1.82
400	a) 0.128	0.132	0.64-1	0.323
800	a) 0.18-1	0.10-1	0.41-2	0.32-1

Table 5.10

Four-state plane-wave translation factor cross sections for capture into 2s, 2po, $2p^{\pm}1$ states and n=2 level of $^4He^+$. 12 impact parameter results are labelled by a); 30 impact parameter results by b). Cross sections are in units of $10^{-16}cm^2$.(0.16-1 = 0.16 x 10^{-1}).

Switching function	$^4He^{2+}$ Laboratory energy (keV)								
	1	2.4	5	10	20	40	100	400	800
$-F(R)\eta$	a) 0.46-1 b) 0.36-1	0.854 0.808	3.03 3.16	8.31 8.39	15.01 15.03	16.99 17.01	14.81 14.81	9.73 9.73	8.17 8.17
$-F(R)\cos\theta$	a) –	–	2.90	–	–	15.91	–	7.17	5.01
$-F(R)\eta^3$	a) –	–	3.31	–	–	19.20	–	14.00	12.15
$-F(R)\tanh 3\eta$	a) 0.43-1 b) 0.33-1	0.792 0.752	2.73 2.87	7.40 7.46	13.01 13.05	14.16 14.18	10.64 10.64	4.83 4.83	3.81 3.81

Table 5.11

Four-state switching function translation factor cross sections for capture into the n = 2 level of $^4He^+$. 12 impact parameter results are labelled by a) ; 30 impact parameter results by b). Cross sections are in units of $10^{-16}cm^2$. (0.46-1 = 0.46 x 10^{-1}).

Fig. 5·4 $^4He^{2+} + H(1s) \longrightarrow {}^4He^{+}(n=2) + H^{+}$

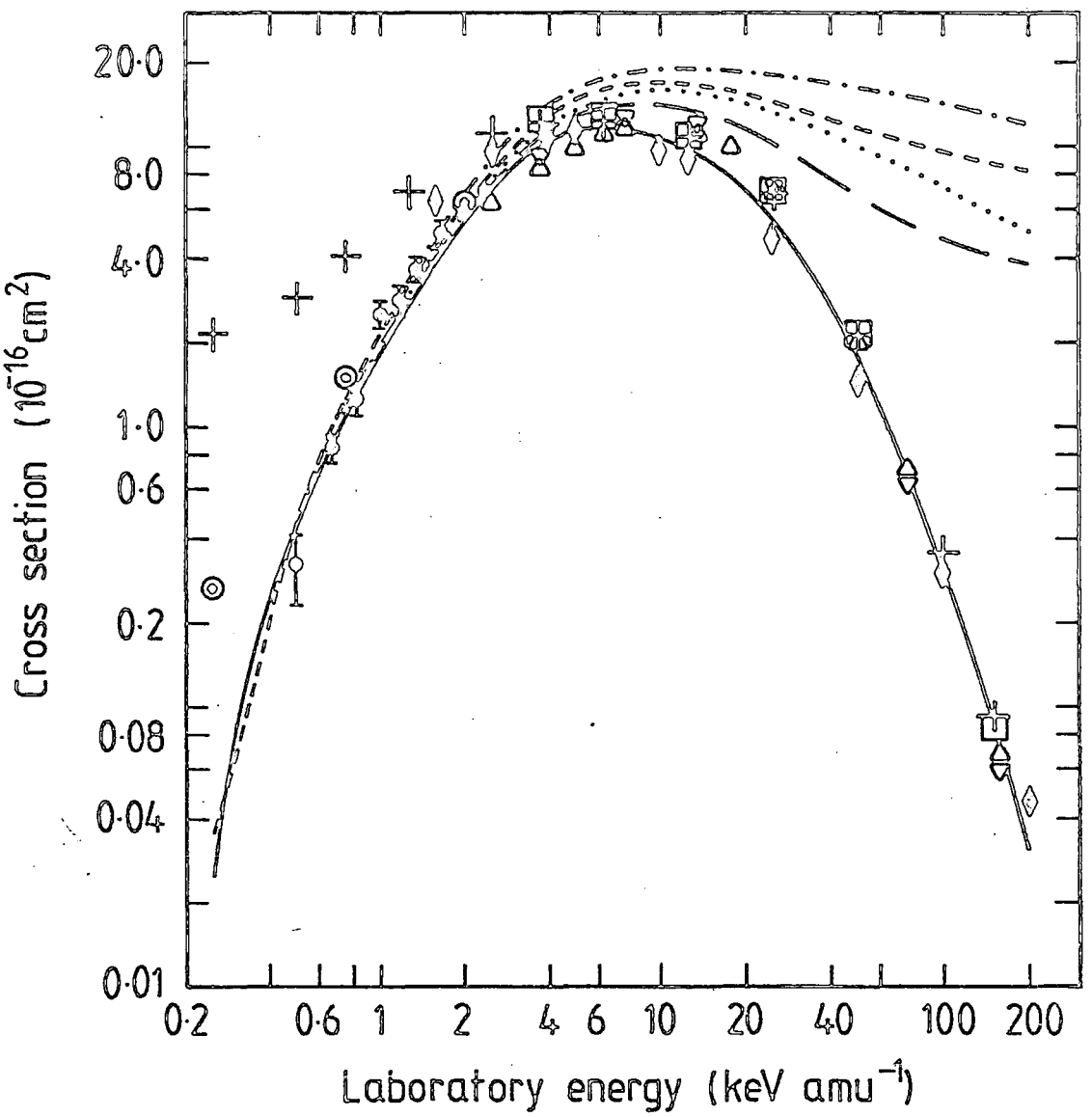

Key to Figure 5.4

Cross sections for electron capture into the n=2 level of $^4He^+$ with comparative total capture data (lab. energy $\leqslant 2.5$ keV amu^{-1}).

Theoretical cross sections :

———— , four-state atomic expansion with plane-wave translation factors, n = 2 capture, present work;

– – – – – , four-state atomic expansion with simple switching function translation factors, n = 2 capture, present work;

····· , four-state atomic expansion with Schneiderman and Russek switching function translation factors, n = 2 capture, present work;

·–·–·–· , four-state atomic expansion with cubic switching function translation factors, n = 2 capture, present work;

═══ ═══ , four-state atomic expansion with tanh switching function translation factors, n = 2 capture, present work;

△ , eight-state atomic expansion, n = 2 capture, Bransden and Noble (1981);

▽ , twenty-state atomic expansion, n = 2 capture, Bransden et al. (1983);

◇ , eight-state atomic expansion, n = 2 capture, Msezane and Gallaher (1973);

+ , eight-state and □ , eleven-state atomic expansion, n = 2 capture, Rapp (1974);

◎ , ten-state molecular expansion, total capture, Hatton et al. (1979).

Experimental cross section :

I , total capture, Nutt et al. (1978).

As with the 2s capture graph in figure 5.3, there is a large discrepancy in the high energy region of the energy range covered between the present switching function translation factor cross sections and the plane-wave translation factor cross sections, both of which were calculated using a four-state atomic expansion (1s target state and 2s, 2po and $2p^{\pm}1$ projectile states). In the low energy region the four switching function cross section curves almost merge into the plane-wave cross section curve. The switching function results begin to diverge from the plane-wave results before the cross section's maximum at about 2.5 keV amu^{-1}. This corresponds to a velocity of about 0.3 a.u. which is about the same velocity as where divergence occurred with the two-state work. Also the four individual switching function cross sections begin to diverge among one another at this velocity. In the low energy region the four switching function cross sections agree well and only the simple switching function cross sections are plotted therefore. The plane-wave and switching function cross section results plotted on the graph are divided into 12 impact parameter and 30 impact parameter results. The 30 impact parameter cross sections are those corresponding to energies up to and including 2.5 keV amu^{-1} Above this energy 12 impact parameter cross sections are plotted.

Above an energy of 50 keV amu^{-1} there is excellent agreement between the presentfour-state plane-wave results

and the eight-state and twenty-state plane-wave results of Bransden and Noble (1981) and Bransden et al. (1983). This is hardly surprising since the same programs were used to compute the four-state results as were used to compute the eight- and twenty-state results, the programs being written by Noble (see subsection 5.3.4). In the eight-state work of Bransden and Noble (1981), four-state runs of the programs were performed to compare the results with those produced by Malaviya (1969) who used the same size of basis in his expansion. It should be noted that the present four-state results are in agreement with Malaviya's results which are not plotted. There is also good agreement with the data of Rapp (1974) who used an eight- and eleven-state atomic expansion, and with the data of Msezane and Gallaher (1973) who used an eight-state atomic expansion. In the energy region from the maximum ($\approx$ 6 keV amu^{-1}) to 50 keV amu^{-1} the agreement between the present four-state plane-wave data and other theoretical data is not as good as that in the region of 50 keV amu^{-1} and above. On the low energy side of the cross section's maximum it can be seen that some experimental data have been plotted. These data due to Nutt et al. (1978) are for total capture not capture into the n = 2 level of $^{4}He^{+}$. Similarly some theoretical data for total capture, which were produced by Hatton et al. (1969) using ten molecular states with plane-wave translation factors, are plotted. At the energies being considered in this low energy region ($\lesssim$ 2.5 keV amu^{-1}) virtually all the total cross section is due to capture

into the n = 2 level and so it is valid to make a comparison with these total capture data. It can be seen that there is very good agreement between the present plane-wave and switching function results and the theoretical results of Hatton et al. (1969) and the experimental results of Nutt et al. (1978) down to about 0.7 keV amu^{-1}. There is much better agreement between the present four-state results and the ten-state molecular results of Hatton et al. (1969) here than there is between the present two-state results and Hatton et al.'s results for capture into the 2s state of $^4He^+$ (see figure 5.3). One reason for this in the higher number of basis states being used in this low energy region (Bransden and Noble, 1982).

We end this subsection with a table of c.p.u. times for the computation of four-state matrix elements and cross sections for capture into the n = 2 level of $^4He^+$ at a laboratory energy of 400 keV (100 keV amu^{-1}) by the computer programs used in this work, table 5.12.

	Program name	C.p.u. time (s)			
		12i.p.		30i.p.	
PW	M FOURIER	327	N	≈800	N
	C PLANXM	19		≈ 40	
	M PLANEL	2930	N	-	
	C CROSSM	24			
SF	M SWITEL(S)	≈4200	N	7446	D
	C CROSSM	≈ 35		55	
	M SWITEL(SR)	≈7908	N	-	
	C CROSSM	≈ 33			
	M SWITEL(C)	4064	N	-	
	C CROSSM	38			
	M SWITEL(T)	4221	N	7130	D
	C CROSSM	35		58	

Table 5.12

C.p.u. times for computation of matrix elements (M) and cross sections (C) for capture into the n = 2 level of $^4He^+$ at 400 keV for 12 and 30 impact parameters (i.p.). PW : plane-wave factors, SF : switching function factors N : NUMAC (IBM 370/168); D : Daresbury (AS 7000).

5.5 Probability times impact parameter distributions

The probability for electron capture into the 2s state of $^4He^+$ is $|C_{2s}(+\infty)|^2$. The probability for capture into the n = 2 level of $^4He^+$ is $\{ |C_{2s}(+\infty)|^2 + |C_{2p0}(+\infty)|^2 + |C_{2p\pm1}(+\infty)|^2 \}$. We denote either of these probabilities by P_c and plot the values of bP_c against b (b is the impact parameter). The resulting graphs may be of use in finding which impact parameters contribute most to the capture cross section. (Twice the area under the bP_c versus b curve is equal to the cross section in πa_0^2 see equation (3.3.9)). Figures 5.5 to 5.12 show bP_c versus b graphs for capture into the 2s state and the n = 2 level of $^4He^+$ comparing the plane-wave results (full line) with the simple switching function results (broken line). E_{lab} is the $^4He^{2+}$ laboratory energy. The 5 keV graphs (figures 5.5 and 5.9) used 30 impact parameters, the other graphs used 12 impact parameters. The bP_c data points were joined by straight lines for simplicity.

At 5 keV, where the plane-wave and switching function cross sections are in good agreement, similar structure is observed for the plane-wave and switching function graphs figures 5.5 and 5.9. This is especially so for the two-state graph of figure 5.5 where the structure is almost the same down to an impact parameter of about 1.5 a.u. As the laboratory energy, E_{lab}, increases the difference between the areas under the plane-wave

Fig. 5·5 bPc vs. b for $^4He^{2+} + H(1s) \longrightarrow {}^4He^{+}(2s) + H^{+}$

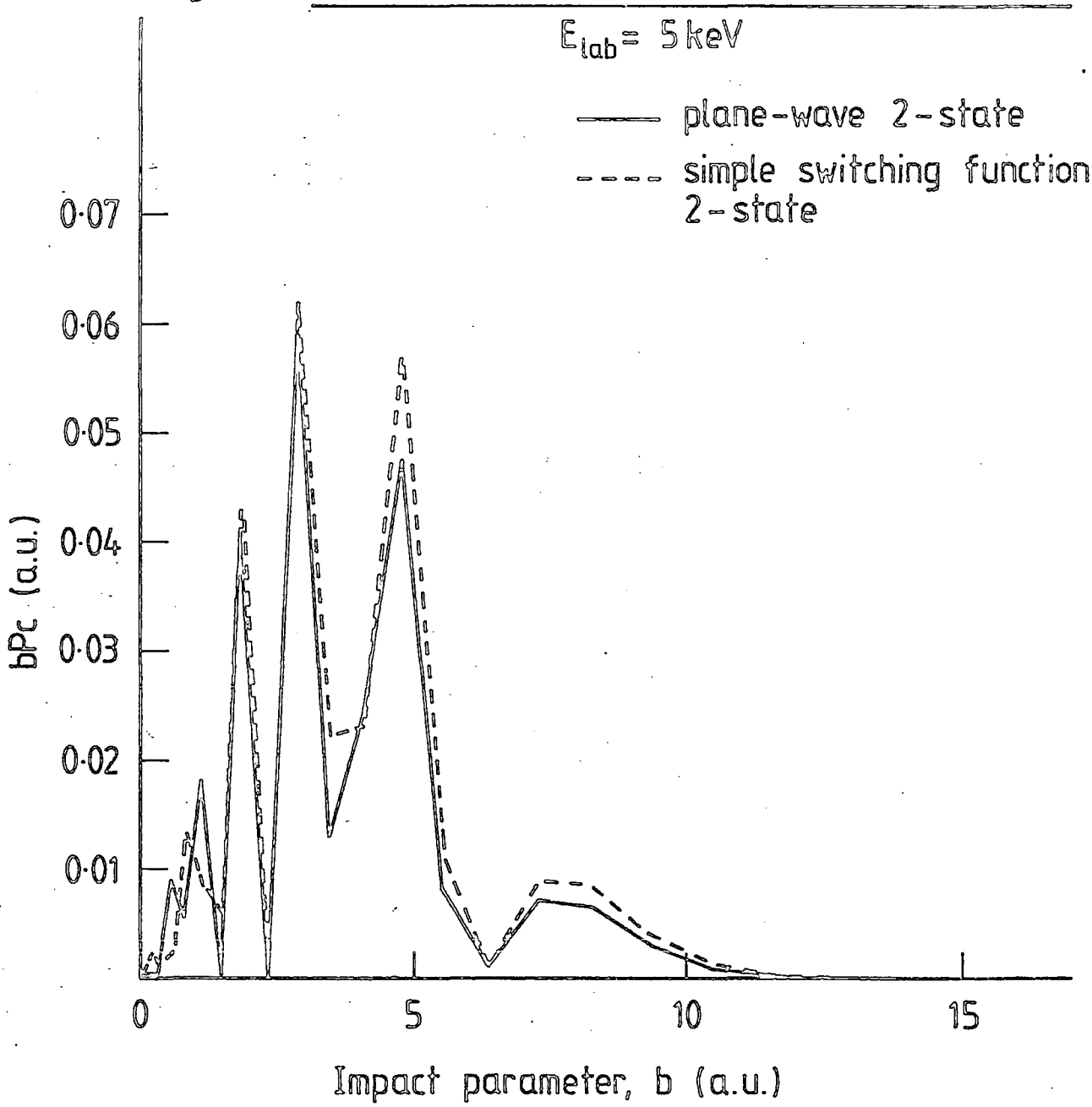

Fig. 5·6 bPc vs. b for $^4He^{2+} + H(1s) \longrightarrow {}^4He^{+}(2s) + H^{+}$

E_{lab} = 20keV

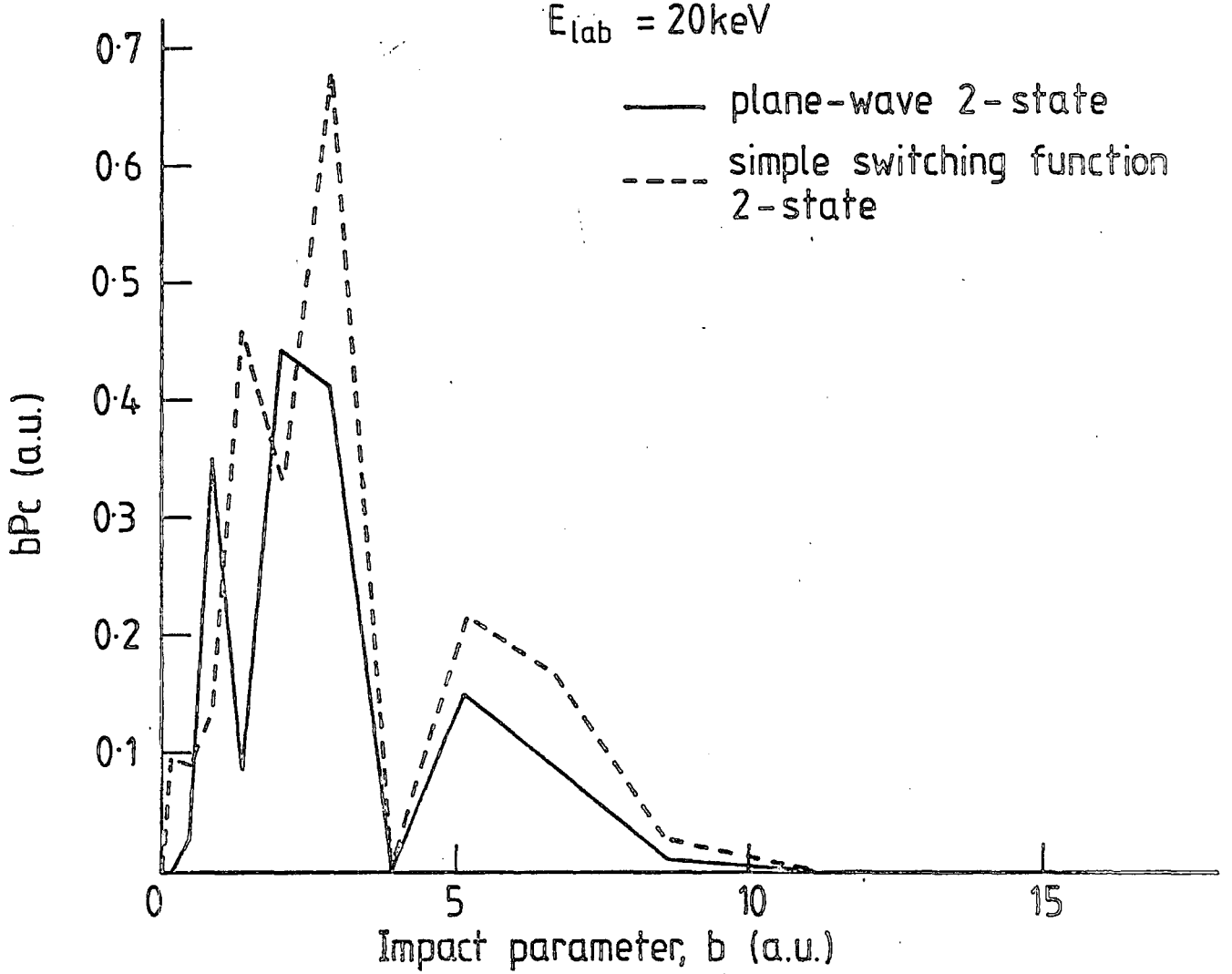

Fig. 5·7 bPc vs. b for $^4He^{2+} + H(1s) \longrightarrow {}^4He^{+}(2s) + H^{+}$

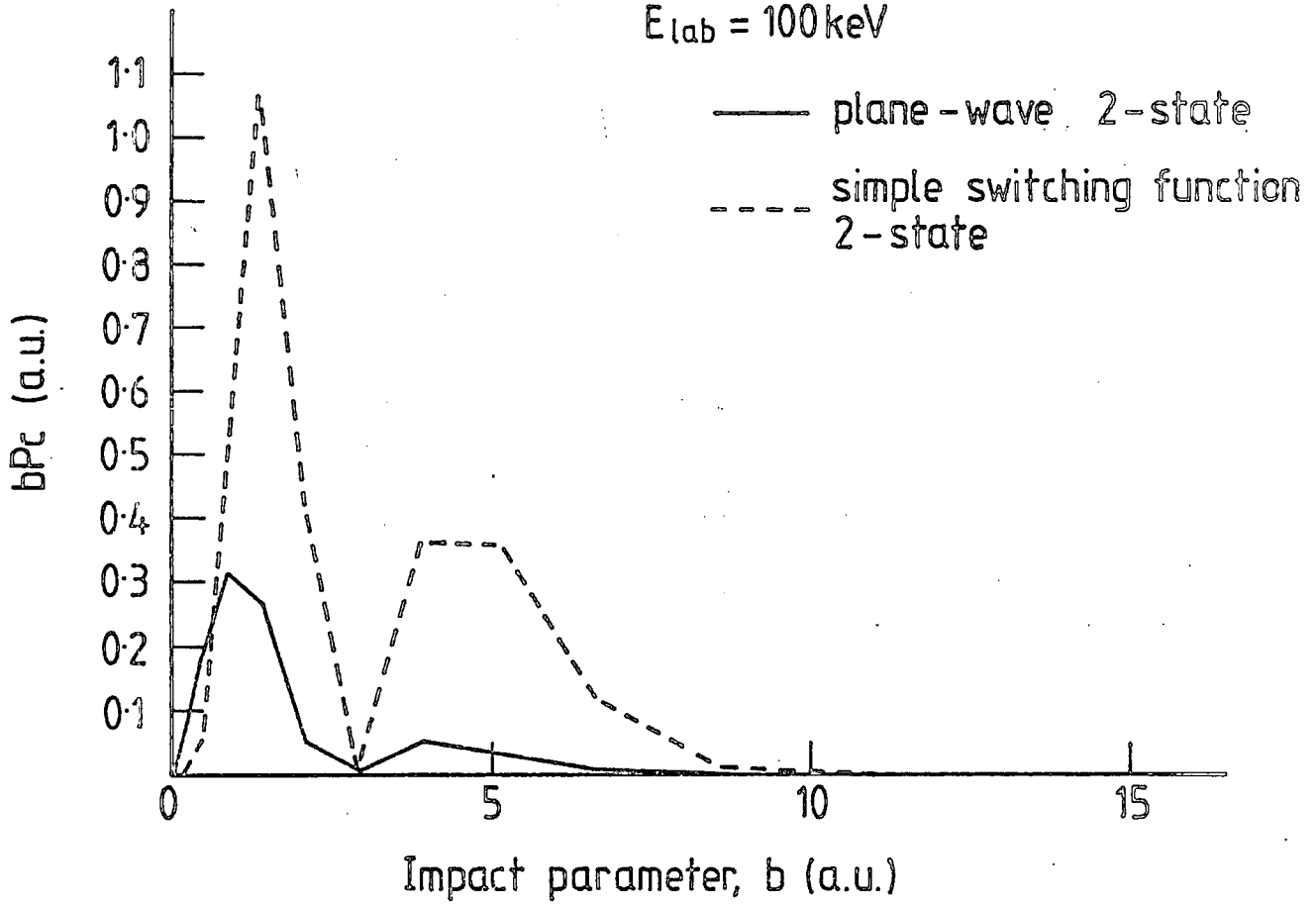

Fig. 5·8 bPc vs. b for $^4He^{2+} + H(1s) \longrightarrow {}^4He^{+}(2s) + H^{+}$

$E_{lab} = 400\,keV$

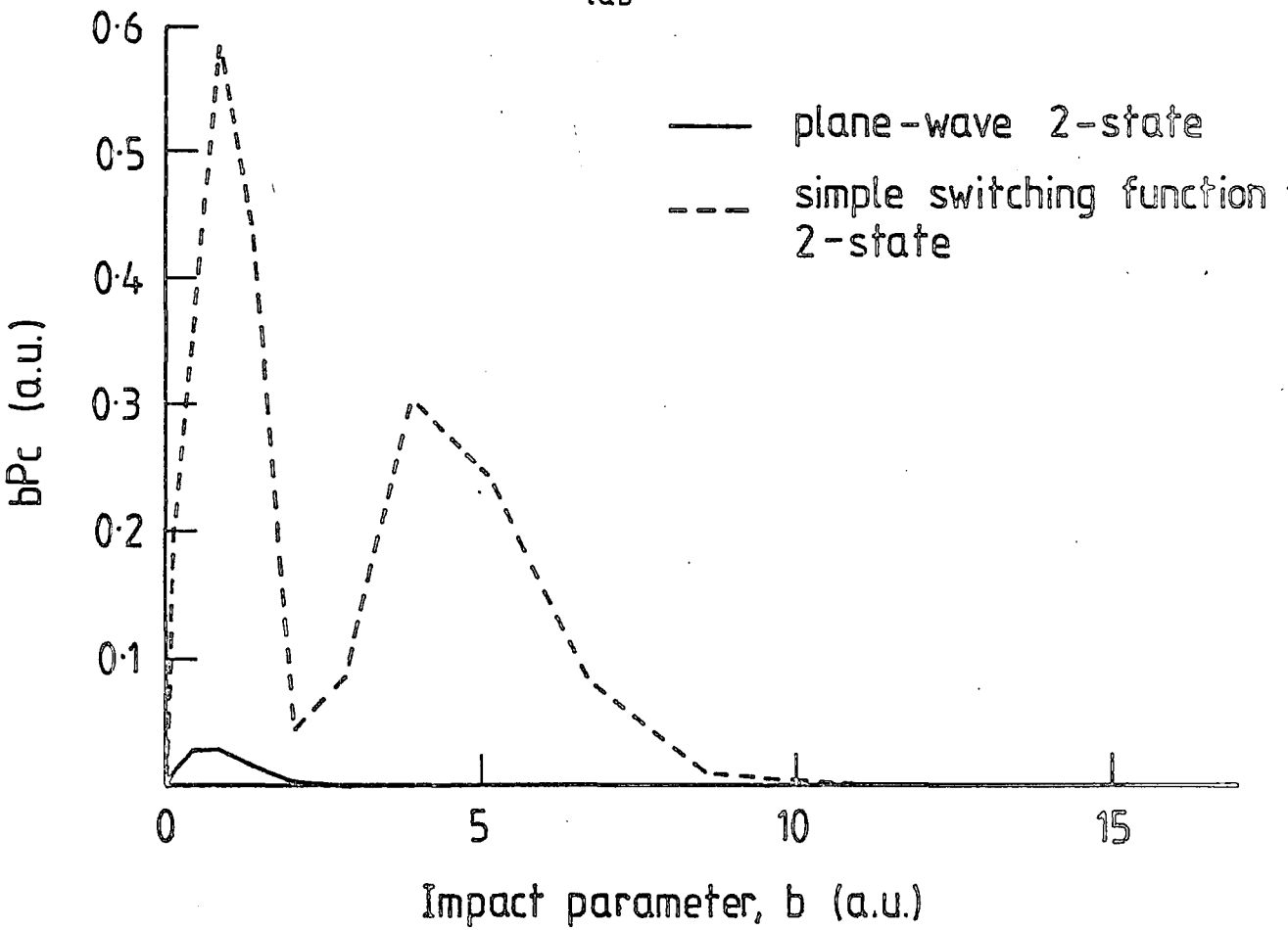

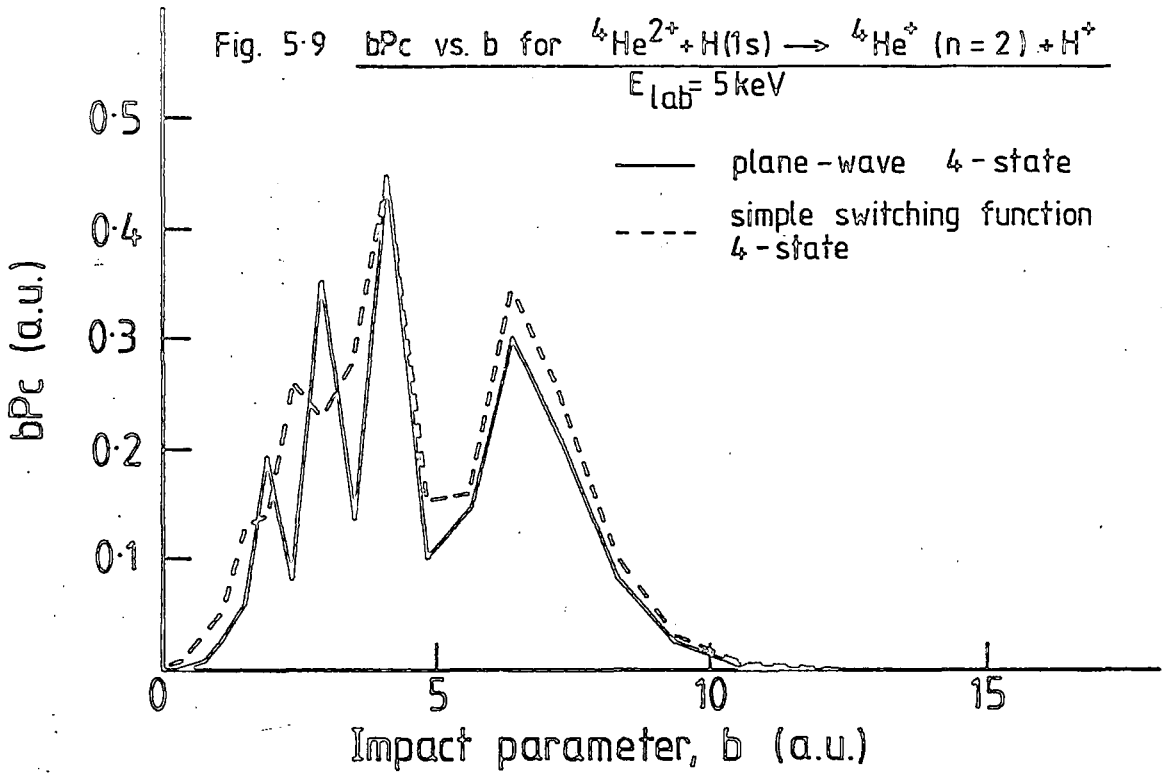

Fig. 5·9 bPc vs. b for $^4He^{2+} + H(1s) \longrightarrow {}^4He^{+}(n=2) + H^{+}$ $E_{lab} = 5\,keV$

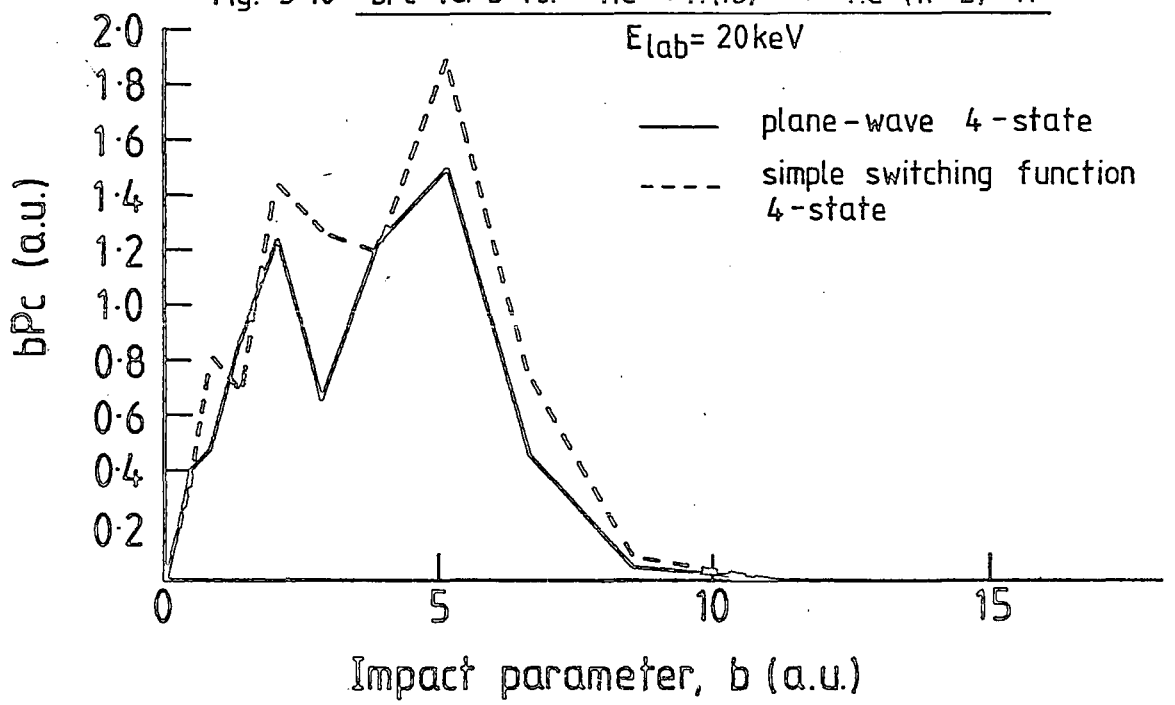

Fig. 5·10 bPc vs. b for $^4He^{2+} + H(1s) \longrightarrow {}^4He^{+}(n=2) + H^{+}$ $E_{lab} = 20\,keV$

Fig. 5·11 bPc vs. b for $^4He^{2+} + H(1s) \rightarrow {}^4He^{+} (n=2) + H^{+}$
$E_{lab} = 100keV$

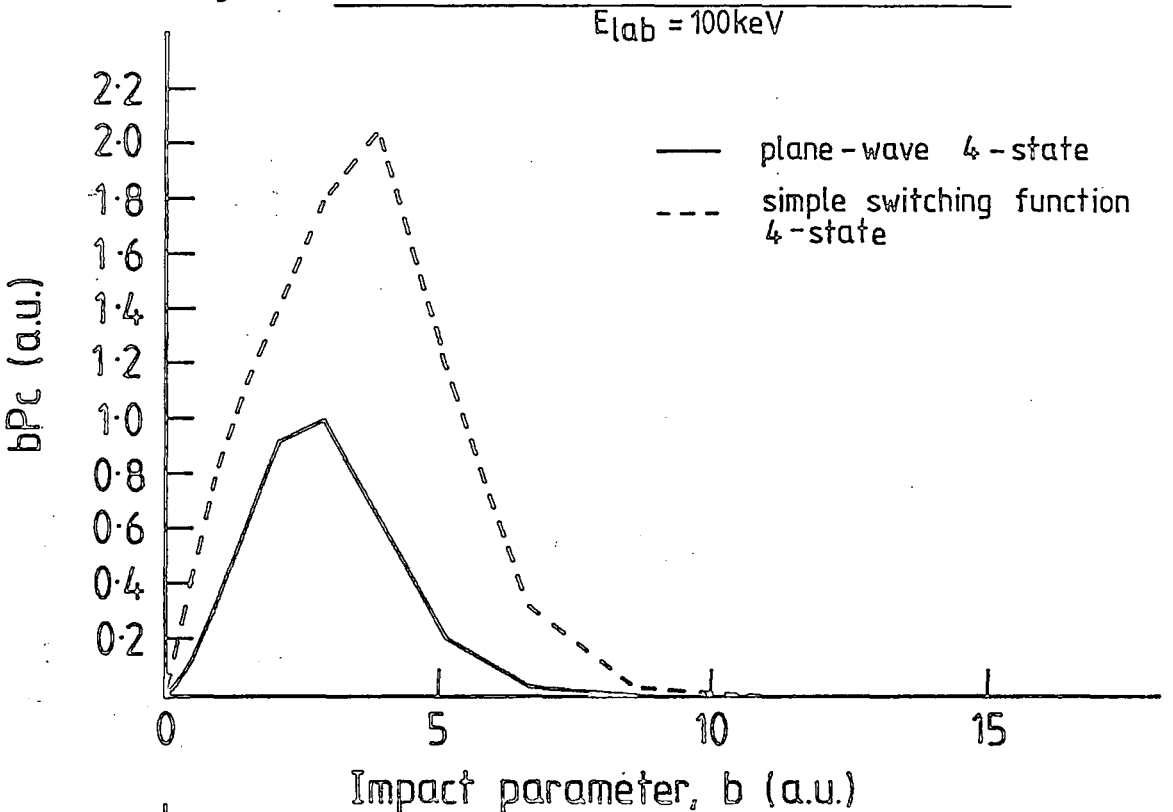

Fig. 5·12 bPc vs. b for $^4He^{2+} + H(1s) \rightarrow {}^4He^{+} (n=2) + H^{+}$
$E_{lab} = 400keV$

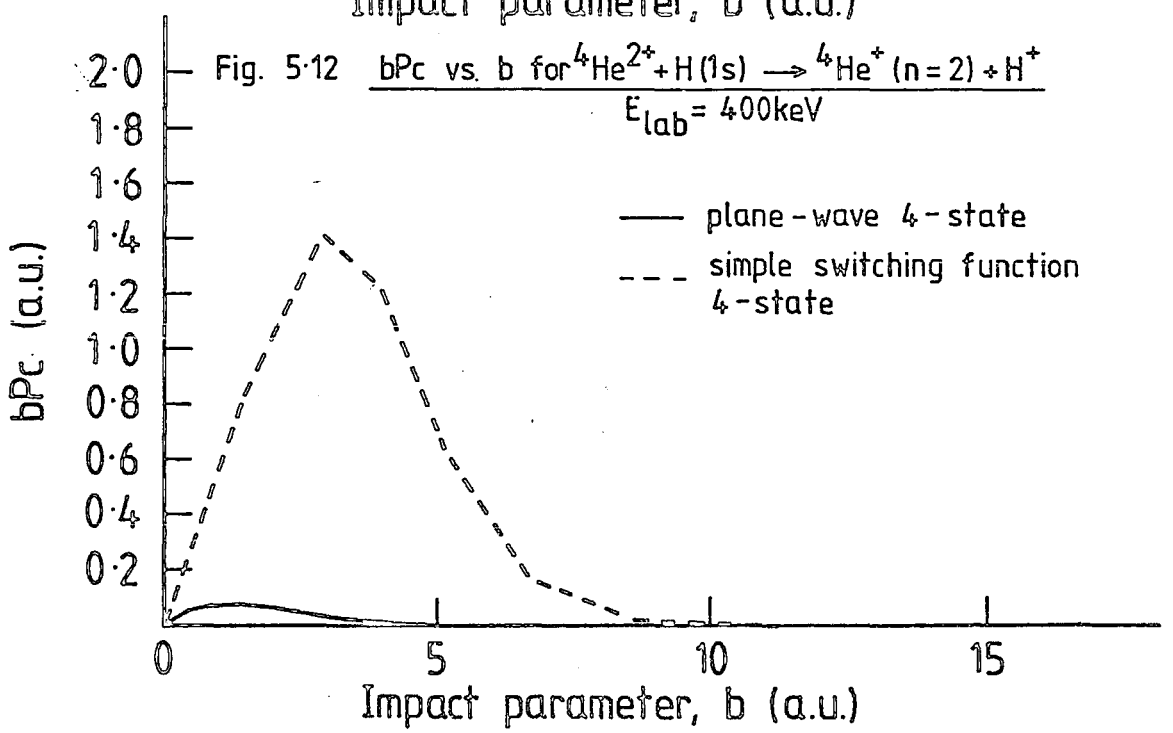

and switching function curves becomes larger which, of course, corresponds to the increasing disagreement between the associated cross sections. Also, as E_{lab} increases, there is a marked loss of structure for both the plane-wave and switching function curves, though the curves do retain similarities in the structures remaining. At the highest energy considered of 400 keV, the two-state switching function curve has become two peaks (figure 5.8) whilst the four-state switching function curve has become one peak (figure 5.12). Probably the most interesting graph is that of figure 5.5 for E_{lab} = 5 keV and two states being used in the expansion. For impact parameters $\gtrsim$ 1.5 a.u. the observed forms of the bP_e plots are virtually the same. This similarity is almost certainly correlated with the fact that at energies of the order of 5 keV and below, the plane-wave and switching function models are in accord with one another.

5.6 The cross sections and the functional form of the switching function

For the two-state, 2s state capture and four-state, n = 2 level capture, the cross sections obtained using switching function translation factors diverge from those obtained using plane-wave translation factors in the intermediate to high energy region of the energy range considered. In addition in this energy region the cross sections obtained using different functional forms of the switching function display significant

differences between one another which must be due to their different forms.

In the early stages of the work presented here the switching functions used were the simple switching function f_s and the Schneiderman and Russek switching function f_{sR} . The motivation for the use of these switching functions was twofold: the simple switching function had a very simple form (hence its name), and the Schneiderman and Russek switching function was the first switching function to be proposed (Schneiderman and Russek, 1969). However, when the divergence at high energies became apparent with the production of results, it was decided to try and use a switching function in the translation factor that would have such a form as to make the translation factors behave somewhat like plane-wave translation factors in an attempt to reproduce results close in value to the ones obtained using plane-wave factors.

If we consider the simple switching function, f_s

$$f_s = -F(R)\eta \qquad (5.6.1)$$

where

$$F(R) = \frac{R^2}{R^2 + P^2} \,, \qquad (5.6.2)$$

we see that it is of the form

$$f = -F(R)g(\eta) \qquad (5.6.3)$$

the function f_s being obtained when $g(\eta) = \eta$. The correct united atom limit is produced by the function $F(R)$ which tends to zero as R tends to zero. Figure 5.13 shows a sketch of $F(R)$ for $p = 1/2$.

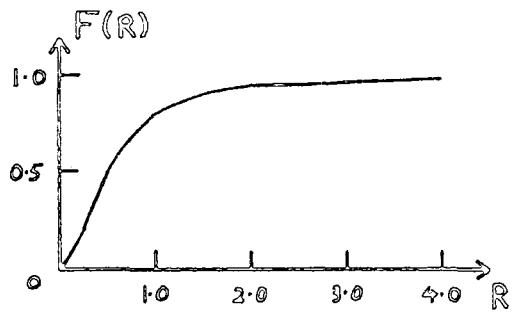

Figure 5.13
Sketch of $F(R)$ for $p = 1/2$.

In the case of the simple switching function $g(\eta)$ is a straight line ($g(\eta) = \eta$), (see figure 5.14).

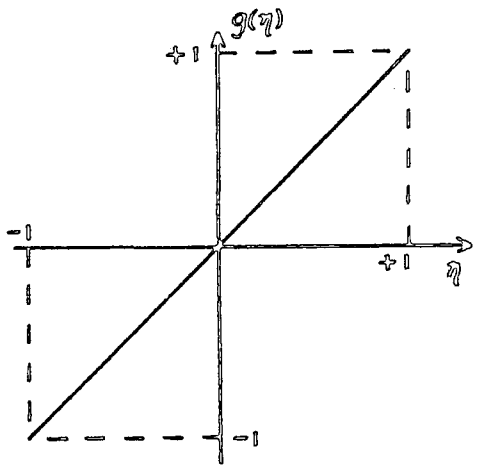

Figure 5.14
Sketch of $g(\eta)$ for the simple switching function, f_s for $|\eta| \leq 1$.

As η varies between plus and minus one so too does $g(\eta)$ and the switching behaviour of the switching function is produced. In the case of the plane-wave translation factors, the electron is attached to either one centre or the other. In terms of the function $g(\eta)$ this should correspond very nearly to $g(\eta)$ being of the form shown in figure 5.15.

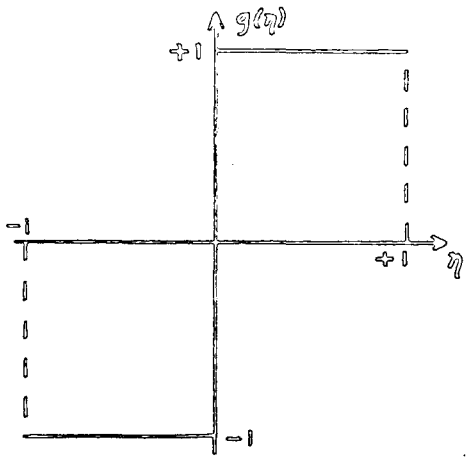

Figure 5.15
Function $g(\eta)$ for plane-wave translation factor, $|\eta| \leq 1$.

With this in mind the function $tanh(\alpha\eta)$ where $\alpha \geq 3$ was a good candidate for the function $g(\eta)$ such that the translation factor would be more like a plane-wave translation factor. The value of α was chosen to be 3 in the present work. Also the function η^3 was such that it was very nearly $tanh 3\eta$ reflected about the line $g(\eta) = \eta$ and so should produce an opposite effect to that of $tanh 3\eta$, see figure 5.16.

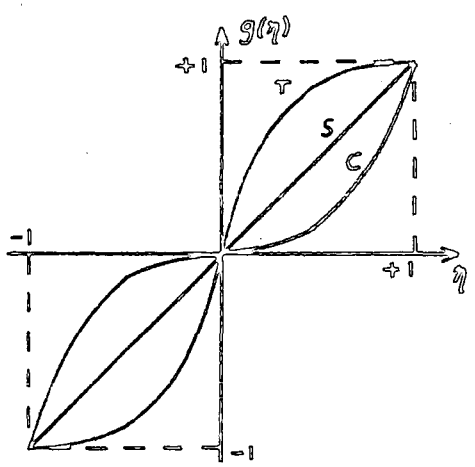

Figure 5.16.
Curve T : $g(\eta) = tanh 3\eta$.
Curve S : $g(\eta) = \eta$.
Curve C : $g(\eta) = \eta^3$.

The results obtained show that indeed the four-state, n = 2 level capture cross sections associated with the tanh switching function in the translation factors are closer to those obtained using the plane-wave translation factors than the cross sections obtained using the simple switching function in the translation factor. Also the cross sections obtained using the cubic switching function in the translation factor are furthest away from the plane-wave translation factor cross sections (see figure 5.4). However, for the two-state, 2s state capture cross sections, this is only true up to about 75 keV amu^{-1} (see figure 5.3). Above an energy of about 60 keV amu^{-1} the cross section associated with the tanh switching function starts increasing, as indeed does the cross section associated with the cubic switching function. No such behaviour appears for the four-state, n = 2 level capture cross sections, though it may appear at higher energies than were considered. This behaviour is somewhat puzzling but leaving this aside, it does appear that the tanh switching function does improve the cross section results with respect to the other switching function cross section results. However, the improvement is not great enough so as to produce results in accord with those obtained using plane-wave translation factors. This may be because the tanh switching function translation factors do not behave like the plane-wave translation factors in the small $\mathbb{R}$ (internuclear separation) region. The fact

that the improvement in the results is not very great with respect to the plane-wave results may be indicative of the behaviour of the switching function translation factors in the small internuclear separation region being quite significant in its effect and thereby responsible for the divergence of the present switching function results from the plane-wave results at high energies.

5.7 Closing comments

In this chapter the results of this work have been presented together with some discussion. In the next and final chapter of this thesis the results and their implications will be discussed in more detail. Suggestions for future work will also be made.

CHAPTER 6

CONCLUDING CHAPTER

6.1 Discussion of the results

The results presented in the previous chapter would seem to indicate that for both two-state and four-state atomic expansion methods applied to electron capture into the 2s state and the n=2 level of $^4He^+$ respectively, the use of electron translation factors incorporating a switching function $f(\vec{r}, \vec{R})$ predicts capture cross sections in the intermediate to high energy region of the energy range considered that are in poor to extremely poor agreement with the capture cross sections predicted by the use of plane-wave translation factors. Indeed, at a laboratory energy of 200 keV amu^{-1} the disagreement is somewhat greater than two orders of magnitude. For both two-state and four-state methods the use of other (albeit similar) forms of switching function would appear to make little improvement to the switching function cross section results as compared with the plane-wave results, even though there are significant differences between the individual switching function cross sections which must be attributed to their different forms. In the low energy region ($\lesssim$2.5 keV amu^{-1}) the agreement between the switching function and plane-wave capture cross sections is good.

Before taking the discussion further, let us briefly review the main reasons for use of switching functions in the theory of ion-atom collisions. As we saw in Section

2.5 of Chapter 2, the basic molecular expansion method, the PSS (perturbed stationary state) method has two major defects, namely that the coupling matrix elements are dependent upon the choice of the origin of co-ordinates, and that some of the couplings do not vanish at large internuclear separation. However, the wavefunction expansion in terms of orthonormal adiabatic molecular states is very simple in form and gives rise to straightforward coupled equations. Bates and McCarroll (1958) introduced plane-wave translation factors into the formulation in order that the wavefunction describing the electronic motion should be a solution of the Schrödinger equation at large internuclear separation. The result of the plane-wave factors' introduction is the elimination of the two problems inherent to the PSS method; the coupling matrix elements are independent of the origin and they all vanish at large internuclear separation. Unfortunately the simple form of the original PSS expansion has been lost. Now it is necessary to divide the expansion into two parts corresponding to the direct and rearrangement channels. This gives rise to much more complicated coupled equations, and matrix elements which are difficult and time consuming to evaluate owing to the presence in some of them of the momentum transfer factors $exp(\pm i\vec{v}.\vec{r})$ which arise due to the plane-wave factors being present in the wavefunction expansion.

The basic theoretical defect of the Bates and McCarroll method is that the introduction of plane-wave translation factors causes the electron to be associated with either

one centre or the other. This is correct at large internuclear separations where, indeed, this is the case. However, at small internuclear separations to associate the electron with either one centre or the other is clearly incorrect as the electron is, in fact, associated with both centres. Plane-wave translation factors have been used with good success in two-centre atomic basis expansion methods for modelling ion-atom collisions in the intermediate and above energy region. Here the need to describe the dynamics of the electron at small internuclear separation is not as important as the electron spends most of its time either upon one centre or the other, hence the reason for atomic basis states being used. In the low energy, adiabatic region, though, the electron spends a significant amount of its time neither bound to one centre nor the other but rather it is in some state of the quasimolecule formed by the two centres and the electron hence the use of molecular basis states in the expansion is appropriate. In essence, the plane-wave translation factors should really be associated with atomic basis states used in a two-centre expansion. They clearly have an "atomic" character as they theoretically associate the electron to one centre or the other. At energies in the intermediate and above region this is a good feature, but at low energies it is not. It is an interesting paradox that plane-wave translation factors were introduced into ion-atom collision theory in conjunction with a molecular basis expansion.

The use of a switching function goes a long way in

solving the problems associated with the use of plane-wave translation factors. As we have seen, translation factors are important and necessary if the theory is to be origin independent and devoid of asymptotic couplings that are non-vanishing. However, the switching function being incorporated into the translation factor gives it much more flexibility. At large internuclear separation it is either plus one or minus one and the translation factor becomes a plane-wave one. However, as the system relaxes as the internuclear separation becomes smaller, the switching function becomes smaller in value, tending asymptotically to zero as the internuclear separation goes to zero. This is called the united atom limit. Thus the translation factors are no longer plane-wave in form but rather they have modified in accordance with the electron moving into the situation where it is in a quasimolecular state. In contrast to the plane-wave translation factors, switching function translation factors have a "molecular" character, hence their applicability to low energy collisions where molecular basis expansions are employed. Apart from their obvious theoretical advantage in modelling the small internuclear separation region effectively, yet giving the correct asymptotic form to the wavefunction for the electronic motion at large internuclear separation, their flexibility results in there being no need to separate the direct and rearrangement channels. This, again, is a reflection of their molecular character.

As far as the author is aware, switching functions have never been used in conjunction with a two-centre atomic basis expansion. Hence the work described in this thesis may be of some importance in ion-atom collision theory. There would appear to be two advantages in the use of a switching function with an atomic basis. The one is that the matrix elements are easier to evaluate. When one considers the complicated expressions which were presented in Chapter 3 for the direct and exchange matrix elements, this may appear to be of little value. Indeed, the computer programs used to compute the matrix elements numerically were not economic in computer time, and, indeed, this was the overriding reason why calculations using larger basis sets were not employed. However, despite the large number of elements to be calculated, compared to the overlap and exchange elements arising from the use of plane-wave factors with their awkward momentum transfer factors $\exp(\pm i\vec{v}.\vec{r})$, the individual elements are easier to evaluate. Also almost all of the individual elements are proportional to the collision velocity or the square of it. The notable exceptions are the overlap and potential elements. This means that a calculation can be done at a particular collision energy, that is, collision velocity and then the matrix elements, having been stored, used to generate elements specific to other collision velocities by simple multiplication of some of the elements by ratios or squared ratios of the collision velocity at which the new elements are required to the collision velocity used

in the first calculation. Certainly if any serious use of the two-centre atomic basis switching function method were to be made, this would be an attractive means of obtaining the matrix elements. The other advantage gained by using a switching function with a two-centre atomic basis expansion is that a much better description of the small internuclear separation region should be achieved, that is, the switching function translation factor has a greater flexibility over the plane-wave translation factor and thereby introduces molecular character into the atomic basis expansion. In theory, this should give the atomic basis expansion more ability to model collisions of ions and atoms in the low energy region where molecular effects are important. As far as the high energy region is concerned, the molecular effects are of limited importance and so there would appear to be no advantage in the introduction of a switching function. If the results presented in this thesis are correct, then it would appear that the introduction of a switching function for modelling intermediate to high energy collisions is a positive disadvantage. In the light of this discussion, let us now return to the results of this work.

In the low energy ($\lesssim 2.5$ keV amu^{-1}) region it would appear that there is nothing to be gained by the use of switching function translation factors as opposed to plane-wave translation factors, even though the switching function results are in good to fair agreement with the plane-wave

results. Any molecular character, introduced by virtue of the inclusion of the switching function, would appear to be small if any. At energies $\gtrsim 2.5$ keV amu^{-1} it is clear that the two-centre atomic basis method with switching function translation factors is not appropriate. The implication of this is that the switching function approach with a molecular basis expansion is likewise not appropriate at such energies, with possibly a similar divergence between molecular basis switching function results and atomic basis plane-wave results. With this in mind, it is therefore interesting to consider some recent total cross section results for proton-lithium electron capture obtained by Ermolaev (1983), together with results for the same process obtained by Allan et al. (1983).

Both Ermolaev and Allan et al. were considering electron capture of the outer 2s electron from lithium atoms in the ground state by protons. In the work of Ermolaev a two-centre atomic basis expansion with plane-wave translation factors was used. Two-state, thirteen-state and nineteen-state calculations were performed. Allan et al. used a molecular basis expansion with the adiabatic switching function (factor) suggested by Dickinson and McCarroll (1983). Six and, in certain cases, seven states were used in the molecular expansion. The H^+ laboratory energy range used was 30 eV - 15 keV. Figure 6.1, reproduced by permission from the paper of Ermolaev (1983), displays graphically Ermolaev's atomic basis results (AO - atomic orbital)

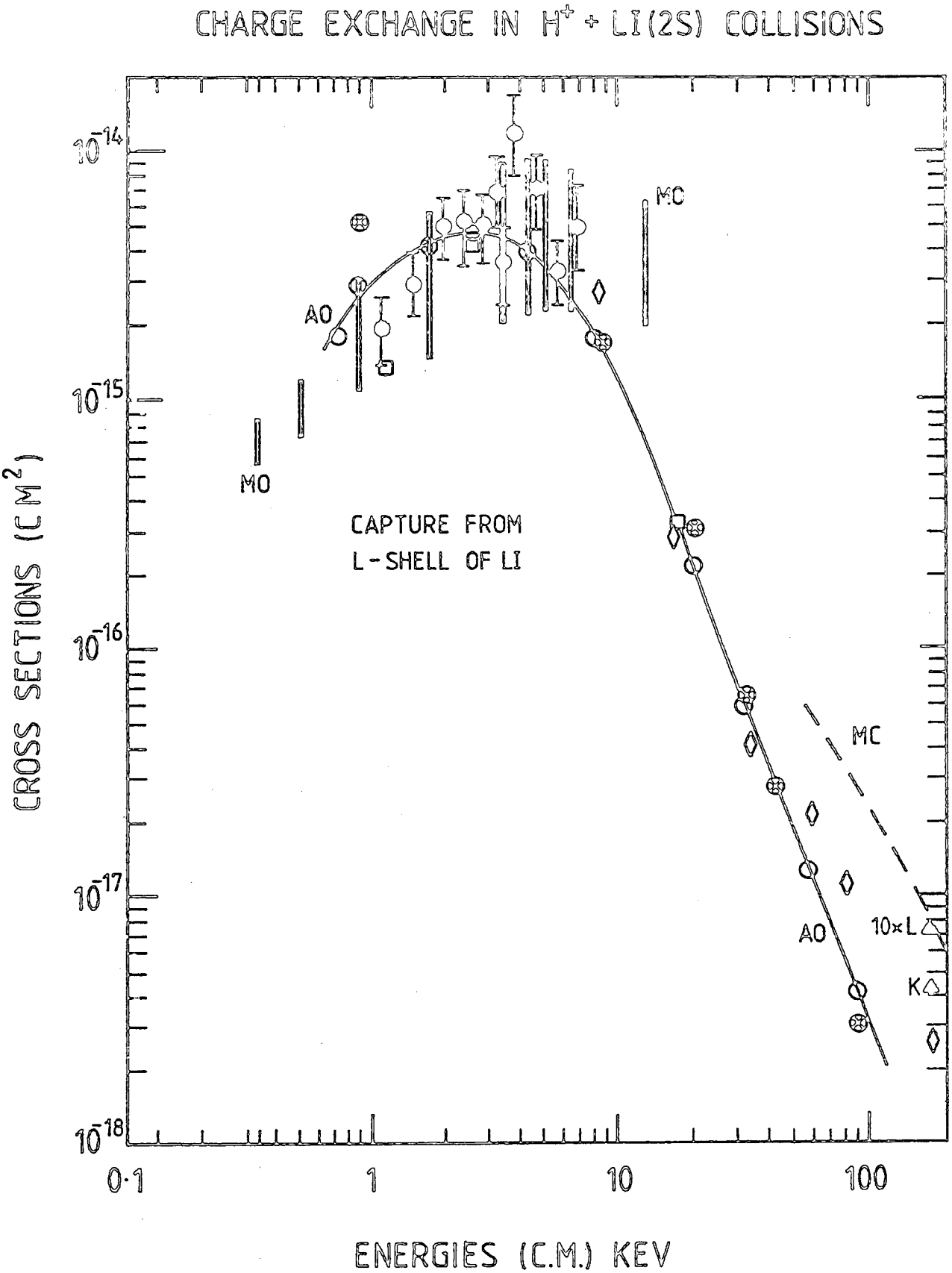

Figure 6.1 (Caption overleaf)

Caption to Figure 6.1

Total cross sections for production of H in H^+ + Li collisions (L-shell capture). Theoretical data : MO-molecular expansion of Allan et al. (1983). Atomic expansions: ⊗ 2-state, present work; O 13-state, present work; □ 19-state, present work; MC - classical trajectory Monte Carlo, Olson (1982); L, K △ CDW, Banyard and Shirtcliffe (1979) for L- and K-shell capture respectively. Experimental data : ⌶ - Grüebler et al. (1970); ◇ - Il'in et al. (1967a, 1967b), D'yachkov and Zinenko (1968).

and the molecular basis results (MO - molecular orbital) of Allan et al. (1983), together with comparative theoretical and experimental data. It should be noted that the results of Allan et al. were origin dependent and hence thin, open rectangles are used on the graph to represent the upper and lower limits for the cross section. The width of the rectangles has no significance. The reason for this origin dependence will be stated shortly. It can be seen that the atomic basis results agree well with the experimental results of Il'in et al. (1967a, 1967b) and D'yachkov and Zinenko (1968). The atomic basis results of Ermolaev at high energies are also in the same general region of the graph as the classical trajectory Monte Carlo calculations of Olson (1982) and the CDW calculations of Banyard and Shirtcliffe (1979). The molecular basis results are in good accord with the atomic basis results and the

experimental results of Grüebler et al. (1970) from about 1 to 3 keV (centre of mass, C.M.). However, for C.M. energies greater than about 5 keV the molecular basis results diverge from the atomic basis results quite drastically. If we consider the molecular basis (MO) data rectangle furthest to the right, the discrepancy between its centre and the atomic basis (AO) curve is abouta factor of 5.

The laboratory energy corresponding to this data rectangle is 15 keV amu^{-1}; this corresponds to a velocity of 0.77 a.u. This divergence between the switching function results of Allan et al. (1983) and the plane-wave results of Ermolaev (1983) is very similar to that observed in the present work. Also the velocity region where the divergence becomes significant is about the same in both cases, 0.4 - 0.5 a.u. One qualifying fact that ought to be stated is that the switching function used by Allan et al. (1983) was not of the same type as that used in the present work. Allan et al. used the adiabatic switching function of Dickinson and McCarroll (1983), which was quoted in equations (2.5.70) in Chapter 2. Reference to those equations shows that it is a function of time only unlike the one used in the present work which was a function of electronic and internuclear co-ordinates $\vec{r}$ and $\vec{R}$. Also the adiabatic switching function was zero within the interaction region which corresponded to the $|t| < t_0$ part of the time axis where $t_0\ (>0)$ was some suitable time value. Outside the interaction region the adiabatic switching function was

$1-\exp(-\gamma|t-t_0|)$ where γ was a frequency which was low compared with the natural frequency of the problem. Essentially the adiabatic switching function is a means whereby the problem can be dealt with using the PSS method in the interaction region, but with the bonus of the basis states having the correct asymptotic behaviour. The origin dependence mentioned earlier arises due to the method used by Allan et al. being a modified PSS method. Whether the adiabatic switching function is a true switching function is open to question.

The cause for the divergence between the switching function results and the plane-wave results of the present work above about 2.5 keV amu^{-1} laboratory energy must be attributed to the effect of the switching function upon the two-centre atomic basis expansion. It has been stated earlier that plane-wave translation factors have essentially an "atomic" character whilst switching function translation factors have a "molecular" character, they being able to model the electronic dynamics in the small internuclear separation region quite effectively. It is possible that their molecular character is somehow responsible for the increasing divergence with respect to increasing collision energy of the switching function results from the plane-wave results. At low energies, in the adiabatic region, the molecular basis expansion is appropriate for modelling ion-atom collisions as only a small number of states are strongly coupled. This is not the case at high energies,

in the non-adiabatic region. Here a fairly large molecular basis set is required. It may be that the introduction of a switching function into an atomic basis expansion with a small number of states gives the expansion sufficient molecular character so as to be of no practical use for calculating capture cross sections at energies which are not in the low energy region. Investigations using larger basis sets might shed light upon this question. Recently Bransden (1983p) in a private communication has stated that T. A. Green has shown that without the momentum transfer factors $exp(\pm i\vec{v}.\vec{r})$ in the exchange matrix elements, it is impossible to obtain the rapid decrease of the capture cross section at high energies.

6.2 Conclusions and suggestions for future work

The main conclusion of this work would appear to be that the use of a two-centre atomic basis expansion with switching function translation factors for calculating electron capture cross sections has no advantage over the use of a two-centre atomic basis expansion with plane-wave translation factors when only a small number of basis states are retained in the expansion. In addition, at high energies there occurs a dramatic divergence of the switching function capture cross section results from the plane-wave results owing, presumably, to the inability of the switching function basis expansion to model the collision effectively. Calculations upon other systems and using extended basis sets are required. Further investigations into the functional form of the switching function may also be of value.

APPENDIX A1

Effect of the operators H_{el} and $-i\,\partial/\partial t]_F$ upon the basis functions $F_j^S(\vec{r},t)$ and $G_k^S(\vec{r},t)$

The expressions for the direct and exchange matrix elements presented in Chapter 3, Section 3.3 equations (3.3.30) to (3.3.33) are obtained by considering the effect of the operators H_{el} and $-i\,\partial/\partial t]_F$ upon the basis functions $F_j^S(\vec{r},t)$ and $G_k^S(\vec{r},t)$.

We have

$$H_{el} = -\tfrac{1}{2}\nabla_F^2 + V_{eA} + V_{eB} + V_{AB} \,, \qquad \text{(A1.1)}$$

and

$$F_j^S(\vec{r},t) = \phi_j^B(\vec{r}_B)\exp -i\left[\varepsilon_j t + \tfrac{1}{8}v^2 t - \tfrac{1}{2}f(\vec{r},\vec{R})\vec{v}.\vec{r}\right] \qquad \text{(A1.2)}$$

$$G_k^S(\vec{r},t) = \chi_k^A(\vec{r}_A)\exp -i\left[\eta_k t + \tfrac{1}{8}v^2 t - \tfrac{1}{2}f(\vec{r},\vec{R})\vec{v}.\vec{r}\right] . \qquad \text{(A1.3)}$$

Expressions for $H_{el}F_j^S(\vec{r},t)$ and $H_{el}G_k^S(\vec{r},t)$.

We begin by considering the effect of ∇_F^2 upon $F_j^S(\vec{r},t)$.

$$\nabla_F^2 F_j^S(\vec{r},t) = e^{-i(\varepsilon_j + \frac{1}{8}v^2)t}\nabla_F^2\left[\phi_j^B(\vec{r}_B)e^{if(\vec{r},\vec{R})\vec{v}.\vec{r}/2}\right] \qquad \text{(A1.4)}$$

Now

$$\nabla_F^2\left[A(\vec{r})B(\vec{r})\right] = A(\vec{r})\nabla_F^2 B(\vec{r}) + 2\vec{\nabla}_F A(\vec{r}).\vec{\nabla}_F B(\vec{r}) + B(\vec{r})\nabla_F^2 A(\vec{r}) \qquad \text{(A1.5)}$$

and so (omitting the arguments of the function f)

$$\nabla_F^2\left[\phi_j^B(\vec{r}_B)e^{if\vec{v}.\vec{r}/2}\right] = e^{if\vec{v}.\vec{r}/2}\nabla_F^2\phi_j^B(\vec{r}_B) + 2\vec{\nabla}_F\phi_j^B(\vec{r}_B).\vec{\nabla}_F\left(e^{if\vec{v}.\vec{r}/2}\right) + \phi_j^B(\vec{r}_B)\nabla_F^2\left(e^{if\vec{v}.\vec{r}/2}\right). \qquad \text{(A1.6)}$$

It is straightforward to show that

$$\vec{\nabla}_r\left(e^{if\vec{v}.\vec{r}/2}\right) = \frac{i}{2}\left[(\vec{v}.\vec{r})\vec{\nabla}_r f + f\vec{v}\right]e^{if\vec{v}.\vec{r}/2}, \qquad \text{(A1.7)}$$

and that

$$\nabla_r^2\left(e^{if\vec{v}.\vec{r}/2}\right) = \frac{i}{2}(\vec{v}.\vec{r})(\nabla_r^2 f)e^{if\vec{v}.\vec{r}/2}$$

$$+ i(\vec{v}.\vec{\nabla}_r f)e^{if\vec{v}.\vec{r}/2} - \frac{1}{2}f(\vec{v}.\vec{r})(\vec{v}.\vec{\nabla}_r f)e^{if\vec{v}.\vec{r}/2}$$

$$-\frac{1}{4}f^2v^2e^{if\vec{v}.\vec{r}/2} - \frac{1}{4}(\vec{v}.\vec{r})^2(\vec{\nabla}_r f)^2 e^{if\vec{v}.\vec{r}/2}. \qquad \text{(A1.8)}$$

We note that $\phi_j^B(\vec{r}_B)$ satisfy the equation

$$\left(-\frac{1}{2}\nabla_r^2 + V_{eB}\right)\phi_j^B(\vec{r}_0) = \varepsilon_j\,\phi_j^B(\vec{r}_B). \qquad \text{(A1.9)}$$

Using equations (A1.1), (A1.4) and equations (A1.6) to (A1.8) plus equation (A1.9) we obtain

$$H_{el} F_j^s(\vec{r},t) = \varepsilon_j F_j^s(\vec{r},t) + (V_{eA} + V_{AB}) F_j^s(\vec{r},t)$$

$$-\frac{i}{2} e^{-i(\varepsilon_j + \frac{1}{8}v^2)t} e^{if\vec{v}.\vec{r}/2} f \vec{v}.\vec{\nabla}_{\vec{r}} \phi_j^B(\vec{r}_B)$$

$$-\frac{i}{2} e^{-i(\varepsilon_j + \frac{1}{8}v^2)t} e^{if\vec{v}.\vec{r}/2} (\vec{v}.\vec{r})(\vec{\nabla}_{\vec{r}} f).\vec{\nabla}_{\vec{r}} \phi_j^B(\vec{r}_B)$$

$$-\frac{i}{2}(\vec{v}.\vec{\nabla}_{\vec{r}} f) F_j^s(\vec{r},t) - \frac{i}{4}(\vec{v}.\vec{r})(\nabla^2 f) F_j^s(\vec{r},t)$$

$$+\frac{1}{8}v^2 f^2 F_j^s(\vec{r},t) + \frac{1}{4} f(\vec{v}.\vec{r})(\vec{v}.\vec{\nabla}_{\vec{r}} f) F_j^s(\vec{r},t)$$

$$+\frac{1}{8}(\vec{v}.\vec{r})^2 (\vec{\nabla}_{\vec{r}} f)^2 F_j^s(\vec{r},t). \qquad \text{(A1.10)}$$

In a similar fashion we obtain

$$H_{el} G_k^s(\vec{r},t) = \eta_k G_k^s(\vec{r},t) + (V_{eB} + V_{AB}) G_k^s(\vec{r},t)$$

$$-\frac{i}{2} e^{-i(\eta_k + \frac{1}{8}v^2)t} e^{if\vec{v}.\vec{r}/2} f \vec{v}.\vec{\nabla}_{\vec{r}} \chi_k^A(\vec{r}_A)$$

$$-\frac{i}{2} e^{-i(\eta_k + \frac{1}{8}v^2)t} e^{if\vec{v}.\vec{r}/2} (\vec{v}.\vec{r})(\vec{\nabla}_{\vec{r}} f).\vec{\nabla}_{\vec{r}} \chi_k^A(\vec{r}_A)$$

$$-\frac{i}{2}(\vec{v}.\vec{\nabla}_{\vec{r}} f) G_k^s(\vec{r},t) - \frac{i}{4}(\vec{v}.\vec{r})(\nabla_{\vec{r}}^2 f) G_k^s(\vec{r},t)$$

$$+\frac{1}{8}v^2 f^2 G_k^s(\vec{r},t) + \frac{1}{4} f(\vec{v}.\vec{r})(\vec{v}.\vec{\nabla}_{\vec{r}} f) G_k^s(\vec{r},t)$$

$$+\frac{1}{8}(\vec{v}.\vec{r})^2 (\vec{\nabla}_{\vec{r}} f)^2 G_k^s(\vec{r},t). \qquad \text{(A1.11)}$$

Expressions for $(-i\partial/\partial t]_{\vec{r}})F_j^s(\vec{r},t)$ and $(-i\partial/\partial t]_{\vec{r}})G_k^s(\vec{r},t)$.

We have

$$\frac{\partial}{\partial t}\Big]_{\vec{r}} F_j^s(\vec{r},t) = \frac{\partial}{\partial t}\Big]_{\vec{r}} \left\{ \phi_j^B(\vec{r}_B) e^{-i(\varepsilon_j + \frac{1}{8}v^2)t} e^{if\vec{v}.\vec{r}/2} \right\} \tag{A1.12}$$

$$= \phi_j^B(\vec{r}_B) e^{if\vec{v}.\vec{r}/2} \frac{\partial}{\partial t}\Big]_{\vec{r}} e^{-i(\varepsilon_j + \frac{1}{8}v^2)t}$$

$$+ \phi_j^B(\vec{r}_B) e^{-i(\varepsilon_j + \frac{1}{8}v^2)t} \frac{\partial}{\partial t}\Big]_{\vec{r}} e^{if\vec{v}.\vec{r}/2}$$

$$+ e^{-i(\varepsilon_j + \frac{1}{8}v^2)t} e^{if\vec{v}.\vec{r}/2} \frac{\partial}{\partial t}\Big]_{\vec{r}} \phi_j^B(\vec{r}_B). \tag{A1.13}$$

Now

$$\frac{\partial}{\partial t}\Big]_{\vec{r}} e^{-i(\varepsilon_j + \frac{1}{8}v^2)t} = -i\left\{ \varepsilon_j + \frac{1}{8}\left[v^2 + t\frac{d(v^2)}{dt} \right] \right\} e^{-i(\varepsilon_j + \frac{1}{8}v^2)t}, \tag{A1.14}$$

$$\frac{\partial}{\partial t}\Big]_{\vec{r}} e^{if\vec{v}.\vec{r}/2} = \frac{i}{2}\left\{ (\vec{v}.\vec{r}) \frac{\partial}{\partial t}\Big]_{\vec{r}} f(\vec{r},\vec{R}(t)) + f\vec{r}.\frac{d\vec{v}}{dt} \right\} e^{if\vec{v}.\vec{r}/2} \tag{A1.15}$$

and

$$\frac{\partial}{\partial t}\Big]_{\vec{r}} \phi_j^B(\vec{r}_B) = \frac{\partial}{\partial t}\Big]_{\vec{r}_0} \phi_j^B(\vec{r}_0) + \frac{\partial \vec{r}_B}{\partial t}.\vec{\nabla}_{\vec{r}_B} \phi_j^B(\vec{r}_B) \tag{A1.16}$$

$$= \frac{\partial}{\partial t}\Big]_{\vec{r}_B} \phi_j^B(\vec{r}_B) + \frac{1}{2}\vec{v}.\vec{\nabla}_{\vec{r}} \phi_j^B(\vec{r}_B) \tag{A1.17}$$

as

$$\vec{r}_B = \vec{r} + \frac{1}{2}\vec{R}(t) \tag{A1.18}$$

and putting

$$\vec{\nabla}_{\vec{r}} \equiv \vec{\nabla}_{\vec{r}_B}. \tag{A1.19}$$

Using the results of the previous page we find

$$-i\left.\frac{\partial}{\partial t}\right]_{\vec{r}} F_j^s(\vec{r},t) = -\left\{\varepsilon_j + \frac{1}{8}\left[v^2 + t\,\frac{d(v^2)}{dt}\right]\right\} F_j^s(\vec{r},t)$$

$$+\frac{1}{2}(\vec{v}.\vec{r})\left\{\left.\frac{\partial}{\partial t}\right]_{\vec{r}} f(\vec{r},\vec{R})\right\} F_j^s(\vec{r},t) + \frac{1}{2} f\,\vec{r}.\frac{d\vec{v}}{dt}\,F_j^s(\vec{r},t)$$

$$-\frac{i}{2}\,e^{-i(\varepsilon_j+\frac{1}{8}v^2)t}\,e^{if\vec{v}.\vec{r}/2}\,\vec{v}.\vec{\nabla}_{\vec{r}}\,\phi_j^B(\vec{r}_B). \qquad \text{(A1.20)}$$

Similarly, using

$$\left.\frac{\partial}{\partial t}\right]_{\vec{r}} X_k^A(\vec{r}_A) = \left.\frac{\partial}{\partial t}\right]_{\vec{r}_A} X_k^A(\vec{r}_A) - \frac{1}{2}\vec{v}.\vec{\nabla}_{\vec{r}}\,X_k^A(\vec{r}_A) \qquad \text{(A1.21)}$$

we find

$$-i\left.\frac{\partial}{\partial t}\right]_{\vec{r}} G_k^s(\vec{r},t) = -\left\{\eta_k + \frac{1}{8}\left[v^2 + t\,\frac{d(v^2)}{dt}\right]\right\} G_k^s(\vec{r},t)$$

$$+\frac{1}{2}(\vec{v}.\vec{r})\left\{\left.\frac{\partial}{\partial t}\right]_{\vec{r}} f(\vec{r},\vec{R})\right\} G_k^s(\vec{r},t) + \frac{1}{2} f\,\vec{r}.\frac{d\vec{v}}{dt}\,G_k^s(\vec{r},t)$$

$$+\frac{i}{2}\,e^{-i(\eta_k+\frac{1}{8}v^2)t}\,e^{if\vec{v}.\vec{r}/2}\,\vec{v}.\vec{\nabla}_{\vec{r}}\,X_k^A(\vec{r}_A). \qquad \text{(A1.22)}$$

APPENDIX A2

Derivation of the integral identity used in simplifying the matrix element expressions

We define the integral I_1, where I_1 is given by

$$I_1 = \int_v \Phi^*(\vec{r})\,\vec{\nabla} f(\vec{r}).\vec{\nabla}\Psi(\vec{r})\,d\vec{r}\ , \qquad \text{(A2.1)}$$

where the integration is over all space.

The functions $\Phi(\vec{r})$ and $\Psi(\vec{r})$ are complex functions which tend asymptotically to zero as $r \to \infty$. The function $f(\vec{r})$ is real.

Integrating I_1 by parts

$$I_1 = \left[\Phi^*(\vec{r}) f(\vec{r}) \vec{\nabla}\Psi(\vec{r})\right]_{\substack{\text{all}\\ \text{space}}} - \int_v f(\vec{r})\vec{\nabla}\Phi^*(\vec{r}).\vec{\nabla}\Psi(\vec{r})\,d\vec{r} - \int_v \Phi^*(\vec{r}) f(\vec{r}) \nabla^2\Psi(\vec{r})\,d\vec{r}. \qquad \text{(A2.2)}$$

As $\Phi(\vec{r})$ and $\Psi(\vec{r})$ tend to zero as $r \to \infty$, the first term in square brackets of equation (A2.2) is zero. Thus we have

$$I_1 = -\int_v f(\vec{r})\vec{\nabla}\Phi^*(\vec{r}).\vec{\nabla}\Psi(\vec{r})\,d\vec{r} - \int_v \Phi^*(\vec{r}) f(\vec{r}) \nabla^2\Psi(\vec{r})\,d\vec{r}. \qquad \text{(A2.3)}$$

We define next the integral I_2.

$$I_2 = \int_v f(\vec{r})\vec{\nabla}\Phi^*(\vec{r}).\vec{\nabla}\Psi(\vec{r})\,d\vec{r}. \qquad \text{(A2.4)}$$

Integrating I_2 by parts and ignoring the first term as we did for I_1, we obtain

$$I_2 = -\int_v \Psi(\vec{r})\vec{\nabla}f(\vec{r}).\vec{\nabla}\Phi^*(\vec{r})\,d\vec{r} - \int_v \Psi(\vec{r})f(\vec{r})\nabla^2\Phi^*(\vec{r})\,d\vec{r}. \qquad \text{(A2.5)}$$

We see from equations (A2.3) and (A2.4) that

$$I_1 = -I_2 - \int_v \Phi^*(\vec{r})f(\vec{r})\nabla^2\Psi(\vec{r})\,d\vec{r}. \qquad \text{(A2.6)}$$

Substituting for I_2 from equation (A2.5) we obtain

$$I_1 = \int_v \Psi(\vec{r})\vec{\nabla}f(\vec{r}).\vec{\nabla}\Phi^*(\vec{r})\,d\vec{r} + \int_v \Psi(\vec{r})f(\vec{r})\nabla^2\Phi^*(\vec{r})\,d\vec{r} - \int_v \Phi^*(\vec{r})f(\vec{r})\nabla^2\Psi(\vec{r})\,d\vec{r}. \qquad \text{(A2.7)}$$

We define the integral I_3

$$I_3 = \int_v \Psi(\vec{r})\vec{\nabla}f(\vec{r}).\vec{\nabla}\Phi^*(\vec{r})\,d\vec{r} \qquad \text{(A2.8)}$$

and integrate I_3 by parts, ignore the first term and we have

$$I_3 = -\int_v \Phi^*(\vec{r})\vec{\nabla}f(\vec{r}).\vec{\nabla}\Psi(\vec{r})\,d\vec{r} - \int_v \Phi^*(\vec{r})\Psi(\vec{r})\nabla^2 f(\vec{r})\,d\vec{r}. \qquad \text{(A2.9)}$$

If we examine equation (A2.7) we see that I_3 is the first term in the expression and so substituting for I_3 from equation (A2.9) we obtain

$$I_1 = -\int_v \Phi^*(\vec{r})\vec{\nabla}f(\vec{r}).\vec{\nabla}\Psi(\vec{r})\,d\vec{r}$$

$$-\int_v \Phi^*(\vec{r})\Psi(\vec{r})\nabla^2 f(\vec{r})\,d\vec{r}$$

$$+\int_v \Psi(\vec{r})f(\vec{r})\nabla^2\Phi^*(\vec{r})\,d\vec{r}$$

$$-\int_v \Phi^*(\vec{r})f(\vec{r})\nabla^2\Psi(\vec{r})\,d\vec{r}. \qquad \text{(A2.10)}$$

The first term in equation (A2.10) is I_1 (from equation (A2.1)) and so transferring this to the left hand side of equation (A2.10) we obtain

$$2I_1 = -\int_v \Phi^*(\vec{r})\Psi(\vec{r})\nabla^2 f(\vec{r})\,d\vec{r}$$

$$+\int_v \Psi(\vec{r})f(\vec{r})\nabla^2\Phi^*(\vec{r})\,d\vec{r}$$

$$-\int_v \Phi^*(\vec{r})f(\vec{r})\nabla^2\Psi(\vec{r})\,d\vec{r}. \qquad \text{(A2.11)}$$

Substituting the expression for I_1 given by equation (A2.1) in equation (A2.11) and rearranging slightly we obtain the final result

$$2\int_v \Phi^*(\vec{r})\vec{\nabla}f(\vec{r}).\vec{\nabla}\Psi(\vec{r})\,d\vec{r} + \int_v \Phi^*(\vec{r})\left\{\nabla^2 f(\vec{r})\right\}\Psi(\vec{r})\,d\vec{r}$$

$$= \int_v \left\{\nabla^2\Phi^*(\vec{r})\right\}f(\vec{r})\Psi(\vec{r})\,d\vec{r} - \int_v \Phi^*(\vec{r})f(\vec{r})\nabla^2\Psi(\vec{r})\,d\vec{r}, \qquad \text{(A2.12)}$$

where the ∇^2 operator acts only upon the function to its right. This is indicated by the curly brackets.

The relation of equation (A2.12) is equivalent to

$$\left[f(\vec{r}), H_{el}\right] = \frac{1}{2}\nabla_{\vec{r}}^2 f(\vec{r}) + \vec{\nabla}_{\vec{r}} f(\vec{r}).\vec{\nabla}_{\vec{r}} \qquad \text{(A2.13)}$$

where H_{el} is the electronic Hamiltonian given by equation (3.3.2) of Chapter 3. The expression of equation (A2.13) was noted by Taulbjerg et al. (1975).

APPENDIX A3

An expression for the space-fixed real spherical harmonics in terms of body-fixed real spherical harmonics

We begin with the expression for space-fixed spherical harmonics $Y^{SF}_{\ell m}(\theta,\phi)$ in terms of body-fixed spherical harmonics $Y^{BF}_{\ell m}(\theta',\phi')$.

$$Y^{SF}_{\ell m}(\theta,\phi)=\sum_{m'=-\ell}^{m'=\ell} D^{\ell}_{m'm}(\alpha,\beta,0)\,Y^{BF}_{\ell m'}(\theta',\phi'). \qquad (A3.1)$$

For the system with which we are concerned

$$\alpha=0 \qquad \text{and} \qquad \beta=\frac{\pi}{2}+\delta \qquad (A3.2)$$

where δ is the angle between the internuclear vector $\vec{R}$ and the (space-fixed) x-axis (see figure 4.2, Chapter 4). We thus have

$$Y^{SF}_{\ell m}(\theta,\phi)=\sum_{m'=-\ell}^{m'=\ell} D^{\ell}_{m'm}(0,\beta,0)\,Y^{BF}_{\ell m'}(\theta',\phi'). \qquad (A3.3)$$

The general rotation matrix elements $D^{\ell}_{m'm}(\alpha,\beta,\gamma)$ may be written in terms of Wigner simplified rotation matrix elements, (also known as Wigner reduced rotation matrix elements) $d^{\ell}_{m'm}(\beta)$, (Rose, 1957),

$$D^{\ell}_{m'm}(\alpha,\beta,\gamma)=e^{-im'\alpha}\,d^{\ell}_{m'm}(\beta)\,e^{-im\gamma}. \qquad (A3.4)$$

We see, therefore, that equation (A3.3) may be written

$$Y^{SF}_{\ell m}(\theta,\phi)=\sum_{m'=-\ell}^{m'=\ell} d^{\ell}_{m'm}(\beta)\,Y^{BF}_{\ell m'}(\theta',\phi'). \qquad (A3.5)$$

From now on the angular arguments of the spherical harmonics will be omitted. Splitting the summation in equation (A3.5) we have

$$Y^{SF}_{\ell m} = \sum_{m'=-\ell}^{m'=-1} d^{\ell}_{m'm}(\beta) Y^{BF}_{\ell m'} + \sum_{m'=0}^{m'=\ell} d^{\ell}_{m'm}(\beta) Y^{BF}_{\ell m'} . \qquad (A3.6)$$

Using the relations

$$d^{\ell}_{m'm} = (-1)^{m'} d^{\ell}_{-m'm} , \qquad (A3.7)$$

and

$$Y_{\ell,-m} = (-1)^{m} Y^{*}_{\ell m} , \qquad (A3.8)$$

the first summation in equation (A3.6) over negative m' indices may be replaced by one over positive m' indices and hence equation (A3.6) becomes

$$Y^{SF}_{\ell m} = \sum_{m'=1}^{m'=\ell} d^{\ell}_{m'm}(\beta) Y^{BF\,*}_{\ell m'} + \sum_{m'=0}^{m'=\ell} d^{\ell}_{m'm}(\beta) Y^{BF}_{\ell m'} . \qquad (A3.9)$$

Using equation (A3.7) and re-arranging slightly we obtain from equation (A3.9)

$$Y^{SF}_{\ell m} = d^{\ell}_{0m}(\beta) Y^{BF}_{\ell 0} + \sum_{m'=1}^{m'=\ell} \left[d^{\ell}_{m'm}(\beta) Y^{BF}_{\ell m'} + (-1)^{m'} d^{\ell}_{-m'm}(\beta) Y^{BF\,*}_{\ell m'} \right] . \qquad (A3.10)$$

Hence, taking the complex conjugate, equation (A3.10) yields

$$Y^{SF\,*}_{\ell m} = d^{\ell}_{0m}(\beta) Y^{BF\,*}_{\ell 0} + \sum_{m'=1}^{m'=\ell} \left[(-1)^{m'} d^{\ell}_{-m'm}(\beta) Y^{BF}_{\ell m'} + d^{\ell}_{m'm}(\beta) Y^{BF\,*}_{\ell m'} \right] . \qquad (A3.11)$$

The real spherical harmonics, in the space-fixed frame, are given by

$$\overline{Y}^{SF}_{\ell m} = N_m \left[Y^{SF}_{\ell m} + Y^{SF\,*}_{\ell m} \right] \qquad (A3.12)$$

where the N_m factors are defined by equations (4.2.6a) and (4.2.6b), (Chapter 4). Substituting for $Y^{SF}_{\ell m}$ and $Y^{SF\,*}_{\ell m}$ in equation (A3.12) and using the expression for the body-fixed real spherical harmonics given by

$$\bar{Y}^{BF}_{\ell m} = N_m \left[Y^{BF}_{\ell m} + Y^{BF\,*}_{\ell m} \right] \qquad \text{(A3.13)}$$

we obtain

$$\bar{Y}^{SF}_{\ell m} = \frac{N_m}{N_0} d^{\ell}_{0m}(\beta) \bar{Y}^{BF}_{\ell 0} + \sum_{m'=1}^{\ell} \frac{N_m}{N_{m'}} \left[d^{\ell}_{m'm}(\beta) + (-1)^{m'} d^{\ell}_{-m'm}(\beta) \right] \bar{Y}^{BF}_{\ell m'} . \qquad \text{(A3.14)}$$

This may be written in a more compact form as follows:-

$$\bar{Y}^{SF}_{\ell m} = \sum_{m'=0}^{\ell} \mathcal{D}^{\ell}_{m'm}(\beta) \bar{Y}^{BF}_{\ell m'} \qquad \text{(A3.15)}$$

where

$$\mathcal{D}^{\ell}_{m'm}(\beta) = \frac{N_m}{N_{m'}} \left[d^{\ell}_{m'm}(\beta) + (-1)^{m'} d^{\ell}_{-m'm}(\beta) \right] \frac{1}{\delta_{m'0} + 1} . \qquad \text{(A3.16)}$$

We have thus obtained an expression for the $\bar{Y}^{SF}_{\ell m}$ in terms of the $\bar{Y}^{BF}_{\ell m}$.

APPENDIX A4

An expression for the rotation angle δ for the Coulomb trajectory

In this appendix an expression will be derived for the angle δ for the case of the nuclear trajectories being Coulombic.

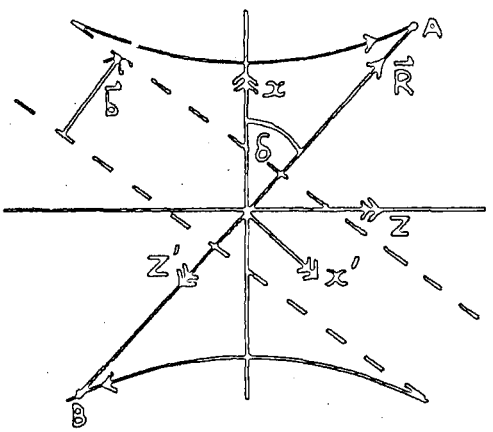

Figure A4.1
Diagram showing space-fixed and body-fixed frames and angle δ.

Figure A4.1 shows the angle δ. It is the angle between the x-axis (space-fixed) and the vector $\vec{R}$.

The initial relative velocity of the nuclei A and B is v_i and so by conservation of angular momentum we have

$$v_i b = R^2 \frac{d\delta}{dt} \qquad \text{(A4.1)}$$

where b is the modulus of the impact parameter vector $\vec{b}$ (Figure A4.1).

The parametric equations for the trajectory motion are

$$R = (\gamma^2 + b^2)^{1/2} \cosh w + \gamma \qquad \text{(A4.2)}$$

$$t = \frac{1}{v_i}\left[(\gamma^2 + b^2)^{1/2} \sinh w + \gamma w\right] . \qquad \text{(A4.3)}$$

We know that these may be re-written in terms of a new

parameter τ given by

$$\tau = (\gamma^2+b^2)^{1/2} \sinh w \qquad \text{(A4.4)}$$

and we thus have

$$R(\tau) = (\tau^2+\gamma^2+b^2)^{1/2} + \gamma \qquad \text{(A4.5)}$$

$$t(\tau) = \frac{1}{V_i}\left[\tau + \gamma \sinh^{-1}\frac{\tau}{(\gamma^2+b^2)^{1/2}}\right] . \qquad \text{(A4.6)}$$

Returning to equation (A4.1), we have

$$V_i b = R^2 \frac{d\delta}{d\tau}\cdot\frac{d\tau}{dt} \qquad \text{(A4.7)}$$

or

$$V_i b = R^2 \frac{d\delta}{d\tau}\cdot\frac{1}{T(\tau)} \qquad \text{(A4.8)}$$

where

$$T(\tau) = dt/d\tau . \qquad \text{(A4.9)}$$

From equation (A4.6) we find that $T(\tau)$ is given by

$$T(\tau) = \frac{1}{V_i}\left[1 + \frac{\gamma}{(\tau^2+\gamma^2+b^2)^{1/2}}\right] \qquad \text{(A4.10)}$$

and from (A4.5) this becomes

$$T(\tau) = \frac{R}{V_i(R-\gamma)} . \qquad \text{(A4.11)}$$

Substituting for $T(\tau)$ in equation (A4.8) and re-arranging we obtain an expression for $d\delta/d\tau$ which is

$$\frac{d\delta}{d\tau} = \frac{b}{R(R-\gamma)} . \qquad \text{(A4.12)}$$

We now proceed to integrate equation (A4.12). Substituting the expression for $R(\tau)$ in equation (A4.12) and setting

$$c^2 = \gamma^2+b^2 \qquad \text{(A4.13)}$$

we find

$$\frac{d\delta}{d\tau} = \frac{b}{\tau^2 + c^2 + \gamma(\tau^2 + c^2)^{1/2}} \quad . \tag{A4.14}$$

We know that when $\tau = 0$, $\delta = 0$ and so

$$\delta = b\int_0^{\tau} \frac{d\tau}{\tau^2 + c^2 + \gamma(\tau^2 + c^2)^{1/2}} \quad . \tag{A4.15}$$

Putting

$$\tau = c\sinh z \tag{A4.16}$$

the integral in equation (A4.15) transforms into

$$\delta = b\int_0^{z} \frac{dz}{c\cosh z + \gamma} \quad . \tag{A4.17}$$

This may be integrated using the half-angle method applied to hyperbolic integrals, that is, we put

$$t = \tanh\frac{z}{2} \quad . \tag{A4.18}$$

From equation (A4.18) we obtain

$$dz = \frac{2\,dt}{1 - t^2} \tag{A4.19}$$

and also

$$\cosh z = \frac{1 + t^2}{1 - t^2} \quad . \tag{A4.20}$$

Equation (A4.17) becomes

$$\delta = b\int_0^{t} \frac{2\,dt}{(c - \gamma)t^2 + c + \gamma} \quad , \quad (c > \gamma) \, . \tag{A4.21}$$

This may be integrated to yield

$$\delta = 2\tan^{-1}\left(\frac{c - \gamma}{c + \gamma}\right)^{1/2} t \quad , \tag{A4.22}$$

where use has been made of equation (A4.13). We need to find t in terms of τ . We know that

$$\sinh z = \frac{\tau}{c} \tag{A4.23}$$

and so

$$z = \sinh^{-1}\left(\frac{\tau}{c}\right) = \log_e \frac{\left[\tau + (\tau^2 + c^2)^{1/2}\right]}{\tau} \; . \tag{A4.24}$$

From equation (A4.18) we obtain

$$t = \tanh \frac{z}{2} = \frac{(\tau^2 + c^2)^{1/2} - c}{\tau} \tag{A4.25}$$

Substituting for t in equation (A4.22) and using equation (A4.13) we obtain the final expression

$$\delta = 2 \tan^{-1}\left\{ \frac{(\gamma^2 + b^2)^{1/2} - \gamma}{b} \cdot \frac{\left[(\tau^2 + \gamma^2 + b^2)^{1/2} - (\gamma^2 + b^2)^{1/2}\right]}{\tau} \right\} . \tag{A4.26}$$

APPENDIX A5

Expressions for quantities occurring in the body-fixed integrals in terms of the prolate spheroidal co-ordinates (ξ, η, ϕ)

Various quantities must be expressed in terms of (ξ, η, ϕ) co-ordinates in order to perform the integrals needed to calculate the matrix elements in the body-fixed frame. In this appendix expressions for these quantities will be obtained.

We begin by reminding ourselves of the definition of the (ξ, η, ϕ) co-ordinates

$$\xi = \frac{1}{R}(r_A + r_B), \quad 1 \leq \xi < \infty \tag{A5.1a}$$

$$\eta = \frac{1}{R}(r_A - r_B), \quad -1 \leq \eta \leq 1 \tag{A5.1b}$$

$$\phi \text{ (azimuthal angle)}, \quad 0 \leq \phi \leq 2\pi . \tag{A5.1c}$$

From equations (A5.1a) and (A5.1b) we have

$$r_A = \frac{R}{2}(\xi + \eta) , \tag{A5.2a}$$

$$r_B = \frac{R}{2}(\xi - \eta) . \tag{A5.2b}$$

Also it can be shown that

$$r_A^2 + r_B^2 = \frac{R^2}{2}(\xi^2 + \eta^2) , \tag{A5.3a}$$

$$r_A^2 - r_B^2 = R^2 \xi \eta , \tag{A5.3b}$$

and

$$r_A r_B = \frac{R^2}{4}(\xi^2 - \eta^2) . \tag{A5.3c}$$

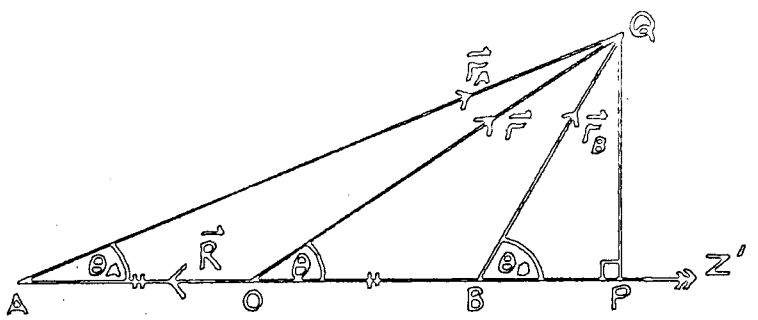

Figure A5.1
Figure required for calculation of quantities in (ξ, η, ϕ) co-ordinates.

Figure A5.1 shows the familiar electron capture co-ordinate system. The z'-axis is one of the body-fixed co-ordinates. We note the introduction of the angles θ_A, θ_B and θ. These are measured from the z'-axis.

Using the cosine rule for triangle AOQ we have

$$r_A^2 = r^2 + \frac{R^2}{4} + Rr\cos\theta \,, \qquad \text{(A5.4)}$$

and for triangle BOQ applying the cosine rule

$$r_B^2 = r^2 + \frac{R^2}{4} - Rr\cos\theta \,. \qquad \text{(A5.5)}$$

From equations (A5.4) and (A5.5) we find that

$$r_A^2 + r_B^2 = 2r^2 + \frac{R^2}{2} \qquad \text{(A5.6)}$$

and

$$r_A^2 - r_B^2 = 2Rr\cos\theta \,. \qquad \text{(A5.7)}$$

Comparing equation (A5.7) with equation (A5.3b) we find that

$$r\cos\theta = \frac{R}{2}\xi\eta \qquad \text{(A5.8)}$$

and comparing equation (A5.6) with equation (A5.3a) we find that

$$r = \frac{R}{2}(\xi^2+\eta^2-1)^{1/2} \,. \qquad \text{(A5.9)}$$

It follows immediately from equations (A5.8) and (A5.9) that

$$\cos\theta = \frac{\xi\eta}{(\xi^2+\eta^2-1)^{1/2}} \,. \qquad \text{(A5.10)}$$

Using the well-known relation

$$\sin^2\theta + \cos^2\theta = 1 \qquad \text{(A5.11)}$$

gives

$$\sin\theta = \frac{[(\xi^2-1)(1-\eta^2)]^{1/2}}{(\xi^2+\eta^2-1)^{1/2}} \,. \qquad \text{(A5.12)}$$

It follows from Figure A5.1 that

$$r\cos\theta = \frac{R}{2} + r_B\cos\theta_B \qquad \text{(A5.13)}$$

and

$$r_A\cos\theta_A = R + r_B\cos\theta_B \,. \qquad \text{(A5.14)}$$

Using equations (A5.2b) and (A5.8), equation (A5.13) gives

$$\cos\theta_B = \frac{\xi\eta-1}{\xi-\eta} \,. \qquad \text{(A5.15)}$$

From this

$$\sin\theta_B = \frac{\left[(\xi^2-1)(1-\eta^2)\right]^{1/2}}{\xi-\eta} \quad . \tag{A5.16}$$

In a similar manner equation (A5.14) may be used to give

$$\cos\theta_A = \frac{\xi\eta+1}{\xi+\eta} \tag{A5.17}$$

which gives in turn

$$\sin\theta_A = \frac{\left[(\xi^2-1)(1-\eta^2)\right]^{1/2}}{\xi+\eta} \quad . \tag{A5.18}$$

Drawing together the results of this analysis we have

$$r = \frac{R}{2}(\xi^2+\eta^2-1)^{1/2} \quad , \tag{A5.19a}$$

$$r\cos\theta = \frac{R}{2}\xi\eta \quad , \tag{A5.19b}$$

$$\sin\theta = \frac{\left[(\xi^2-1)(1-\eta^2)\right]^{1/2}}{(\xi^2+\eta^2-1)^{1/2}} \quad , \tag{A5.19c}$$

and

$$\cos\theta = \frac{\xi\eta}{(\xi^2+\eta^2-1)^{1/2}} \quad . \tag{A5.19d}$$

$$r_A = \frac{R}{2}(\xi+\eta) \quad , \tag{A5.20a}$$

$$\sin\theta_A = \frac{\left[(\xi^2-1)(1-\eta^2)\right]^{1/2}}{\xi+\eta} \quad , \tag{A5.20b}$$

and

$$\cos\theta_A = \frac{\xi\eta+1}{\xi+\eta} \quad . \tag{A5.20c}$$

$$r_B = \frac{R}{2}(\xi-\eta) \quad , \tag{A5.21a}$$

$$\sin\theta_B = \frac{\left[(\xi^2-1)(1-\eta^2)\right]^{1/2}}{\xi-\eta} \quad , \tag{A5.21b}$$

and

$$\cos\theta_B = \frac{\xi\eta-1}{\xi-\eta} \quad . \tag{A5.21c}$$

This concludes this appendix.

APPENDIX A6

Azimuthal angular integrals

In this appendix a prescription will be presented for determining the azimuthal integrals required in the integration of the matrix elements.

The integrals are

$$ {}^{\phi}I_1(m_1,m_2)=\int_0^{2\pi} \cos m_1\phi \cos m_2\phi \, d\phi , \qquad (A6.1) $$

$$ {}^{\phi}I_2(m_1,m_2)=\int_0^{2\pi} \cos m_1\phi \cos m_2\phi \cos\phi \, d\phi , \qquad (A6.2) $$

$$ {}^{\phi}I_3(m_1,m_2)=\int_0^{2\pi} \cos m_1\phi \cos m_2\phi \cos^2\phi \, d\phi . \qquad (A6.3) $$

The ${}^{\phi}I_1$ -integral is a standard integral and will be used in the analysis upon the other two integrals ${}^{\phi}I_2$ and ${}^{\phi}I_3$. It is given by (Gröbner and Hofreiter, 1961)

$$ {}^{\phi}I_1=\begin{cases} 0 & \text{for } m_1\neq m_2 \\ \pi & \text{for } m_1=m_2\neq 0 \\ 2\pi & \text{for } m_1=m_2=0 . \end{cases} \qquad (A6.4) $$

To find an expression for ${}^{\phi}I_2$ we begin with the well-known formula

$$ \cos A\cos B=\tfrac{1}{2}\left[\cos(A+B)+\cos(A-B)\right] . \qquad (A6.5) $$

Setting $A=m_1\phi$ and $B=\phi$ yields

$$ \cos m_1\phi\cos\phi=\tfrac{1}{2}\left[\cos(m_1+1)\phi+\cos(m_1-1)\phi\right] $$

$$ =\tfrac{1}{2}\left[\cos(m_1+1)\phi+\cos|m_1-1|\phi\right] . \qquad (A6.6) $$

Using this result the integral ${}^{\phi}I_2$, equation (A6.2), becomes

$$^{\phi}I_2 = \frac{1}{2}\int_0^{2\pi} \cos(m_1+1)\phi \cos m_2\phi \, d\phi + \frac{1}{2}\int_0^{2\pi} \cos|m_1-1|\phi \cos m_2\phi \, d\phi \, . \tag{A6.7}$$

Denoting the integrals in equation (A6.7) as follows:-

$$^{\phi}J_1 = \int_0^{2\pi} \cos(m_1+1)\phi \cos m_2\phi \, d\phi \tag{A6.8a}$$

$$^{\phi}J_2 = \int_0^{2\pi} \cos|m_1-1|\phi \cos m_2\phi \, d\phi \tag{A6.8b}$$

we have

$$^{\phi}I_2 = \frac{1}{2}\left(^{\phi}J_1 + {}^{\phi}J_2\right) \tag{A6.9}$$

where

$$^{\phi}J_1 = \begin{cases} 0 & \text{for } m_1+1 \neq m_2 \\ \pi & \text{for } m_1+1 = m_2 \neq 0 \\ 2\pi & \text{for } m_1+1 = m_2 = 0 \end{cases} \tag{A6.10}$$

and

$$^{\phi}J_2 = \begin{cases} 0 & \text{for } |m_1-1| \neq m_2 \\ \pi & \text{for } |m_1-1| = m_2 \neq 0 \\ 2\pi & \text{for } |m_1-1| = m_2 = 0 \, , \end{cases} \tag{A6.11}$$

The expression for $^{\phi}I_3$ is found by using the formula

$$\cos^2\phi = \frac{1}{2}(1+\cos 2\phi) \, . \tag{A6.12}$$

Substituting for $\cos^2\phi$ in equation (A6.3) we obtain

$$^{\phi}I_3 = \frac{1}{2}\left(^{\phi}I_1 + {}^{\phi}K\right) \tag{A6.13}$$

where

$$^{\phi}K = \int_0^{2\pi} \cos m_1\phi \cos m_2\phi \cos 2\phi \, d\phi \, . \tag{A6.14}$$

Using the formula of equation (A6.5), setting $A = m_1\phi$ and $B = 2\phi$ we obtain

$$^{\phi}K = \frac{1}{2}\int_0^{2\pi} \cos(m_1+2)\phi \cos m_2\phi \, d\phi + \frac{1}{2}\int_0^{2\pi} \cos|m_1-2|\phi \cos m_2\phi \, d\phi . \quad \text{(A6.15)}$$

Thus denoting the integrals in equation (A6.15) as follows:-

$$^{\phi}K_1 = \int_0^{2\pi} \cos(m_1+2)\phi \cos m_2\phi \, d\phi \quad \text{(A6.16a)}$$

$$^{\phi}K_2 = \int_0^{2\pi} \cos|m_1-2|\phi \cos m_2\phi \, d\phi \quad \text{(A6.16b)}$$

we have

$$^{\phi}K = \frac{1}{2}(^{\phi}K_1 + {}^{\phi}K_2) \quad \text{(A6.17)}$$

and so

$$^{\phi}I_3 = \frac{1}{4}(2\,{}^{\phi}I_1 + {}^{\phi}K_1 + {}^{\phi}K_2) \quad \text{(A6.18)}$$

where

$$^{\phi}K_1 = \begin{cases} 0 & \text{for } m_1+2 \neq m_2 \\ \pi & \text{for } m_1+2 = m_2 \neq 0 \\ 2\pi & \text{for } m_1+2 = m_2 = 0 \end{cases} \quad \text{(A6.19)}$$

and

$$^{\phi}K_2 = \begin{cases} 0 & \text{for } |m_1-2| \neq m_2 \\ \pi & \text{for } |m_1-2| = m_2 \neq 0 \\ 2\pi & \text{for } |m_1-2| = m_2 = 0 \end{cases} . \quad \text{(A6.20)}$$

APPENDIX A7

Associated Legendre functions in terms of prolate spheroidal co-ordinates

Associated Legendre functions $P_\ell^m(x)$ are solutions of the associated Legendre equation which is

$$(1-x^2)v'' - 2xv' + \left[\ell(\ell+1) - \frac{m^2}{1-x^2}\right]v = 0 \qquad \text{(A7.1)}$$

where $$v \equiv P_\ell^m(x) \qquad \text{(A7.2)}$$

and $$x \equiv \cos\theta \,. \qquad \text{(A7.3)}$$

(Section 12.5, Arfken, 1970).

The associated Legendre functions are (up to $\ell = 2$)

$$P_0^0(x) = 1 \qquad \text{(A7.4)}$$

$$P_1^0(x) = x = \cos\theta \qquad \text{(A7.5a)}$$

$$P_1^1(x) = (1-x^2)^{1/2} = \sin\theta \qquad \text{(A7.5b)}$$

$$P_2^0(x) = (3x^2-1)/2 = (3\cos^2\theta - 1)/2 \qquad \text{(A7.6a)}$$

$$P_2^1(x) = 3x(1-x^2)^{1/2} = 3\sin\theta\cos\theta \qquad \text{(A7.6b)}$$

$$P_2^2(x) = 3(1-x^2) = 3\sin^2\theta \,. \qquad \text{(A7.6c)}$$

Using the expressions for $\sin\theta_A$, $\cos\theta_A$, $\sin\theta_B$ and $\cos\theta_B$ derived in Appendix A5, equations, (A5.20b), (A5.20c), (A5.21b) and (A5.21c), we obtain the following expressions for the associated Legendre functions $P^{(m-o)_i}_{(\ell_A)_k}(\cos\theta_A)$ and $P^{(m-o)_j}_{(\ell_B)_j}(\cos\theta_B)$ for values of $(\ell_A)_k$ and $(\ell_B)_j$ up to and including 2.

1. $P^{(m_A)_k}_{(\ell_A)_k}(\cos\theta_A)$

$$P^0_0(\cos\theta_A) = 1 \tag{A7.7}$$

$$P^0_1(\cos\theta_A) = \frac{\xi\eta+1}{\xi+\eta} \tag{A7.8a}$$

$$P^1_1(\cos\theta_A) = \frac{\left[(\xi^2-1)(1-\eta^2)\right]^{1/2}}{\xi+\eta} \tag{A7.8b}$$

$$P^0_2(\cos\theta_A) = \frac{1}{2}\left[\frac{3(\xi\eta+1)^2-(\xi+\eta)^2}{(\xi+\eta)^2}\right] \tag{A7.9a}$$

$$P^1_2(\cos\theta_A) = \frac{3(\xi\eta+1)\left[(\xi^2-1)(1-\eta^2)\right]^{1/2}}{(\xi+\eta)^2} \tag{A7.9b}$$

$$P^2_2(\cos\theta_A) = \frac{3(\xi^2-1)(1-\eta^2)}{(\xi+\eta)^2} \tag{A7.9c}$$

2. $P^{(m_B)_j}_{(\ell_B)_i}(\cos\theta_B)$

$$P^0_0(\cos\theta_B) = 1 \tag{A7.10}$$

$$P^0_1(\cos\theta_B) = \frac{\xi\eta-1}{\xi-\eta} \tag{A7.11a}$$

$$P^1_1(\cos\theta_B) = \frac{\left[(\xi^2-1)(1-\eta^2)\right]^{1/2}}{\xi-\eta} \tag{A7.11b}$$

$$P^0_2(\cos\theta_B) = \frac{1}{2}\left[\frac{3(\xi\eta-1)^2-(\xi-\eta)^2}{(\xi-\eta)^2}\right] \tag{A7.12a}$$

$$P^1_2(\cos\theta_B) = \frac{3(\xi\eta-1)\left[(\xi^2-1)(1-\eta^2)\right]^{1/2}}{(\xi-\eta)^2} \tag{A7.12b}$$

$$P^2_2(\cos\theta_B) = \frac{3(\xi^2-1)(1-\eta^2)}{(\xi-\eta)^2} \tag{A7.12c}$$

APPENDIX A8

A8.1 Expressions for the BA-, BB- and AA- type matrix elements in terms of Ω -triple integrals

All the expressions given are for when the "simple" switching function f_s is used where f_s is given by

$$f_s = -\frac{R^2}{R^2+\rho^2}\eta \,. \tag{A8.1}$$

We have $$F(R) = R^2/(R^2+\rho^2) \,. \tag{A8.2}$$

1. BA- type elements

$$N_{jk}^{BA} = \langle \phi_j^B(\vec{r}_B) | \chi_k^A(\vec{r}_A) \rangle \,, \tag{A8.3}$$

$$N_{jk}^{BA} = \beta_j \alpha_k \frac{R^3}{8}\left[{}^{A}_{\Omega}I_{jk}^{BA}(2,0) - {}^{A}_{\Omega}I_{jk}^{BA}(0,2)\right] \,. \tag{A8.4}$$

$$A_{jk}^{BA} = \langle \phi_j^B(\vec{r}_B) | V_{eB} | \chi_k^A(\vec{r}_A) \rangle \,, \tag{A8.5}$$

$$A_{jk}^{BA} = -Z_B \beta_j \alpha_k \frac{R^2}{4}\left[{}^{A}_{\Omega}I_{jk}^{BA}(1,0) + {}^{A}_{\Omega}I_{jk}^{BA}(0,1)\right] \,. \tag{A8.6}$$

$$G_{jk}^{BA} = \langle \phi_j^B(\vec{r}_B) | f_s^2 | \chi_k^A(\vec{r}_A) \rangle \,, \tag{A8.7}$$

$$G_{jk}^{BA} = \beta_j \alpha_k \frac{R^2[F(R)]^2}{8}\left[{}^{A}_{\Omega}I_{jk}^{BA}(2,2) - {}^{A}_{\Omega}I_{jk}^{BA}(0,4)\right] \,. \tag{A8.8}$$

$$H_{jk}^{BA} = \langle \phi_j^B(\vec{r}_B) | f_s(\vec{v}.\vec{r})\vec{v}.\vec{\nabla}_i f_s | \chi_k^A(\vec{r}_A) \rangle \,, \tag{A8.9}$$

$$\begin{aligned} H_{jk}^{BA} = {} & \beta_j \alpha_k \frac{[F(R)]^2 R}{32}\left[\frac{d(R^2)}{dt}\right]^2\left[{}^{A}_{\Omega}I_{jk}^{BA}(2,2) - {}^{A}_{\Omega}I_{jk}^{BA}(2,4)\right] \\ & + \beta_j \alpha_k \frac{[F(R)]^2 R}{8}\cdot\frac{d(R^2)}{dt}\cdot b V_i\left[{}^{B}_{\Omega}I_{jk}^{BA}(1,3) - \tfrac{1}{2}\,{}^{B}_{\Omega}I_{jk}^{BA}(1,1)\right] \\ & + \beta_j \alpha_k \frac{[F(R)]^2 R}{8}\cdot b^2 V_i^2\left[{}^{C}_{\Omega}I_{jk}^{BA}(2,4) - {}^{C}_{\Omega}I_{jk}^{BA}(2,2)\right. \\ & \left. + {}^{C}_{\Omega}I_{jk}^{BA}(0,2) - {}^{C}_{\Omega}I_{jk}^{BA}(0,4)\right] . \end{aligned} \tag{A8.10}$$

$$K_{jk}^{BA} = \langle \phi_j^B(\vec{r}_B) | (\vec{v}.\vec{F}) \left\{ \frac{\partial}{\partial t} \right\} f_s | \chi_k^A(\vec{r}_A) \rangle \,, \tag{A8.11}$$

$$K_{jk}^{BA} = \beta_j \alpha_k \frac{R^2 F'(R)}{64} \left[\frac{d(R^2)}{dt} \right]^2 \left[{}^{A}_{\Omega}I_{jk}^{BA}(3,2) - {}^{A}_{\Omega}I_{jk}^{BA}(1,4) \right]$$

$$+ \beta_j \alpha_k \frac{R F(R)}{64} \left[\frac{d(R^2)}{dt} \right]^2 \left[{}^{A}_{\Omega}I_{jk}^{BA}(1,4) - {}^{A}_{\Omega}I_{jk}^{BA}(1,2) \right]$$

$$+ \beta_j \alpha_k \frac{R^2 F'(R)}{32} . \frac{d(R^2)}{dt} . b v_i \left[{}^{B}_{\Omega}I_{jk}^{BA}(0,3) - {}^{B}_{\Omega}I_{jk}^{BA}(2,1) \right]$$

$$+ \beta_j \alpha_k \frac{R F(R)}{32} . \frac{d(R^2)}{dt} . b v_i \left[{}^{B}_{\Omega}I_{jk}^{BA}(0,1) - {}^{B}_{\Omega}I_{jk}^{BA}(0,3) - {}^{B}_{\Omega}I_{jk}^{BA}(2,1) \right]$$

$$+ \beta_j \alpha_k \frac{R F(R)}{16} . b^2 v_i^2 \left[{}^{C}_{\Omega}I_{jk}^{BA}(3,0) - {}^{C}_{\Omega}I_{jk}^{BA}(1,0) - {}^{C}_{\Omega}I_{jk}^{BA}(3,2) + {}^{C}_{\Omega}I_{jk}^{BA}(1,2) \right] . \tag{A8.12}$$

$$\Lambda_{jk}^{BA} = \langle \phi_j^B(\vec{r}_B) | f_s \vec{F} . \frac{d\vec{v}}{dt} | \chi_k^A(\vec{r}_A) \rangle \,, \tag{A8.13}$$

$$\Lambda_{jk}^{BA} = \beta_j \alpha_k \frac{R F(R)}{16} . \left(R^3 \frac{d^2 R}{dt^2} - b^2 v_i^2 \right) \left[{}^{A}_{\Omega}I_{jk}^{BA}(3,2) - {}^{A}_{\Omega}I_{jk}^{BA}(1,4) \right] . \tag{A8.14}$$

$$\bar{A}_{jk}^{BA} = \langle \phi_j^B(\vec{r}_B) | V_{cA} | \chi_k^A(\vec{r}_A) \rangle \,, \tag{A8.15}$$

$$\bar{A}_{jk}^{BA} = - Z_A \beta_j \alpha_k \frac{R^2}{4} \left[{}^{A}_{\Omega}I_{jk}^{BA}(1,0) - {}^{A}_{\Omega}I_{jk}^{BA}(0,1) \right] . \tag{A8.16}$$

$$V_{jk}^{BA} = \langle \phi_j^B(\vec{r}_B) | f_s (\vec{v}.\vec{F}) V_{cB} | \chi_k^A(\vec{r}_A) \rangle \,, \tag{A8.17}$$

$$V_{jk}^{BA} = - \beta_j \alpha_k Z_B \frac{R^2 F(R)}{16} . \frac{d(R^2)}{dt} \left[{}^{A}_{\Omega}I_{jk}^{DA}(1,3) + {}^{A}_{\Omega}I_{jk}^{BA}(2,2) \right]$$

$$+ \beta_j \alpha_k Z_B \frac{R^2 F(R)}{8} . b v_i \left[{}^{B}_{\Omega}I_{jk}^{BA}(1,1) + {}^{B}_{\Omega}I_{jk}^{BA}(0,2) \right] . \tag{A8.18}$$

$$W_{jk}^{BA} = \langle \phi_j^B(\vec{r}_B) | f_s (\vec{v}.\vec{F}) V_{cA} | \chi_k^A(\vec{r}_A) \rangle \,, \tag{A8.19}$$

$$W_{jk}^{BA} = \beta_j \alpha_k Z_A \frac{R^2 F(R)}{16} . \frac{d(R^2)}{dt} \left[{}^{A}_{\Omega}I_{jk}^{BA}(1,3) - {}^{A}_{\Omega}I_{jk}^{BA}(2,2) \right]$$

$$+ \beta_j \alpha_k Z_A \frac{R^2 F(R)}{8} . b v_i \left[{}^{B}_{\Omega}I_{jk}^{BA}(1,1) - {}^{B}_{\Omega}I_{jk}^{BA}(0,2) \right] . \tag{A8.20}$$

$$U_{jk}^{BA} = \langle \phi_j^B(\vec{r}_B) | f_s(\vec{v}.\vec{r}) | \chi_k^A(\vec{r}_A) \rangle , \tag{A8.21}$$

$$U_{jk}^{BA} = \beta_j \alpha_k \frac{R^3 F(R)}{32} . \frac{d(R^2)}{dt} \left[{}_A^A I_{jk}^{BA}(3,2) - {}_A^A I_{jk}^{BA}(1,4) \right]$$

$$+ \beta_j \alpha_k \frac{R^3 F(R)}{16} . bv_i \left[{}_A^B I_{jk}^{BA}(0,3) - {}_A^B I_{jk}^{BA}(2,1) \right] . \tag{A8.22}$$

The L_{jk}^{BA} element is given by

$$L_{jk}^{BA} = \langle \phi_j^B(\vec{r}_B) | (\vec{v}.\vec{r}) V_{eB} | \chi_k^A(\vec{r}_A) \rangle$$

$$- \langle \phi_j^B(\vec{r}_B) | (\vec{v}.\vec{r}) V_{eA} | \chi_k^A(\vec{r}_A) \rangle$$

$$- (\varepsilon_j - \eta_k) \langle \phi_j^B(\vec{r}_B) | (\vec{v}.\vec{r}) | \chi_k^A(\vec{r}_A) \rangle \tag{A8.23}$$

from equation (4.4.8) of Section 4.4. Thus

$$L_{jk}^{BA} = V_{jk}^{BA}\Big|_{f_s=1} - W_{jk}^{BA}\Big|_{f_s=1} - (\varepsilon_j - \eta_k) U_{jk}^{BA}\Big|_{f_s=1} . \tag{A8.24}$$

$$V_{jk}^{BA}\Big|_{f_s=1} = \langle \phi_j^B(\vec{r}_B) | (\vec{v}.\vec{r}) V_{eB} | \chi_k^A(\vec{r}_A) \rangle , \tag{A8.25}$$

$$V_{jk}^{BA}\Big|_{f_s=1} = \beta_j \alpha_k Z_B \frac{R^2}{16} . \frac{d(R^2)}{dt} \left[{}_A^A I_{jk}^{BA}(1,2) + {}_A^A I_{jk}^{BA}(2,1) \right]$$

$$- \beta_j \alpha_k Z_B \frac{R^2}{8} . bv_i \left[{}_A^B I_{jk}^{BA}(1,0) + {}_A^B I_{jk}^{BA}(0,1) \right] . \tag{A8.26}$$

$$W_{jk}^{BA}\Big|_{f_s=1} = \langle \phi_j^B(\vec{r}_B) | (\vec{v}.\vec{r}) V_{eA} | \chi_k^A(\vec{r}_A) \rangle , \tag{A8.27}$$

$$W_{jk}^{BA}\Big|_{f_s=1} = \beta_j \alpha_k Z_A \frac{R^2}{16} . \frac{d(R^2)}{dt} \left[{}_A^A I_{jk}^{BA}(2,1) - {}_A^A I_{jk}^{BA}(1,2) \right]$$

$$- \beta_j \alpha_k Z_A \frac{R^2}{8} . bv_i \left[{}_A^B I_{jk}^{BA}(1,0) - {}_A^B I_{jk}^{BA}(0,1) \right] . \tag{A8.28}$$

$$U_{jk}^{BA}\Big|_{f_s=1} = \langle \phi_j^B(\vec{r}_B) | (\vec{v}.\vec{r}) | \chi_k^A(\vec{r}_A) \rangle , \tag{A8.29}$$

$$U_{jk}^{BA}\Big|_{f_s=1} = \beta_j \alpha_k \frac{R^3}{32} \cdot \frac{d(R^2)}{dt}\left[{}^{A}_{\Omega}I_{jk}^{BA}(1,3) - {}^{\hat{}}_{\Omega}I_{jk}^{BA}(3,1)\right]$$

$$+\beta_j \alpha_k \frac{R^3}{16} \cdot bv_i\left[{}^{B}_{\Omega}I_{jk}^{BA}(2,0) - {}^{B}_{\Omega}I_{jk}^{BA}(0,2)\right]. \qquad \text{(A8.30)}$$

2. BB-type Elements

$$A_{jk}^{BB} = \langle \phi_j^B(\vec{r}_B) | V_{CA} | \phi_k^B(\vec{r}_B) \rangle , \qquad \text{(A8.31)}$$

$$A_{jk}^{BB} = -Z_A \beta_j \beta_k \frac{R^2}{4}\left[{}^{A}_{\Omega}I_{jk}^{BB}(1,0) - {}^{A}_{\Omega}I_{jk}^{BB}(0,1)\right]. \qquad \text{(A8.32)}$$

The G_{jk}^{BB}, H_{jk}^{BB}, J_{jk}^{BB}, K_{jk}^{BB} and Λ_{jk}^{BB} elements are given by the expressions for their corresponding BA-type elements but with β_k instead of α_k, and Ω-triple integrals labelled BB instead of BA, e.g. ${}^{A}_{\Omega}I_{jk}^{BB}(0,1)$ instead of ${}^{A}_{\Omega}I_{jk}^{BA}(0,1)$.

$$\bar{U}_{jk}^{BB} = (\varepsilon_j - \varepsilon_k)\langle \phi_j^B(\vec{r}_B) | f_s(\vec{v}.\vec{r}) | \phi_k^B(\vec{r}_B) \rangle , \qquad \text{(A8.33)}$$

$$\bar{U}_{jk}^{BB} = (\varepsilon_j - \varepsilon_k)\beta_j \beta_k \frac{R^3 F(R)}{32} \cdot \frac{d(R^2)}{dt}\left[{}^{A}_{\Omega}I_{jk}^{BB}(3,2) - {}^{A}_{\Omega}I_{jk}^{BB}(1,4)\right]$$

$$-(\varepsilon_j - \varepsilon_k)\beta_j \beta_k \frac{R^3 F(R)}{16} \cdot bv_i\left[{}^{B}_{\Omega}I_{jk}^{BB}(0,3) - {}^{B}_{\Omega}I_{jk}^{BB}(2,1)\right]. \qquad \text{(A8.34)}$$

The L_{jk}^{BB} element is given by

$$L_{jk}^{BB} = -(\varepsilon_j - \varepsilon_k)\langle \phi_j^B(\vec{r}_B) | (\vec{v}.\vec{r}) | \phi_k^B(\vec{r}_B) \rangle$$

$$= -\bar{U}_{jk}^{BB}\Big|_{f_s=1} \qquad \text{(A8.35)}$$

from equation (4.4.4), Section 4.4.

$$L_{jk}^{BB} = (\varepsilon_j - \varepsilon_k)\beta_j\beta_k \frac{R^3}{32} \cdot \frac{d(R^2)}{dt}\left[{}^{A}_{\Omega}I_{jk}^{BB}(3,1) - {}^{A}_{\Omega}I_{jk}^{BB}(1,3)\right]$$

$$+ (\varepsilon_j - \varepsilon_k)\beta_j\beta_k \frac{R^3}{16} \cdot bv_i\left[{}^{B}_{\Omega}I_{jk}^{BB}(0,2) - {}^{B}_{\Omega}I_{jk}^{BB}(2,0)\right]. \qquad \text{(A8.36)}$$

3. AA-type Elements

$$A_{jk}^{AA} = \langle X_j^A(\vec{r}_A) | V_{eB} | X_k^A(\vec{r}_A) \rangle , \qquad \text{(A8.37)}$$

$$A_{jk}^{AA} = -Z_B \alpha_j \alpha_k \frac{R^2}{4}\left[{}^{A}_{\Omega}I_{jk}^{AA}(1,0) + {}^{A}_{\Omega}I_{jk}^{AA}(0,1)\right]. \qquad \text{(A8.38)}$$

The G_{jk}^{AA}, H_{jk}^{AA}, J_{jk}^{AA}, K_{jk}^{AA} and Λ_{jk}^{AA} elements are given by the BA-type expressions but with α_j instead of β_j, and Ω -triple integrals labelled AA instead of BB.

$$\bar{U}_{jk}^{AA} = (\eta_j - \eta_k)\langle X_j^A(\vec{r}_A) | f_s(\vec{v}.\vec{r}) | X_k^A(\vec{r}_A) \rangle , \qquad \text{(A8.39)}$$

$$\bar{U}_{jk}^{AA} = (\eta_j - \eta_k)\alpha_j\alpha_k \frac{R^3 F(R)}{32} \cdot \frac{d(R^2)}{dt}\left[{}^{A}_{\Omega}I_{jk}^{AA}(3,2) - {}^{A}_{\Omega}I_{jk}^{AA}(1,4)\right]$$

$$+ (\eta_j - \eta_k)\alpha_j\alpha_k \frac{R^3 F(R)}{16} \cdot bv_i\left[{}^{B}_{\Omega}I_{jk}^{AA}(0,3) - {}^{B}_{\Omega}I_{jk}^{AA}(2,1)\right]. \qquad \text{(A8.40)}$$

The L_{jk}^{AA} element is given by

$$L_{jk}^{AA} = -(\eta_j - \eta_k)\langle X_j^A(\vec{r}_A) | (\vec{v}.\vec{r}) | X_k^A(\vec{r}_A) \rangle$$

$$= -\bar{U}_{jk}^{AA}\Big|_{f_s=1} \qquad \text{(A8.41)}$$

from equation (4.4.5), Section 4.4.

$$L_{jk}^{AA} = (\eta_j - \eta_k)\alpha_j\alpha_k \frac{R^3}{32} \cdot \frac{d((R^2))}{dt}\left[{}_{A}^{A}I_{jk}^{AA}(3,1) - {}_{A}^{A}I_{jk}^{AA}(1,3)\right]$$

$$+(\eta_j - \eta_k)\alpha_j\alpha_k \frac{R^3}{16} \cdot bv_i\left[{}_{A}^{B}I_{jk}^{AA}(0,2) - {}_{A}^{B}I_{jk}^{AA}(2,0)\right]. \qquad \text{(A8.42)}$$

J. Phys. B: Atom. Molec. Phys. 13 (1980) 4245–4255. Printed in Great Britain

Electron capture by fully stripped ions of helium, lithium beryllium and boron from atomic hydrogen

B H Bransden, C W Newby and C J Noble†
The University of Durham, Durham DH1 3LE England

Received 1 May 1980

Abstract. A two-state approximation based on atomic wavefunctions is used to calculate cross sections for electron capture by He^{2+}, Li^{3+}, Be^{4+} and B^{5+} from atomic hydrogen in the ground state. The velocity range covered is from $v = 0{\cdot}44$ to $v = 2{\cdot}8$ au which corresponds to a laboratory energy range of from 5 to 200 keV amu^{-1}. Reasonable agreement is obtained with the experimental data for He^{2+}, Li^{3+} and B^{5+}.

1. Introduction

Electron capture by fully and partially stripped ions from atomic hydrogen has attracted a great deal of experimental and theoretical interest because of the importance of a knowledge of the corresponding cross sections in fusion research (Gilbody 1979). The reactions concerned are of the form

$$X^{q+} + H(1s) \rightarrow X^{(q-1)+} + H^{+} \tag{1}$$

where X^{q+} represents the incident ion. If the incident ion is fully stripped so that q is equal to the nuclear charge, the ion X^{q+} is hydrogenic and characterised by a set of single-electron quantum numbers nlm. When the velocity of the incident ion is slow compared with the Bohr velocity of the target electron, the wavefunction for the system can be represented in terms of combinations of molecular orbitals; but at higher velocities it is more appropriate to base approximations on truncated two-centre atomic expansions (Briggs 1976, Bransden 1972, 1979a, b). Over a range of laboratory energies of from about 5 to 200 keV amu^{-1}, the truncated expansion approach works when the nuclear charge is $q = 1$ or $q = 2$, because capture is, for these cases, predominantly into states with $n = 1$ or $n = 2$ respectively, so that the number of important channels is small. Correspondingly, reasonably accurate total capture cross sections can be obtained if only those terms representing the important channels are retained in the truncated expansions, although for high accuracy it is necessary to use elaborate expansions including pseudostates. As q increases the principal quantum number of the most likely final state also increases and in addition the total number of final states of significance becomes rather large. For this reason it is impracticable to include all the states of importance in a coupled channel calculation. Fortunately, it has been shown by Lin and collaborators (Lin 1978a, b, Lin *et al* 1978, Lin and Tunnell 1979) in connection with their work on capture from inner shells of heavy ions that over an

† Now at the Daresbury Laboratory of the Science Research Council, Daresbury, Cheshire, England.

0022-3700/80/214245+11$01.50

energy range about the energy at which the cross section reaches its maximum value, a simple two-state approximation can provide useful cross sections. In this approximation, originally due to Bates (1958), only those terms representing the initial and final atomic states are retained in the truncated expansion.

In the present work, we apply the two-states method to capture by He^{2+}, Li^{3+}, Be^{4+} and B^{5+} over the range of incident laboratory energies of 5–200 keV amu^{-1} which allows comparison with the experimental data of Gilbody and his collaborators (Shah and Gilbody 1978, Shah *et al* 1978, Nutt *et al* 1978, Goffe *et al* 1979) with the distorted-wave model of Ryufuku and Watanabe (1978, 1979a, b) and the classical model of Olson and Salop (1977).

2. Theory

The coupled channel approximation has frequently been described in the literature and only a summary will be given here for convenience. For further details reference may be made to Bransden (1970, 1972) or to McDowell and Coleman (1970). The approximation is applied within the impact parameter framework in which the nuclear motion is treated classically and the wavefunction for the electron satisfies the time-dependent Schrödinger equation (in atomic units)

$$\left(H - i\frac{\partial}{\partial t}\right)\Psi(\boldsymbol{r}, t) = 0 \tag{2a}$$

where

$$H = -\tfrac{1}{2}\nabla_r^2 - \frac{q}{r_A(t)} - \frac{1}{r_B(t)} + \frac{q}{R(t)}. \tag{2b}$$

In equation (2), r_A and r_B are the distances of the electron from the incident nucleus X and from the proton, respectively, and $\boldsymbol{r}$ is the position vector of the electron with respect to the mid-point of the internuclear line. The internuclear separation R is a function of t which is determined by the classical trajectory describing the nuclear motion and in this work is taken to be a straight line defined by a constant impact parameter b and constant velocity v.

In the two-state approximation the wavefunction is written as

$$\Psi(\boldsymbol{r}, t) = a(t)\phi(r_B)\exp(-i\epsilon t)\exp[i(-\tfrac{1}{2}\boldsymbol{v}\cdot\boldsymbol{r} + \tfrac{1}{8}v^2 t)]$$
$$+ c(t)\chi_{nlm}(r_A)\exp(-i\eta_n t)\exp[i(\tfrac{1}{2}\boldsymbol{v}\cdot\boldsymbol{r} + \tfrac{1}{8}v^2 t) \tag{3}$$

where ϕ is the 1s ground-state wavefunction of atomic hydrogen with eigen-energy ϵ and χ_{nlm} is the wavefunction of the ion $X^{(q-1)+}$ in the state (nlm) with corresponding eigen-energy η_n. The velocity-dependent factors are required in order for the Schrödinger equation to be satisfied in the limits $t \to \pm\infty$. Coupled first-order differential equations for the amplitudes $a(t)$ and $c(t)$ can be found from a variational principle and take the form

$$\begin{aligned} i[\dot{a} + S\dot{c}] &= Ha + Kc \\ i[S^*\dot{a} + \dot{c}] &= \bar{K}a + \bar{H}c \end{aligned} \tag{4}$$

where the matrix elements S, H, $\bar{H}$, K and $\bar{K}$ are defined as

$$S = \int \phi^*(r_B)\chi_{nlm}(r_A)\exp(iv\cdot r)\,dr \exp[i(\epsilon-\eta_n)t]$$

$$H = q\int |\phi(r_B)|^2\left(-\frac{1}{r_A}+\frac{1}{R}\right)dr$$

$$\bar{H} = \int |\chi_{nlm}(r_A)|^2\left(-\frac{1}{r_B}+\frac{q}{R}\right)dr \qquad (5)$$

$$K = \int \phi^*(r_B)\chi_{nlm}(r_A)\exp(iv\cdot r)\left(-\frac{1}{r_B}+\frac{q}{R}\right)dr \exp[i(\epsilon-\eta_n)t]$$

$$\bar{K} = \int \chi^*_{nlm}(r_A)\phi(r_B)\exp(-iv\cdot r)\left(-\frac{q}{r_A}+\frac{q}{R}\right)dr \exp[i(\eta_n-\epsilon)t].$$

We note the relation

$$i\dot{S} = \bar{K}^* - K \qquad (6)$$

which ensures the conservation of probability.

Equation (4) is solved subject to the boundary conditions $a(t=-\infty)=1$, $c(t=-\infty)=0$ for each value of the impact parameter b. The capture cross section into the state with quantum numbers nlm is then

$$Q_{nlm} = 2\pi\int_0^\infty |c(t=+\infty)|^2 b\,db \qquad (7)$$

and the total capture cross section is

$$Q = \sum_{nlm} Q_{nlm} \qquad (8)$$

where, for each n, the sums over m and l range over all the allowed values of l and m; $|m|\leq l$ and $0\leq l\leq(n-1)$.

The evaluation of the direct matrix elements H and $\bar{H}$ is elementary, and the principal numerical problem is the efficient evaluation of the overlap S and the exchange matrix elements K and $\bar{K}$. A standard computer package has been developed to enable the matrix elements for any values of n, l and m to be calculated (Noble 1980) using the Fourier transform method of Sin Fai Lam (1967). This package can be obtained on request from the CPC Program Library.

In the case of incident He^{2+} ions, previous calculations in the two-state approximation have been made for capture into the 2s and 2p states of He^+ by Malaviya (1969). This affords an independent check on the numerical accuracy of the results, as rather different numerical methods were used in the two calculations. It is very satisfactory that agreement with Malaviya's cross section was obtained to the three significant figures published.

3. Results and discussion

Calculations were carried out at incident energies between 5 and 200 keV amu^{-1} for capture into all final states with $n\leq 4$ for He^{2+} and Li^{3+} and for $n\leq 5$ for Be^{4+} and B^{5+}.

The cross sections, $\sigma_n = \Sigma_{lm} \sigma_{lm}$, for capture into each complete shell are shown in table 1. To compare these with the experimental data for the total capture cross section $\sigma = \Sigma_n \sigma_n$, a correction must be made for capture into shells with higher n. This was made by assuming a behaviour of the cross section which is shown by the Brinkman–Kramers cross section at high velocities (McDowell and Coleman 1970 p 379). Of course, the Brinkman–Kramers cross section is incorrect in magnitude, but it is effective in predicting cross section ratios (Crothers and Todd 1980, Chan and Eichler 1979). If n_{max} is the largest value of n for which two-state calculations have been made, our correction is to use the expression

$$\sigma(n) = \sigma(n_{max})(n_{max}/n)^3 \tag{9}$$

for all $n > n_{max}$. The total cross sections found in this way are included in table 1.

Table 1. Calculated cross sections for capture by ions of He^{2+}, Li^{3+}, Be^{4+} and B^{5+} from H(1s), units of 10^{-16} cm^2.

E (kev amu^{-1})†	$\sigma(n)$ $n=1$	2	3	4	5	$\sigma = \Sigma\sigma(n)$‡
He^{2+}						
5	0·0020	10·53	0·034	0·0095		10·60
10	0·024	11·21	0·490	0·037		11·82
25	0·086	5·79	1·49	0·410		8·41
50	0·172	1·79	0·868	0·376		3·79
100	0·102	0·314	0·179	0·093		0·84
200	0·025	0·031	0·016	0·008		0·094
Li^{3+}						
5	0·000	20·72	2·43	0·009		23·17
10	0·000	18·94	6·89	0·328		26·67
25	0·002	8·54	6·68	2·04		20·45
50	0·002	2·83	2·80	1·47		9·39
100	0·001	0·611	0·589	0·377		2·18
200	0·001	0·081	0·064	0·039		0·25
Be^{4+}						
5	0·000	5·89	43·4	0·38	0·05	49·86
10	0·000	6·99	31·6	3·16	0·22	42·43
25	0·000	4·42	14·20	6·49	2·17	31·74
50	0·000	1·96	5·06	3·53	1·96	16·53
100	0·000	0·597	1·089	0·879	0·584	4·35
200	0·001	0·112	0·138	0·104	0·069	0·57
B^{5+}						
5	§	2·10	49·63	12·98	0·14	65·14
10		2·16	37·19	18·45	1·37	62·00
25		1·75	16·46	14·40	5·59	49·65
50		1·03	6·14	6·23	3·91	25·34
100		0·41	1·45	1·51	1·11	6·78
200		0·11	0·21	0·20	0·15	0·97

† E is the laboratory energy of the incident ion on a stationary target.
‡ Allowance made for $n > n_{max}$ as in equation (9).
§ Ground-state capture cross sections ($n = 1$) are very small and not given.

From table 1, we can see that over this energy region capture into the ground state is quite unimportant except for the case of He^{2+} where it amounts to 26% of the total cross section at the highest energy of 200 keV amu^{-1} ($v = 2{\cdot}8$ au). At lower energies only one or two values of n are important; but, as the energy increases, so does the number of n values of significance. The behaviour of the cross section as a function of incident charge q is of interest. For a given relative velocity, Crothers and Todd (1980) have shown that high-energy approximations, such as the Brinkman–Kramers, the continuum distorted-wave and the continuum intermediate-state models lead to a q^3 variation of the cross section.† However, at lower energies the variation may be closer to q^2 (Presnyakov and Ulantsev 1975). In our model the variation is roughly q^2 over the energy range 10–100 keV amu^{-1} with deviations at the highest and lowest energies (see table 2). It is clear that the assumption of proportionality to a power of q is rather too simple and that simultaneous scaling of cross sections and velocities as in the work of Ryufuku and Watanabe (1979a) or of Gardner *et al* (1977) is likely to be more accurate. However, such a procedure amounts to an empirical interpolation formula, since there does not appear to be any good theoretical reason to suppose that the velocity should scale.

Table 2. Calculated total cross sections for electron capture divided by q^2, units of 10^{-16} cm^2.

E (keV amu^{-1})	He^{2+}	Li^{3+}	Be^{4+}	B^{5+}
5	2·65	2·57	3·11	2·69
10	2·95	2·96	2·65	2·48
25	2·10	2·27	1·98	1·99
50	0·94	1·04	1·03	1·01
100	0·21	0·24	0·27	0·27
200	0·024	0·028	0·035	0·039

For a given n at the lowest energies the capture probability increases with l up to the maximum value allowed, $l = n - 1$. As the energy increases, the higher l values begin to be suppressed. A similar trend is found in the Brinkman–Kramers approximation (Golden *et al* 1978), the eikonal approximation (Chan and Eichler 1979) and in the distorted-wave calculations of Ryufuku and Watanabe (1979b). This is illustrated in table 3 in the case of capture by B^{5+} into the $n = 5$ level of B^{4+}.

Table 3. Cross sections for capture by B^{5+} from H(1s): distribution in l for the shell $n = 5$, units of 10^{-16} cm^2.

E (keV amu^{-1})	$l = 0$	1	2	3	4
10	0·069	0·204	0·315	0·358	0·430
50	0·131	0·385	0·668	1·288	1·441
200	0·004	0·021	0·062	0·049	0·011

† At very large values of v, the Brinkman–Kramers cross section is proportional to q^5, see equation (8.2.16) of McDowell and Coleman (1970).

Our calculated cross sections are compared with other theoretical calculations and with experiment in figures 1–4. The most extensive theoretical work at intermediate energies covering all the cases we have considered has been by Olson and Salop (1977) using the classical Monte Carlo method of Abrines and Percival (1966a, b) and Ryufuku and Watanabe (1978, 1979a, b) using a unitarised distorted-wave approach. The classical calculations, which cover an energy range of 40–200 keV amu^{-1}, are comparable in magnitude with the two-state calculations and with experiment, but the shape of the cross section as a function of energy appears rather different, the cross sections decreasing with increasing energy more rapidly than might be expected. This may be due to large statistical errors being associated with the calculation of the two points of highest energy, as noted by Olson and Salop in their paper. The work of Ryufuku and Watanabe is based on the distorted-wave solution of equation (4). The

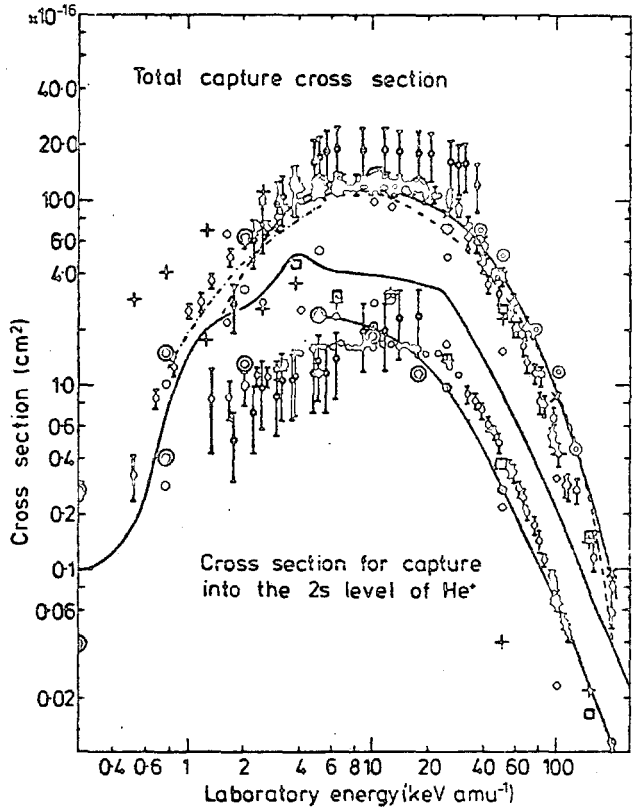

Figure 1. Cross sections for electron capture by He^{2+} from H(1s). Total cross sections are shown in the upper part of the figure and cross sections for capture into the 2s state of He^+ are shown in the lower half of the figure. Theoretical cross sections: ——×——, two-state atomic expansion (present work) for total cross sections; ——○——, two-state atomic expansion (present work) for 2s capture; – – – – –, unitarised distorted-wave approximation (UDWA) Ryufuku and Watanabe (1978); ●, classical method, Olson and Salop (1977); ◇, eight-state atomic expansion, Msezane and Gallaher (1973); +, eight-state and □, eleven-state atomic expansion, Rapp (1974); ⊗, three-state molecular orbital expansion, Piacentini and Salin (1977); – · – · – · –, twenty-state molecular orbital expansion, Winter and Lane (1978); ⊙, ten-state molecular orbital expansion, Hatton *et al* (1979). Experimental cross sections: ◇, Shah and Gilbody (1978), Nutt *et al* (1978); ◇, Bayfield and Khayrallah (1975); ◇, Olson *et al* (1977).

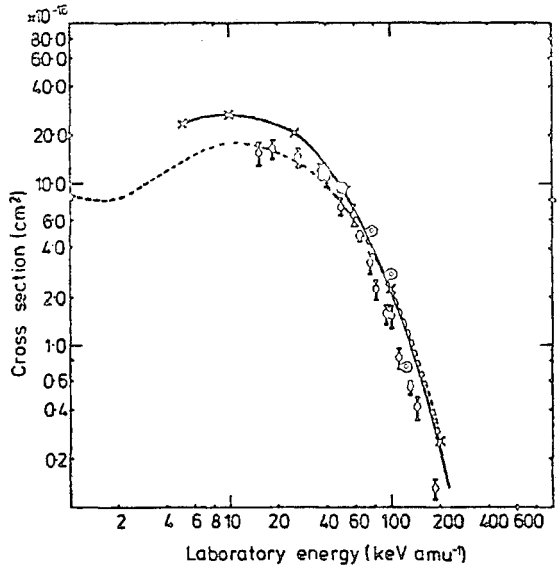

Figure 2. Total cross sections for electron capture by Li^{3+} from H(1s). Theoretical cross sections: ——×——, two-state atomic expansion (present work); – – – – –, unitarised distorted-wave approximation (UDWA), Ryufuku and Watanabe (1979a); ©, classical method, Olson and Salop (1977). Experimental cross sections: ◊, Shah *et al* (1978).

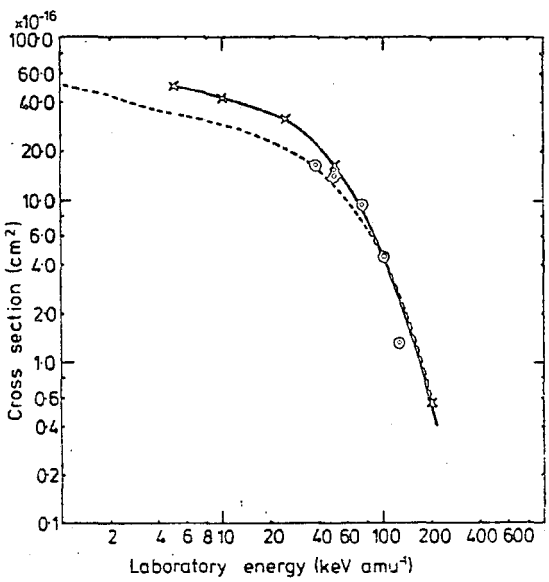

Figure 3. Theoretical total cross sections for electron capture by Be^{4+} from H(1s). ——×——, two-state atomic expansion (present work); – – – – –, unitarised distorted-wave approximation (UDWA), Ryufuku and Watanabe (1979a); **O**, classical method, Olson and Salop (1977).

distorted-wave charge exchange amplitude is (Bates 1958)

$$C^{\mathrm{DW}}(t=\infty)=\int_{-\infty}^{\infty}\mathrm{d}t\left(\frac{\bar{K}-S^{*}H}{1-|S|^{2}}\right)\exp\mathrm{i}(\delta_{a}(t)-\delta_{c}(t)) \tag{10}$$

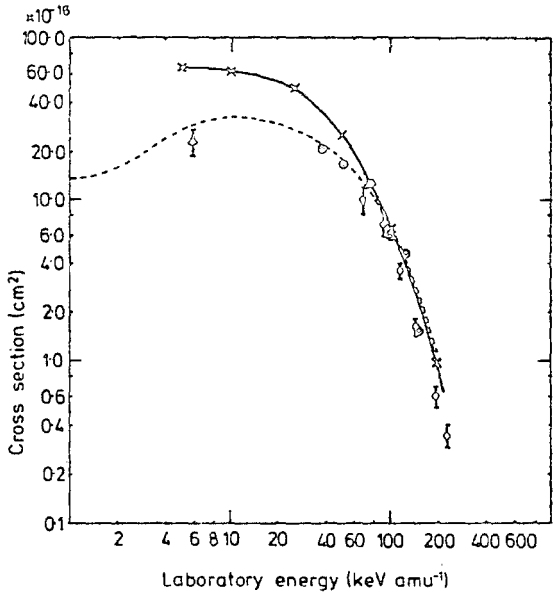

Figure 4. Total cross sections for electron capture by B^{5+} from H(1s). Theoretical cross sections: ——×——, two-state atomic expansion (present work); - - - - -, unitarised distorted-wave approximation, Ryufuku and Watanabe (1979a); ○, classical method, Olson and Salop (1977). Experimental cross sections: △, Crandall *et al* (1979); ▽, Goffe *et al* (1979).

where

$$\delta_a(t) = \int_{-\infty}^{t} \mathrm{d}t' \left(\frac{H - S\bar{K}}{1 - |S|^2} \right) \qquad \delta_c(t) = \int_{-\infty}^{t} \mathrm{d}t' \left(\frac{\bar{H} - S^* K}{1 - |S|^2} \right). \tag{11}$$

Ryufuku and Watanabe make the approximation of neglecting S^2 in the denominators of these expressions and this should be a good approximation in most cases. They then unitarise the total probability for capture $P(b)$, defined as

$$p(b) = \sum_{nlm} |C_{nlm}^{\mathrm{DW}}(t = \infty)|^2 \tag{12}$$

by writing

$$P(b) = \sin^2(p(b))^{1/2}. \tag{13}$$

They derived this expression from the perturbation series by (i) neglecting time ordering and (ii) omitting the even ordered terms from the series. The latter approximation is very much open to question. Examination of the coupled channel approximations of Rapp (1974), for example, in the case of $He^{2+} + H(1s)$ shows that at the lower energies where the two-state approximation begins to break down, corrections arise from couplings to the $n = 2$ levels of H and these couplings do not occur in the unitarised distorted-wave model (UDWA). From figures 1–4, we see that for He^{2+}, the UDWA cross sections are rather close to the two-state cross sections, above 5 keV amu^{-1}. For Li^{3+}, Be^{4+} and B^{5+}, the UDWA cross sections, while agreeing reasonably with the two-state cross sections at the higher energies, are considerably smaller at the lower energies, where the unitarisation procedure produces large corrections to the DW cross section. It is, of course, hardly necessary to point out that coupled channel calculations automatically preserve unitarity (in the two-state case if equation (6) is satisfied), but while unitarity is a virtue, it does not guarantee the accuracy of a method.

At the higher energies the calculated two-state approximation produces cross sections which are close to those of the distorted-wave approximation of equations (10) and (11); in other words 'back coupling' is small. To take an explicit example, Saha *et al* (1980) have recently calculated the $He^{2+} + H(1s) \rightarrow He^{+}(3s) + H^{+}$ cross section from 6·25 to 200 keV amu^{-1} in the DW approximation. Above 25 keV amu^{-1} the DW and two-state cross sections agree to three significant figures, but below this energy the DW cross section is too large, exceeding the two-state cross section by a factor of about five at 6 keV amu^{-1}.

3.1. He^{+}

The case of helium is interesting in that not only the total cross section has been measured, but also the cross section for capture into the 2s level of He^{+}. From figure 1 we see that the two-state calculations (and the UDWA cross sections) agree rather well with the total cross section data of Shah and Gilbody (1978) and Nutt *et al* (1978) from 5 keV amu^{-1}, becoming a little larger than the data at higher energies. The agreement between the present calculations and the data for 2s capture is less good, but is not surprising as Malaviya's (1969) work shows that while the $n = 2$ capture cross section given by the two-state approximation agrees closely with the results of the more elaborate five-state approximation above 6 keV amu^{-1}, the coupling between the degenerate 2s and 2p levels is of importance in determining the cross sections for capture into the individual 2s, $2p_0$ and $2p_{\pm 1}$ levels.

The results of the more elaborate eight-state atomic expansion calculations of Rapp (1974) and Msezane and Gallaher (1973) are also shown in figure 1. As Rapp remarks, these calculations should agree, but in fact there are considerable differences between them. For this reason it is difficult to comment on the agreement of these calculations (or of the eleven-state work of Rapp) with the two-state calculations and with the data. Other calculations at the lower energies, based on the MO expansion are shown. Of these, the recent work of Hatton *et al* (1979), which is the only MO calculation which is completely translationally invariant, is in good agreement with the data.

3.2. Li^{3+}, Be^{4+} and B^{5+}

For lithium, the two-state cross section agrees rather well in shape with the data of Shah *et al* (1978), but is a little greater in magnitude (see figure 2). For beryllium there is no data, while for boron the two-state cross section has a similar energy variation to that of the Belfast data (Goffe *et al* 1979) and again the calculated cross section is somewhat greater in magnitude. The lowest energy in the Belfast experiment was around 65 keV amu^{-1} but there is a single measured point at 6 keV amu^{-1} by Crandall *et al* (1979). As can be seen from figure 4, this point is in much better agreement with the UDWA cross section than with the present calculations. Clearly further measurements in this energy region would be desirable.

4. Conclusions

Over the intermediate energy range we have considered (5–200 keV amu^{-1}), the two-state approximation appears to represent the electron capture cross section to a fair degree of accuracy. At lower energies, where the molecular aspects of the system will

become important, the two-state approximation can be improved by using the variable charge method of Cheshire (1968) and it is our intention to explore this, as well as to extend our work to cases with $q > 5$. At higher energies, continuum intermediate states are important and methods such as the CDW or CIS approximations should be employed (Belkić *et al* 1979). It is unfortunate that, as noted above, there is some disagreement between the different authors on the results of many-state atomic expansion calculations for He^{2+}. To clear up this question, we are planning to repeat the eight-state calculations and to extend them by adding suitable pseudostates.

Acknowledgments

This work was supported, in part, by the Science Research Council. One of us (CWN) wishes to acknowledge the receipt of a Science Research Council studentship.

References

Abrines R and Percival I C 1966a *Proc. Phys. Soc.* **88** 861–72
—— 1966b *Proc. Phys. Soc.* **88** 873–83
Bates D R 1958 *Proc. R. Soc.* A **274** 294–301
Bayfield J E and Khayrallah G A 1975 *Phys. Rev.* A **12** 869–75
Belkić D E, Gayet R and Salin A 1979 *Phys. Rep.* **56** 279–369
Bransden B H 1970 *Atomic Collision Theory* (New York: Benjamin)
—— 1972 *Rep. Prog. Phys.* **35** 949–1005
—— 1979a *Phys. Mag.* **1** 11–36
—— 1979b *Advances in Atomic and Molecular Physics* vol 15, ed D R Bates and I Estermann (New York: Academic) pp 263–91
Briggs J S 1976 *Rep. Prog. Phys.* **39** 217–89
Chan F T and Eichler J 1979 *Phys. Rev. Lett.* **42** 58–61
Cheshire I M 1968 *J. Phys. B: Atom. Molec. Phys.* **1** 428–37
Crandall D H, Phaneuf R A and Meyer F W 1979 *Phys. Rev.* A **19** 504–14
Crothers D S F and Todd N R 1980 *J. Phys. B: Atom. Molec. Phys.* **13** 2277–94
Gardner L D, Bayfield J E, Koch P M, Kim H J and Stelson P H 1977 *Phys. Rev.* A **16** 1415–8
Gilbody H B 1979 *Advances in Atomic and Molecular Physics* vol 15, ed D R Bates and I Estermann (New York: Academic) pp 293–328
Goffe T V, Shah M B and Gilbody H B 1979 *J. Phys. B: Atom. Molec. Phys.* **12** 3763–73
Golden J E, McGuire J H and Omidvar K 1978 *Phys. Rev.* A **18** 2373–6
Hatton G J, Lane N F and Winter T G 1979 *J. Phys. B: Atom. Molec. Phys.* **12** L571–7
Lin C D 1978a *J. Phys. B: Atom. Molec. Phys.* **11** L185–90
—— 1978b *J. Phys. B: Atom. Molec. Phys.* **11** L595–9
Lin C D, Song S C and Tunnell L N 1978 *Phys. Rev.* A **17** 1646–54
Lin C D and Tunnell L N 1979 *J. Phys. B: Atom. Molec. Phys.* **12** L485–90
McDowell M R C and Coleman J P 1970 *An Introduction to the Theory of Ion Atom Collisions* (Amsterdam: North Holland)
Malaviya V 1969 *J. Phys. B: Atom. Molec. Phys.* **2** 843–50
Msezane A and Gallaher D F 1973 *J. Phys. B: Atom. Molec. Phys.* **6** 2334–54
Noble C J 1980 *Commun. Comput. Phys.* **19** 327–35
Nutt W L, McCullough R W, Brady K, Shah M B and Gilbody H B 1978 *J. Phys. B: Atom. Molec. Phys.* **11** 1457–62
Olson R E and Salop A 1977 *Phys. Rev.* A **16** 531–41
Olson R E, Salop A, Phaneuf R A and Meyer F W 1977 *Phys. Rev.* A **16** 1867–72
Piacentini R D and Salin A 1977 *J. Phys. B: Atom. Molec. Phys.* **10** 1515–22
Presnyakov L P and Ulantsev A D 1975 *Sov. J. Quantum Electron.* **4** 1320–4
Rapp D 1974 *J. Chem. Phys.* **61** 3777–9

Ryufuku H and Watanabe T 1978 *Phys. Rev.* A 18 2005–15
—— 1979a *Phys. Rev.* A 19 1538–49
—— 1979b *Phys. Rev.* A 20 1828–37
Saha H P, Maiti N and Sil N C 1980 *J. Phys. B: Atom. Molec. Phys.* 13 327–42
Shah M B and Gilbody H B 1978 *J. Phys. B: Atom. Molec. Phys.* 11 121–31
Shah M B, Goffe T V and Gilbody H B 1978 *J. Phys. B: Atom. Molec. Phys.* 11 L233–6
Sin Fai Lam L T 1967 *Proc. Phys. Soc.* 92 67–74
Winter T G and Lane N F 1978 *Phys. Rev.* A 17 66–79

REFERENCES

Abramowitz M. and Stegun I.A., 1965, "Handbook of Mathematical Functions", (Dover, New York).

Allan R.J., Dickinson A.S. and McCarroll R., 1983, J. Phys. B: At. Mol. Phys. 16, 467.

Anderson D.G.M., Antal M.J. and Mc Elroy M.B., 1974, J. Phys. B: At. Mol. Phys. 7, L118.

Arfken G., 1970, "Mathematical Methods for Physicists", (Academic Press, New York).

Baer M., 1975, Chem. Phys. Lett. 35, 112.

Banyard K.E. and Shirtcliffe G.W., 1979, J. Phys. B: At. Mol. Phys. 12, 3247.

Basu D., Bhattacharya D.M. and Chatterjee G., 1967, Phys. Rev. 163, 8.

Basu D., Mukherjee S.C. and Sural D.P., 1978, Phys. Reports 42C, 145.

Bates D.R., 1958, Proc. Roy. Soc. A247, 294.

Bates D.R. and McCarroll R., 1958, Proc. Roy. Soc. A245, 175.

Bates D.R. and Williams, D.A., 1964, Proc. Phys. Soc. 83, 425.

Bates D.R., Massey H.S.W. and Stewart A.L., 1953, Proc. Roy. Soc. A216, 437.

Bayfield J.E., 1969, Phys. Rev. 185, 105.

Bayfield J. E. and Khayrallah G.A., 1975, Phys. Rev. A12, 869.

Becker R.L., Ford A.L. and Reading J.F., 1980, J. Phys. B: At. Mol. Phys. 13, 4059.

Belkic Dz. and Gayet R., 1977, J. Phys. B: At. Mol. Phys. 10, 1911.

Belkic Dz. and Janev R.K., 1973, J. Phys. B: At. Mol. Phys. 6, 1020.

Belkic Dz. and McCarroll R., 1977, J. Phys. B: At. Mol. Phys. 10, 1933.

Belkic Dz., Gayet R. and Salin A., 1979, Phys. Reports 56, 279.

Born M. and Fock V., 1928, Z. Phys. 51, 165.

Born M. and Oppenheimer J.R., 1927, Ann. Physik 84, 457.

Bransden B.H., 1972, Rep. Prog. Phys. 35, 949.

Bransden B.H., 1983, "Atomic Collision Theory", 2nd ed., (Benjamin/Cummings, New York).

Bransden B.H., 1983p, private communication.

Bransden B.H. and Noble C.J., 1981, J. Phys. B: At. Mol. Phys. 14, 1849.

Bransden B.H. and Noble C.J., 1982, J. Phys. B: At. Mol. Phys. 15, 451.

Bransden B.H. and Sin Fai Lam L. T., 1966, Proc. Phys. Soc. 87, 653.

Bransden B.H., Newby C.W. and Noble C.J., 1980, J. Phys. B: At. Mol. Phys. 13, 4245.

Bransden B.H., Noble C.J. and Chandler J., 1983, J. Phys. B: At. Mol. Phys. - to be published.

Briggs J.S. and Taulbjerg K., 1975, J. Phys. B: At. Mol. Phys. 8, 1909.

Brinkman H.C. and Kramers H. A., 1930, Proc. Acad. Sci. Amst. 33, 973.

Callaway J. and Wooten J.W., 1974, Phys. Rev. A9, 1924.

Campos D., Ramirez C. and de Garcia A., 1983, J. Phys. B: At. Mol. Phys. 16, 853.

Chatterjee G., Bhattacharya D.M. and Sil N.C., 1967, Indian J. Phys. 41, 934.

Cheshire I.M., 1964, Proc. Phys. Soc. 84, 89.

Cheshire I.M., 1967, Proc. Phys. Soc. 92, 862.

Cheshire I.M., 1968, J. Phys. B: At. Mol. Phys. 1, 428.

Cheshire I.M., Gallaher D.F. and Taylor A.J., 1970, J. Phys. B: At. Mol. Phys. 3, 813.

Chidichimo-Frank M.C. and Piacentini R.D., 1974, J. Phys. B: At. Mol. Phys,. 7, 548.

CRC Handbook of Chemistry and Physics, 1975, 56th edition, ed. R.C. Weast, (CRC Press, Cleveland, Ohio).

Crothers D.S.F. and Hughes J.G., 1978, Proc. Roy. Soc. A359, 345.

Crothers D.S.F. and Hughes J.G., 1979, Philos. Trans. Roy. Soc. 292, ser.A, 539.

Crothers D.S.F. and Todd N.R., 1981a, J. Phys. B: At. Mol. Phys. 14, 2233.

Crothers D.S.F. and Todd N.R., 1981b, J. Phys. B: At. Mol. Phys. 14, 2251.

Dalgarno A. and Yadav H.N., 1953, Proc. Phys. Soc. A66, 173.

Delos J.B., 1981, Revs. of Mod. Phys. 53, 287.

Dickinson A.S. and McCarroll R., 1983, J. Phys. B: At. Mol. Phys. 16, 459.

Dose V. and Semini C., 1974, Helv. Phys. Acta 47, 609.

Drisko R.M., 1955, Ph.D. Thesis, Carnegie Inst. Tech.

D'yachkov B.A. and Zinenko V.I., 1968, Sov. At. Energy 24, 16.

Ermolaev A.M., 1983, J. Phys. B: At Mol. Phys. - submitted for publication.

Farina J.E.G., 1975, "Quantum Theory of Scattering Processes : General Principles and Advanced Topics", (Pergamon Press, Oxford).

Fitchard E., Ford A.L. and Reading J.F., 1977, Phys. Rev. A16, 1325.

Flannery M.R., 1969, J. Phys. B: At. Mol. Phys. 2, 1044.

Ford A.L., Fitchard E. and Reading J.F., 1977, Phys. Rev. A16, 133.

Ford A.L., Reading J.F. and Becker R.L., 1979a, J. Phys. B: At. Mol. Phys. 12, 2905.

Ford A.L., Reading J.F. and Becker R.L., 1981, Phys. Rev. A23, 510.

Ford A.L., Reading J.F. and Becker R.L., 1982, J. Phys. B: At. Mol. Phys. 15, 3257.

Ford A.L., Becker R.L., Swafford G.L. and Reading J.F., 1979b, J. Phys. B: At. Mol. Phys. 12, L491.

Fritsch W. and Lin C.D., 1982a, J. Phys. B: At. Mol. Phys. 15, 1255.

Fritsch W. and Lin C.D., 1982b, Phys. Rev. A26, 762.

Fritsch W. and Lin C.D., 1982c, J. Phys. B: At. Mol. Phys. 15, L281.

Fritsch W. and Lin C.D., 1983, J. Phys. B: At. Mol. Phys. 16, 1595.

Fritsch W. and Wille U., 1977, J. Phys. B: At. Mol. Phys. 10, L165.

Fujiwara K., 1981, J. Phys. B: At. Mol. Phys. 14, 3977.

Fulton M.J. and Mittleman M.H., 1965, Ann. Phys. (N.Y.) 33, 65.

Gallaher D.F. and Wilets L., 1968, Phys. Rev. 169, 139.

Green T.A., 1965, Proc. Phys. Soc. 86, 1017.

Green T.A., 1981a, Phys. Rev. A23, 519.

Green T.A., 1981b, Phys. Rev. A23, 532.

Green T.A., Shipsey E.J. and Browne J.C., 1981, Phys. Rev. A23, 546.

Green T.A., Shipsey E.J. and Browne J. C., 1982, Phys. Rev. A25, 1364.

Greenland P.T., 1982, Phys. Reports 81, 131.

Gröbner W. and Hofreiter N., 1961, Integraltafel, unbestimmte und bestimmte Integrale, (Springer-Verlag, Wien und Innsbruck, Austria).

Grüebler W., Schmelzbach P.A., König V. and Marmier P., 1970, Helv. Phys. Acta 43, 254.

Harel C. and Salin A., 1977, J. Phys. B: At. Mol. Phys. 10, 3511.

Hatton G.J., Lane N.F. and Winter T.G., 1979, J. Phys. B: At. Mol. Phys. 12, L571.

Heil T.G. and Dalgarno A., 1979, J. Phys. H: At. Mol. Phys. 12, L557.

Hildebrand F.B., 1974, "Introduction to Numerical Analysis", 2nd ed.,(McGraw-Hill, New York).

Il'in R.N., Oparin V.A., Solov'ev E.S. and Fedorenko N.V., 1967a, Sov. Phys. - JETP Lett. 2, 197.

IL'in R.N., Oparin V.A., Solov'ev E.S. and Fedorenko N.V., 1967b, Sov. Phys. - Tech. Phys. 11, 921.

Kimura M. and Thorson W.R., 1981a, Phys. Rev. A24, 1780.

Kimura M. and Thorson W.R., 1981b, Phys. Rev. A24, 3019.

Kimura M. and Thorson W.R., 1983, J. Phys. B: At. Mol. Phys. 16, 1471.

Landau L.D., 1932, Physik Z. Sowjetunion 2, 46.

Landau L.D. and Lifshitz E.M., 1960, "Mechanics", vol. 1 of "Course of Theoretical Physics", (Pergamon Press, Oxford).

Lebeda C.F., Thorson W.R. and Levy H., 1971, Phys. Rev. A4, 900.

Levy H. and Thorson W.R., 1969a, Phys. Rev. 181, 244.

Levy H. and Thorson W.R., 1969b, Phys. Rev. 181, 252.

Lin C.D., 1978a, J. Phys. B: At. Mol. Phys. 11, L185.

Lin C.D., 1978b, J. Phys. B: At. Mol. Phys. 11, L595.

Lin C.D. and Tunnell L.N., 1979, J. Phys. B: At. Mol. Phys. 12, L485.

Lin. C.D., Soong S.C. and Tunnell L.N., 1978, Phys. Rev. A17, 1646.

Lovell S.E. and McElroy M.B., 1965, Proc. Roy. Soc. A283, 100.

Lüdde H.J. and Dreizler R.M., 1981, J. Phys. B: At. Mol. Phys. 14, 2191.

Lüdde H.J. and Dreizler R.M., 1982a, J. Phys. B: At. Mol. Phys. 15, 2703.

Lüdde H.J. and Dreizler R.M., 1982b, J. Phys. B: At. Mol. Phys. 15, 2713.

Lüdde H.J. and Dreizler R.M., 1983, J. Phys. B: At. Mol. Phys. 16, 1009.

McCarroll R., 1961, Proc. Roy. Soc. A264, 547.

McCarroll R., 1982, in "Atomic and Molecular Collision Theory", ed. F.A. Gianturco, (Plenum, New York), p165.

McCarroll R. and Salin A., 1968, J. Phys. B: At. Mol. Phys. 1, 163.

McCarroll R., Piacentini R.D. and Salin A., 1970, J. Phys. B: At. Mol. Phys. 3, 137.

McDowell M.R.C. and Coleman J.P., 1970, "Introduction to the Theory of Ion-Atom Collisions", (North-Holland, Amsterdam).

McDowell M. R. C. and Ferendeci A.M. (eds.), 1980, "Atomic and Molecular Processes in Controlled Thermonuclear Fusion", (Plenum, New York).

Malaviya V., 1969, J. Phys. B: At. Mol. Phys. 2, 843.

Massey H.S.W. and Smith R.A., 1933, Proc. Roy. Soc. A142, 142.

Morrison H.G. and Öpik U., 1978, J. Phys. B: At. Mol. Phys. 11, 473.

Morse P.M. and Feshbach H., 1953, "Methods of Theoretical Physics", (McGraw-Hill, New York).

Mott N.F., 1931, Proc. Camb. Phil. Soc. 27, 553.

Mott N. F. and Massey H.S.W., 1965, "The Theory of Atomic Collisions", 3rd ed., (Oxford University Press, London).

Msezane A. and Gallaher D.F., 1973, J. Phys. B: At. Mol. Phys. 6, 2334.

Neumann J. von and Wigner E., 1929, Physik Z. 30, 467.

Noble C.J., 1980, Comput. Phys. Commun. 19, 327.

Nutt W.L., McCullough R.W., Brady K., Shah M.B. and Gilbody H.B., 1978, J. Phys. B: At. Mol. Phys. 11, 1457.

Olson R.E., 1982, J. Phys. B: At. Mol. Phys. 15, L163.

Oppenheimer J.R., 1928, Phys. Rev. 31, 349.

Park J.T., Aldag J. E., George J.M., Peacher J.L. and McGuire J.H., 1977, Phys. Rev. A15, 508.

Peart B., Grey R. and Dolder K.T., 1977, J. Phys. B: At. Mol. Phys. 10, 2675.

Piacentini R.D. and Salin A., 1974, J. Phys. B: At. Mol. Phys. 7, 1666.

Piacentini R.D. and Salin. A., 1976, J. Phys. B: At. Mol. Phys. 9, 563.

Piacentini R.D. and Salin A., 1977, J. Phys. B: At. Mol. Phys. 10, 1515.

Ponce V.H., 1979, J. Phys. B: At. Mol. Phys. 12, 3731.

Rankin J. and Thorson W.R., 1978, Phys. Rev. A18, 1990.

Rapp D., 1973, J. Chem. Phys. 58, 2043.

Rapp D., 1974, J. Chem. Phys. 61, 3777.

Rapp D. and Dinwiddie D., 1972, J. Chem. Phys. 57, 4919.

Rapp D., Dinwiddie D., Storm D. and Sharp T.E., 1972, Phys. Rev. A5, 1290.

Reading J.F. and Ford A.L., 1979, J. Phys. B: At. Mol. Phys. 12, 1367.

Reading J.F., Ford A.L. and Becker R.L., 1981, J. Phys. B: At. Mol. PHys. 14, 1995.

Reading J.F., Ford A.L. and Becker R.L., 1982, J. Phys. B: At. Mol. Phys. 15, 625.

Reading J.F., Ford A.L. and Fitchard E., 1976, Phys. Rev. Lett. 36, 573.

Reading J.F., Ford A.L., Swafford G.L. and Fitchard A., 1979, Phys. Rev. A20, 130.

Riley M.E. and Green T.A., 1971, Phys. Rev. A4, 619.

Rose M.E., 1957, "Elementary Theory of Angular Momentum", (Wiley, New York).

Ryding G., Wittkower A.B. and Gilbody H.B., 1966, Proc. Phys. Soc. 89, 547.

Ryufuku H., 1982, Phys. Rev. A25, 720.

Ryufuku H. and Watanabe T., 1978, Phys. Rev. A18, 2005.

Ryufuku H. and Watanabe T., 1979a, Phys. Rev. A19, 1538.

Ryufuku H. and Watanabe T., 1979b, Phys. Rev. A20, 1828.

Salop A. and Olson R.E., 1977, Phys. Rev. A16, 1811.

Salop A. and Olson R.E., 1979. Phys. Rev. A19, 1921.

Schiff L.I., 1955, "Quantum Mechanics", (McGraw-Hill, New York).

Schneiderman S.B. and Russek A., 1969, Phys. Rev. 181, 311.

Sethu Raman V., Thorson W.R. and Lebeda C.F., 1973, Phys. Rev. A8, 1316.

Shah M.B. and Gilbody H.B., 1978, J. Phys. B: At. Mol. Phys. 11, 121.

Shakeshaft R., 1976, Phys. Rev. A14, 1626.

Shakeshaft R., 1978a, Phys. Rev. A17, 1011.

Shakeshaft R., 1978b, Phys. Rev. A18, 1930.

Shampine L.F. and Gordon M.K., 1975, "Computer Solution of Ordinary Differential Equations : The Initial Value Problem", (Freeman, San Francisco).

Shipsey E.J., Green T.A. and Browne J.C., 1983, Phys. Rev. A27, 821.

Sil N.C., 1954, Indian J. Phys. 28, 232.

Simony P.R. and McGuire J.H., 1981, J. Phys. B: At. Mol. Phys. 14, L737.

Sin Fai Lam L.T., 1967, Proc. Phys. Soc. 92, 67.

Smith F.T., 1969, Phys. Rev. 179, 111.

Sookne D.J., 1973, J. of Research NBS-B. Mathematical Sciences, 77A, 125.

Stebbings R.F., Young R.A., Oxley C.L. and Ehrhardt H., 1965, Phys. Rev. 138A, 1312.

Stückelberg E.C.G., 1932, Helv. Phys. Acta 5, 369.

Sullivan J., Coleman J.P. and Bransden B.H., 1972, J. Phys. B: At. Mol. Phys. 5, 2061.

Taulbjerg K., Vaaben J. and Fastrup B., 1975, Phys. Rev. A12, 2325.

Teller E., 1937, J. Phys. Chem. 41, 109.

Thomas L.H., 1927, Proc. Roy. Soc. A114, 561.

Thorson W.R. and Delos J.B., 1978a, Phys. Rev. A18, 117.

Thorson W.R. and Delos J.B., 1978b, Phys. Rev. A18, 135.

Thorson W.R. and Levy H., 1969. Phys. Rev. 181, 230.

Thorson W.R., Kimura M., Choi J.H. and Knudson S.K., 1981, Phys. Rev. A24, 1768.

Vaaben J. and Briggs J.S., 1977, J. Phys. B: At. Mol. Phys. 10, L521.

Vaaben J. and Taulbjerg K., 1979, "Proc. 11th Int. Conf. on Physics of Electronic and Atomic Collisions", ed. K. Takayanagi. (Kyoto : Society for Atomic Collision Research). Contributed paper, p 566.

Vaaben J. and Taulbjerg K., 1981, J. Phys. B: At. Mol. Phys. 14, 1815.

Wilets L. and Gallaher D.F., 1966, Phys. Rev. 147, 13.

Winter T.G., 1982, Phys. Rev. A25, 697.

Winter T.G. and Hatton G.J., 1980, Phys. Rev. A21, 793.

Winter T.G. and Lane N.F., 1978, Phys. Rev. A17, 66.

Winter T.G., Hatton G.J. and Lane N.F., 1980, Phys. Rev. A22, 930.

Wittkower A.B., Ryding G. and Gilbody H.B., 1966, Proc. Phys. Soc. 89, 541.

Young R.A., Stebbings R.F. and McGowan J.M., 1968, Phys. Rev. 171, 85.

Zener C., 1932, Proc. Roy. Soc. A137, 696.